EASTERN SCHELDT INLET MORPHODYNAMICS

EASTERN SCHELDT INLET MORPHODYNAMICS

PROEFSCHRIFT

Ter verkrijging van de graad van doctor
aan de Technische Universiteit Delft,
op gezag van de Rector Magnificus prof. ir. K.C.A.M. Luyben,
voorzitter van het College voor Promoties,
in het openbaar te verdedigen op woensdag 27 maart 2013 om 12:30 uur

door

Menno EELKEMA
civiel ingenieur
geboren te Bilthoven

Dit proefschrift is goedgekeurd door de promotoren:

Prof. Dr. Ir. M.J.F. Stive

Prof. Dr. Ir. Z.B. Wang

Samenstelling promotiecommissie:

Rector Magnificus,	voorzitter
Prof. Dr. Ir. M.J.F. Stive,	Technische Universiteit Delft, promotor
Prof. Dr. Ir. Z.B. Wang,	Technische Universiteit Delft, promotor
Prof. Dr. Ir. H.J. de Vriend,	Technische Universiteit Delft
Prof. Dr. Ir. J.A. Roelvink,	UNESCO-IHE/Technische Universiteit Delft
Prof. Dr. Ir. P. Hoekstra,	Universiteit Utrecht
Dr. A.J.F. van der Spek,	Deltares
Dr. Ir. A. Hibma,	Van Oord BV

The work presented in this thesis is carried out as part of the innovation program Building with Nature. The Building with Nature program is funded from several sources, including the Subsidieregeling Innovatieketen Water (SIW, Staatscourant nrs 953 and 17009) sponsored by the Dutch Ministry of Transport, Public Works and Water Management and partner contributions of the participants to the Foundation EcoShape. The program receives co-funding from the European Fund for Regional Development EFRO and the Municipality of Dordrecht.

Additional funding was provided by the Dr. Ir. Cornelis Lely Foundation.

ISBN 978-90-9027347-1

Printed by Haveka, the Netherlands

Sources cover images:	Lighthouse photograph:	Jos de Witte
	Inlet bathymetry	Menno Eelkema
	Other pictures:	https://beeldbank.rws.nl/

Undertow

I've been struck dumb
By a voice that speaks from deep
Beneath the endless waters.
It's twice as clear as heaven
And twice as loud as reason.
It's deep and rich like silt on a riverbed
And just as never-ending.
The current's mouth below me
Opens up around me
Suggests and beckons all while swallowing
Surrounds and drowns and sweeps me away.

I've been baptized
By a voice that screams from deep
Beneath the cold black waters.
It's half as high as heaven
And half as clear as reason.
It's cold and black like silt on a riverbed
And just as never-ending.
The current's mouth below me
Opens up around me
Suggests and beckons all while swallowing
Surrounds and drowns and sweeps me away.

- Maynard James Keenan

SUMMARY

In the south-western part of the Netherlands, the system of estuaries, tidal basins and islands has been shaped and studied by humans for centuries. By far the largest event that determined its current configuration was the storm surge that occurred in 1953. This giant flooding gave rise to one of the largest engineering programs in the world: the Delta Plan. The aim of this plan was to ensure safety against flooding, while at the same time allow for other utilisations of the Delta. This system of dams, barriers and sluices has had, and is still having a strong effect on the morphology of the Delta coast and basins, especially the Eastern Scheldt tidal basin. The objective of this thesis is to gain understanding of the mechanisms that govern the exchange of sediment between the Eastern Scheldt basin and its ebb-tidal delta, and the effects of human interventions on these mechanisms.

In order to gain better understanding of the processes determining the morphology of the inlet, analysis of bathymetric and hydraulic data is combined with process-based numerical modelling. As part of this research a dedicated numerical model of the Delta as a whole and the Eastern Scheldt in particular is made. This approach is applied to four different stages in the evolution of the Eastern Scheldt. The first stage concerns the Eastern Scheldt estuary before any part of the Delta Plan was implemented. The second stage deals with the construction of several back-barrier dams in the nineteen sixties. The third stage describes how the storm surge barrier affected the ebb-tidal delta between 1986 and 2010. The fourth stage consists of an outlook on the next 100 to 200 years.

The Eastern Scheldt is the former mouth of the Scheldt River. During the middle ages, the Western Scheldt took over the function of main river mouth. Historical records on land reclamations and inundations around the Eastern Scheldt estuary show a continuous effort by humans throughout the centuries to reclaim the shallow flats around the estuary. However, the largest change in the surface area of the estuary was caused by the inundation of South-Beveland by a storm surge in 1530 A.D. This inundation started a long period of tidal prism growth and sediment export. Model simulations show that the growth of both the prism and the export was hampered by the presence of an erosion-resistant clay layer underneath the inundated area of South-Beveland.

The inundation also initiated the migration of the shallow tidal watershed between the Eastern Scheldt and Grevelingen estuary towards the Grevelingen. Consequently, the tidal influence of the Eastern Scheldt began to reach into the Volkerak channel. Model simulations show that this migration was most likely caused by the changes in tidal phase and amplitude on the Eastern Scheldt's side of the watershed in response to the inundation. This watershed migration caused the tidal prism to grow even further, sustaining the sediment export out of the inlet. By 1950, the Eastern Scheldt estuary was still exporting significant amounts of sediment. This indicates that by this time, the estuary was still in the process of adapting its morphology towards an equilibrium.

In response to the storm surge of 1953, the decision was made to close off most of the inlets along the Delta coast. The first phase of this so-called Delta Plan consisted of constructing several back-barrier dams. These dams, located in the Grevelingen estuary and Volkerak channel, turned the Eastern Scheldt from an estuary into a basin. The dams cut off all river influence, and also amplified the tidal range in the Eastern Scheldt. The increase in tidal prism resulted in a larger sediment export than there already was. Because of the increased flow velocities, channels scoured and the tidal flats experienced a slight increase in elevation. The erosive trend in the channels was not observed in the entire basin. The Keeten channel experienced accretion, probably because it was overloaded by the sediment supply coming from the Volkerak.

The ebb-tidal delta grew rapidly in sediment volume during this period which lasted from 1969 to 1986. The entire ebb-tidal delta became wider by accretion of shoals on their seaward sides and channels pushing their ebb-shields seaward. The sediment from the basin was primarily deposited on the shoals. The main channels became larger and straightened.

In 1986 the final stage of the Delta Plan was finalised with the construction of the storm surge barrier and two more back-barrier dams inside the Eastern Scheldt basin. The hydrodynamic effect of this was a strong decrease in tidal flow velocities inside the basin and on the ebb-tidal delta. The bathymetry of the ebb-tidal delta responded in two ways. First of all, the main channels and shoals experienced a small clockwise rotation. Secondly, the ebb-tidal delta sediment volume began to decrease, while also the morphological activity saw a sharp decline. The strongest erosion is seen on the shallow parts above 10 m depth. Results from a process-based model indicate that wave-action in combination with the tidal current is largely responsible for this erosion. This tidal current has decreased, but not enough to turn the ebb-tidal delta into a totally wave-dominated regime as is observed on the Grevelingen ebb-tidal delta after the total closure of the Grevelingen inlet. The tidal current on the Eastern Scheldt ebb-tidal delta is still strong enough to transport sediment away from the shoals with the help of wave stirring. However, the decreased tidal current, in combination with the lack of sediment supply, causes that the sediment transport towards the shoals is insufficient, resulting in net erosion of these shoals.

Most of the channels have turned into sinks for sediment, although some notable exceptions exist. The channels running closest to the coast have experienced erosion instead of accretion. This development is a part of the overall rotation of the ebb-tidal delta, and is a result of the altered tidal hydrodynamics brought on by the barrier. Due to the presence of the barrier, the alongshore component of the tide has become stronger relative to the cross-shore component coming out of the inlet. As a result, the ebb-tidal delta rotated, and the channels running close to the coast scoured. Application of a process-based model reveals that although the average

magnitude of the tidal current velocity on the ebb-tidal delta has decreased in response to the barrier's construction, tide-residual currents and current velocity asymmetries have increased in some places, most notably on the Banjaard shoal and the Krabbengat channel.

It is not entirely clear where the eroded sediment has ended up. The storm surge barrier is effectively acting as a barrier for sediment transport, judging from the sediment budget of the basin which is not gaining any significant quantities of sediment. The remaining transport path over the ebb-tidal delta is directed from south-west to north-east. The eroded sediment most likely ends up on the southern side of the Grevelingen ebb-tidal delta, where a large abandoned channel, called the Brouwershavense gat channel, acts as a sink. However, this area cannot account for the total amount of sediment that has been eroded from the Eastern Scheldt's ebb-tidal delta.

It is important to have knowledge on how long the adaptation of the ebb-tidal delta will take. In most other cases when inlets are affected by human intervention, the sediment exchange between basin and ebb-tidal delta remains unimpeded. In this case, however, the ebb-tidal delta is not losing sediment towards the basin because of the barrier. This makes that the timescale of the adaptation of the ebb-tidal delta is most likely relatively long. The ebb-tidal delta will most likely experience erosion of the shallow parts and the seaward edge. As the seaward edge erodes, the shoals closer to the barrier become less sheltered from waves. In this way, the erosion sustains itself. It is also to be expected that this development will cause an increase in the maximum significant wave heights just seaward of the barrier.

From the entire study on the Eastern Scheldt and its surroundings, it has become clear that the Eastern Scheldt is a basin that has been shaped strongly by a multitude of human interventions. It will take in the order of centuries before the morphological effects of these interventions will have levelled out.

SAMENVATTING

De rivieren en estuaria van de Nederlandse Delta worden al eeuwen lang bestudeerd en beïnvloed door mensen. Met name de stormvloed van 1953 heeft de hedendaagse vorm van de Delta in hoge mate bepaald. Deze grote stormvloed gaf aanleiding tot een van de grootste waterbouwprojecten in de wereld: De Deltawerken. Het doel van deze Deltawerken was om veiligheid tegen overstroming te vergroten, met in achtneming van de andere functies van de Delta. Dit systeem van dammen, keringen en sluizen heeft nog steeds een sterke invloed op de morfologie van de Delta bassins en kustlijn, in het bijzonder de Oosterschelde. Het doel van dit onderzoek is om inzicht te verkrijgen in de mechanismen die de uitwisseling van sediment tussen de bassins en de kust bepalen, en de effecten van menselijke ingrepen op deze mechanismen.

Om meer inzicht te krijgen in de processen die de morfologie van het zeegat van de Oosterschelde bepalen, worden gemeten data van bathymetrie en hydrodynamica gecombineerd met process-gebaseerde modellen. Als onderdeel van dit onderzoek is er een gedetailleerd model van de zuidwestelijke delta en de Oosterschelde gemaakt. Deze aanpak is toegepast op vier verschillende periodes in de levensloop van de Oosterschelde. De eerste periode behelst de tijd van voor de Deltawerken, toen de Oosterschelde nog een estuarium was. De tweede periode beslaat de jaren van 1970 tot 1986, toen de Oosterschelde door meerdere dammen werd afgesloten van de grote rivieren. De derde periode, van 1986 tot aan 2012, wordt gedomineerd door de effecten van de stormvloedkering. De vierde periode is een vooruitzicht op de langetermijneffecten van de stormvloedkering in de komende honderd tot tweehonderd jaar.

De Oosterschelde is de voormalige monding van de rivier de Schelde. In de middeleeuwen heeft de Westerschelde de functie van riviermonding geleidelijk overgenomen. Historische beschrijvingen van landaanwinningen en landverlies rond de Oosterschelde laten zien dat er een continue inspanning was om de ondiepe slikken rond het estuarium in te polderen. Echter, de grootste verandering in de totale oppervlakte van het estuarium kwam door het onderlopen van Zuid Beveland door de Sint Felixvloed in 1530. Dit landverlies zorgde voor een lange periode waarin het getijprisma langzaam groeide en het estuarium sediment exporteerde. Modelsimulaties laten zien dat de groei van zowel het getijprisma als de sedimentexport werd gehinderd door de slecht erodeerbare kleilaag onder Zuid Beveland.

Het onderlopen van Zuid Beveland veroorzaakte eveneens het verplaatsen van het wantij tussen de Oosterschelde en de Grevelingen. Als gevolg hiervan begon de getij-

invloed van de Oosterschelde tot in het Volkerak te reiken. Modelsimulaties geven aan dat deze verplaatsing richting de Grevelingen waarschijnlijk het resultaat was van de veranderingen in de fase en amplitude van het getij aan de Oosterschelde-zijde van het wantij. Deze veranderingen waren een effect van het onderlopen van Zuid Beveland. De verplaatsing van het wantij zorgde ervoor dat het getijprisma van de Oosterschelde nog verder groeide. Deze groei zorgde op zijn beurt voor een aanhoudende export van sediment. Gedurende de eerste helft van de twintigste eeuw exporteerde het Oosterschelde estuarium nog steeds aanzienlijke hoeveelheden sediment richting zee. Dit geeft aan dat de effecten van de inpolderingen en overstromingen nog niet waren uitgewerkt op het moment dat men begon met het uitvoeren van de Deltawerken.

Na de watersnoodramp van 1953 werd besloten om de zeegaten van Zeeland af te sluiten, met uitzondering van de Westerschelde. De eerste stap van deze Deltawerken bestond uit de bouw van meerdere dammen achter in de estuaria. Deze dammen, gelegen in de Grevelingen en het Volkerak, veranderden de Oosterschelde in een bassin wat afgesneden was van rivierafvoer. Deze dammen versterkten de getijslag en vergrootten het getijprisma. Dit resulteerde in een toename van de sediment export. Vanwege de toename in stroomsnelheden werden de geulen groter en de platen hoger. De erosie in de geulen vond niet overal in het bassin plaats. In de Keeten vond er lichte aanzanding plaats, waarschijnlijk vanwege de grote sedimentaanvoer vanuit het Volkerak en het Zijpe. In deze periode, die duurde van 1969 tot 1986, vond er een snelle groei plaats van het sedimentvolume van de buitendelta. De buitendelta werd wijder door aanzanding van de ondieptes en door geulen die deze ondieptes verder zeewaarts drukten.

Het laatste onderdeel van het Deltaplan kwam gereed in 1986 met de bouw van de stormvloedkering in de Oosterschelde, gecombineerd met nog twee dammen achter in het bassin. Het hydrodynamische effect van deze ingrepen was een sterke afname van het getijprisma en stroomsnelheden in het bassin en op de buitendelta. De bathymetrie van de buitendelta reageerde op twee manieren op deze afname. Ten eerste ondergingen de geulen en ondieptes een kleine rotatie met de klok mee. Ten tweede begonnen het sedimentvolume en de morfologische activiteit van de buitendelta af te nemen. De meeste erosie vond plaats op de ondiepe gebieden met waterdieptes kleiner dan 10 meter. Resultaten van een proces-gebaseerd model geven aan dat deze erosie voornamelijk het resultaat zijn van korte golven in combinatie met de getijstroming. Door de afname in getijstroming is de afbrekende werking van de golven relatief sterker geworden, en als gevolg daarvan nemen de ondieptes af in hoogte. Deze afname in de stroming is niet groot genoeg om de buitendelta geheel gedomineerd door golfwerking te laten worden. Dit gebeurde wel met de voordelta van de Grevelingen na de sluiting van het Brouwershavense gat. De stroming op de buitendelta van de Oosterschelde is nog steeds sterk genoeg om sediment van de ondieptes naar dieper water te transporteren, waarbij het geholpen wordt door de opwoeling door golven. Echter, de afname in getijstroming, in combinatie met de gebrekkige sediment aanvoer, zorgt ervoor dat er te weinig sediment richting de ondieptes getransporteerd wordt. Als gevolg hiervan eroderen deze ondieptes.

Sinds de bouw van de stormvloedkering zijn de meeste geulen op de buitendelta kleiner geworden door aanzanding vanaf de eroderende ondieptes. Echter, de geulen die dicht onder de kust langs lopen, zoals de Onrust en het Krabbengat, zijn juist groter en dieper geworden. Deze ontwikkeling is een onderdeel van de heroriëntatie van de buitendelta, en is een effect van de verandering die de stormvloedkering teweeg heeft gebracht in de getijstroming. Vanwege de kering is de kustlangse component van de getijstroming sterker geworden in verhouding tot de stroming die uit het zeegat komt. Als gevolg hiervan vindt er een heroriëntatie van de buitendelta plaats, en slijpen de geulen vlak voor de kust verder uit. Resultaten van een procesgebaseerd model laten zien dat alhoewel de getijgemiddelde magnitude van de stroomsnelheid is afgenomen als gevolg van de stormvloedkering, de residuele stromingen en de stromingsasymmetrie nemen toe op sommige plekken.

Het is niet geheel eenduidig waar het geërodeerde sediment naartoe is getransporteerd. De stormvloedkering laat nagenoeg geen sediment door, afgaande op de sedimentbalans van het bassin wat geen significante toename van sedimentvolume laat zien. De hoofdrichting van het sedimenttransport op de buitendelta gaat van zuidwest naar noordoost. De meest voor de hand liggende bestemming voor het geërodeerde sediment is de zuidelijke kant van de buitendelta van de Grevelingen. Dit gebied wordt gedomineerd door een afgesloten geul genaamd het Brouwershavense Gat, dat sinds de bouw van de Brouwersdam veel sediment vergaart. Echter, de totale hoeveelheid gemeten sedimentatie in dit gebied is kleiner dan het volume wat geërodeerd is van de Oosterschelde buitendelta.

Het is van belang om inzicht te hebben in de tijdschaal waarop de buitendelta zich aanpast aan de nieuwe situatie. Bij veel andere buitendelta's die beïnvloed zijn door menselijk ingrijpen, kunnen bassin en buitendelta vrijuit sediment met elkaar uitwisselen. Echter, in het geval van de Oosterschelde verhindert de stormvloedkering dat de buitendelta zijn overschot aan sediment aan het bassin kwijt kan. Dit zorgt er voor dat de aanpassingstijd van de buitendelta waarschijnlijk langer is dan normaal. Naar alle waarschijnlijkheid zullen de ondiepe delen en de buitenste rand van de buitendelta verder blijven eroderen. Als deze delen eroderen, zullen de binnenste delen minder beschut zijn tegen golfaanval. Op deze manier houdt de erosie zichzelf in stand.

Deze gehele studie naar de geschiedenis en toekomst van de Oosterschelde geeft een beeld van een bassin dat sterk door menselijke ingrepen is veranderd. Het zal naar verwachting nog enkele eeuwen duren voordat de morfologische effecten van deze ingrepen zijn uitgewerkt.

TABLE OF CONTENTS

Chapter 1

INTRODUCTION

In the south-western part of the Netherlands, the system of estuaries, tidal basins and islands, known as the Delta in Dutch terminology (Figure 1.1), has been shaped and studied by humans for centuries. By far the largest event that determined its current configuration was the storm surge that occurred in 1953. This giant flooding gave rise to one of the largest engineering programs in the world: the Delta Plan. The aim of this plan was to ensure safety against flooding, while at the same time allow for other utilisations of the Delta. This system of dams, barriers and sluices has had, and is still having a strong effect on the morphology of the Delta basins and coast.

Tidal basins like these often act as effective sediment traps but can also release large quantities of sediment (e.g. Elias, 2006). Therefore, they play an important role in the sediment budget of the coastal system and thus influence the long-term evolution of the coastal zone. Besides their role in the sediment exchange between land and sea, estuaries and tidal basins attract a large array of human activities such as navigation, industry, fishing, mining, and recreation. Because of their location on the interface between salt and fresh water, these systems also accommodate some of the most valuable ecosystems in the world. Apart from the economic and ecologic value, the population living around the estuary also desires safety against flooding. All these different kinds of utilisation and interests make that sound management of these zones is crucial.

The use and management of these areas are often restricted by national and international law and regulation. They are further complicated by the fact that these systems are characterized by complicated interactions between water motion, sediment exchange, and biological activity. In the Netherlands processes such as sea-level rise, land subsidence, and the fact that one third of the country is located below sea level add to the complexity as well as the urgency. To aid in these management issues, it is important to have a good understanding of the morphological behaviour in the past, present and future. This behaviour has changed in response to the Delta Plan. Therefore, the objective of this thesis is to gain understanding of the mechanisms that govern the exchange of sediment between these basins, in particular the Eastern Scheldt, and the coast that connects them, and the effects of human interventions on these mechanisms.

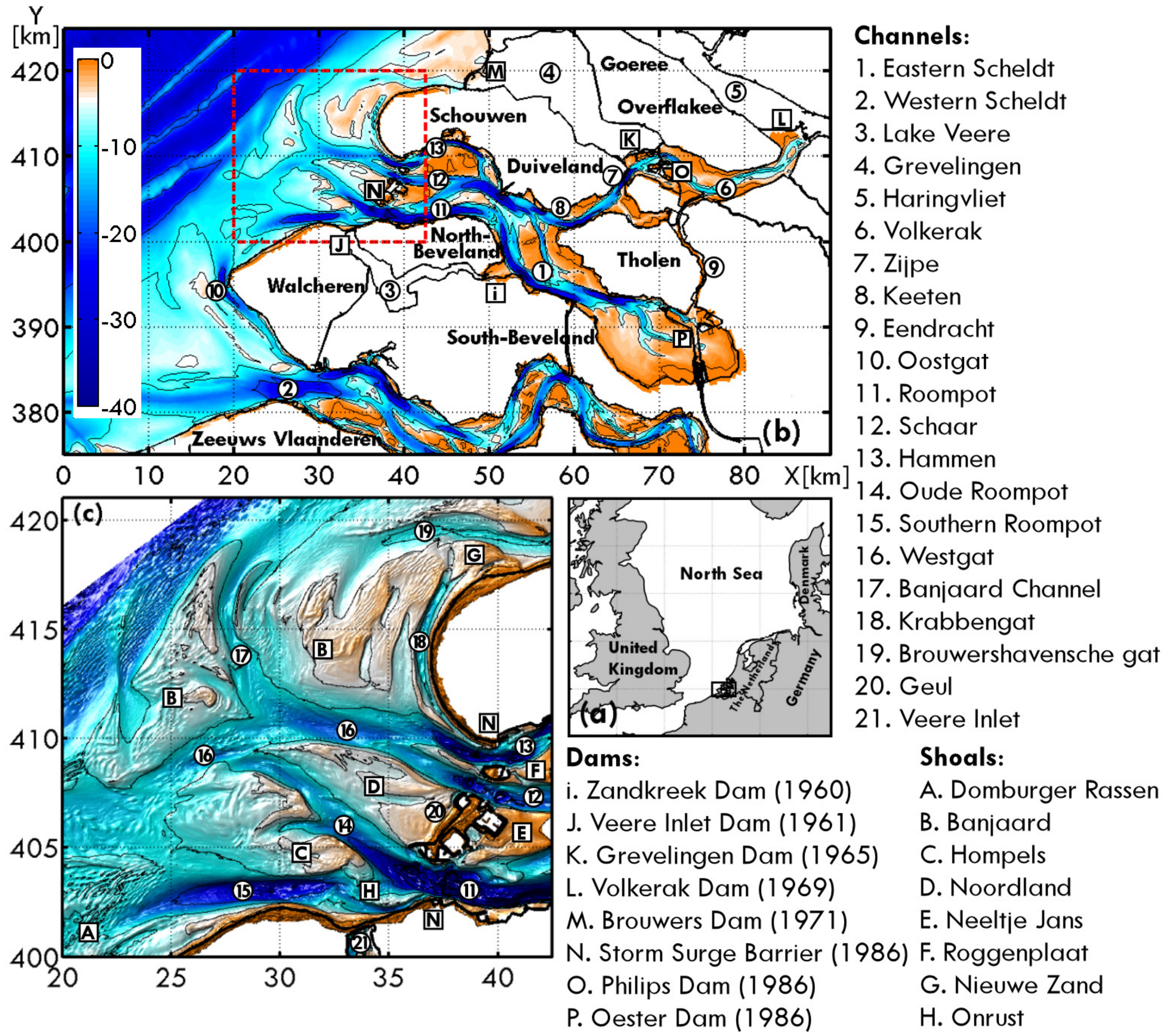

Figure 1.1: Overview of the Dutch Delta and the Eastern Scheldt ebb-tidal delta in 2008.

1.1 The Eastern Scheldt tidal inlet

In the night of January 31st 1953 a severe north-western storm caused a storm surge along the Delta Coast of 3 meters above mean sea level which lasted for almost two days. This surge, combined with a springtide, caused local water levels of more than 4 meters above mean sea level (Rijkswaterstaat, 1961). The levees in the Dutch Delta were not designed to counter a surge of this magnitude, and many failed after overtopping water eroded the inner slopes. The inundations that followed killed 1835 people, drowned approximately 30.000 pieces of livestock, caused the evacuation of some 30.000 people, damaged or destroyed approximately 50.000 buildings, and left 1700 km^2 flooded.

In response to this catastrophe, within a decade a plan was drawn to increase the level of safety of the Delta. This plan, known as the “Delta Plan”, consisted of the construction of a series of dams to close off all the Delta branches except for the

Western Scheldt and the Nieuwe Waterweg. This choice of effectively shortening the coastline was preferred because it was much cheaper than strengthening all the estuarine levees, and apparently also easier to realise. The two northernmost inlets (Grevelingen and Haringvliet) were closed off from the sea with dams during the nineteen sixties. The Western Scheldt and Nieuwe Waterweg were not to be closed due to their function as entrances to the harbours of Antwerp and Rotterdam, respectively.

In the nineteen seventies a public and political discussion erupted about whether the Eastern Scheldt estuary should be completely closed off. Opposition to the original plan grew due to the Eastern Scheldt's importance to local wildlife and fishery. The choice was made to alter the plan: The Eastern Scheldt was to retain as much of its tidal influence as possible while at the same time still be safe from storm surges. This would be accomplished by means of a permeable barrier on the location of the originally planned dam. This storm surge barrier would allow the tide to pass through the inlet under normal weather conditions, but would close during storm surges. Aside from the storm surge barrier, two compartmentalisation dams were to be built in the landward part of the basin in order to retain as much of the original tidal range as possible. This new plan was executed during the nineteen seventies and eighties, and was finalised in 1986.

Morphological effects of the Delta Plan on the basins and the coast became apparent quite quickly (e.g. Haring, 1978; Van den Berg, 1986; Ten Brinke, 1993; Louters *et al.,* 1998). That these effects would occur had been predicted (e.g. De Vriend *et al.*, 1989), although the exact amplitude and timescale of these effects proved harder to predict. The dams in the Grevelingen and Haringvliet inlets caused the sediment of these ebb-tidal deltas to be reworked shoreward by wave action, thereby silting up the old channels. Since the construction of the storm surge barrier, the tidal flats inside the Eastern Scheldt basin have been deteriorating in height, area, and volume. This is because the barrier caused a decrease in tidal current. Tidal currents inside a basin transport sediment towards the tidal flats and build them up, while wind waves break them down. Although the currents have decreased, the waves inside the Eastern Scheldt have hardly decreased in strength since the construction of the storm surge barrier. As a result, the tidal flats are eroding. The decrease in tidal currents also means that the channels are too large with respect to the currents running through them, and so these channels act as sediment traps for the sediment eroded from the tidal flats.

This process of deteriorating shoals and accreting channels is commonly known as the 'sediment hunger'. In geological terms this is coined as positive accommodation space. The sediment demand would be less of a problem if the basin and the ebb-tidal delta could exchange sediment like they would normally be able to do. In that case the deficit of sediment inside the basin would be replenished from the surplus of sediment on the ebb-tidal delta. However, from studying the basin's sediment budget it appears as if the basin has not been receiving any significant quantities of sediment from outside. From this observation it is assumed that the storm surge barrier is also acting as a barrier for sediment transport into the basin (Ten Brinke, 1993). It is not understood well why the barrier causes this sediment blockage. It is estimated that the channels require approximately 400 million m^3 of sediment to regain equilibrium

(Kohsiek *et al.,* 1987). The tidal flats can only offer around 150 million m^3, and apparently no sediment is entering the basin from the sea. This would mean that on the long term the tidal flats in the Eastern Scheldt would be lost if no measures were taken. This disappearance would be detrimental for many biological species, e.g. the aquatic birds feeding on these tidal flats.

Compared to the basin, the ebb-tidal delta of the Eastern Scheldt has received less scientific attention, even though its history and the presence of the storm surge barrier make this a unique opportunity for studying ebb-tidal delta morphology under the influence of human intervention. It is also unclear what effect the storm surge barrier exactly has on the ebb-tidal delta. After the construction of the storm surge barrier the morphological trends on the Eastern Scheldt's ebb-tidal delta have not been as clear as on other deltas.

The barrier drastically changed the flow patterns around the inlet and creates large amounts of local turbulence. The sediment blockage also means the ebb-tidal delta is not losing sediment towards the basin. This combination of effects has created a unique situation. Therefore, it remains to be determined what the overall long-term trends of the ebb-tidal delta's shape and sediment budget really are. This knowledge on the behaviour of the Eastern Scheldt's ebb-tidal delta is crucial if the ebb-tidal delta is to be involved in finding and evaluating solutions to the problems in the Eastern Scheldt.

1.2 RESEARCH QUESTIONS

The main research question addressed in this thesis is:

What are the effects of the Delta Plan on the Eastern Scheldt tidal inlet?

Answering the main question is done by answering several key questions, each with its own subquestions:

- **Key question 1: What was the state of the Eastern Scheldt before the Delta Plan was implemented?**
  - What were the morphological effects of the land reclamations and inundations around the Eastern Scheldt in the previous centuries up until 1960?
  - Is it possible to identify a 'natural' or 'equilibrium' state of the Eastern Scheldt in its history?
- **Key question 2: What was the state of the Eastern Scheldt by the time the storm surge barrier was constructed?**
  - What were the effects on the Eastern Scheldt of the first phase of the Delta Plan, viz. the closure of the Grevelingen and Volkerak?
- **Key question 3: What were the short-term hydrodynamic and morphological effects of the storm surge barrier on the ebb-tidal delta?**
  - What changes in hydrodynamics can be observed on the ebb-tidal delta?

   - What morphological effects can be discerned, and what are their trends?
- **Key question 4: What are the possible long-term effects of the storm surge barrier?**
   - Towards what kind of long-term state will the ebb-tidal delta evolve?
   - On what time scale does this adaptation take place?

1.3 RESEARCH APPROACH

De Vriend (1991; 1996) distinguishes two types of approaches in coastal research: a behaviour orientated approach and a process-based approach. Both these approaches have their advantages and shortcomings. A behaviour orientated approach uses a downscaling approach by analysing large-scale observations in order to derive trends or empirical relationships, which makes this method suitable for predicting long-term large-scale behaviour. However, its major shortcoming lies in the lack of comprehensive descriptions of the physics that underlie the observed dynamics, making these models unable to describe small-scale processes in detail.

Process-based models, on the other hand, use an upscaling approach; micro-scale processes such as water motion and sediment transport are simulated by applying a series of coupled equations describing the conservation of mass and momentum of water, and the conservation and transport of sediment or other constituents. The major advantage of process-based models is their ability to give detailed information on flow patterns and sediment transports on small spatial and temporal scales. However, their ability to accurately model long-term macro- and mega-scale morphological behaviour is limited.

In the research on the morphodynamics of Texel inlet, Elias (2006) successfully used a 'mixed' approach as suggested in De Vriend (1991), in which behaviour oriented modelling and process-based modelling are combined and integrated. The same approach is used in this thesis in order to give answers to the research questions formulated in the previous section. Analysis of bathymetric and hydraulic data is combined with process-based numerical modelling in order to form conceptual models of the different stages of ebb-tidal delta development. As part of this research a dedicated numerical model of the Delta as a whole and the Eastern Scheldt in particular is made.

This study is performed as part of a case study within the larger Building with Nature program, which also provided funding. The Building with Nature program is an innovation program aimed at designing new techniques for dealing with coastal management problems. These new techniques incorporate and make use of natural processes as much as possible. One of the case studies within Building with Nature, called the South-Western Delta case study, aims at applying the Building with Nature philosophy in order to find solutions for the problems within and around the Eastern Scheldt.

1.4 THESIS OUTLINE

The structure of this thesis will be largely chronological with the events shaping the Eastern Scheldt inlet (Figure 1.2). Chapter 2 describes the historical morphological development of the Eastern Scheldt until 1960, before any parts of the Delta Plan were implemented. Chapter 3 describes the morphological evolution of the ebb-tidal delta between 1960 and 1983. This is the period in which the Eastern Scheldt experienced the effects of the first phase of the Delta Plan, which ended around 1983 when construction on the storm surge barrier begun. Chapter 4 picks up where chapter 3 left off, and describes the evolution between 1983 and the present day. This period is characterized by the initial effects of the storm surge barrier. Chapter 5 offers an outlook on how the ebb-tidal delta might behave in coming decades. The knowledge and lessons learned from all these different periods are summarized in the conclusions in chapter 6. This chapter also gives recommendations on coastal maintenance strategies for the Eastern Scheldt system, possible further research, and integration of the findings of this study into the Building with Nature framework.

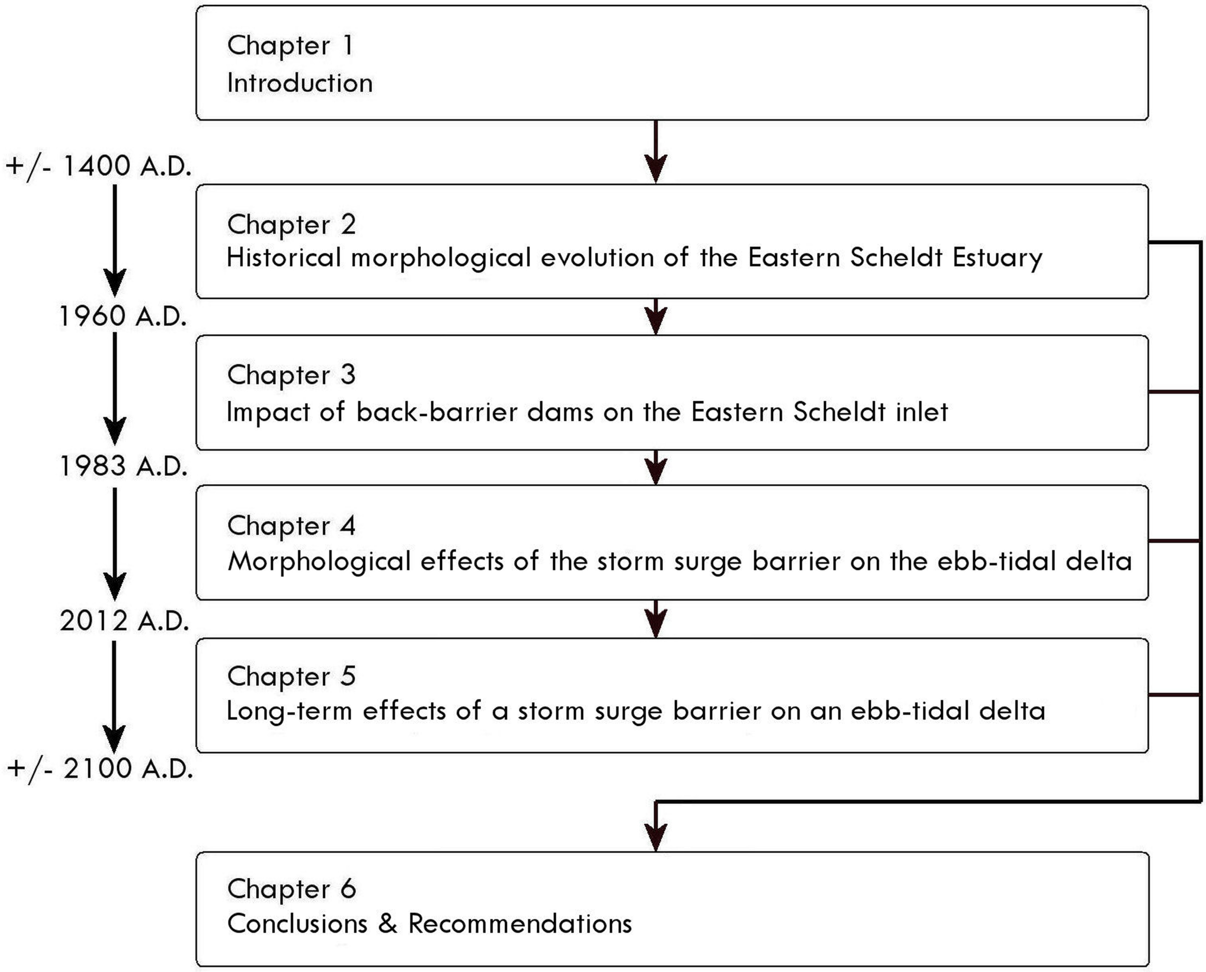

Figure 1.2: Overview of thesis outline

Chapter 2

HISTORICAL MORPHOLOGICAL EVOLUTION OF THE EASTERN SCHELDT ESTUARY

2.1 INTRODUCTION

The Eastern Scheldt estuary and ebb-tidal delta have seen large changes in both shape and size throughout their lifetime. Especially the configuration of the estuary has been changed dramatically by human influence as well as extreme events. These changes have not only had their impact on the system of flats and channels within the estuary, but also on its neighbouring estuaries and the ebb-tidal delta.

The objective of this chapter is to describe the evolution of the Eastern Scheldt estuary in the centuries leading up to 1960. A better understanding of the historical evolution of this estuary will give more insight into the present-day situation. Section 2.2 gives a short general overview on tidal inlet processes. In section 2.3 an analysis is made of historical observations and data regarding bathymetry, land reclamations and inundations. This analysis is used to formulate hypotheses on possible links between different developments inside the estuary. In sections 2.4 and 2.5 these hypotheses are tested using a two-dimensional numerical flow model (Delft3D) of the Eastern Scheldt with a simplified geometry. The knowledge from the observations and the model study are combined and integrated in the conclusions in section 2.6.

2.2 TIDAL INLETS

Tidal inlets are openings along barrier coastlines connecting the sea to estuaries and tidal basins, which are maintained by tidal currents (Escoffier, 1940; Fitzgerald *et al.*, 2002). A tidal inlet system is usually subdivided in a back-barrier basin, an inlet gorge, an ebb-tidal delta and the adjacent coast. The geometry of the basin and the tidal range determine the tidal prism, which is the total amount of water flowing through the inlet per tidal cycle. This tidal prism in turn determines the size of the inlet cross-section (O'Brien, 1969), the channel volume inside the basin (Eysink, 1990), and the sediment volume of the ebb-tidal delta (Walton and Adams, 1976).

The geometry of the ebb-tidal delta is dependent, among other factors, on the ratio between wave and tidal energy (e.g. Oertel, 1975; Hayes, 1979). Wave energy tends to push sediment towards the coast, while tidal motion tends to push the ebb-tidal offshore. In case of significant littoral drift, there are several ways in which the sediment can bypass the tidal inlet from the updrift to the downdrift barrier island (Fitzgerald *et al.*, 2000). At smaller inlets, the sediment usually bypasses by means of migrating shoals and channels, while at larger inlets the main channels remain in position, and simply deposit sediment on their downdrift sides. The type of bypassing, as well as the overall stability of the inlet, is determined by the ratio between the littoral drift and the tidal prism (Bruun and Gerritsen, 1959).

In the Netherlands, most inlets are either tide-dominated or mixed-energy inlets which tend to be stable in their location. Most ebb-tidal deltas of this type of inlet share common characteristics in their bathymetries (Hayes, 1980). These include (Figure 2.1a):

- A main ebb channel in the central part of the inlet,
- Marginal flood channels running close to the shoreline,
- Channel margin linear bars between the ebb and flood channels,
- A terminal lobe located at the seaward end of the main ebb-channel,
- Swash platforms, which are large shoals dominated by wave action.

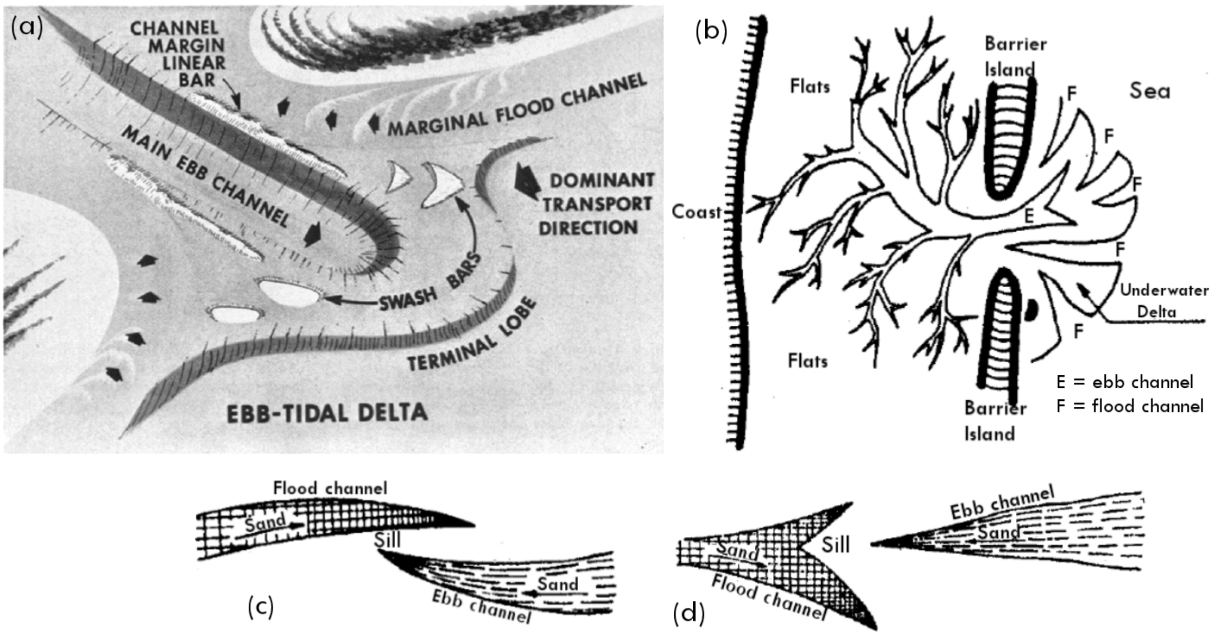

Figure 2.1: (a) Conceptual inlet model by Hayes (1980). (b) Sketch by Van Veen *et al.*, (2005) of a typical submarine delta along the Dutch Coast. (c) and (d) Sketches of mutually evading flood- and ebb-channels (Van Veen *et al.*, 2005).

In the case of most Dutch tidal inlets, the general direction of the main channels is a function of the strength and phase of the tide coming out of the inlet relative to the tide propagating along the Dutch coast (Sha and Van den Berg, 1993). The ebb and flood channels are usually not directly connected, but rather move around each other, separated by sub-tidal sills (Van Veen *et al.,* 2005) (Figure 2.1c&d).

Human intervention or other large scale disturbances in and around tidal inlet systems can have far reaching consequences on the behaviour of tidal inlets and the basins and coasts which they connect (Stive and Wang, 2003). Depending on the magnitude of the disturbance, the state of a tidal inlet system can be brought far out of morphological equilibrium. The system will typically evolve back towards a new equilibrium state by redistributing sediment between its elements. The time required for the sediment surpluses and deficits to level out depends on the size of the elements, how strongly each of these elements is disturbed, and how strong these elements are interacting with each other (Kragtwijk *et al.*, 2004).

The net sediment transports through a tidal channel are usually a result of asymmetries in the tidal current. Due to the fact that the crest of the tidal wave can propagate at a different speed from the through, the shape of the tidal wave becomes distorted, leading to differences in the duration of ebb and flood (Speer and Aubrey, 1985). Because both phases generally have to transport an equal amount of water, this distortion leads to differences between the average ebb and flood currents. Because the sediment transport is proportional to a third or higher power of the current velocity, this asymmetry leads to net transport in ebb- or flood direction, depending on the type of asymmetry (Van de Kreeke and Robaczewska, 1993). The phase speed is proportional to the square root of the average water depth, so at sea the crest of the tidal wave will propagate faster than the through, leading to flood-asymmetry and flood-directed sediment transports. In estuaries, however, the presence of intertidal area can sometimes lead to a geometry in which the high tide propagates slower than low tide, giving rise to ebb-asymmetry and ebb-directed transports (Friedrichs and Aubrey, 1988).

2.3 GEOLOGICAL EVOLUTION

2.3.1 General geological evolution of the Dutch coast

Up until the twentieth century the shape of the Dutch coast was mostly the result of processes that have been going on since the last ice age (e.g. Zagwijn, 1986; Van den Berg, 1986; Van der Spek, 1994; Cleveringa, 2000). Since the end of this ice age (±10.000 BP), the relative sea level rose at an average rate of 1 m per century due to melting ice covers, thermal expansion, post-glacial rebound, and land subsidence. Around 8000 BP the North Sea obtained its present-day configuration (Beets and Van der Spek, 2000). Further rise in sea level caused the coastal dune barrier to be driven eastward, and caused old river valleys and other low-lying areas to be inundated (Figure 2.2a). The supply of sediment was still too low to keep up with the rapid sea level rise, resulting in the overall transgression of the Dutch coast.

This situation changed around 6000 BP for the central Netherland coast. A decrease in the rate of sea level rise meant the sediment supply could keep up with the rise, resulting in a period of coastal progradation (Beets *et al.,* 1992). The lagoons along the Belgian and Holland coast started to fill in with sediment, and by 3300 BP the coast of the Netherlands consisted of a more or less continuous dune barrier coastline stretching from the Belgian coast to what is now Texel island (Figure 2.2b&c). This coastline was interrupted only by the mouths of the Rhine, Meuse and Scheldt rivers. The area behind these dune barriers consisted of large peat bogs and lakes which were former lagoons cut off from the sea (Beets and Van der Spek, 2000). North of this Holland coast, the prevailing hydrodynamic conditions caused that the sediment supply was still insufficient to fill up the estuaries. This caused this part of the coast to turn into a slowly receding barrier island coast with the shallow Wadden sea basin behind it.

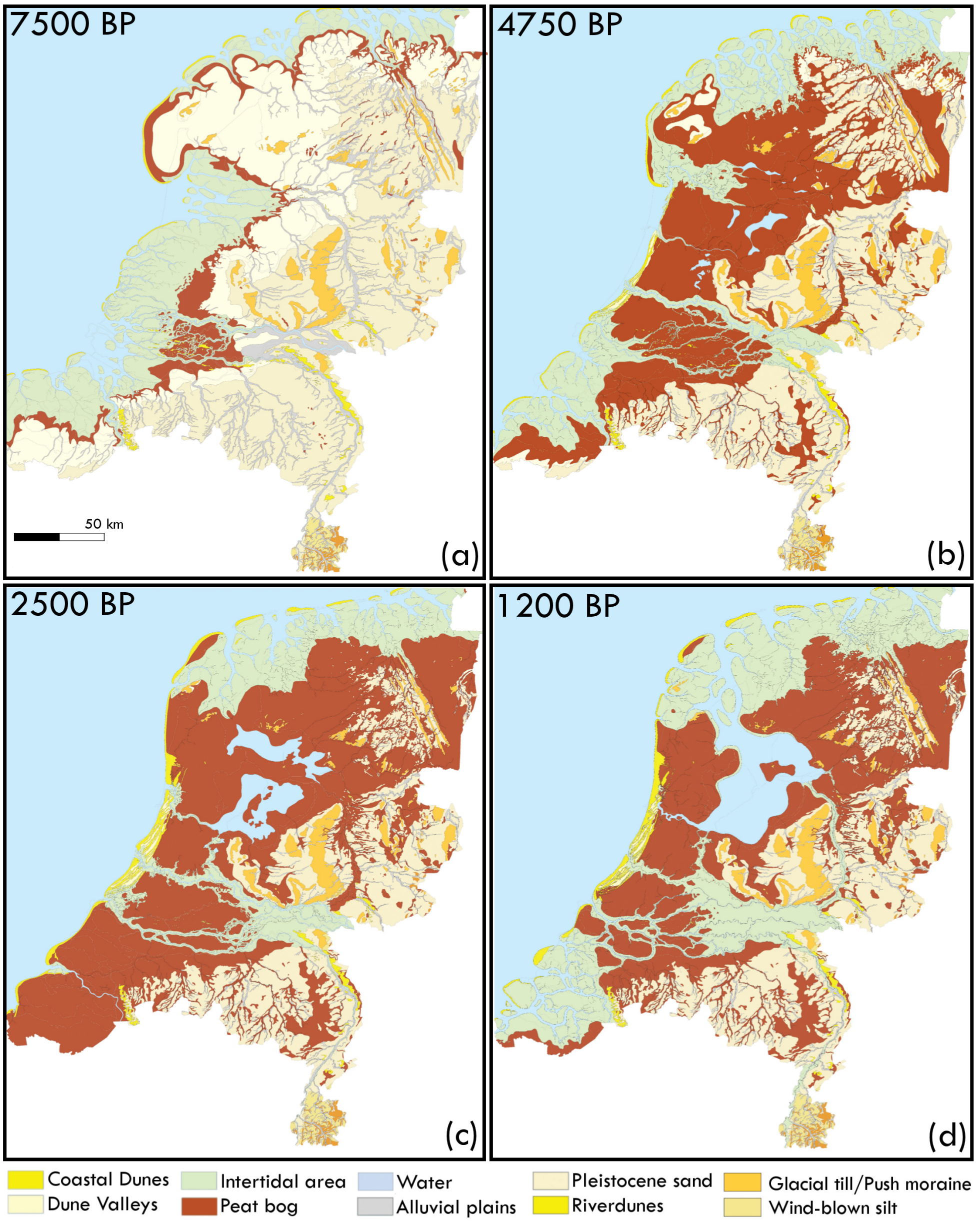

Figure 2.2: Geological evolution of the Netherlands between 7500 BP and 1200 BP (from Vos *et al.*, 2011).

2.3.2 Geological evolution of the Delta coast

Before 6000 BP, Zeeland consisted of a tidal landscape with tidal flats, channels, and lagoons, rimmed with peat bogs (Figure 2.3a). This landscape was the result of the sea invading the Scheldt River valley system due to the rapid sea-level rise. During this age, the path of the Scheldt River was oriented more northward than in the present day, and flowed into sea roughly at the location of the modern day Haringvliet. The tidal basin currently known as the Eastern Scheldt became connected to the Scheldt River around 6000 BP (Figure 2.3b) and remained its main mouth until the Western Scheldt basin also became connected during the Middle Ages.

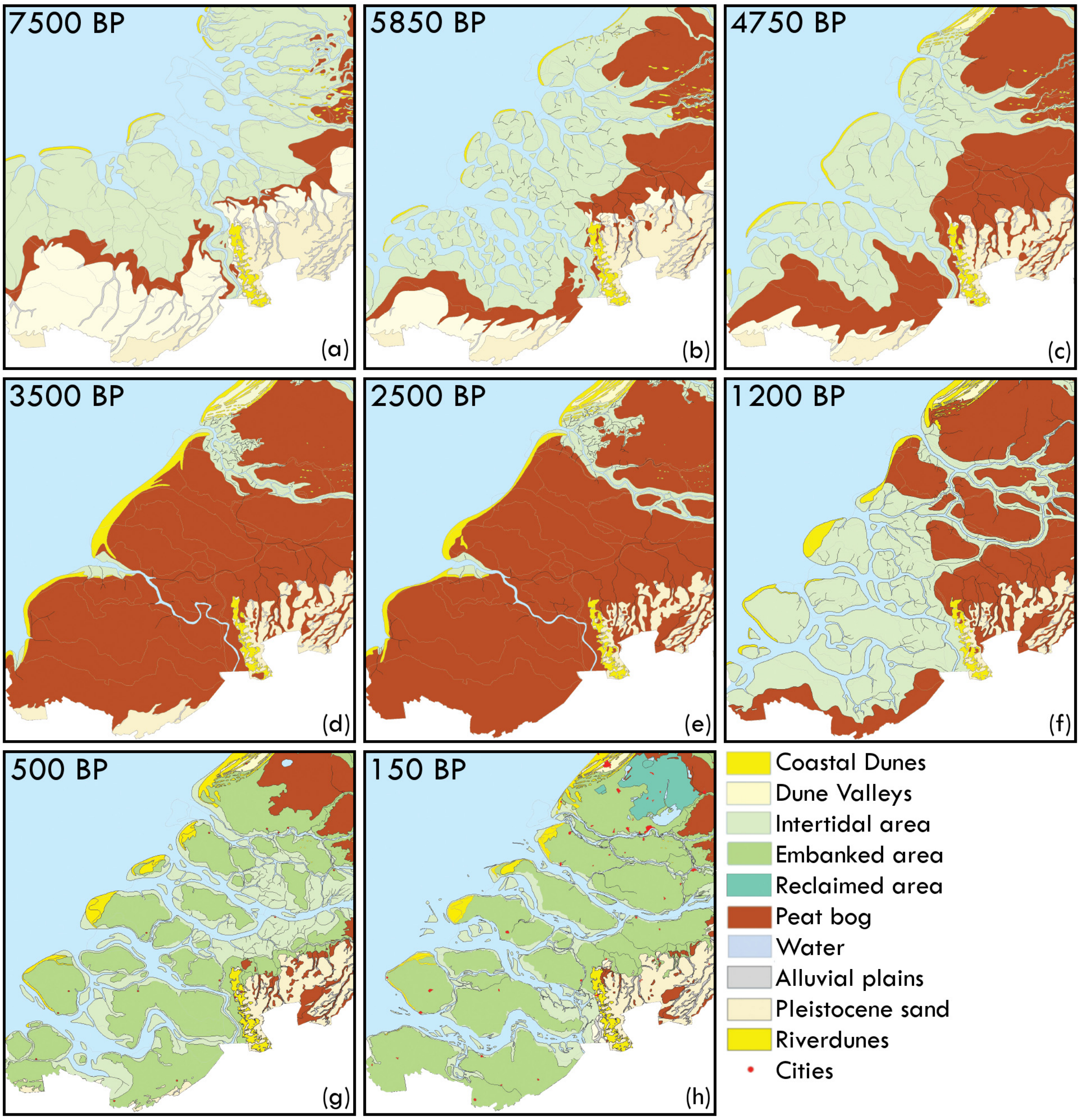

Figure 2.3: Geological evolution of the Dutch delta from 7500 BP to 150 BP (from Vos *et al.*, 2011).

The coastal plain in the Zeeland area silted up between 5000 and 4500 BP, and the barrier stabilized (Beets and Van der Spek, 2000). This was due to a deceleration of the sea-level rise in combination with abundant sediment availability coming from the eroding headlands of Walcheren and Flanders (Vos and Van Heeringen, 1997). The remaining tidal inlets closed, and the area behind the dune barrier turned into an extensive peat marsh (Figure 2.3d&e). This situation lasted until roughly 2000 BP.

From Roman times onwards, the sea-level rise and subsequent changes in estuarine conditions along the Scheldt caused the peat cushions to collapse. This process was enhanced by local inhabitants digging ditches, which caused subsidence of the peat (Vos and Van Heeringen, 1997). This development created large amounts of potential tidal prism. As a result, breaches of the coastal barrier and newly formed tidal channels washed most of the peat away, and turned this area into a system of wide estuaries with channels, mud flats, and salt marshes (Figure 2.3f). Between 2000 and 1000 BP most of the areas between the main channels silted up to high-tide level. During the same period humans began to embank these areas.

In the same period, a new inlet began to develop south of the Eastern Scheldt. This new inlet grew rapidly throughout the centuries. It eventually connected to the Scheldt River during the middle ages, when it became known as the Western Scheldt (Van der Spek, 1997). Due to this connection and subsequent scouring of the Western Scheldt, the Eastern Scheldt gradually lost most of its river influence. By the 14th century, the Western Scheldt became the primary shipping route to the city of Antwerp. The Eastern Scheldt was still connected to the Western Scheldt through two shallow tidal watersheds called Sloe (between Walcheren and South-Beveland) and Kreekrak (between South-Beveland and the mainland). These watersheds were gradually closed off by land reclamations in the following centuries. To the north the Eastern Scheldt was connected to the Grevelingen estuary through a shallow watershed known as the Zijpe.

2.3.3 Land reclamations and inundations

References to inhabitation of the islands around the Eastern Scheldt date back as far as Roman times. Local inhabitants have made a continuous effort to build embankments and reclaim the salt marshes and mudflats surrounding the islands (Figure 2.4). By 1500 AD most of the flats around Tholen and Duiveland had been reclaimed (Wilderom, 1964). The improved artificial drainage of the former marshlands and mudflats caused further subsidence of the land.

Land reclamation efforts were not always successful. During the 15th century, the southern shore of Schouwen island began to erode under the attack of the newly-formed Hammen channel. This erosion continued until the end of the 16th century (Beekman, 2007). Also the northern edge of North-Beveland experienced similar erosion (Wilderom, 1961). Several polders on the northern side of this island had to be abandoned over the centuries.

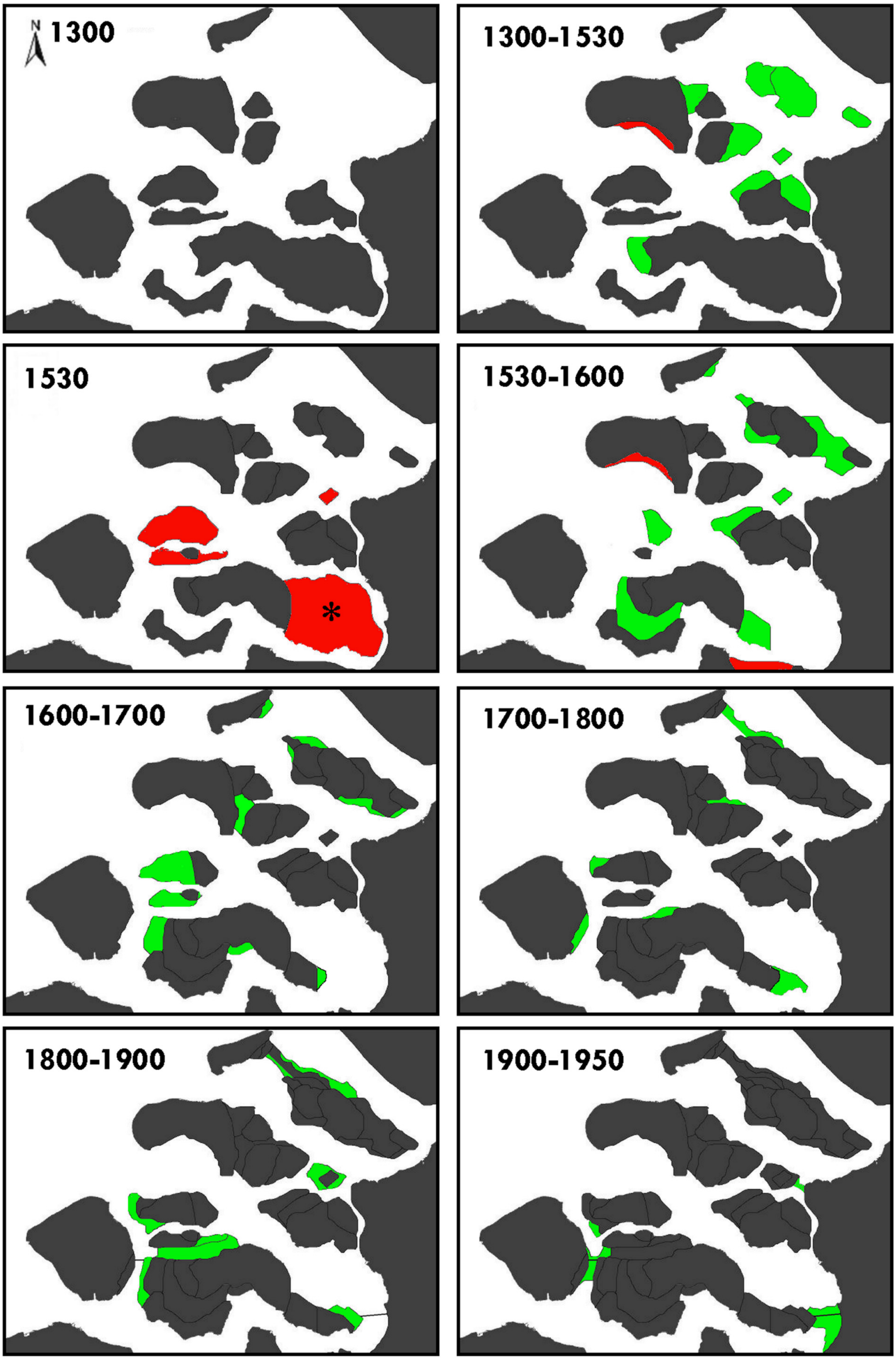

Figure 2.4: Land reclamations (green) and inundations (red) in the Dutch delta. The asterisk denotes the drowned land of South-Beveland.

In 1530 and 1532 AD two large storm surges, the St. Felix flood and the All-Saints flood, inundated almost 200 km^2 of agricultural land. Most of this area, around 150 km^2, consisted of the eastern part of South-Beveland, in the south-eastern part of the estuary. Along with this, North-Beveland and parts of Tholen became flooded. Over the course of the next 100 years most inundated parts of North-Beveland and Tholen were reclaimed again. However, a large part of South-Beveland ($\pm$ 95 km^2) remained inundated (Van den Berg, 1986).

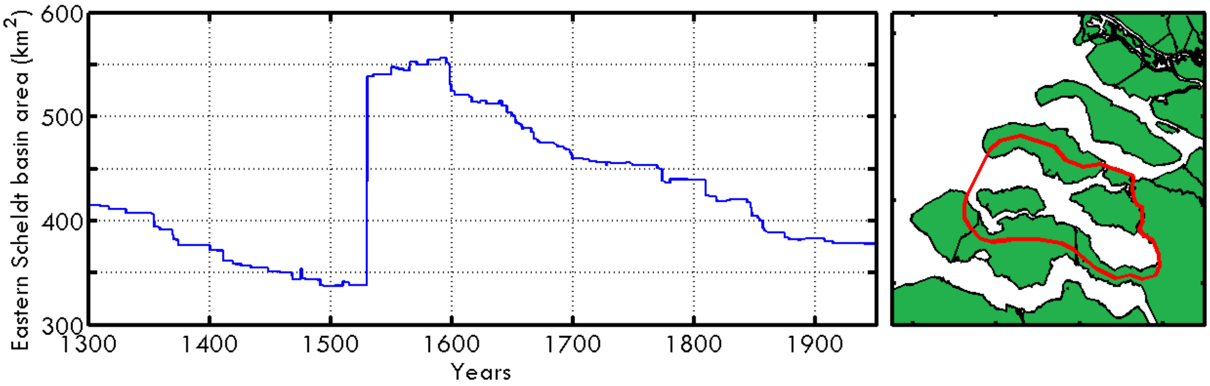

Figure 2.5: Basin area within the red polygon.

These reclamations and inundations must have had an effect on the morphology of the estuaries between the islands. The shape and total area of an estuary are important parameters which have large influence on the tidal prism, the amplification of the tide, and the availability of sediment. From the data on lost and reclaimed land around the Eastern Scheldt, the evolution of the basin area over time can be derived. This is done by taking the basin area from the present day, and then calculating backward in time by either subtracting reclaimed area or adding inundated area.

The evolution of the basin area calculated in this way is shown in Figure 2.5. The red polygon shown in the same figure indicates the area and polders considered for this calculation. This calculation is performed under the assumption that the tidal influence of the Eastern Scheldt is limited to this polygon.

Figure 2.5 shows that during the 17th century (the Dutch "Golden Age"), the number of reclamations per period of time reached its highest value. Approximately 60 km^2 of basin area was reclaimed around the Eastern Scheldt alone. However, most of this activity was merely reclaiming some of the land that was lost in the floods of 1530 and 1532. In the 19th centuries the rate at which new polders were built was lower than in the previous centuries. However, the polders themselves became much larger, so the gain in reclaimed area remained roughly as high as during the 17th century. By 1900, the basin area had stabilised.

2.3.4 Morphological evolution inside the estuary

At the beginning of the 16th century, the width of the Eastern Scheldt at its mouth was roughly as large as it is in the present day. The width tapered off towards the estuary's eastern connection with the Scheldt River (Wilderom, 1968). It was connected to neighbouring estuaries through several shallow tidal channels. The connections to the Scheldt River, called Sloe and Kreekrak, silted up after the Western Scheldt became connected to the river. Eventually both connections were closed off with dams during the 19th century.

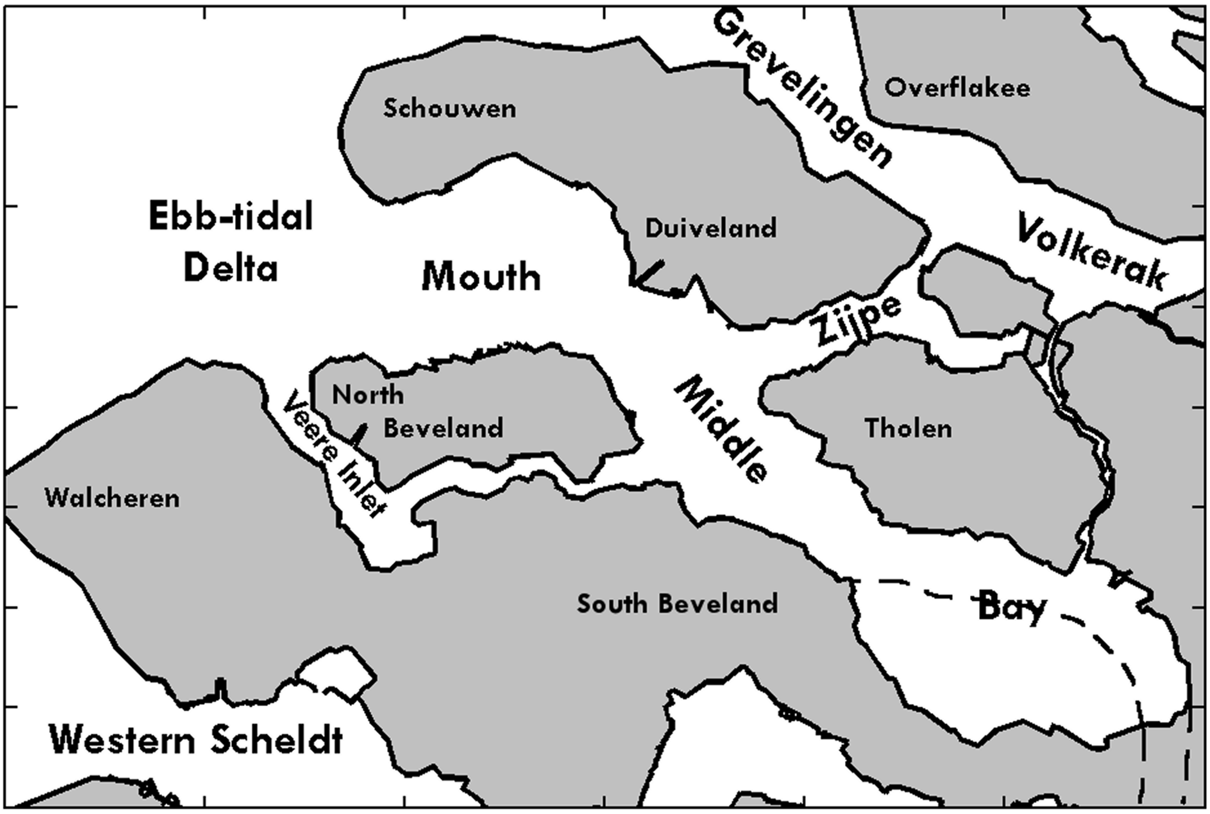

Figure 2.6: Overview of the names used in this chapter for different parts of the Eastern Scheldt. The dotted line shows the approximate location of the pre-1530 embankment of South-Beveland.

After the two cataclysmic floods in the years 1530 and 1532, the morphology began to change. The large addition of intertidal area must have resulted in a large increase in tidal prism. The cross-sectional area of tidal channels is proportional to this tidal prism (O'Brien, 1969). As a result of this relation, the main channels throughout the estuary began to scour in response to the inundation (Table 2.1), and the estuary must have started to export sediment out to sea (Beekman, 2007). This is especially visible in the mouth area, where the shores of Schouwen and North-Beveland began to erode under the strain of the expanding Hammen and Roompot channels close to the shore. Another effect of the increase in tidal flow velocities was sedimentation on the flats and banks.

Table 2.1: Depths in meters of the main inlet channels derived from historic charts (Beekman, 2007).

Year of chart	1600	1623	1774	1800	1827	1872	1910	1920	1950
Roompot	9	13	9	15	27	26	24	18	24
Hammen	11	19	11	14	23	29	36	36	32
Westgat	-	-	-	24	28	23	24	18	19

The export of sediment since the inundation of South-Beveland can also be explained from a tidal hydrodynamic point of view. The addition of large intertidal areas in the back end of the estuary must also have had an effect on the shape of the tidal wave (Friedrichs and Aubrey, 1988). In general, more intertidal area means that the celerity of the high water phase of the tide is retarded more relative to the celerity of the low water phase. This can be observed as an ebb phase that lasts shorter than the flood. As a consequence of this asymmetry, the average flow velocities during ebb are higher than during flood. Because sediment transport is a non-linear function of this flow velocity, more sediment is exported during the ebb phase than is imported during the flood phase. The same effect is observed when channels inside an estuary become deeper.

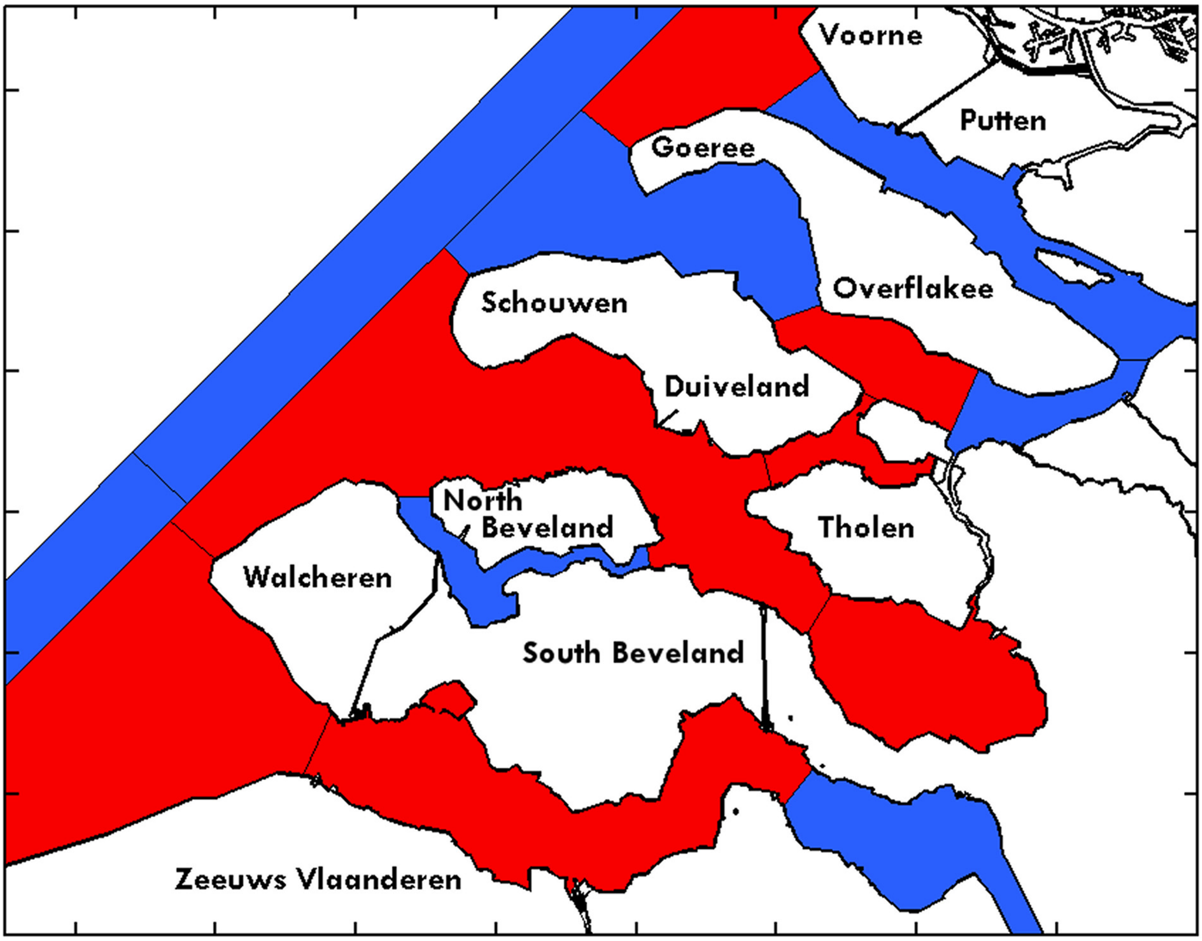

Figure 2.7: Sediment budget between 1872 and 1952 (red=erosion, blue=accretion). Adapted from Haring, 1955.

Haring (1978) made an extensive study of the sediment budget of the Delta estuaries in the 19th and first half of the 20th century (Figure 2.7). Although the bathymetrical measurements used for this study were less accurate than modern day measurements, some trends still stand out. According to the study, the Eastern Scheldt estuary exported approximately 280 Mm^3 of sediment in the period between 1872 and 1950. This means that during this period the estuary was still exporting sediment at an average rate of 3.5 Mm^3 per year. Apparently, the Eastern Scheldt's sediment budget was still adapting at this time. This amount of sediment cannot be accounted for in the ebb-tidal delta (Haring, 1978). Therefore, some of the export might have been through the Zijpe channel towards the Grevelingen estuary and Volkerak channel.

The possible effects of the land reclamations that were carried out between 1530 and 1950 were that the increase in tidal prism from the inundation might have been reduced. Aside from this, reduction of the intertidal storage volume might have also reduced the ebb asymmetry of the tide, according to the theory of Friedrichs and Aubrey (1988). However, even by the end of the 19^{th} century, the basin area was still greater than what it used to be before South-Beveland was inundated.

The inundated part of the bay area (Figure 2.6), also known as the drowned land of South-Beveland, must have experienced relatively little erosion during the last 400 years. The average bed level around 1950 AD was only 80 cm below mean sea level (Wilderom, 1968). This is also the elevation at which foundations of old buildings are found which were lost in the inundation. When a constant sea level rise of 20 cm per century is taken into account, the 1950 bed-level must have been around the mean sea level which existed at the beginning of the 16^{th} century.

According to Haring (1953), an average erosion of 30 cm was measured in the entire bay area between 1872 and 1951. Since it is known that the 1950 average bed level is probably more or less the same as the 1530 bed level, the observation of erosion between 1872 and 1950 means that this area must have experienced some accretion since the floods of 1530 and 1532. Another observation from the present-day situation is that most of the channels in the bay are relatively narrow, but also reach depths of 20 m (Figure 2.8).

The evolution of the drowned land of South-Beveland could be related to the clay layer that lies underneath most of this former polder. This clay layer starts at roughly 1 m below present-day mean sea level, and has a thickness varying between 3 and 7 m. The soil underneath this clay layer consists of sand (www.dinoloket.nl). It is possible that this layer has kept the amount of erosion in this area limited. It could also explain the narrow, yet deep channels through this area. Hypothetically, once a channel has cut through the clay layer, the sand underneath it is more easily erodible. The growing channel will go for the path of least resistance, and will thus grow deep instead of wide.

Before the 18^{th} century, the connection between the Eastern Scheldt and the Grevelingen estuary to the north consisted of a channel known as the Zijpe. Historians have reported that in the 16^{th} century people could cross this channel on foot at low tide (Wilderom, 1964), so apparently there existed a tidal watershed in this channel. However, at the beginning of the 18^{th} century this tidal watershed began to scour, and by the end of the century the Zijpe had reached a depth of more than 20 meters.

A tidal watershed can be defined morphologically as a continuous shallow area separating two tidal basins (Vroom, 2011). It can also be defined in a hydraulic way as the point between two basins with the smallest standard deviation of the flow velocity. The location of this hydraulic watershed depends on the tidal phases and amplitudes on both sides of the watershed. After a large-scale disturbance in an estuary, such as an inundation, these tidal phases and amplitudes can change. Consequently, the location of the hydraulic tidal watershed will move, after which the morphological watershed will erode and move towards the new location of the hydraulic watershed.

Van den Berg (1986) explains the disappearance of the tidal watershed in the Zijpe area by looking at the effects of the inundation of South-Beveland. Because of the subsequent deepening of the Eastern Scheldt estuary, the celerity of the tidal wave through this estuary began to increase. This would mean the tidal wave also reached the tidal watershed sooner than before. However, the location of a tidal watershed depends on the phases as well as the amplitudes of the tidal waves on both sides of the watershed (Vroom, 2011). If the phase of the vertical tide at one side of the watershed decreases, the watershed will be pushed in the other direction. According to the same study, the tidal watershed will be located towards the side with the largest tidal range. This means that there are multiple possible explanations for the migration of the watershed. The migration occurred either because the tidal phase at the Eastern Scheldt side decreased, or because the tidal amplitude decreased, or due to a combination of these two causes.

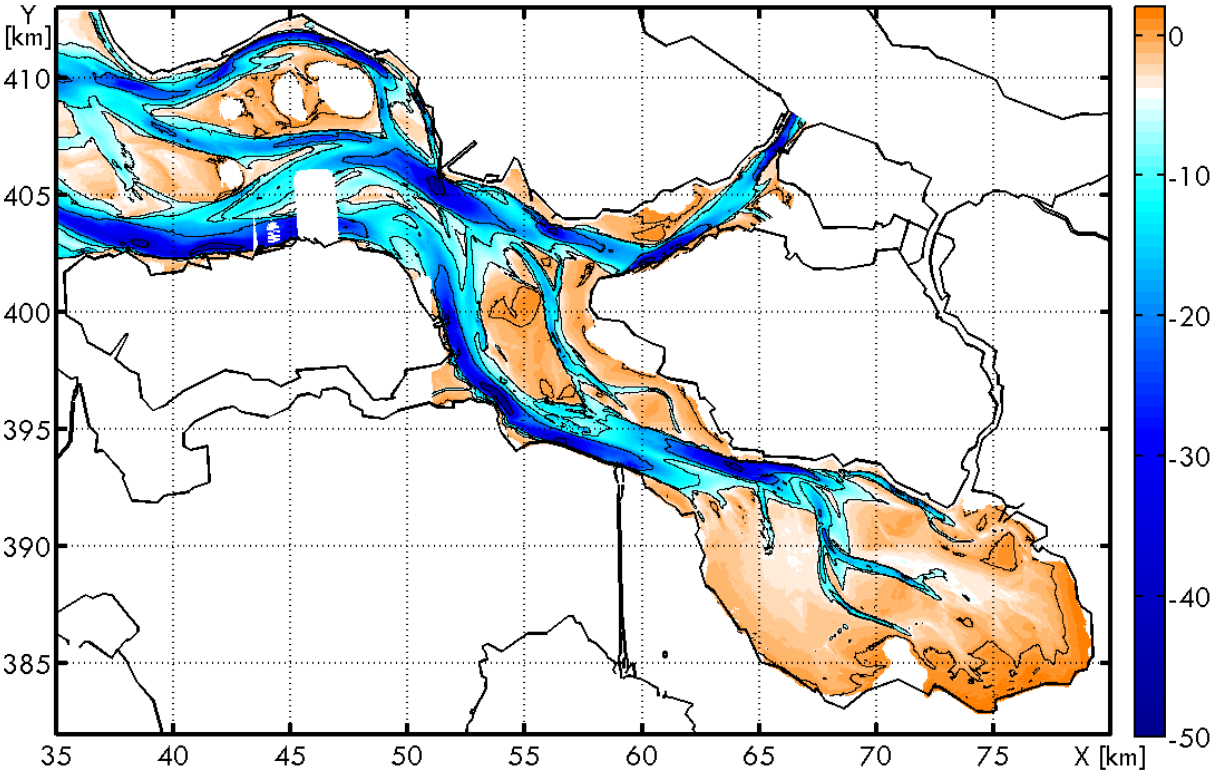

Figure 2.8: Bathymetry of the Eastern Scheldt measured in 1968.

After the disappearance of the watershed, the tidal influence of the Eastern Scheldt began to reach into the Volkerak channel (see Figure 2.6 for locations). This process must have further increased the tidal prism, amplifying the scouring in the Zijpe and Eastern Scheldt channels. In this way, the advancement of the Eastern Scheldt's tidal influence into the Volkerak could have strengthened itself. In the twentieth century, the Zijpe channel was still growing in cross-sectional area (Haring, 1978), and the whole Zijpe channel connecting the Eastern Scheldt and Grevelingen lost 32 Mm^3 of sediment between 1872 and 1950.

This incorporation of the Volkerak channel to the Eastern Scheldt is mirrored in the development of the Grevelingen estuary. The mouth of the Grevelingen lost between 7000 and 8000 m^2 of its cross-sectional area between 1860 and 1951 (Haring, 1955). The entire Grevelingen estuary gained 60 Mm^3 of sediment during the same period. This development points towards a decrease in tidal flow through this inlet. A simple explanation for this development is that the incorporation of the Volkerak by the Eastern Scheldt meant a graduate decrease in tidal volume flowing from the Volkerak into the Grevelingen. This decrease could have strengthened the Eastern Scheldt's tidal influence over the Volkerak even more.

2.3.5 Morphological evolution of the ebb-tidal delta

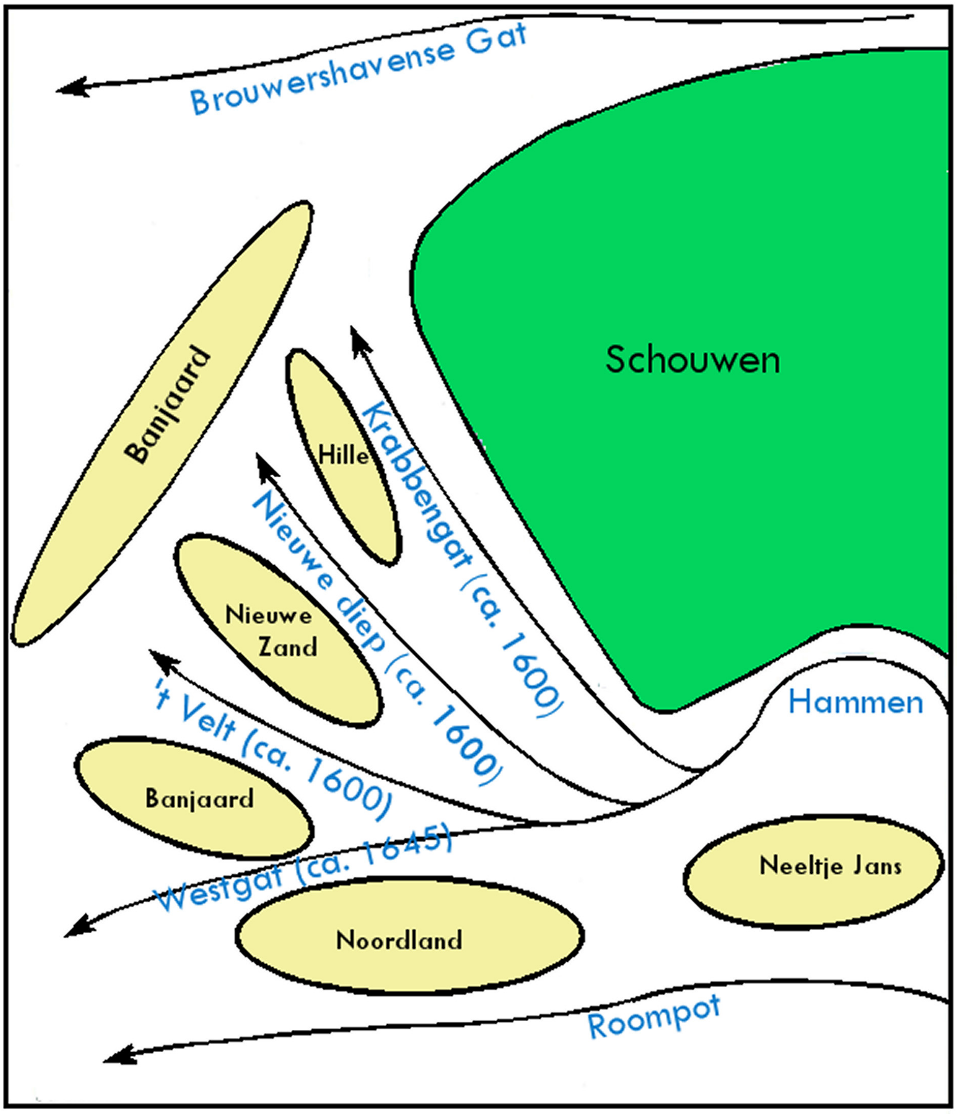

Figure 2.9: Sketch of the ebb-tidal delta channels around 1600 AD, adapted from Beekman (2007). Years indicate the time when channels were first observed.

Descriptions of the ebb-tidal delta of the Eastern Scheldt from before 1800 are rather sketchy. Until around 1600 AD the ebb-tidal delta consisted of a large shoal, called the Banjaard, attached to the beach of Schouwen, and was bound on the south by the

Roompot channel (Beekman, 2007). There are no reports of channels running through this shoal. This situation changed at the end of the 16th century, when the first charts appeared that displayed a channel separating the shoal from the beach of Schouwen. During the next century this single channel split up into at least two more channels cutting through the Banjaard shoal. Around 1650 AD a fourth channel, called the Westgat, was reported to run through the south side of the Banjaard, cutting off a new shoal called the Noordland (Figure 2.9). All these new channels were probably fed by the ebb current out of the Hammen channel. This Hammen channel used to be connected to the Roompot channel. However, by the 17th century this channel had probably separated from the Roompot channel, and started to feed the new system of channels running through the Banjaard shoal. During all this time the Roompot and Hammen channels deepened continuously (Beekman, 2007).

The first reasonably accurate map of the inlet bathymetry was made in 1800 by French cartographer C.F. Beautemps-Beaupré (Figure 2.10). This map, as well as bathymetric maps made in 1827, 1872, 1886, 1910, 1933 and 1953, give more insight into the configuration of channels and shoals on the ebb-tidal delta (Figure 2.11). From these maps, it seems that in the decades before 1953 the Eastern Scheldt ebb-tidal delta was morphologically highly active. The slow but steady increase in tidal volumes over the years described by Haring (1978) and Van Den Berg (1986), caused the main channels to scour, which in turn carried large amounts of sediment from the basin towards the ebb-tidal delta.

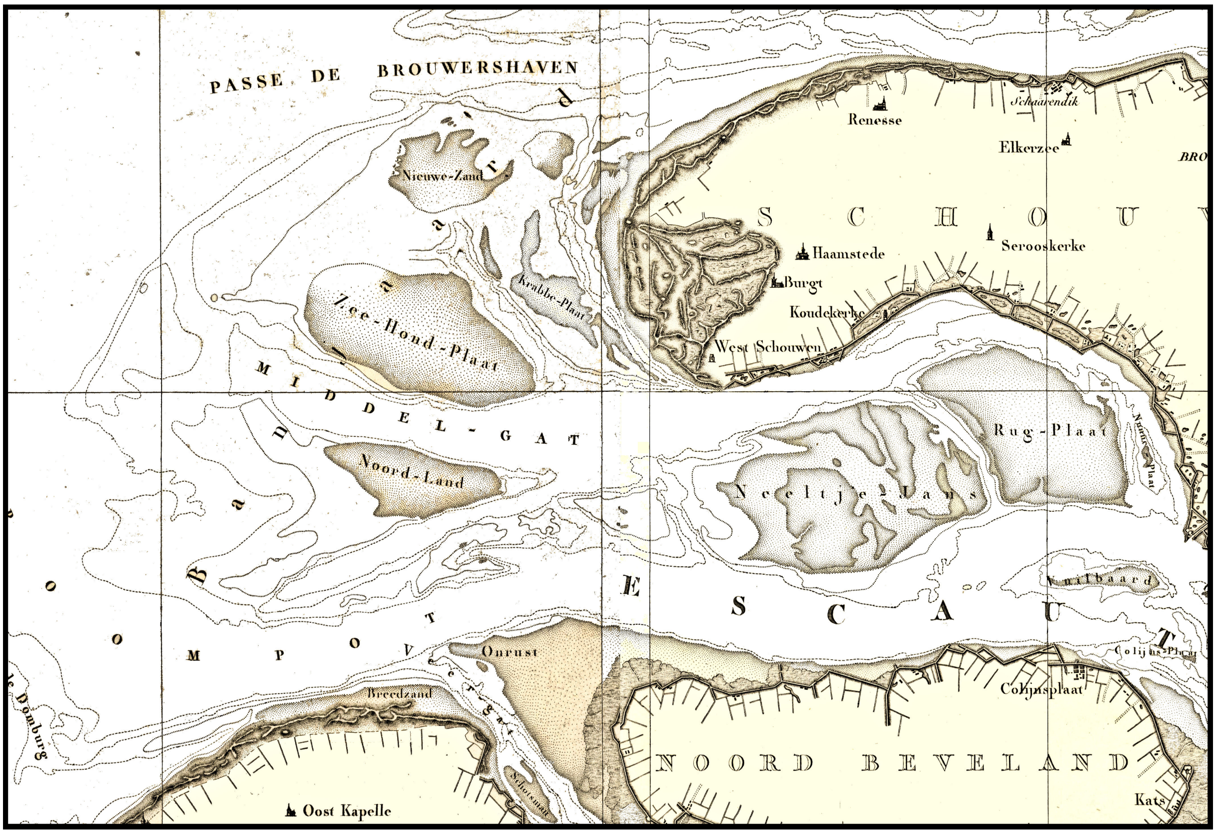

Figure 2.10: Detail of the bathymetric map of the Eastern Scheldt inlet around 1800 AD made by C.F. Beautemps-Beaupré. The Westgat channel is called 'Middelgat' on this map.

According to the bathymetrical maps, this delta grew steadily outward, being fed with sediment from the main channels through a number of rapidly shifting smaller ebb-channels. The northern swash platform, called the Banjaard, was intersected by three of these channels. From west to east these were called the Westgat channel, Hondengat channel, and Krabbengat channel. Between 1827 and 1910 the Westgat channel straightened, and shifted southward. In the decades before 1953 Hondengat channel became more or less abandoned. However, from 1933 onward a new channel crossing the Banjaard shoal began to develop at the location where the Westgat channel used to end. By 1953 this Geul van de Banjaard (henceforth called Banjaard Channel) intersected the Banjaard shoal almost all the way to the seaward shoreface, cutting off the western part of the Banjaard which formed the terminal lobe of the ebb-tidal delta. Meanwhile, nearly all of the intertidal area on the Banjaard and Noordland shoals disappeared.

The Westgat channel did not show any clearly definable cyclic behaviour. Between 1827 and 1862 the seaward end of this channel did seem to switch from a north-western to a south-western, updrift orientation, much like the outer channel shifting described by Fitzgerald *et al.* (2000), and also observed at Texel Inlet (Elias, 2006). However, this development is not followed by a northward migration of this new outer channel. This development is possibly an effect of the increased tidal discharge through the Hammen channel, which feeds the Westgat. This increase can be deduced from the apparent deepening of the Hammen channel between 1800 and 1910 (Table 2.1). The Banjaard Channel, positioned at the location where the Westgat used to end in 1827, has remained stable in its location for its entire existence. It seems that there has always been at least 1 large ebb-channel crossing the Banjaard shoal.

The area where the Roompot channel flows onto the ebb-tidal delta exhibited dynamic, and maybe even cyclic behaviour. The Roompot channel coming out of the inlet interacted with both the Southern Roompot[1] flood-channel on its south-western side, and the Westgat to the north. It seems as if the Roompot was constantly pushed in clockwise direction. In the 1886 and 1910 bathymetries this channel, now called the Geul channel, even connected directly to the Westgat channel. However, at the same time a new ebb-channel developed south of the Geul. This new channel, again called the Oude Roompot channel, took over the function as main ebb-channel, and the Geul channel silted up in the following decades. Meanwhile, the Oude Roompot channel regained the same curved shape visible in the 1827 bathymetry. The interaction of the Oude Roompot with its neighbouring channels during this period looks similar to the mutual evading channels with ‘flank attack’ described by Van Veen *et al.* (2005) (Figure 2.1c).

In the period from 1886 to 1953, the large tidal flat just east of the inlet, called the Roggenplaat, began to break up. A number of small ebb- and flood-chutes across this flat linked up and became a new main inlet channel, called the Schaar van de Roggenplaat (henceforth simply called Schaar channel). This again points towards a tendency of the inlet to increase its cross-sectional area.

[1] The name ‘Southern Roompot’ is not used in literature or on bathymetrical maps, where it is referred to simply as ‘Roompot’. In this thesis, the name ‘Southern Roompot’ is introduced in order to distinguish this particular channel from the other channel called ‘Roompot’.

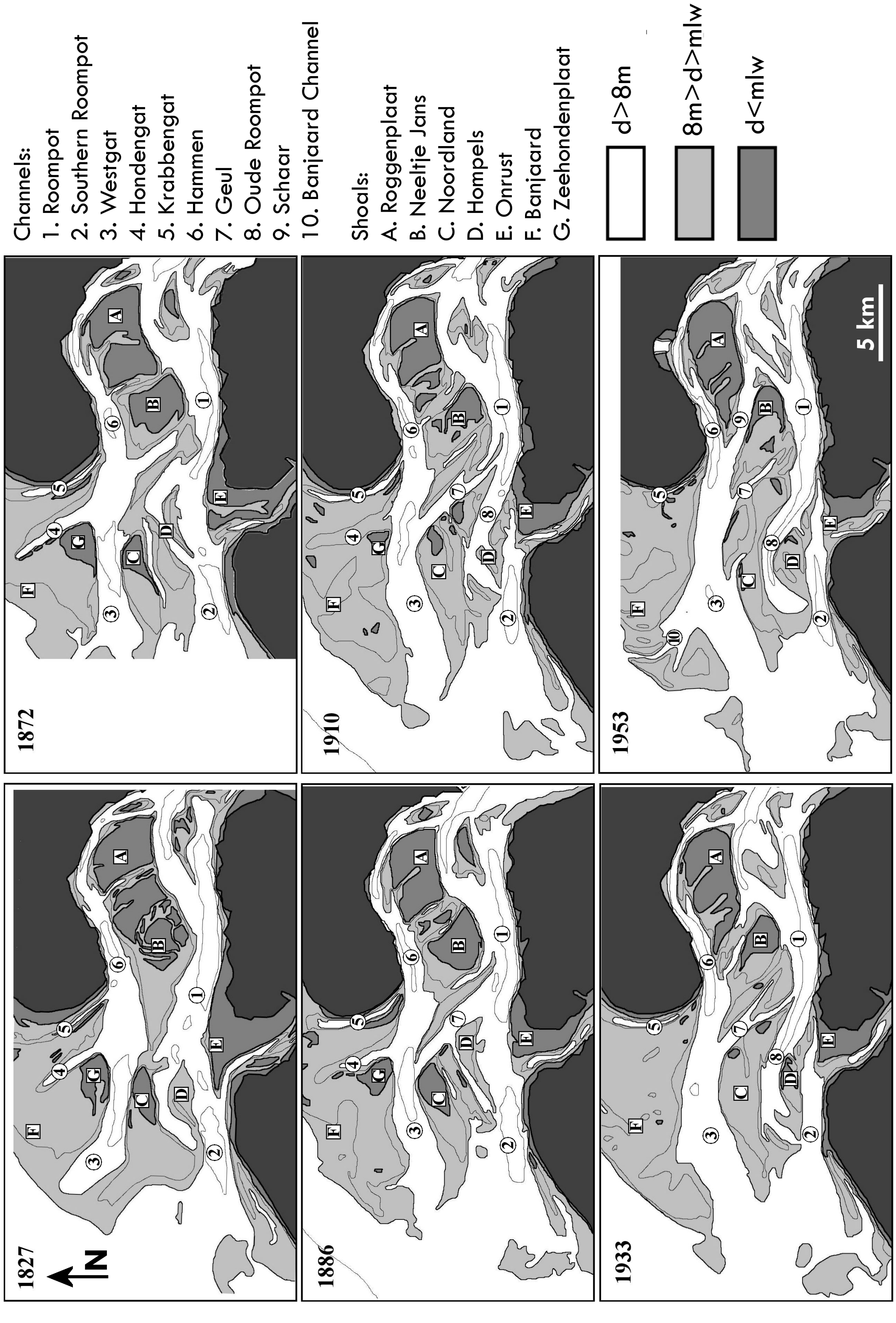

Figure 2.11: Bathymetry of the ebb-tidal delta between 1827 and 1953 (Haring, 1978).

2.4 PROCESS-BASED MODELLING

2.4.1 Approach

By 1950 AD the Eastern Scheldt estuary was still exporting considerable amounts of sediment per year. The hypothesis behind this development is that the inundation of South-Beveland created the circumstances which turned the estuary into a sediment exporting estuary, and that the estuary has been exporting sediment ever since. Due to the addition of large shallow areas in the backward end of the estuary, the tidal flow velocities should have become more ebb-dominant. This ebb-dominance in the flow caused the export of sediment. The increase in intertidal storage area also increased the tidal prism, which in turn caused scour of the channels.

This development is also part of the hypothesis behind the disappearance of the tidal watershed in the Zijpe channel. Due to the scour in the Eastern Scheldt estuary, the tidal wave propagated faster. This caused the tidal watershed between the Eastern Scheldt and the Grevelingen to be pushed northward out of the Zijpe channel. Another hypothesis behind the disappearance is that this happened due to a temporary decrease in tidal range in the Eastern Scheldt caused by the inundation.

However, these hypotheses have not been tested. In order to test them, a process-based numerical model is applied. For this particular study, the model application is designed and applied in accordance with the 'realistic analogue' modelling strategy, as described by Roelvink and Reniers (2011). In this modelling strategy, the goal is not so much to reproduce the exact same morphology as found in reality. Instead, the goal is to let the model create morphology with similar patterns as found in reality, and to use this model as a numerical laboratory to study the effects of different interventions in a more qualitative way (e.g. Van der Wegen and Roelvink, 2008; Dastgheib *et al.*, 2008).

The model domain of this study consists of the Eastern Scheldt geometry without the Volkerak channel and without the inundated part of South-Beveland. This model geometry will be run to simulate 800 years of morphological development inside the estuary starting from a uniform sloping bed.

This simulation will serve as a baseline simulation in order to compare results from other simulations with a situation which could exist if no inundation ever occurred. The bathymetry generated after 400 years of morphological development will be used in a simulation with the inundation present in the model. This simulation, which runs for another 400 years, will give insight into how the estuarine morphology might have changed in response to the inundation. A comparison between this simulation and the baseline simulation will show the differences in transports, hypsometry, and tidal propagation. The results from these simulations will also show a timescale at which the effects could have taken place. However, these modelled timescales are sensitive to the choices for the sediment transport formulation. Therefore, these timescales should be evaluated qualitatively relative to each other, and not in an absolute quantitative sense.

The aim of this study is to answer two main questions: 1) What were the effects of the inundation of South-Beveland on the morphology of the Eastern Scheldt estuary, and 2) Could the inundation of South-Beveland have been an indirect cause of the migration of the tidal watershed out of the Zijpe channel? It must be noted here that the goal is not to reproduce the exact same morphology or hypsometry as existed by the year 1968, but rather to investigate the effects of the inundation relative to a baseline simulation, and to investigate the possible role of the subsoil of the inundated area.

2.4.2 Model Setup

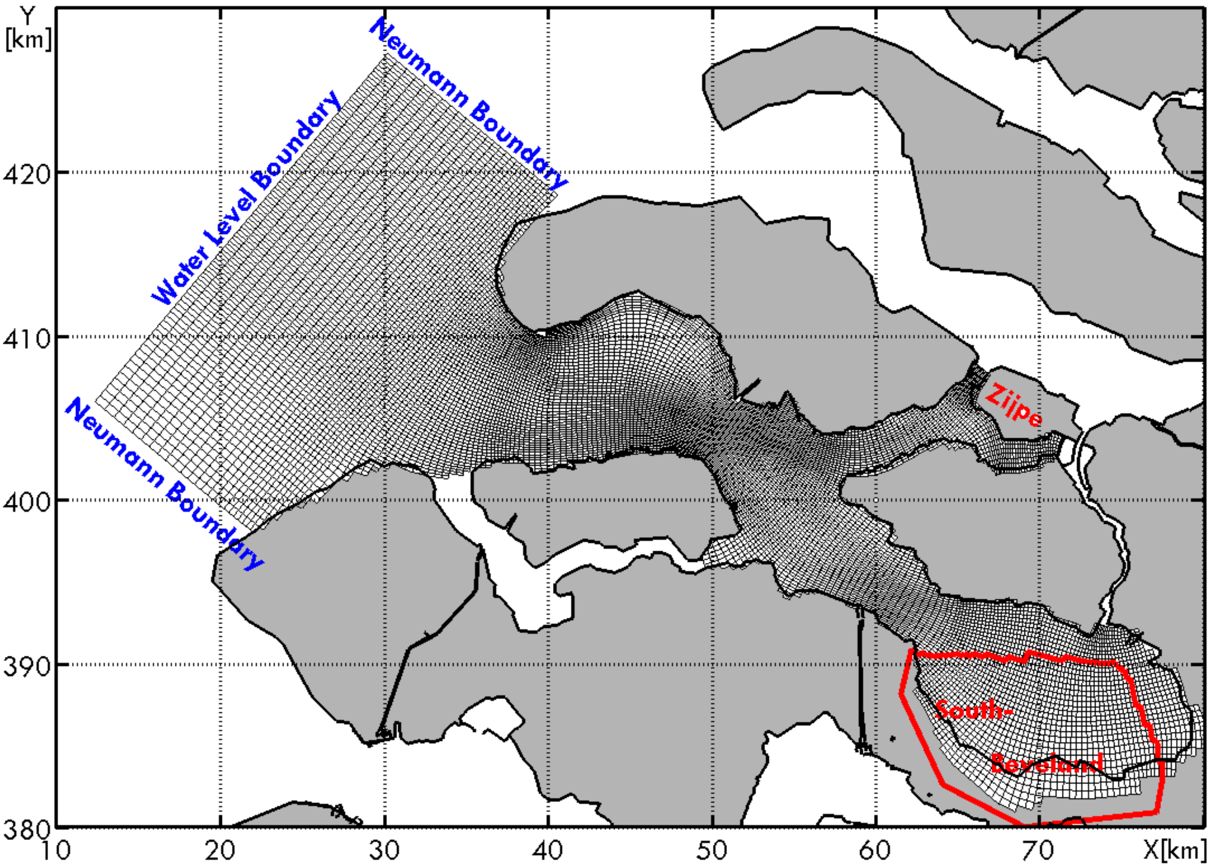

Figure 2.12: Model grid. The red polygon indicates the area that is excluded during the baseline simulation, and included in subsequent simulations in order to simulate the inundation of South-Beveland.

The model geometry consists of the Eastern Scheldt estuary including the northern branch (Figure 2.12). The grid ends where the Grevelingen estuary begins. On the seaward side, the model extends 12 kilometres seaward. The average grid cell size is roughly 150 by 300 m. The boundaries on the seaward side consist of a water level boundary on the long edge, and Neumann boundaries (water level gradient) on the short edges. This type of boundary allows the water levels and current velocities along this boundary to develop freely without disturbances (Roelvink and Walstra, 2004). The water level boundary is simply a pumping mode with an amplitude of 1.4 m and the frequency of the M2-tide. The amplitudes of the Neumann boundaries are kept at zero. This definition of the boundaries means that the model does not reproduce the propagating nature of the real tide along the Zeeland coast. However, the focus of this chapter is on developments inside the estuary. It is assumed that the fact that in reality the tide propagates along the coast does not influence the sediment budget inside the estuary. This definition of the boundaries does mean that the shape of the ebb-tidal delta produced by the model will not resemble the shape found in reality.

The initial bathymetry (Figure 2.13a) consists of a uniform sloping bed with a depth of 10 m at the inlet, and 0 m at the landward end. This gives the estuary an average depth of roughly 5 m. The seaward part of the domain, which starts directly seaward of the 10 m depth contour, has a uniform depth of 20 m.

The fact that the Grevelingen and Volkerak are not included and the Zijpe is modelled as a closed boundary, means that the model cannot reproduce the actual migration or disappearance of the tidal watershed in the Zijpe. However, the focus of this particular study is on how the phase of the tidal wave entering the Zijpe channel could have changed, and not on how this change actually impacted the morphology of the Zijpe, Grevelingen, and Volkerak channels.

The baseline simulation of the model will be run for 4 years of hydrodynamic computation. The morphological changes will be amplified with a morphological factor of 200. Thus, the model computes 800 years of morphological evolution. Van der Wegen and Roelvink (2008) showed that modelling estuarine morphology with a morphological factor of 400 did not lead to significantly different results than a factor of 1. Also, Van der Wegen *et al.* (2008) showed that for similar simulations where there was expected to be a large morphological activity, a factor of 200 was more appropriate. Therefore, for this study a factor of 200 is assumed to be acceptable. The simulations with the inundation will start with the bathymetry from the baseline simulation after 2 years of hydrodynamic computation, and will run for another 2 years with the same morphological factor. Table 2.2 gives an overview of all the simulations performed for this study.

One parameter which contains uncertainty is the level of the land inside the South-Beveland polder before it was flooded. In the present day, foundations of ruins are found between -0.5 and -1m below mean sea level. This level is assumed to be the land level of South-Beveland in 1530. However, the mean sea level has also risen over the centuries. With an average sea level rise of 0.2 m per century, this would mean that by 1530 the mean sea level was also approximately 1 m below present-day mean sea level. Therefore, in the model the land level is initially taken as equal to mean sea level. To see what the effect of a different level might be on the morphological adaptation of the estuary, the simulation with the inundation is performed two times with different values for the level of South-Beveland (MSL - 0m and MSL – 0.5m).

Initially, all simulations are run with a bed composition consisting of an even mixture of three non-cohesive sediment fractions of 100, 300, and 500 microns, respectively. However, another process which might have had a strong effect on the morphology is the clay layer beneath the South-Beveland polder. To investigate this, also simulations are performed which incorporate a layered bed underneath the polder. In these simulations the soil underneath the polder consists of three layers. The top layer consists of sand and is 0.5 m thick. This layer is supposed to represent the loose top soil which was most likely swept away in a short time according to Wilderom

(1968). The second layer consists of cohesive sediment and has a uniform thickness. In reality, this thickness shows spatial variability (www.dinoloket.nl). Therefore, the sensitivity to this thickness is investigated by running this simulation two times with different uniform thicknesses of the clay layer (5m and 7m). Beneath this layer is a non-cohesive base layer, representing the Pleistocene sand underneath the clay.

In all simulations, the non-cohesive sediment transport is calculated using the Van Rijn (1993) formulation. The erosion and deposition of the clay layer is calculated using the Partheniades-Krone formulations (Partheniades, 1965) for cohesive sediment. The sediment comprising the clay layer is assumed to have a dry bed density of 1200 kg/m^3, a settling velocity of 0.25 mm/s, a critical bed shear stress for erosion of 0.5 N/m^2, and an erosion parameter of 0.0001 kg/m^2/s.

Table 2.2: Overview of simulations.

Simulation	Starting bathymetry	Duration	Level South-Beveland polder	Stratigraphy South-Beveland polder
Baseline	Uniform sloping	800 years	N/A	N/A
Sand 1	Baseline after 400 years	400 years	MSL – 0m	Homogeneous sand
Sand 2	Baseline after 400 years	400 years	MSL – 0.5m	Homogeneous sand
Clay 1	Baseline after 400 years	400 years	MSL – 0m	Clay layer from MSL - 0.5m to MSL – 5.5m
Clay 2	Baseline after 400 years	400 years	MSL – 0m	Clay layer from MSL - 0.5m to MSL – 7.5m

2.5 Results

2.5.1 Baseline simulation

The initial morphological development of the baseline simulation consists of the formation of a channel-shoal pattern (Figure 2.13). The quickest and largest development occurs in the narrow parts of the estuary and the northern shore of the inlet. After 400 years of morphological evolution, the channel volume of the estuary has more or less stabilised. However, the pattern of the main channels inside the estuary does not show much correlation with the pattern found in reality (Figure 2.8). The channels look underdeveloped, especially in the middle and landward end. Another 400 years of morphological development does little to change this. The tidal range after 400 years is 2.9 m at the mouth and increases to 3.5 m near the landward end (Figure 2.14). During the second 400 years of the baseline simulation the tidal range near the landward end increases to almost 4 m (dashed black line in Figure 2.14).

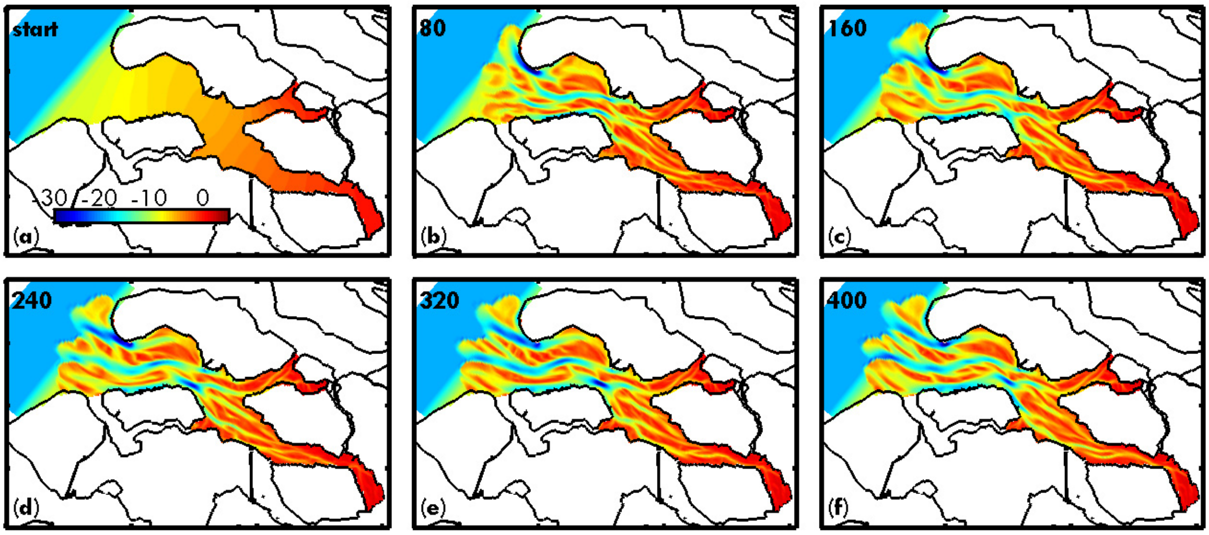

Figure 2.13: Bathymetry during the first 400 years of the baseline simulation. Depths are in m.

2.5.2 Response to inundation with uniform sandy bed

The initial response of the hydrodynamics to the flooding of South-Beveland is a small decrease in tidal prism at the mouth of the estuary (Figure 2.14b). This reduction is due to the significant decrease in tidal range in the bay and middle part of the estuary. This decrease is a direct result of the addition of the inundated area, which acts as a large shallow floodplain tempering the tidal wave. However, due to the development of new channels in the inundated area (Figure 2.15e), the average depth increases, and the channel-to-flat ratio shifts back in favour of the channels. As a result, the tidal range quickly recovers. In less than 50 years the tidal prism has reached its original value, and continues to grow to 150% of this original value. This growth is in part because the tidal range increases (Figure 2.14a), and in part because the intertidal storage volume increases as South-Beveland erodes. However, the tidal range in the bay area measured in the nineteen fifties was closer to 3.8 m (Van den Berg, 1986) instead of the 4.2 m produced by the model, pointing towards a tendency of the model to overestimate these values.

The tidal prism continuously grows during the 400 years of simulation, although it does slow down during the last 200 years. The final value for the tidal prism is around 1400 Mm^3/tide, which is larger than the value of around 1100 Mm^3/tide measured in 1959. If the model would have included the Volkerak channel, as the Eastern Scheldt does in reality, the overestimation of the tidal prism would probably have been even larger. Apparently, running this simulation with a uniform sandy bed results in an overestimation of the tidal prism. Looking at the resulting hypsometry (Figure 2.16a, red and blue lines), it appears that the intertidal storage volume becomes too large. When comparing the real and the simulated hypsometries, it has to be noted that the real 1968 hypsometry is a result of an Eastern Scheldt which includes the Volkerak area. However, the simulations did not include this area, so differences are to be expected.

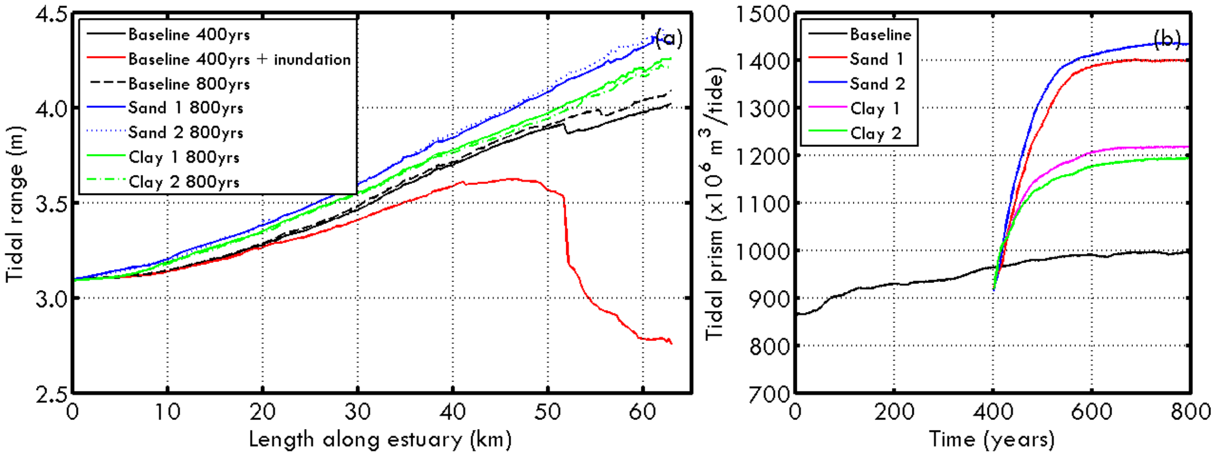

Figure 2.14: (a) Tidal range along the estuary for different simulations. (b) Evolution of the tidal prism at the mouth for different simulations. Sand 1: uniform sand, South-Beveland polder at MSL. Sand 2: uniform sand, polder at MSL-0.5m. Clay 1: clay layer 5m thick underneath South-Beveland polder. Clay 2: clay layer 7m thick underneath South-Beveland polder.

In case of a uniform sand bed, the flooded parts of the bay area immediately start to adapt to the inundation. New channels develop quickly, and the average depth of the area increases rapidly (Figure 2.15e and Figure 2.17g). The tidal volumes coming in and out of the bay area show instantaneous increase in response to the inundation. As a result, the channels in the bay area also grow rapidly, and transport large amounts of sediment into the middle part of the estuary (Figure 2.17f, g, h). Also, the locations of the main channels in the middle part grow closer to the locations found in reality (Figure 2.8).

The tidal volumes and flow velocities in the middle part and the mouth of the estuary also increase. However, these areas initially experience an increase in sediment volume. In the middle part this phase lasts for less than 50 years, in the mouth area for about 100 years (Figure 2.17L). This behaviour is because these parts of the estuary are 'overloaded' with the sediment surplus coming from the bay area. The mouth cannot export all the sediment it receives. Therefore, for a certain period it experiences net accretion of sediment. This process is similar to the 'bump'-behaviour described in Kragtwijk *et al.* (2004).

In the simulations with a uniform sandy bed, after 400 years the channel volumes below -2 m in the bay area are larger than what is actually measured in 1968 (Figure 2.16b red and blue lines). Apparently, the cross-sectional areas of the channels are overestimated by the model. This overestimation is mainly located in the depths between -2 and -20 m.

These model outcomes do not change significantly when the initial bed level of South-Beveland is decreased to -0.5 m below mean sea level. The final results are still the same in the sense that these simulations produce channel volumes and tidal prisms which are too large. This means that although the exact level of the polder is not known precise, its value does not have a dominating influence on the outcome of the simulation.

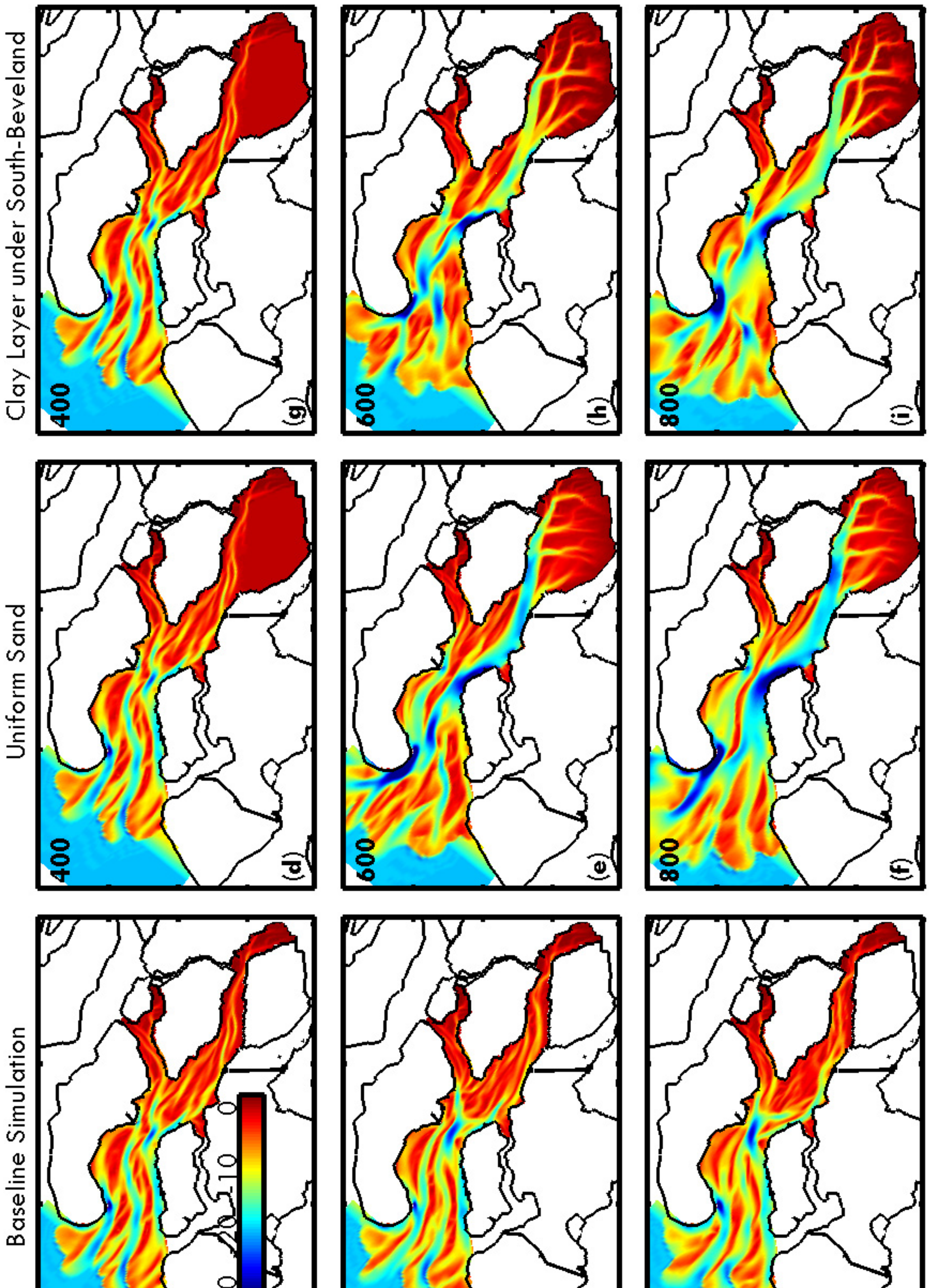

Figure 2.15: Bathymetrical evolution of the second 400 years. (a, b, c) Baseline simulation. (d, e, f) Simulation with inundation. South-Beveland consists of uniform sand. (g, h, i) Simulation with inundation. South-Beveland contains a clay layer 5 m thick.

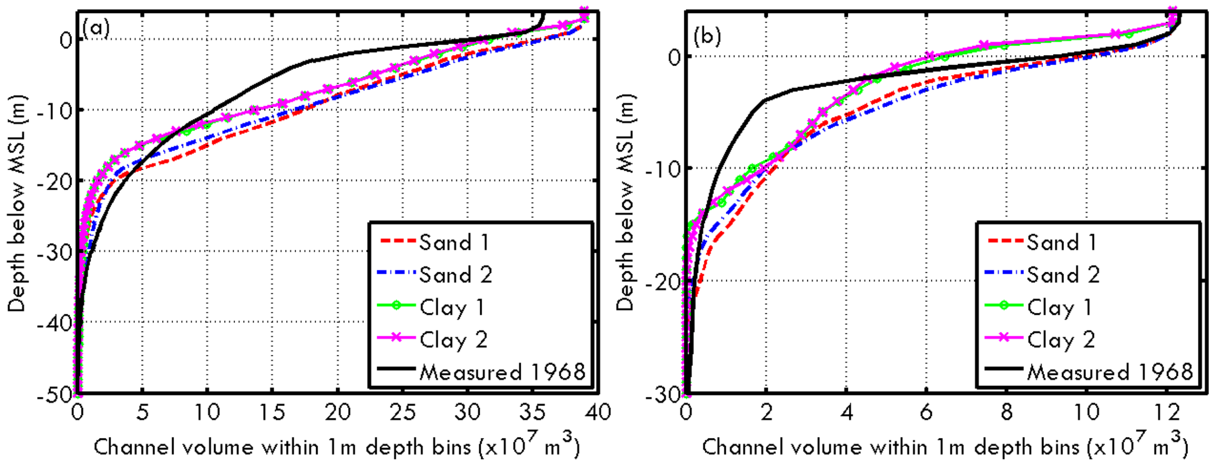

Figure 2.16: measured and modelled hypsometric curves for (a) the Eastern Scheldt estuary, and (b) the bay area.

2.5.3 Response to inundation with clay layer

Apparently, there has been a process which has reduced the increase in depth of the bay area since the inundation, and has also concentrated the erosion to the channels of the bay area, making them relatively deep and narrow. The hypothesis put forward in this study to explain this observation, is that the clay layer beneath South-Beveland hampered the erosion. This could have caused that the storage volume could not grow, and the tidal prism stabilised much sooner. As explained earlier, this clay layer could also explain why the channels in this area are so deep and narrow.

Hypothetically, because the clay layer hampers the erosion of the bay area, the adjacent middle part and mouth area of the Eastern Scheldt receive less sediment, making the deepening of the channels occur on a shorter time scale, because these channels do not have to convey as much sediment coming from the bay.

The model simulations with a clay layer partly strengthen these hypotheses. The tidal prism stabilises sooner, and does not increase as much as in the sandy simulations (Figure 2.14b). Initially, the sediment transport out of the estuary is high, but decreases strongly in the first 200 years (Figure 2.17n). This export would remain high if no layer is incorporated. The increase in sediment volume in the mouth area is still observed, but is not as large as in the other simulations, and also changes into net erosion sooner (Figure 2.17L). The thickness chosen for the clay layer (5 or 7 m) only has a minor influence on the outcome. Apart from this, the clay layer limits the growth of the channel volume below 10 m depth (Figure 2.16b green and pink lines).

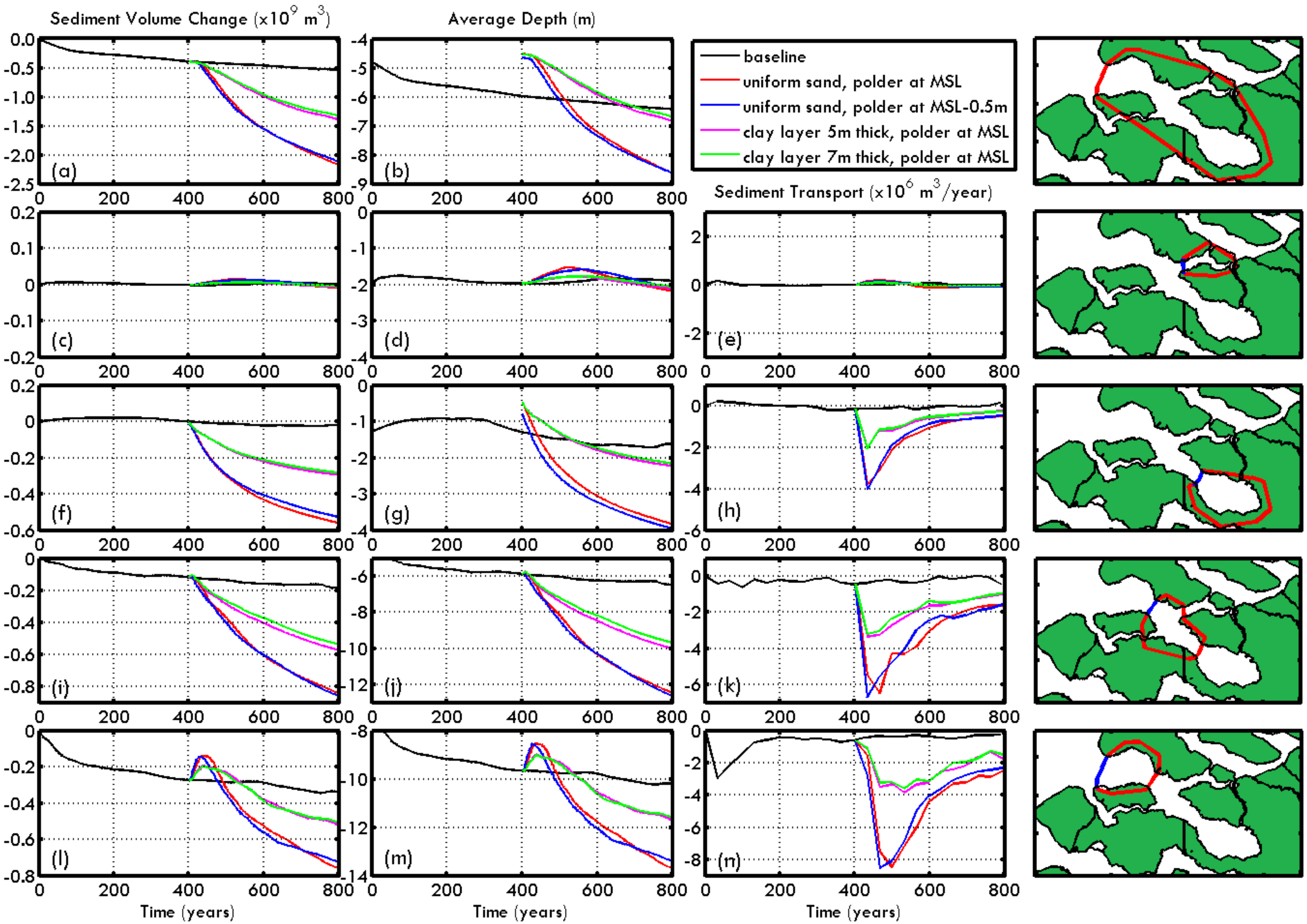

Figure 2.17: Results from long term simulations. First column: cumulative sediment volume change relative to the baseline. Second column: Average depth. Third column: Yearly net transport through the blue transect in the map. Fourth column: maps with the areas considered.

2.5.4 Celerity and amplitude of the tidal wave

Another part of the initial hypothesis dealt with the migration and disappearance of the tidal watershed in the Zijpe channel. According to observations, the Zijpe area started to scour roughly 200 years after South-Beveland flooded. Van den Berg (1986) explains that this process was the result of the deepening of the estuary, which in turn was a consequence of the flooding of South-Beveland. Hypothetically, this deepening should have caused the tidal wave in the Eastern Scheldt to arrive at the watershed sooner, because the celerity of the tidal wave is proportional to the square root of the water depth. However, Vroom (2011) explains that the migration could also be due to a decrease in tidal amplitude on the Eastern Scheldt's side of the watershed.

The development of the average depth of the estuary (Figure 2.17b) seems to be in accordance with the hypothesis of Van den Berg (1986). In all simulations, the average depth shows an initial decrease due to the inclusion of the shallow inundated area. The mouth area also initially decreases in depth, due to the overload of sediment coming from the rest of the estuary (Figure 2.17m). In the simulations without the clay layer the average depth of the estuary takes roughly 100 years of morphological development to overtake the pre-inundation depth. The simulations with the clay layer take about 200 years to overtake their pre-inundation depths.

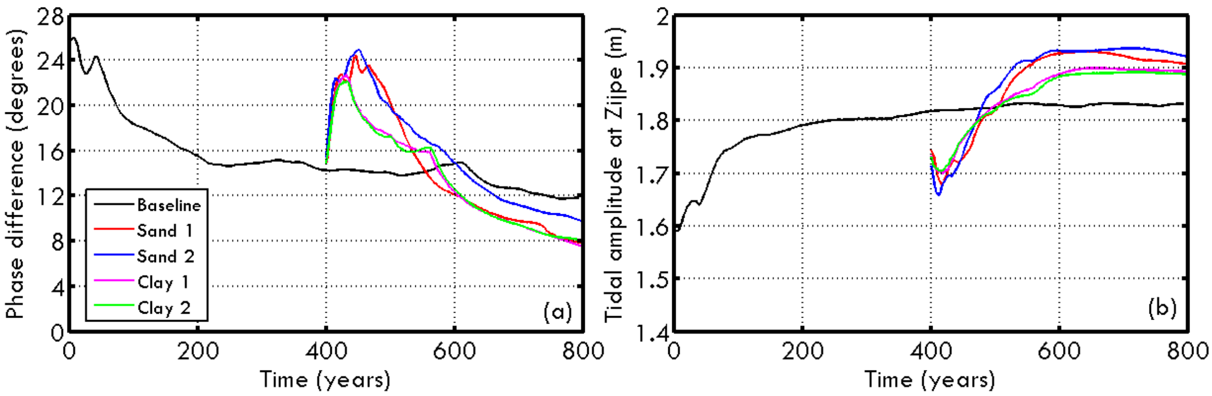

Figure 2.18: (a) Modelled phase difference between the inlet and the Zijpe channel. (b) Tidal amplitude in the Zijpe channel.

The initial decrease and subsequent increase in depth can also be seen in the tidal phases (Figure 2.18a). The time it takes for the tidal wave to travel from the inlet to the Zijpe can be expressed as the phase difference between the inlet and the Zijpe channel. If the tidal wave would travel faster, this would be visible as a smaller phase difference. The initial response of all models which include the inundated South-Beveland is that this phase difference increases, due to the smaller average depth. After this period, the phase difference decreases again due to the scouring of the estuary. Hypothetically, the watershed should have begun migrating after the phase difference decreased below its pre-inundation value. After 200 years, the phase difference in most models has decreased beyond this point, but not by much. Also, according to the same theory, the initial increase in phase difference should have made the tidal watershed migrate in the direction of the Eastern Scheldt, which is not observed.

According to Vroom (2011), the location of a tidal watershed is also influenced by the tidal amplitude. Vroom (2011) explains that a tidal watershed is located towards the side with the larger tidal amplitude. This means that if the amplitude in the Eastern Scheldt decreased, the watershed would have migrated towards the Grevelingen. The model results show that the tidal amplitudes inside the Eastern Scheldt decreased directly in response to the inundation to 92% of its old value (Figure 2.18b). In the Zijpe channel, the amplitude took roughly 100 years to overtake its old value. In the next 200 years, the amplitude grew to 106% of its old value (104% for the simulations including the clay layer).

The observation that the watershed began to migrate towards the Grevelingen 200 years after the inundation of South-Beveland seems to make sense when viewed from the depth perspective. It took between 100 and 200 years for the depth to increase. However, the development of the phase difference and the tidal amplitude in the Zijpe area do not support a clear explanation why the watershed began to migrate at that specific time. Perhaps the effect of the phase difference and the effect of the tidal amplitude were balancing each other during the first 200 years, until the circumstances within the Eastern Scheldt favoured the effect of the phase difference, after which the erosion and migration of the watershed could take place.

These simulations reveal nothing yet about the tidal amplitudes and phases inside the Grevelingen estuary. In order to model the morphology around the tidal watershed more accurately, also the Grevelingen estuary should be included. Besides this, also sea level rise has not been incorporated. This sea level rise added average depth to the estuary on top of the scouring, and thus might have caused a stronger decrease in phase difference between the mouth and Zijpe.

2.6 CONCLUSIONS[2]

The evolution of the Eastern Scheldt estuary over the past 5 centuries is dominated by human intervention. More specifically, the inundation of the polders of South-Beveland in 1530 started a chain of morphological developments which lasted well into the 20th century.

From the limited bathymetrical observations, a view emerges of an estuary which has been constantly deepening itself, first as a response to the South-Beveland inundation, and later due to the incorporation of the Volkerak channel. This incorporation occurred after the tidal watershed in the Zijpe channel disappeared. This disappearance itself was most likely an effect of the deepening brought on by the inundation. The amount of land reclamations around the Eastern Scheldt since 1530 was not large enough to reverse the exporting trend.

The deepening of the estuary resulted in a large and constant supply of sediment out of the inlet and onto the ebb-tidal delta. As a consequence, the channels in the inlet and on the ebb-tidal delta have been growing continuously. Some channels silted up

[2] The author thanks Ad van der Spek for his constructive comments regarding this chapter, and Bert van der Valk for supplying one of the references used in this chapter.

and disappeared over time, but were in most cases quickly replaced by new channels on a different location. Although there are signs of localized cyclic behaviour, there is no real large-scale cyclic behaviour on the ebb-tidal delta. The major shoals and channels have remained in place for centuries.

From the modelling study, it is concluded that the way in which the estuary adapted to the inundation of South-Beveland depends to an extent on the presence of the clay layer underneath the inundated area. Without this layer, the sediment supply to the rest of the estuary would have been far larger. Also, the tidal prism would have grown much larger, because erosion of the inundated South-Beveland would have created a lot of extra intertidal storage volume. This growing tidal prism and subsequent scouring also would have resulted in a bay area that is deeper after 400 years than the real present-day situation.

A noteworthy conclusion from the modelling effort is that the clay layer underneath South-Beveland had a strong influence on the development in the rest of the estuary. This hard layer kept the bed level of this area stable and also limited the growth of the tidal prism. The clay layer also had a strong limiting effect on the sediment supply towards the rest of the estuary. When the clay layer is included in the model, the sediment export out of the estuary decreases strongly in the first 200 years. However, this export must have increased again as the Volkerak channel gradually became part of the Eastern Scheldt system, although the model study could not say anything about this particular development.

The hypothesis by Van den Berg (1986) about the disappearance of the tidal watershed between the Eastern Scheldt and Grevelingen estuaries is partly confirmed. The inundation of South-Beveland and subsequent deepening of the Eastern Scheldt did cause the tidal wave to propagate faster, but only after an initial decrease in propagation speed which lasted for almost 200 years in the model. However, the development of the phase difference and the development of the tidal amplitude in the Zijpe area should have worked against each other with regard to the location of the tidal watershed. The eventual migration of the watershed could be explained by stating that the effect of the phase difference began to grow stronger than the effect of the tidal amplitude at roughly 200 years after the inundation. The model used in this chapter does not include the Grevelingen estuary and Volkerak channel, so it remains to be seen if an extended model which includes these parts can reproduce the migration of the watershed and the expansion of the Eastern Scheldt into the Volkerak channel.

Chapter 3

IMPACT OF BACK-BARRIER DAMS ON THE EASTERN SCHELDT INLET[3]

3.1 INTRODUCTION

As described in the previous chapter, the Eastern Scheldt tidal basin (Figure 3.1) used to be an estuary which was connected to two more estuaries to the north through several deep, narrow channels. These connections were closed off with dams in the nineteen sixties. These dams were part of the Delta Plan, and were built in order to facilitate the eventual closure of the inlets. The finalisation of the back-barrier dams meant the Eastern Scheldt turned from an estuary into a tidal basin. The construction of the back-barrier dams in 1965 and 1969 had a significant impact on the tidal hydrodynamics and sediment transport inside the Eastern Scheldt. The effects of these interventions were still ongoing when the hydrodynamic regime was altered yet again by the construction of the storm surge barrier in the inlet between 1983 and 1986.

The hydrodynamic and morphological evolution of the Eastern Scheldt has been well documented. Most articles describe the developments within the basin in terms of sediment budgets acquired from soundings, and change of the tidal prism in response to human intervention (Mulder and Louters, 1994; Louters *et al.,* 1998; De Bok, 2001). Some studies also incorporate the ebb-tidal delta in this description (Haring, 1978; Van den Berg, 1986; Aarninkhof and Van Kessel, 1999; Cleveringa, 2008). This chapter focuses on the evolution of the inlet and ebb-tidal delta between 1960 and 1982, describing the impact of the first stages of the Delta Plan before the storm surge barrier was implemented. This is done by discussing the aforementioned

[3] An edited version of this chapter was published in the Journal of Coastal Research:
Eelkema, M., Wang, Z.B. and Stive, M.J.F., (2012). Impact of back-barrier dams on the development of the ebb-tidal delta of the Eastern Scheldt. Journal of Coastal Research, 28(6), 1591-1605.

previous studies and reanalyzing the changes in hydrodynamics and bathymetry (section 3.2). A process-based numerical model is then applied to analyze the changes in tidal asymmetry, residual flow, and sediment transport as a result of these back-barrier dams (sections 3.3). Results from this model are presented in section 3.4. In section 3.5 conclusions are drawn by comparing the model outcomes to the observations from section 3.2.

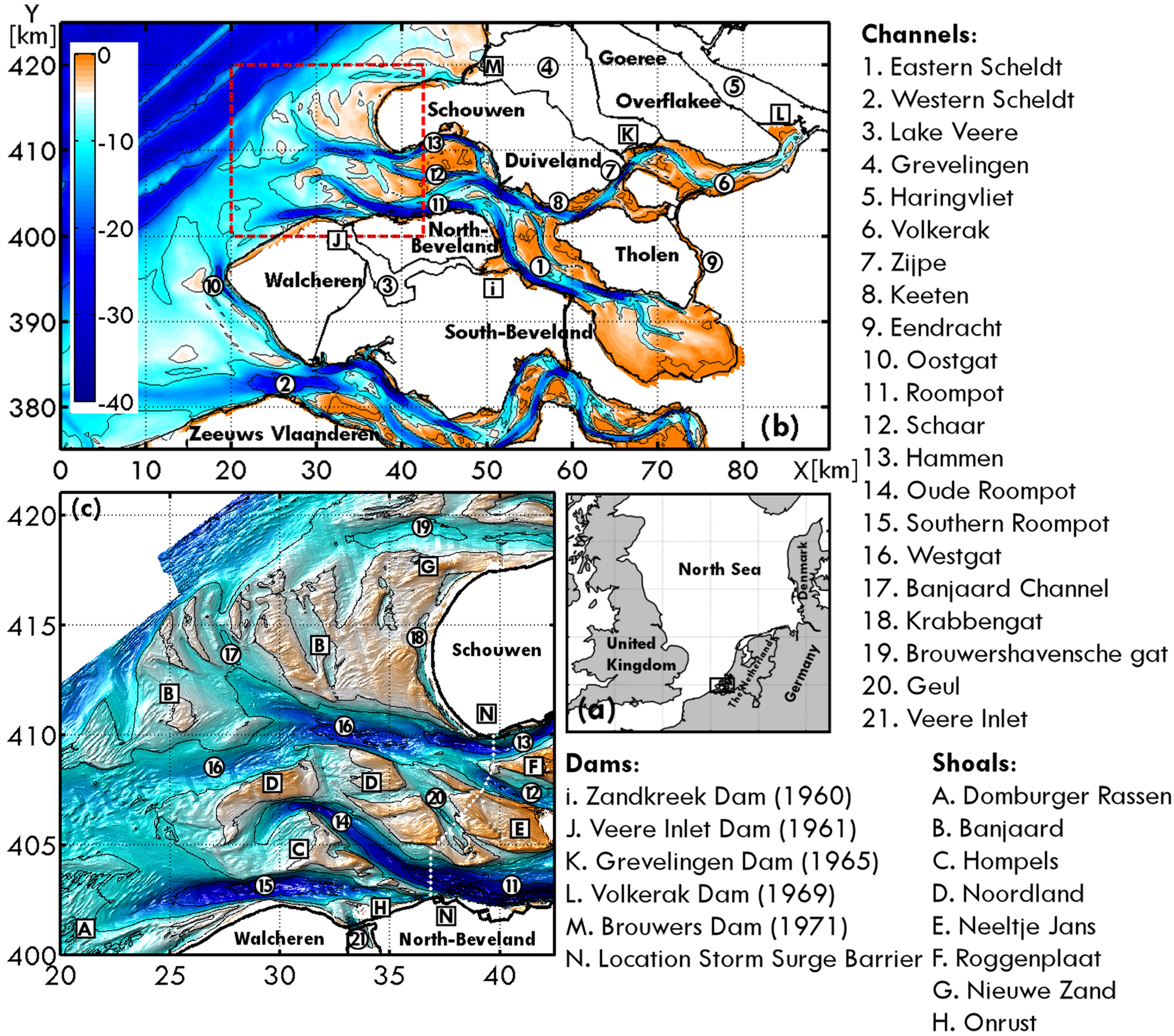

Figure 3.1: Overview of the study area. (a) The North Sea. (b) The south-western delta of the Netherlands. (c) The Eastern Scheldt tidal inlet in 1972. The white dotted line is the location of the storm surge barrier. The years in the legend are the year of completion of a particular dam.

3.2 OBSERVATIONS

3.2.1 The Eastern Scheldt tidal inlet in 1960

The southern part of the North Sea is characterised by a semi-diurnal tide entering the North Sea both from the north around Scotland as well as from the southwest through the English Channel. At the Dutch coast this tide propagates from southwest to northeast as a progressive wave. At the mouth of the Western Scheldt the tidal range is roughly 4 meters, decreasing to about 1.7 meters at the mouth of the Rhine River.

At the inlet of the Eastern Scheldt (Figure 3.1c) the mean tidal range is 2.9 meters. The tidal range increases to roughly 3.5 meters at spring tide, and decreases to 2.3 meters at neap tide.

The wave climate of the southern Dutch coast is largely characterised by locally generated wind waves with only a minor contribution of swell. Most of the wave energy is contained in waves coming from west-southwest, corresponding to the wind climate. However, the northwest direction also contains considerable energy.

The predominant wind direction on the Dutch coast is west-southwest. Although it is usually windy all year through, storms usually only occur during autumn and winter, and it is usually somewhat calmer during summer.

From present-day measurements (Figure 4.5), it is known that the median grain size on the ebb-tidal delta is between 150 and 200 microns on the shoals, and between 200 and 300 microns in the channels. From the same measurements we know that there is hardly any fine sediment (d_{50}<63 microns) present on the ebb-tidal delta.

Section 2.3.5 gives a detailed overview of the evolution of the ebb-tidal delta in the decades leading up to 1960. In short, the main channels delivered sediment from the basin to the ebb-tidal delta under the influence of a growing tidal prism. Some new channels formed on the ebb-tidal delta, while other small channels became abandoned. However, there is no clear large-scale cyclic behaviour. In the inlet, the growth in tidal prism was visible in the growing cross-sectional areas and the creation of a new main channel, called the Schaar.

3.2.2 Changes in hydrodynamics in the period 1960-1982

After the storm surge and flooding of large parts of the Rhine delta in January 1953, it was decided to close off the inlets of the Eastern Scheldt, the Grevelingen, the Haringvliet, and Veere Inlet with dams. To facilitate the construction of these dams, first two secondary dams were to be built inside the Grevelingen and the Volkerak channel. During the nineteen seventies it was decided not to build the dam in the Eastern Scheldt inlet. Instead, a storm surge barrier would be built in order to safeguard against flooding during storms while still allowing tide inside the Eastern Scheldt during normal conditions. This plan of dams and barriers in the Rhine river delta is commonly known as the Delta Plan (Figure 3.2).

The implementation of the Delta Plan between 1960 and 1980 had serious effects on the hydrodynamics of the Eastern Scheldt (Figure 3.3). The chronology of the implementation is important for this development. The first step, the closure of the relatively small Veere Inlet in 1960 and 1961, had no discernable impact on the hydrodynamics and morphology of the Eastern Scheldt as a whole, although there will have been some local effects on the ebb-tidal delta where the Veere Inlet flowed into the larger Southern Roompot channel (see Figure 3.2 for the locations of these dams). The construction of the Grevelingen dam in 1965 caused a small decrease in tidal range in the Eastern Scheldt. The effects of the Grevelingen dam were probably relatively small due to the fact that the Grevelingen dam was built on the tidal watershed between the Grevelingen and the Volkerak channel. Of far greater consequence was the completion of the Volkerak dam in 1969. This closure caused considerable amplification of the tide not only in the northern branch, but also in the rest of the basin. De Bok (2001) showed that the tidal prism increased by almost 7% within a year. The presence of this dam altered the nature of the tidal wave in the northern branch, changing it into a more standing wave. At the connection of the northern branch with the rest of the Eastern Scheldt basin, called the Keeten channel, the tidal volume increased by approximately 17% according to Van den Berg (1986).

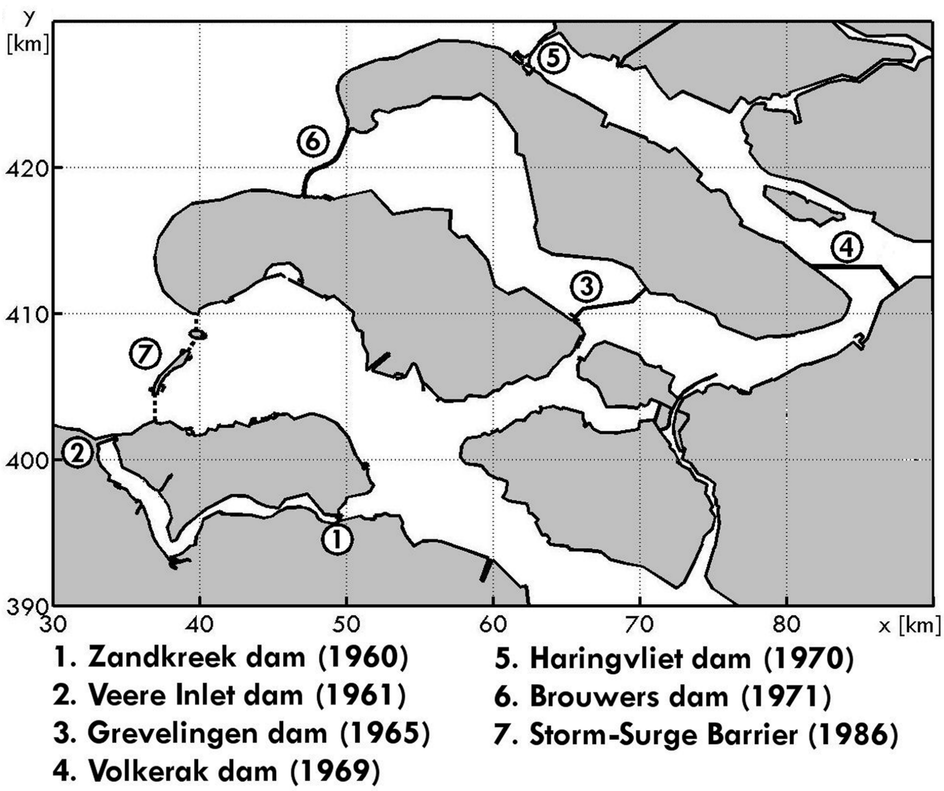

Figure 3.2: Overview of dams constructed between 1960 and 1980.

Before the Volkerak dam was made, the Volkerak was connected to the Haringvliet, which is one of the mouths of the Rhine and Meuse rivers. In spite of this connection, the flow of fresh water into the Eastern Scheldt was rather small due to a surplus of flood discharges from the Eastern Scheldt into the northern tributaries. Only during times of high river discharge there was a measurable dilution of the water inside the

Eastern Scheldt basin (Peelen, 1970). Since completion, there is no significant inflow of fresh water through either Grevelingen dam or Volkerak dam.

According to De Bok (2001), the average tidal range along the basin slowly increased even more after the Volkerak dam was built (Figure 3.3). The cause of this increase is not clear. It could have been the scouring of the main channels which made them more hydraulically efficient, causing more amplification of the tide inside the basin. The cause could also have been the nodal tide, which experienced a low around 1970 and a high approximately 9 years later (De Ronde, 1983). This nodal tide is caused by the 18.6 year rotation of the plane of the lunar orbit. Along the Dutch coast this causes a tidal variation with an amplitude of about 3% of the tidal range. According to De Bok (2001) this increase in tidal range also resulted in a larger tidal prism[4]. However, in the calculation of the tidal prism De Bok (2001) did not include the artificial islands in the inlet made during the seventies. Van den Berg (1986) states that these artificial islands and the canalization of the Eendracht channel caused a decrease in storage capacity which counteracted the increase in tidal range between 1968 and 1982. This seems to be confirmed by the tidal volumes calculated from discharge measurements taken between 1970 and 1980 (also summarized in De Bok (2001)), which show no clear trend for increase or decrease (Figure 3.3). It is probable that the effect of the increased tidal range on the tidal volumes was simply too subtle to be derivable from the limited number of measurements.

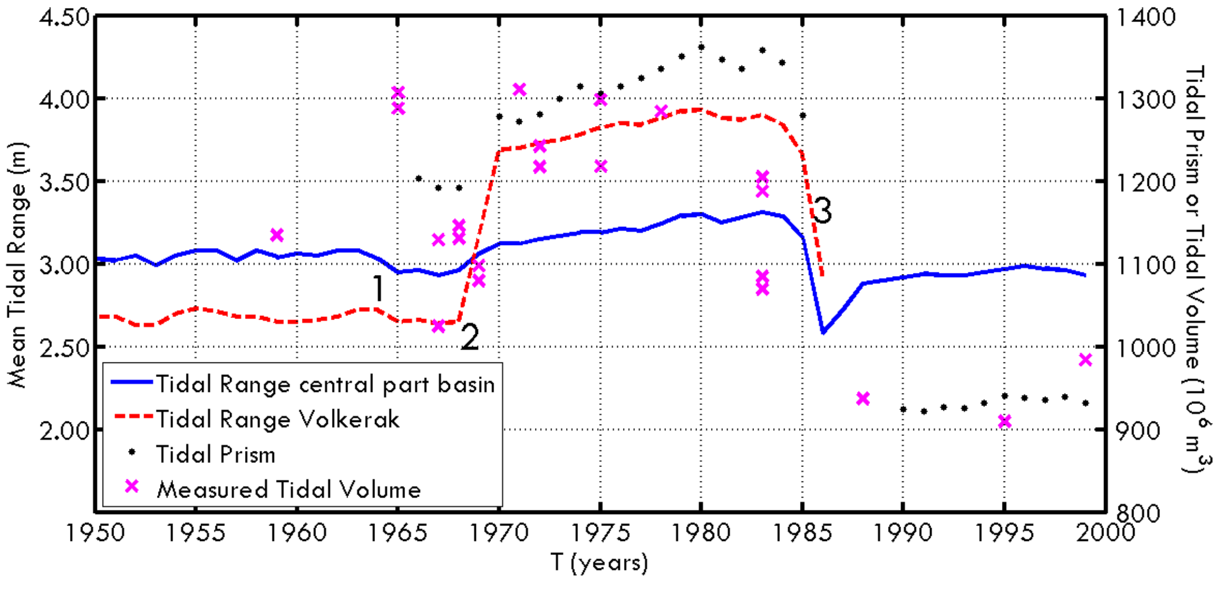

Figure 3.3: Tidal prism and measured tidal volume of the Eastern Scheldt and mean tidal range inside the Keeten and Volkerak channels (De Bok, 2001). Numbers indicate finalization of dams: (1) Grevelingen dam. (2) Volkerak dam. (3) Storm surge barrier.

The final phase of the closure of the Eastern Scheldt inlet began in the spring of 1969 with the construction of two artificial islands in the inlet throat. Both islands were

[4] In literature, the terms 'tidal prism' and 'tidal volume' are often used with interchangeable definitions. For this thesis, the tidal prism is defined as the volume calculated by multiplying the wet surface area of a basin with the local tidal range minus the sediment volume of the flats. The tidal volume is defined as the volume calculated by integrating the tidal discharge through the inlet over 1 flood- or ebb-period.

located on top of two tidal flats, Roggeplaat and Neeltje Jans. Although these islands did not intersect any major channels, they did cause more constriction of the flow through the three main inlet channels. The original plan was to simply close these channels with dams, leaving a fresh water lake without tidal influence at the landward side. Between 1972 and 1974 work was already done on constructing bed protection as foundation for the eventual dams. However, pressure from environmental groups as well as the local fisheries caused re-evaluation of the plans for closure. In 1974 the Dutch government decided for a semi-open barrier, which would ensure safety against flooding by closing during storms, but would otherwise allow tide to flow in and out of the basin. Apart from this, also two compartmentalisation dams would be built in the landward end of the basin, which would cut off the Volkerak and the eastward end of the bay area from the rest of the Eastern Scheldt. Construction of the barrier began in 1976 with the removal of the old bed protection and installation of a new one which was suitable for the barrier itself. Placement of the piers which would hold the gates started in the summer of 1983. The entire storm surge barrier was finalised early 1986.

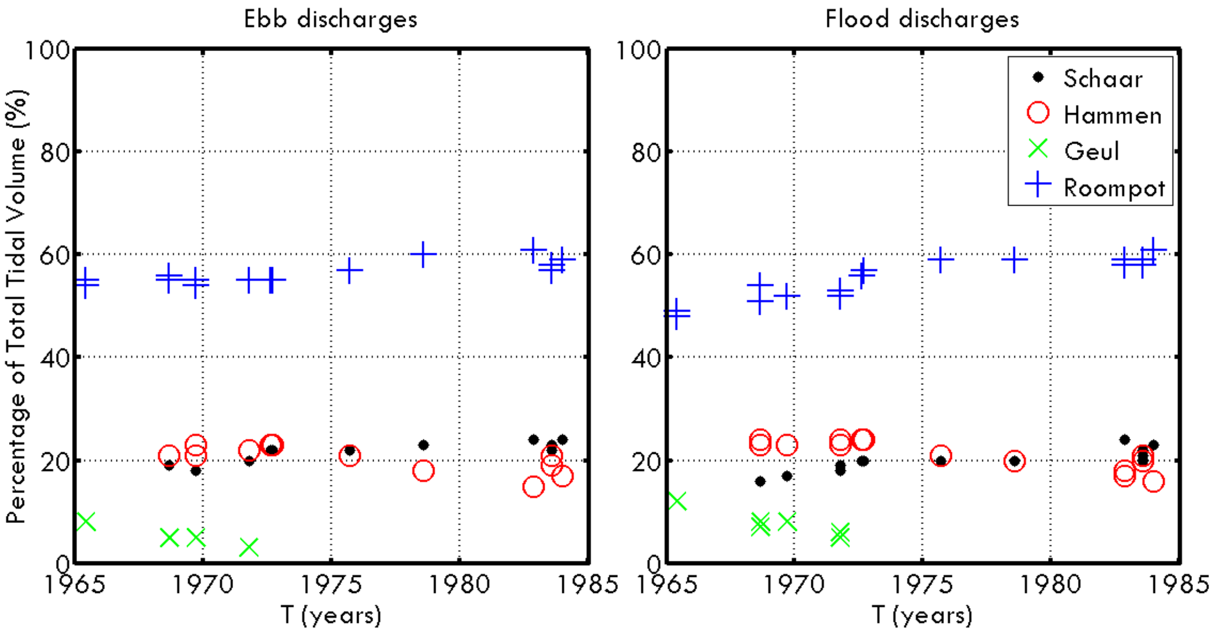

Figure 3.4: Distribution of ebb and flood volumes over the main inlet channels (redrawn after Van den Berg, 1986 and De Bok, 2001).

The tidal flow through the inlet is distributed over the three main channels, the Roompot, Schaar and Hammen (Figure 3.4). Before 1972 there was also a small fourth channel, called Geul, splitting the Neeltje Jans and Noordland shoals. This channel was closed off when the main construction island of Neeltje Jans was built. The distribution of tidal volume over these channels during flood is slightly different than the distribution during ebb. From discharge measurements taken between 1965 and 1982 it seems that around 1965 the Roompot channel took 49% of the total flood volume and 55% of the total ebb volume going through the inlet, and both these volumes increased to 60% in 1982 (De Bok, 2001). This increase seems to start by the time of the closure of the Geul channel. After its closure, the ebb and flood volumes of this Geul channel were distributed evenly over the Roompot and Schaar channels

(Van den Berg, 1986). Regarding the two northern channels, it seems that the Hammen channel lost some of its discharge capacity. The trend in the Hammen seems to be mirrored by the development of the Schaar, although the relative loss is bigger than the gain, resulting in the increased influence of the Roompot. Even though the basin became a closed system after completion of the Volkerak dam, the measurements of the tidal volumes through the inlet hardly ever show equal values for the ebb and flood volumes measured on the same day, due to sub-tidal variation.

3.2.3 Changes in morphology in the period 1960-1982

Digitized bathymetric data of the ebb-tidal delta are well available (De Kruif, 2001). Since 1960, there has been a bathymetrical measurement of the entire ebb-tidal delta every four years. The availability of bathymetric data of the basin in digitized format is somewhat less. For the period between 1960 and 1982 only two bathymetric datasets are available in digitized form, for the years 1968 and 1982. The derivation of morphological effects of the Delta Plan from bathymetric maps is not unambiguous, not only because of measurement inaccuracies, but also because parts of the Eastern Scheldt basin were subject to sand mining, and the amounts of mined material were comparable to, or sometimes even greater than the amounts deposited or eroded by natural means. However, certain natural trends were obvious and persistent, or clearly reversed in response to the construction of the dams.

Developments inside the basin

Prior to the construction of the dams in the Grevelingen and the Volkerak, large parts of the Eastern Scheldt were still deepening, especially in the northern branch. The closure of the Grevelingen and the Volkerak amplified these erosive trends throughout most of the Eastern Scheldt, although some parts experienced accretion (Figure 3.5). According to Louters *et al.* (1998), the basin lost approximately 120 Mm^3 of sediment between 1960 and 1989. About 80 Mm^3 of this is due to sand mining activities, the remaining 40 Mm^3 is due to natural export. If this amount of natural erosion is spread out evenly over the period between 1960 and 1984, an average yearly export between 1 and 2 Mm^3 is the result. However, Louters *et al.* (1998) observed that the export rate reached a peak around 1970 and declined in the following period.

Looking at the northern branch in detail, Van den Berg (1986) noticed that after completion of the Volkerak dam, most of the erosion was located around the Zijpe. Some of the eroded sediment was deposited to the east into the dead end of the Volkerak, while another part was pushed to the south into the Keeten channel, and the remainder was transported to the rest of the Eastern Scheldt. When looking at bathymetrical measurements of the northern branch (Figure 3.5b), it is observed that between 1968 and 1982 some parts of the Keeten channel actually lost cross-sectional area. This means that in spite of an increase in tidal volume running through this channel, the channel cross-section actually decreased (Figure 3.5c). This could be explained by hypothesising that the mouth of the Keeten channel received more sediment from the north than could be transported towards the south. In this sense, the Keeten channel behaved like the ‘bump’-behaviour described in Kragtwijk *et al.* (2004).

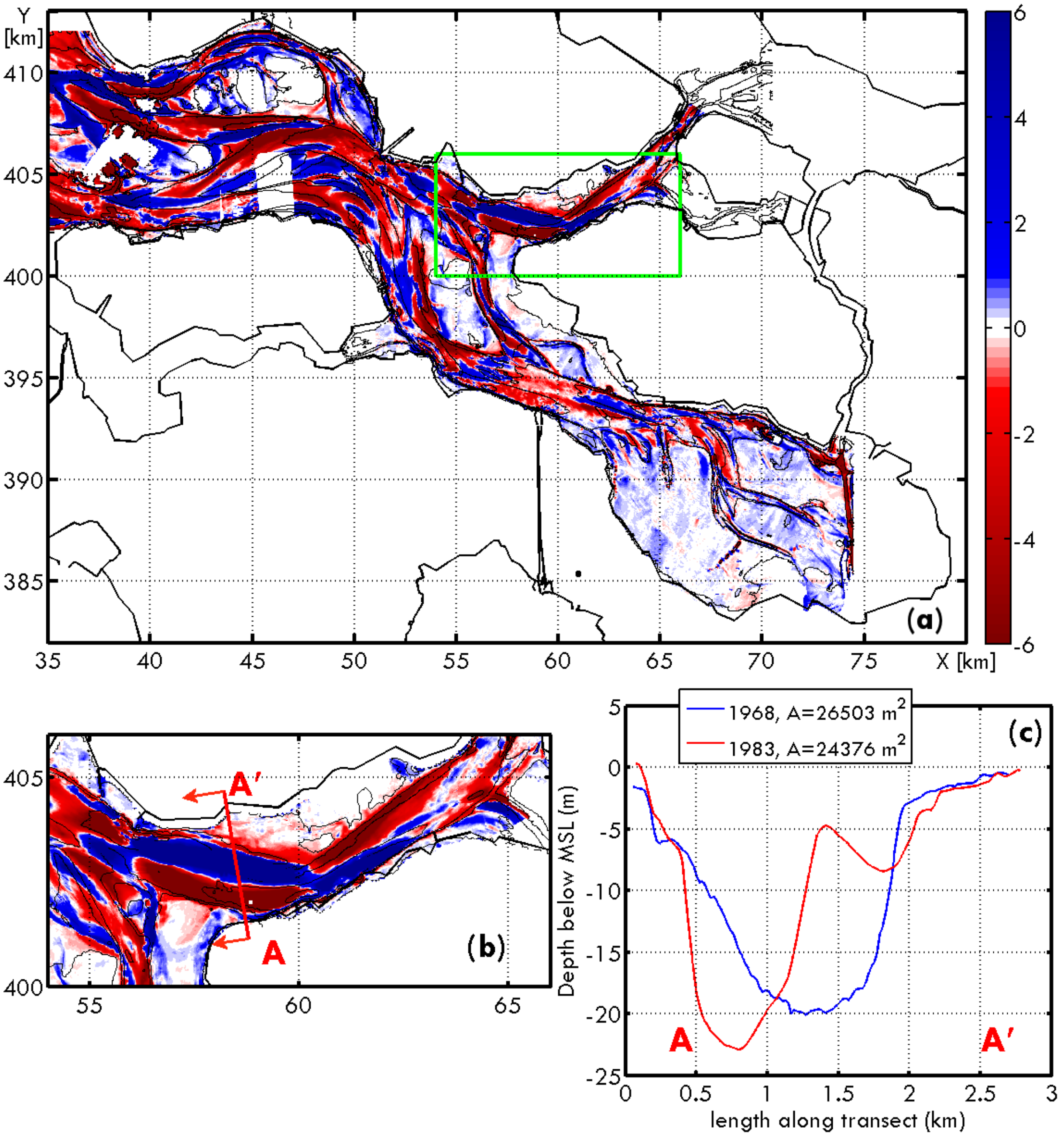

Figure 3.5: (a) Difference in bed-level inside the basin between 1968 and 1982 (red=erosion). (b) Detail of the northern branch. (c) Cross-sectional areas below MSL at transect A-A' in (b).

The occurrence of this ‘bump’ is related to the timescales of the system of morphological elements and the nature of the disturbance. The channel volume of the Keeten apparently responded on a slower timescale than the channels north of it. Another way of looking at it is by saying that the scour from the Volkerak and Zijpe channels overloaded the Keeten with sediment. The Keeten did not have the transport capacity to get rid of this excess sediment, so it started to accrete. As it did, the transport capacity increased. It is hypothesised that if this situation had lasted longer than only 15 years, the Keeten channel would have also started to erode eventually.

Figure 3.5c also shows that the deep part of the Keeten channel moved more towards the southern channel edge. This could be related to a change in the phase of the discharge caused by the Volkerak dam. If the difference between the phases of the discharges in the Keeten channel and the Eastern Scheldt basin changed, this could also change the orientation of the channel as it flows into the basin. This process influencing the orientation is very similar to the mechanism behind ebb-tidal delta orientation described by Sha and Van den Berg (1993).

Developments on the ebb-tidal delta

The cumulative sediment volume of the ebb-tidal delta (Figure 3.6), on the other hand, shows some anomalous behavior. According to the bathymetric measurements, the growth of the ebb-tidal delta sediment volume continued without decreasing in rate until 1980. More than 80 Mm^3 of sediment would have been deposited in only 20 years. Moreover, according to the same data, 30 Mm^3 was eroded in only 4 years between 1980 and 1984. Van den Berg (1986) states that this peak is caused by systematic errors in the 1980 measurement. We think this is likely, because the loss of sediment after 1980, which would be around 8 Mm^3 per year, is not found as a gain of sediment in any of the neighbouring areas. Omission of the 1980 bathymetry also means closer agreement between the gain of sediment on the ebb-tidal delta and the natural loss of 40 Mm^3 from the basin found by Louters *et al.* (1998).

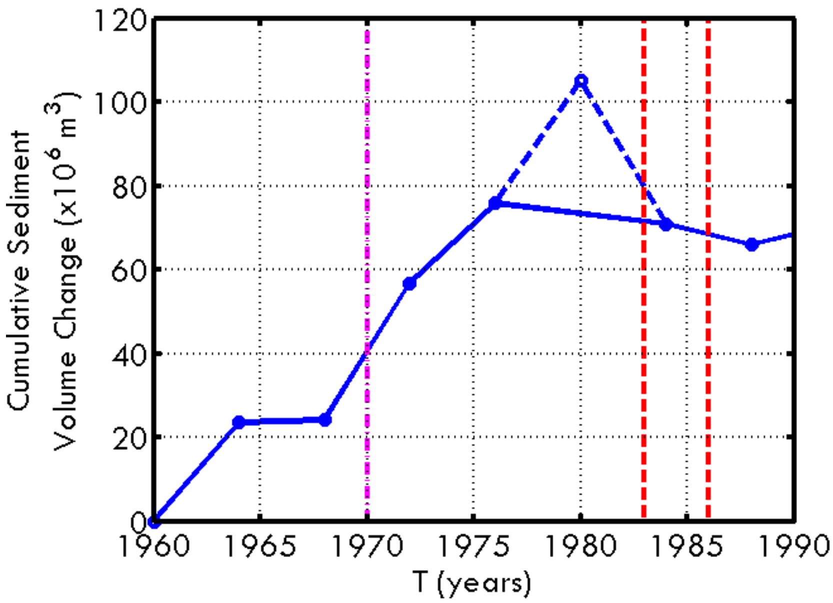

Figure 3.6: Cumulative sediment volume change of the ebb-tidal delta relative to 1960. The dashed blue line shows the volume change with the 1980 data. The solid blue line shows the volume without the 1980 data. The vertical pink line denotes the finalisation of the Volkerak dam. The dashed red lines denote the construction of the storm surge barrier.

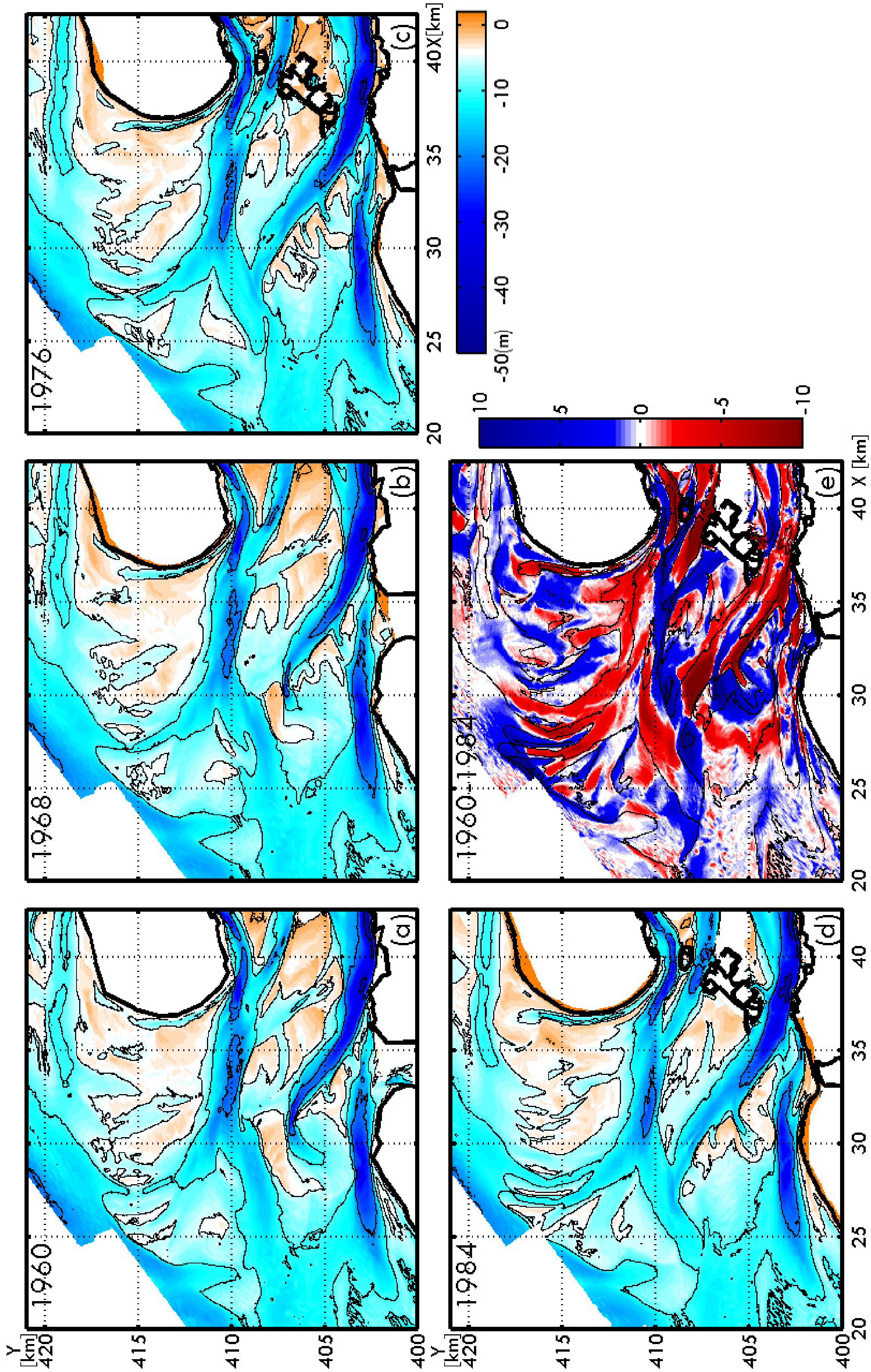

Figure 3.7: Bathymetry of the ebb-tidal delta between 1960 and 1984. (e) Bed-level difference (m) between 1960 and 1984 (red=erosion). Coordinates are in km.

At the location of the inlet, the increase in tidal volumes caused scour of all the main channels. This scour was amplified even more by the construction of two artificial islands on the flats in the inlet during the nineteen seventies (Figure 3.7), constricting the flow to the remaining channels. The changes in hydrodynamic forcing and the sediment budget inside the Eastern Scheldt basin also started to become apparent on the ebb-tidal delta, as has been described by Van den Berg (1986) and Cleveringa (2008). The ebb-tidal delta received large quantities of sediment exported from the basin and grew rapidly in area as a result. The general increase in tidal prism manifested itself in the deepening and lengthening of the main ebb channels. In particular, the Oude Roompot ebb channel expanded rapidly in seaward direction. During this period the spill-over channels on the north-eastern edge of the Hompels shoal migrated northward with rapid speed, moving roughly a kilometer in 4 years. These small ebb channels displayed a highly dynamic cyclic behaviour, in which they seemed to originate from the sub-tidal sill (called Onrust) where the Southern Roompot and Oude Roompot channels meet. Starting as a cut-off on this sill, the channels would initially grow and move north-eastward along the shoal edge. Eventually they would die out as they moved farther away from the inlet. This behaviour is remarkably similar to the behaviour of flood channel cut-offs described by Van Veen *et al.* (2005) (Figure 3.8).

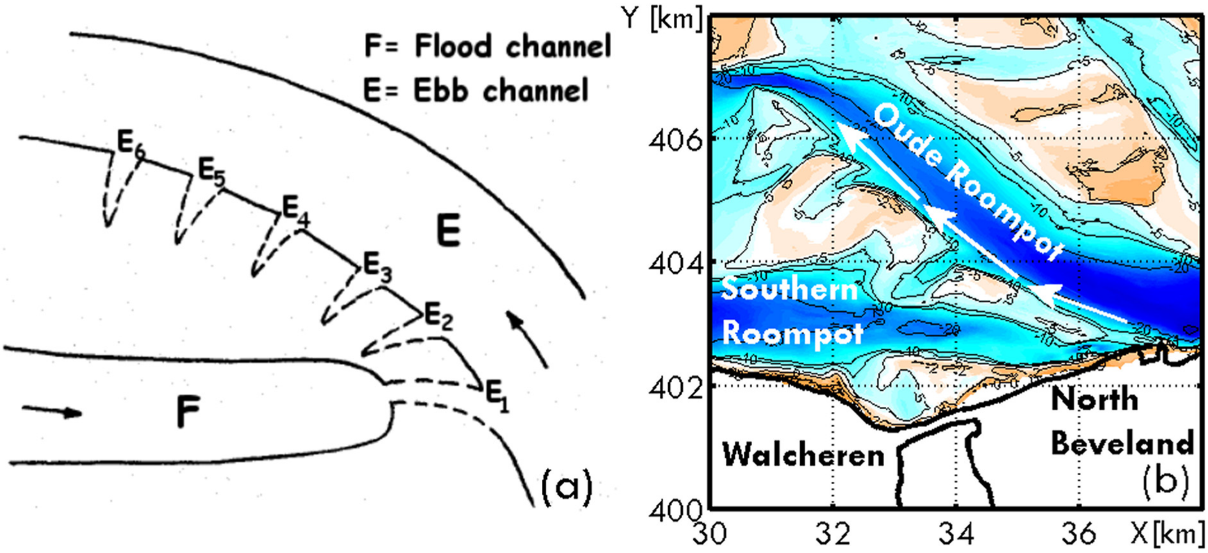

Figure 3.8: (a) Conceptual sketch of migrating ebb channels (E_1 to E_6) generated at the sub-tidal sill (Van Veen *et al.*, 2005). (b) The 1964 bathymetry of the Roompot inlet area. The arrows indicate the migration direction of the small ebb channels.

The Oude Roompot channel used to end in a bend which directed the flow in south-western direction. The northern edge of this bend consisted of a high sill separating the Westgat and Oude Roompot channels. The increased flow from the inlet began to attack this outer bend and eroded the sill. Meanwhile, the south-western end of the bend silted up. Eventually, around 1972 the sill was broken through and thus the Oude Roompot became directly connected to the Westgat channel. This also meant that the Hompels and Noordland shoals were no longer connected. It is tempting to link this breakthrough directly to the changes in tidal flow from the inlet. However, breakthroughs like this one have occurred in the past around the same location. This can be seen in Figure 2.11: Between 1827 and 1886 the shallow part east of the Noordland shoal becomes intersected by a new channel coming from the Roompot, linking the Roompot with the Westgat. Whether the 1972 breakthrough is a direct result of the increase in tidal prism or merely accelerated by it remains unknown.

The Noordland shoal experienced accretion on its northern edge, and as a result straightened in the direction of the Westgat and Roompot channels. As Van den Berg (1986) already pointed out, the Westgat channel showed signs of increased flow as it started to deepen and erode the southern edge of the terminal lobe. Sedimentation-erosion plots of this period also show that the Westgat was pushing a small horse-shoe shaped ridge seaward just south of the terminal lobe (not visible in Figure 3.7). Both these observations are in line with the Westgat receiving more ebb flow from the basin. The development of this horse-shoe shaped sedimentation and erosion pattern is also observed in the seaward part of the Schaar channel, where the increased flow from the inlet scoured the channel and eroded the sill between the Schaar and the Westgat.

The distinctive terminal lobe of the ebb-tidal delta also expanded, mostly in north-western direction, where the Banjaard Channel deposited large quantities of sand on its ebb shield. Also, the entire western edge of the terminal lobe advanced in seaward direction. The Banjaard Channel itself split up and cut into the western end of the Banjaard shoal, creating a linear bar which slowly migrated in westward direction and merged with the terminal lobe in the following decades. This system of Banjaard Channel and bordering linear bars lengthened in northern direction. Between 1972 and 1984 this development did not seem to slow down.

The Krabbengat channel underwent similar development as the Banjaard Channel, scouring and expanding northward and transporting much sediment towards the northern edge of the Banjaard shoal and also onto its own edges. The closure of the Grevelingen basin in 1971 with the completion of the Brouwers dam also played an important role in this development. Due to this dam, the channel marking the northern edge of the Banjaard, called the Brouwershavense Gat, lost most of its discharge. The ebb shield of the Krabbengat channel became much more pronounced and started to move into the Brouwershavense Gat channel. As with the elongation of the Banjaard Channel, this process did not seem to slow down in the period between 1972 and 1984. The Banjaard shoal itself experienced accretion, mostly in the form of old shallow channels filling up.

In its entirety, the ebb-tidal delta seemed to become wider, by means of shoals accreting on their seaward sides and channels pushing their ebb-shields seaward. In our opinion, no reorientation of the ebb-tidal delta is evident from the bathymetrical evolution. The sediment budget shows a distinctive overall increase in sediment volume until 1980 (Figure 3.6). This increase is primarily located on the shoals which gain area and elevation. The main channels show a similar, yet mirrored development, in which they lose sediment because they become deeper.

3.2.4 Research questions

Analysis of the available literature (Haring, 1978; Van den Berg, 1986; Louters *et al.*, 1998) shows that a continuous exporting trend existed for the Eastern Scheldt basin both before and after construction of the dams which cut off the Grevelingen and Haringvliet basins. The sediment budget of the ebb-tidal delta (Figure 3.6) shows a similar, yet mirrored development. The sediment volume increased strongly after 1970, and stabilized around 1980. The peak in volume around 1980 is likely to be erroneous. In the next paragraph we will use a process-based numerical model to investigate whether the development of the tidal asymmetry, residual flow and sediment transport are consistent with these observations. This model is applied as a numerical laboratory, in which certain processes are turned on or off in order to ascertain their importance.

The model is also applied to investigate the influence of the change in tide on the seaward boundary associated with the nodal cycle. Van den Berg (1986) already mentions that the 18.6 year tidal cycle causes an increase of the tidal range between 1969 and 1980. However, Van den Berg (1986) also states that this increase is counteracted by a reduction of the storage capacity brought on by the artificial islands, thereby cancelling out the effect on the tidal prism. As this process occurs on roughly the same timescale as the effect of the interventions, it is important to be able to distinguish between them.

3.3 PROCESS-BASED MODELLING

3.3.1 Method

Process-based numerical models have been used to assist in coastal and estuarine research for the past few decades. These models describe water motion, sediment transport and bed-level changes by solving a coupled set of mathematical equations. The model itself usually consists of several modules, each of which is dedicated to computing a different process. Recent studies (e.g. Elias, 2006; Lesser, 2009) have shown that these types of models are very useful in increasing the spatial and temporal resolution of field measurements (Elias *et al.,* 2006). In this sense the model is applied as a clever way of interpolating or even extrapolating behaviour that is observed in only a limited number of points in space at a limited number of moments in time. One of the prerequisites for this kind of model application is that the model is well-calibrated for those points where measurements are available.

In this study a process-based model is applied in order to gain information on the governing current and sediment transport patterns in different periods, to see how these patterns have changed in response to man-made alterations in basin configuration, and to be able to link the changes in hydrodynamics to the changes in the sediment transport and bathymetrical evolution. It is not the ultimate aim of this study to accurately reproduce the exact transport magnitudes. The aim of this study is to determine how changes in basin geometry and bathymetry influenced the direction and relative magnitudes of the transports caused by the tide.

The focus of this model study will be firstly on the development of the tidal hydrodynamics which force the sediment transport inside and outside the basin. First, the closure of the Volkerak channel in 1969 is modelled to investigate its effect on flow and transport. Next, the same model is run with the bathymetry and tidal forcing of 1982 to see how the adapted bathymetry altered the sediment transport through the inlet. In all these model instances, the model is run for two months. For each time step the model computes flow, sediment transport and bed-level change.

3.3.2 Model Setup

For this research the Delft3D-Flow model (version 3.55.05.00) is used in two-dimensional depth-averaged mode with tidal forcing only. Wave forcing is omitted because we primarily focus on areas which are tide-dominated. Although waves can play an important role in the redistribution of sediment on the shallow parts of the ebb-tidal delta, we assume that their effect on the sediment exchange between basin and ebb-tidal delta is secondary to the effect of the tide. Wang *et al.* (1995) draws a similar conclusion on the influence of waves on the sediment transports between basin and ebb-tidal delta.

The Delft3D-Flow model is discussed in detail in Lesser *et al.* (2004). For application in and around the Eastern Scheldt, a specific model application has been made, called the *KustZuid*-model. The *KustZuid*-model has been designed and constructed as an operational model for predicting water levels for the present-day situation (see Appendix A for the *KustZuid*-model parameter settings). The storm surge barrier is modelled as so-called porous plates across the inlet which cause a loss of energy head. In order to model the period before 1982 these porous plates are simply removed. The model domain uses a well-structured curvilinear grid which incorporates both the Eastern and Western Scheldt basins, the Volkerak channel, and a part of the south-western North Sea coast from the Grevelingen in the north to the Franco-Belgian border in the south (Figure 3.9). The Grevelingen basin, Lake Veere, and Haringvliet estuary have not been included in the grid, because bathymetric data of these areas is lacking for our period of interest. The spatial resolution of the grid varies from more than 2000 m at the seaward boundary, to around 100 m at the Eastern Scheldt inlet. In total, the grid contains 38920 grid points. In order to limit the computational time, only depth-averaged simulations have been made. This is done because the estuary is well-mixed due to the negligible fresh water inflow, and three-dimensional effects have minor influence on the large-scale sediment exchange between basin and ebb-tidal delta. The dilution due to fresh water inflow was already small before the Volkerak dam was built, and became virtually nil after this dam was constructed (Peelen, 1970).

The coastlines of Belgium and Zeeland and the edges of the basins are modelled as closed boundaries with free-slip conditions. Water levels are prescribed on the seaward boundaries as boundary conditions. These boundaries are assumed to be located far away enough from the area of interest (the Eastern Scheldt Inlet). The entire boundary consists of 49 boundary sections, each with its own values for the amplitudes and phases of the astronomical constituents. These values have been derived from a larger-scale model covering the southern North Sea.

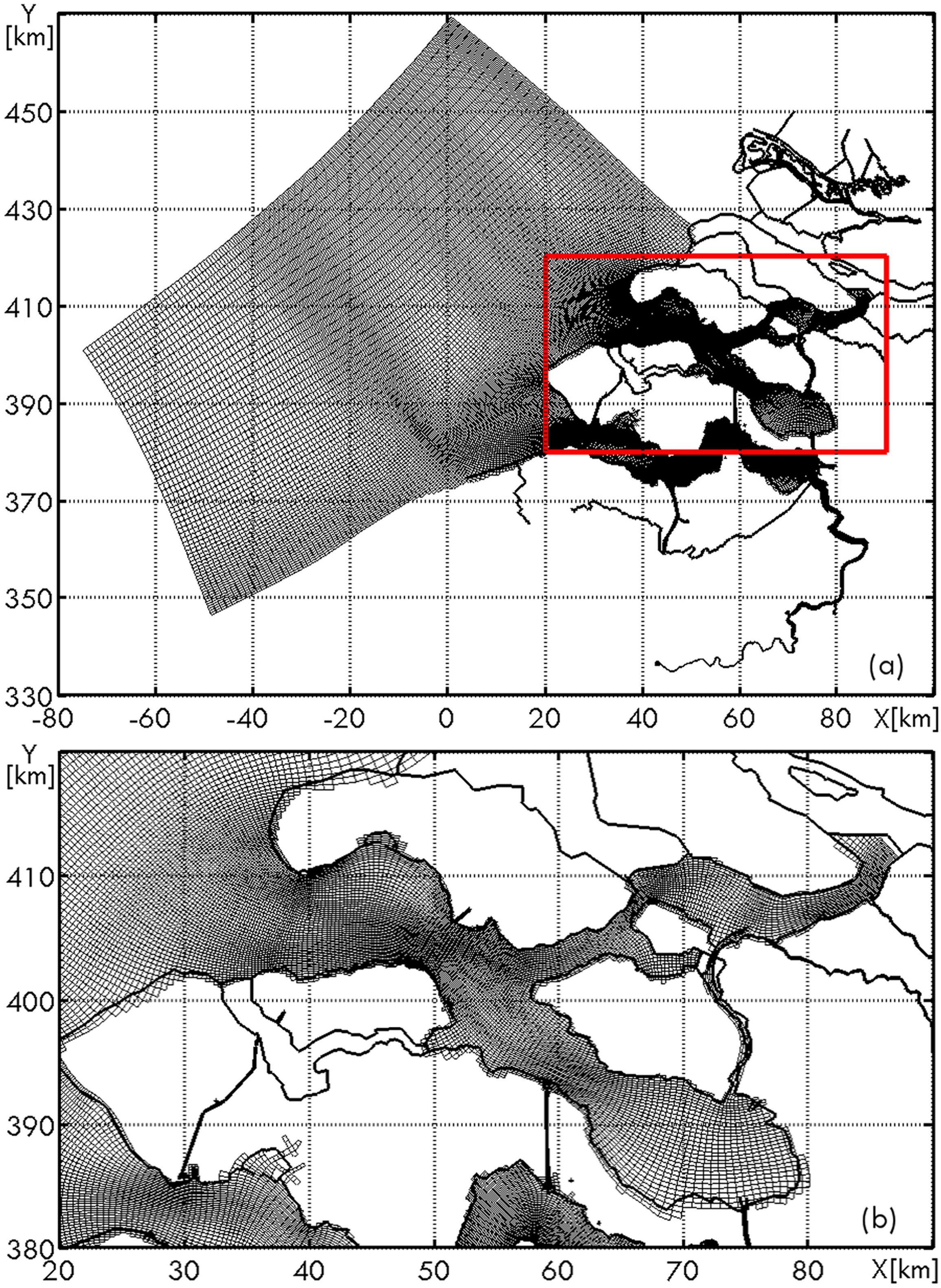

Figure 3.9: (a) KustZuid model grid. (b) Detail of the grid showing the Eastern Scheldt basin.

All model simulations are run for a two-month period. The simulations for investigating the instantaneous effects of the Volkerak dam are run from October 30th to December 30th 1968. The year of 1968 is chosen because the bathymetry of the basin for this simulation is based on the 1968 survey. No other surveys of the basin from the time around 1970 are available in digital format. It has to be noted that the model does not actually portray the real 1968 situation, especially for the ebb-tidal delta, because in 1968 the channels in the Grevelingen inlet were still open. In the model, however, the Grevelingen basin is closed at both ends. The reason for not including the Grevelingen basin in the model is because there is a lack of bathymetrical data for this area for this period.

The simulation for the 1982 period is run from October 30th to December 30th 1982. This simulation period gives us the opportunity to compare model output with discharge measurements performed in November of 1982. A time step of 60 seconds results in a maximum courant number of 15. Reducing the time step to 30 seconds does not result in significant changes in model output. Each run starts from a uniform water level and zero velocities. A period of one day is long enough for the hydrodynamics to spin up before morphological changes are computed. For the eddy viscosity and eddy diffusivity values of 1 m^2/s and 1 m^2/s are chosen. For the bed roughness, a Manning coefficient of 0.025 s/m$^{1/3}$ is applied.

In each run the sediment transport rate is calculated using the Van Rijn (1993) transport formula. From present-day measurements, it is known that the median grain size on the ebb-tidal delta is between 150 and 200 microns on the shoals, and between 200 and 300 microns in the channels. However, no data is available on the spatial distribution of the median grain size for the periods we are interested in. Therefore, we choose to run the simulations with a uniformly distributed median grain size of 200 microns, a sediment density of 2650 kg/m^3, and a dry-bed density of 1600 kg/m^3.

Two different bathymetries are constructed for this study (Table 3.1). Bathymetry A is supposed to represent the 1968 situation of the Eastern Scheldt. This bathymetry is composed of several bathymetrical surveys. For the Eastern Scheldt basin and ebb-tidal delta the 1968 survey is used. For the Volkerak area the 1982 survey is used. No sounding of this area before 1982 was available in a digital format. For the area of the Western Scheldt and the North Sea the survey of 2000 was used. Bathymetry B is supposed to represent the 1982 situation. The basin and Volkerak area are derived from the 1982 survey, the ebb-tidal delta from the 1984 survey. For the area beyond the Eastern Scheldt, again this bathymetry is based on the 2000 survey. The 1982 simulation also incorporates the various construction islands and newly constructed dams. The model for the 1982 situation also involves the scour protection at the location of the storm surge barrier in the form of an unerodable sediment layer at that location. It is very well possible that natural unerodable layers also exist in the basin and inlet area. However, the knowledge on the exact location and nature of these layers is insufficient at present to be incorporated in the model.

Table 3.1: Composition of model bathymetries.

Composed Bathymetry	Bathymetry Volkerak	Bathymetry Eastern Scheldt	Bathymetry ebb-tidal delta	Bathymetry Western Scheldt	Bathymetry North Sea
Bathymetry A	1982	1968	1968	2000	2000
Bathymetry B	1982	1982	1984	2000	2000

For the 1982 situation an extra model run was performed with the 1982 geometry, but with the boundary conditions for 1968 with the Volkerak closed off. In this way we are able to distinguish which changes in transport capacity are due to the changes in bathymetry, and which are due to changes in the tidal forcing.

3.3.3 Model Calibration

The *KustZuid*-model was originally made and calibrated for the present-day situation. This is evident in the reproduction of the tidal propagation. The simulated water levels from a model with the bathymetry and situation from the year 2000 were harmonically analyzed and compared to the harmonic analysis of the observed vertical tide at the same locations. This comparison showed good agreement. However, when the 1982 situation is modelled, i.e. when the barrier is taken out of the model, the amplitude of the M2-component of the vertical tide is overestimated by almost 10 centimetres. Changing the Manning coefficient to a Chézy-coefficient of 50 $m^{1/2}/s$ reduces the amplitudes of M2 to reasonable values (Figure 3.10).

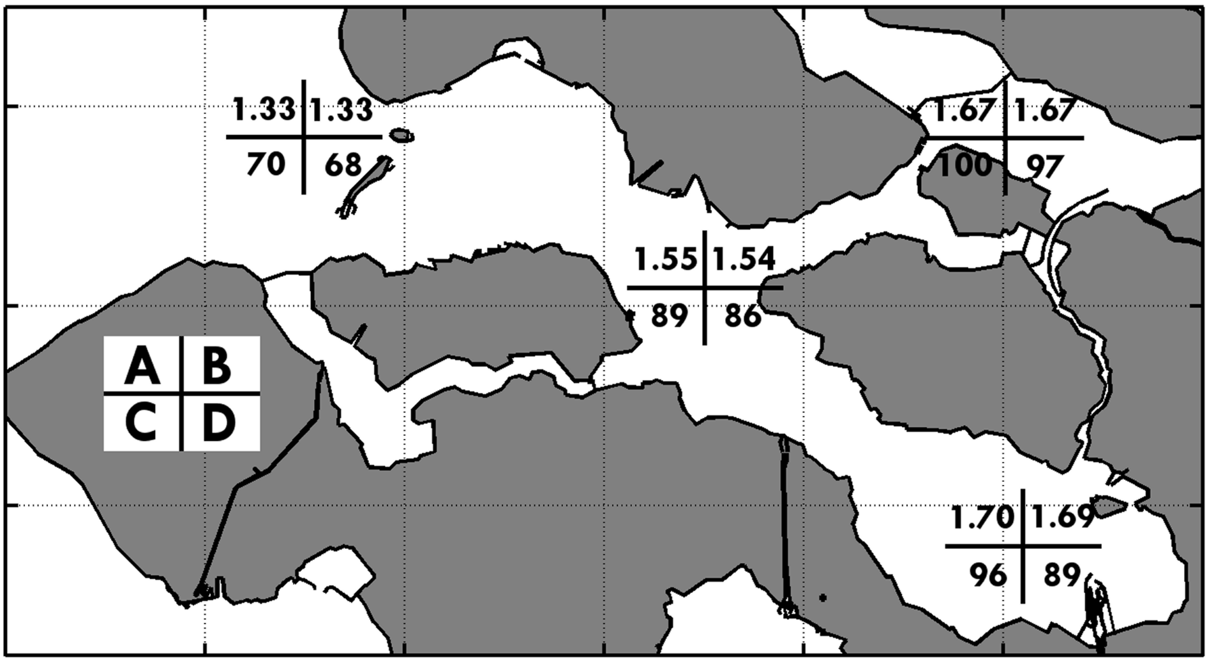

Figure 3.10: Measured and modelled amplitudes and phases of the M2-component of the vertical tide in the Eastern Scheldt basin. A = measured amplitude (m). B = modelled amplitude (m). C = measured phase (degrees). D = modelled phase (degrees).

The distribution of the tidal discharges over the main channels in the inlet is reasonably well represented in the model (Table 3.2). Although the values of the tidal volumes are overestimated, the ratios between these volumes are more or less the same as in reality, both for the 1968 and the 1982 simulation. There are some differences between model and measurements in the changes from the 1968 to 1982 situation. The ebb volumes of the Schaar and Roompot channels decreased in the model, while in the measurements these volumes increased. Comparing flow velocities measured in November 1982 (Rijkswaterstaat 1984)[5] to the flow velocities from the model yields good agreement (Figure 3.11), although some minor underestimation of the peaks is still visible.

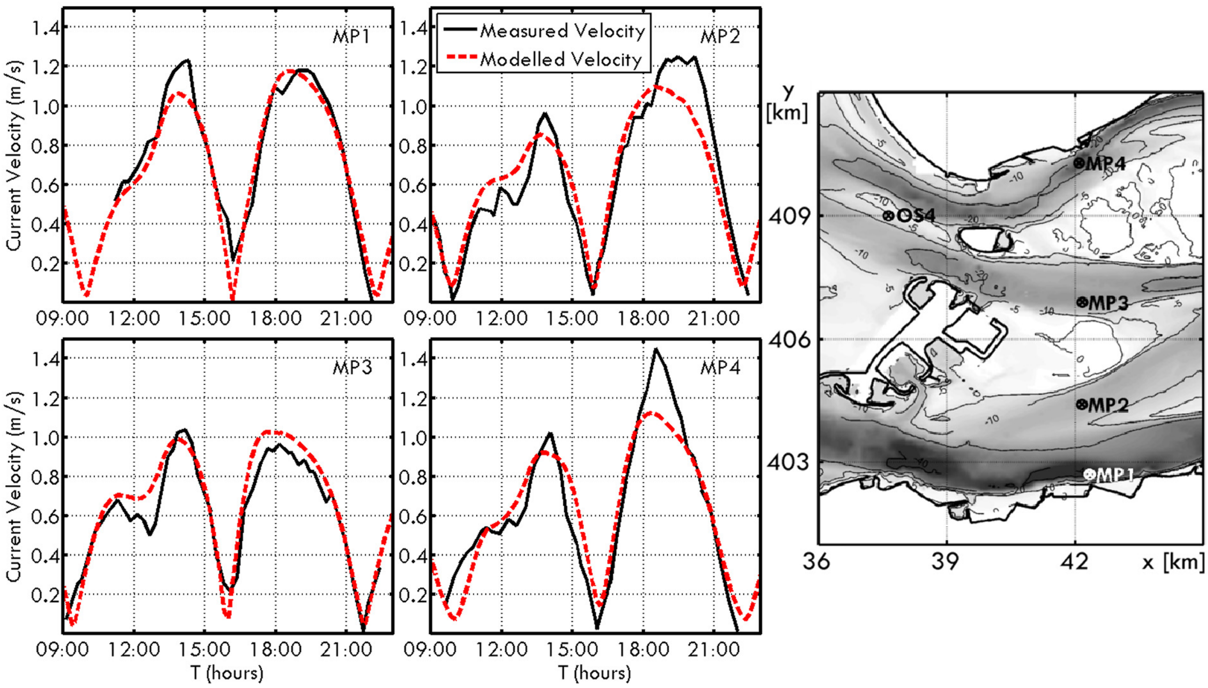

Figure 3.11: Measured and modelled tidal current velocities in the inlet on 02/11/1982.

For the 1968 and 1982 situations, the northern edge of the Volkerak at the location of the Volkerak dam is simply a closed boundary in the model. However, in order to represent the situation that existed before the construction of the Volkerak dam, another boundary condition is needed at the northern end of the Volkerak. This boundary condition is prescribed as a total discharge across the channel. The problem with this method of boundary implementation is that the knowledge on the discharges across this boundary is rather limited. Van den Berg (1986) gives a measured flood volume in 1968 from the Volkerak into the Haringvliet of 120 Mm^3 and a measured ebb volume of 100 Mm^3. This implies there was a residual discharge out of the Eastern Scheldt into the Haringvliet. With this limited knowledge in mind, the boundary is modelled as a total discharge consisting of a component with the M2 frequency and an amplitude of 8500 m^3/s, and a residual discharge out of the Volkerak of 450 m^3/s. The phase of the M2-component is chosen in such a way, that the tidal volumes in the Volkerak and in the more southerly located Keeten channel

[5] Measured data on tidal currents and discharges were kindly provided by Rijkswaterstaat Zeeland with the help of Jan Slager.

approximate the average volumes given by Van den Berg (1986) as close as possible. In this way an M2-phase is derived which is 100 degrees behind the phase of the discharge at the position of the inlet.

Table 3.2: Distribution of tidal volumes in 1971 and 1983 from measurements and model output. Percentages are relative to the total volume.

		Ebb volumes				Flood volumes			
		Measured volume		Modelled volume		Measured volume		Modelled volume	
Inlet channel		m^3 (x10^6)	%	m^3 (x10^6)	%	m^3 (x10^6)	%	m^3 (x10^6)	%
Roompot	07/10/1971	698	56	909	55	717	52	813	53
	26/07/1983	699	57	844	58	698	59	789	58
Schaar	07/10/1971	254	20	329	20	255	19	270	18
	26/07/1983	282	23	325	22	257	22	286	21
Hammen	07/10/1971	284	23	365	22	310	23	379	25
	26/07/1983	237	19	296	20	238	20	287	21
Geul	07/10/1971	35	3	90	5	89	7	122	8
	26/07/1983	0	0	0	0	0	0	0	0
Total	07/10/1971	1256		1653		1367		1542	
	26/07/1983	1219		1458		1192		1355	

3.4 MODEL RESULTS

3.4.1 Simulated changes in flow patterns

Figure 3.12 shows the flow patterns for the 1968 and 1982 situations during maximum flood and ebb flow, all during spring tide. The tide-residual flow field in Figure 3.13a&b shows the intricate patterns that arise from the complex interaction between the flow either entering or leaving the basin, and the shoals that steer and deflect this flow. In the 1968 situation, the southern channel-shoal system consisting of the Hompels shoal and the Roompot channels displays the tide-residual eddy typical for such a main ebb channel (Oude Roompot) and marginal flood channel (Southern Roompot). For the Hompels and Noordland shoals it seems that the direction of the residual flow over these shoals is predominantly flood-directed. On the northern part of the delta, consisting of the Westgat as main ebb channel and the Banjaard shoal, most of the residual flow is directed northward, and no large tide-residual eddies are observed. It is difficult to classify the patterns on the shoal as either flood- or ebb-directed, as a significant part of the flood current flows to the north onto the former Grevelingen ebb-tidal delta. In the Hammen and Schaar channels an interesting circulation pattern is observed. Apparently, most of the flood in this region enters the basin through the Hammen, while most of the ebb is discharged through the Schaar. This is in accordance with the general model of inlet morphology put forward by Hayes (1980), in which the middle part of an inlet is usually an ebb-dominated channel, and the parts of the inlet close to the barrier islands are usually flood-dominated.

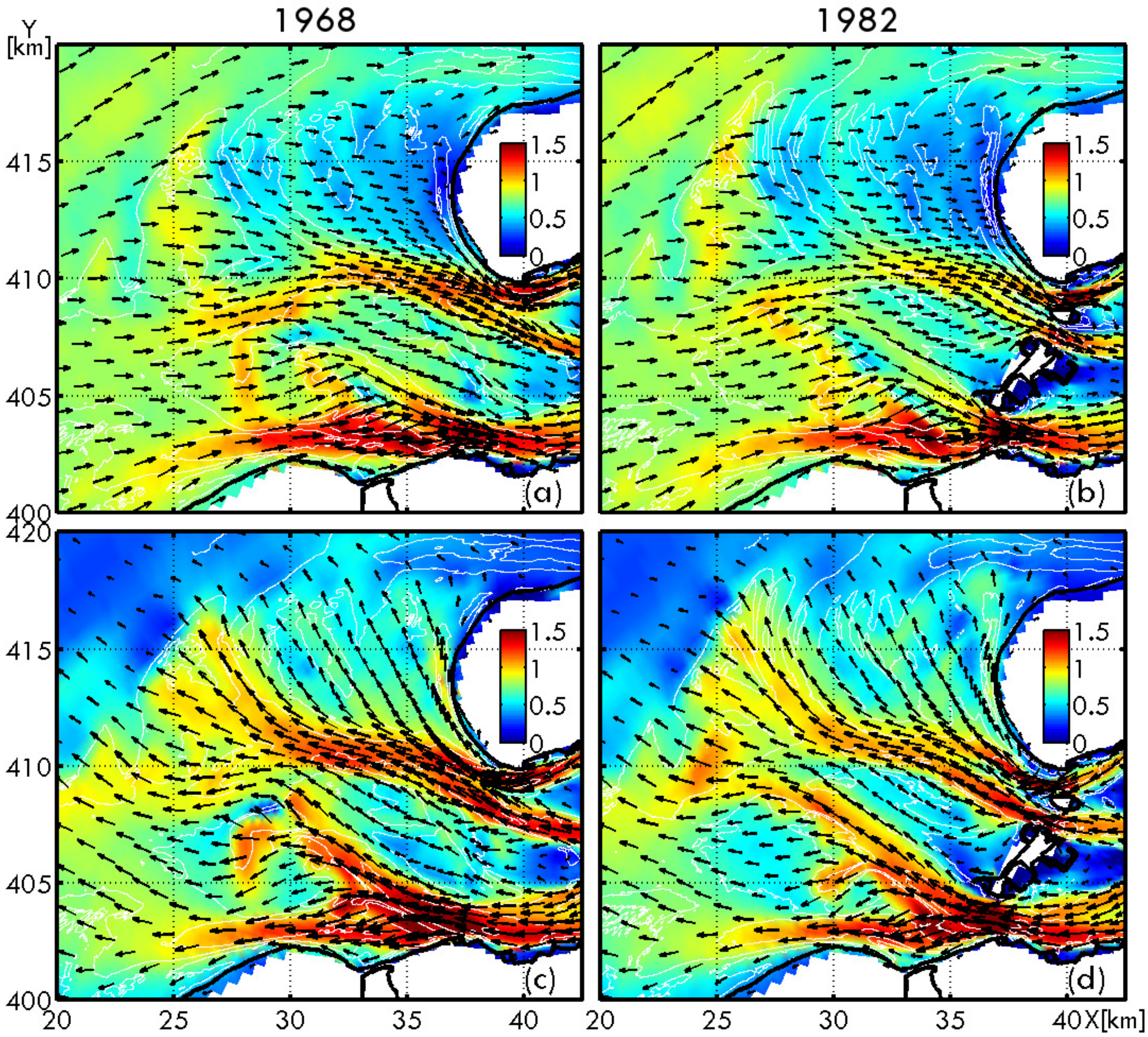

Figure 3.12: (a,b) Maximum flood current in the 1968 and 1982 situation. (c,d) Maximum ebb flow in the 1968 and 1982 situation. Units in the colorbar are in m/s.

When comparing the tidal flow patterns of the situations directly before and after closure of the Volkerak channel, it appears that on the ebb-tidal delta the patterns have not changed. On the other hand, the flow magnitudes increased. No drastic changes in patterns are observed, only the intensity increased. From this it is concluded that the closures in the Volkerak channel have not altered the phase or direction of the tidal flow entering or exiting the inlet in any significant way.

Differences in the patterns between the 1968 and 1982 situations are most noticeable in the south-western part of the delta. The main channels are more elongated, and the ebb jets out of the inlet gaps seem to be more concentrated. As a result the tide-residual eddies are much more eccentric and much weaker, especially around the Roompot-Hompels channel-shoal system.

It is interesting to notice that the residual flow pattern (Figure 3.13a&b) along the Schouwen coast displays a stagnation point. This point is even more clearly visible during maximum flood. North of this point, the current in the Krabbengat channel is predominantly northward directed, even during flood. This northward dominance seems to get stronger going north, both for the 1982 and the 1968 situations. This might have contributed to the growth of the northern Krabbengat end. As it migrated further north, the residual flow driving its development became stronger. However, this analysis cannot investigate how the closure of the Grevelingen inlet in 1971 influenced this development, because the model does not include the Grevelingen basin. Also, wave action is not taken into account, which is likely to be of high importance on shallow areas such as this channel end.

3.4.2 Simulated changes in transport patterns

The same general conclusion on the influence of the closure holds for the tide-averaged sediment transport vectors (Figure 3.13). The construction of the Volkerak dam and the associated tidal volume increase caused the existing pattern to be amplified, but it did not cause these patterns to change shape. The transports through the main inlet channels were already ebb-directed in the period before the dam construction, and these transports merely increased. The residual transport patterns also show strong gradients at the location of the shoal between the Oude Roompot channel and the Westgat channel, in accordance with the observation of the erosion and eventual breach of this shoal. Apart from this, there is also a strong seaward directed transport through the Westgat north-westward into the Banjaard Channel and westward onto the terminal lobe.

A noticeable difference between 1968 and 1982 is seen in the way in which the transport patterns in the vicinity of the Oude Roompot channel have changed. In the 1968 simulation a part of the transport from the inlet is deflected in south-western direction by the Noordland-Hompels shoal connection. At the same time the transports over this shoal connection into the Westgat show large local gradients, signifying the erosion of this shoal. In the 1982 simulation the Oude Roompot is no longer deflected, and flows directly into the Westgat. In this new situation the Oude Roompot seems to be more concentrated and can now reach the southern end of the terminal lobe. A sharp gradient in the transport is observable along this southern end, indicating that the Oude Roompot is in fact feeding this area with sediment.

The residual transport plots show large residual transports towards the sub-tidal Onrust sill between the Southern Roompot and Oude Roompot channels. This is consistent with the observation of the high morphological activity of this area (Figure

3.8). It is also in accordance with the general view on sills put forward by Van Veen *et al.* (2005), who argues that even though at the sill strong currents can occur, the sill maintains its elevation due to large sediment transports towards the sill.

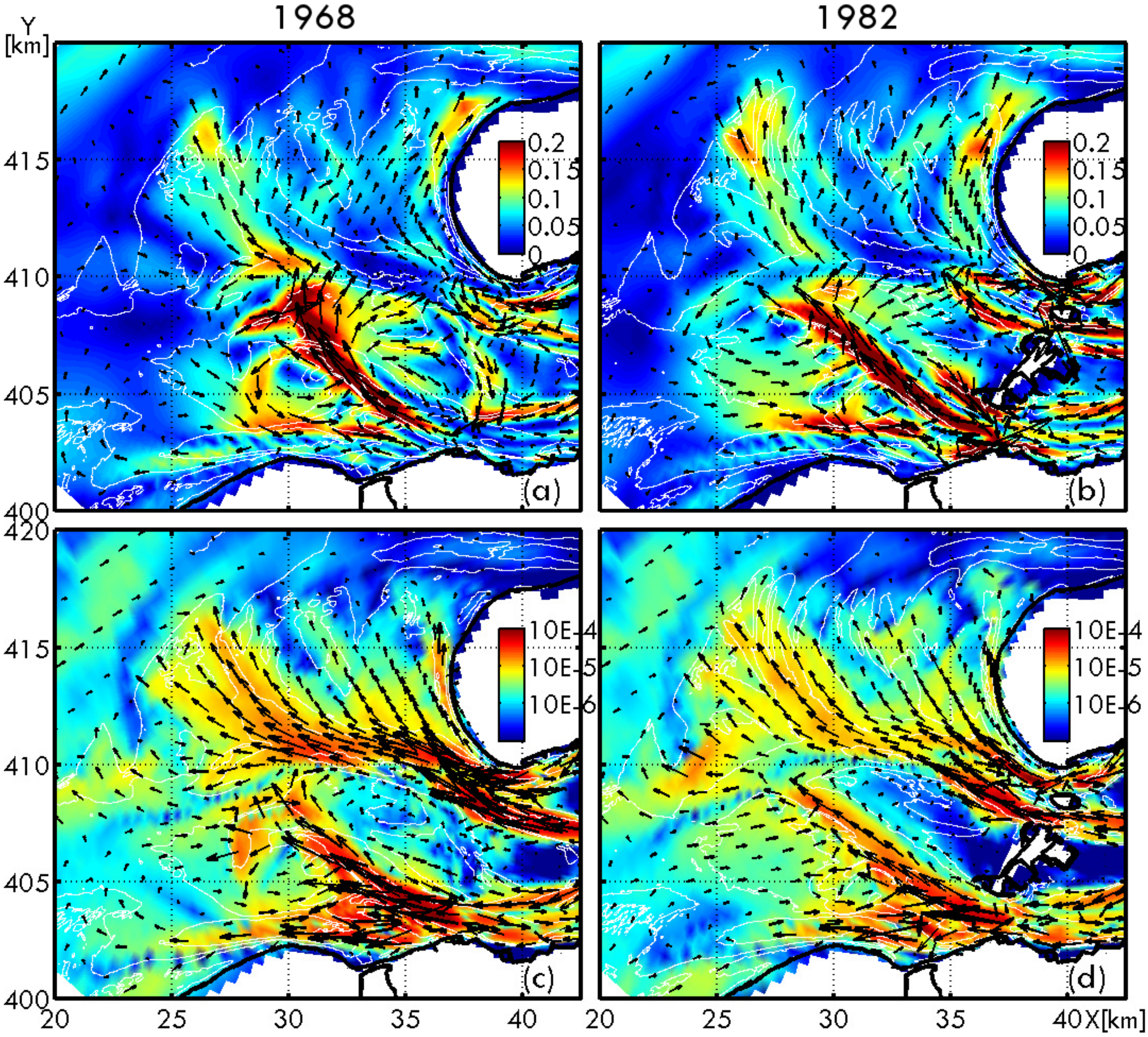

Figure 3.13: (a,b) Tide-residual flow velocities in the 1968 and 1982 situations. Units in m/s. (c,d) Tide-residual sediment transports in the 1968 and 1982 situations. Units in $m^3/m/s$.

The residual transport plots for both the 1968 and 1982 simulations (Figure 3.13) show strong transports from the Westgat to the Banjaard Channel and over the terminal lobe. In both cases these transports seem to terminate at the channel end, which is in accordance with the observation of the growing terminal lobe and channel endings. However, the 1982 transport magnitudes in this region are as high, or in some places even higher than the 1968 magnitudes. This can partly be explained by the development of the Banjaard Channel itself. According to the model, the 1982 Banjaard Channel geometry draws more ebb discharge from the Westgat than the 1968 geometry, even when identical tidal forcing is applied. As mentioned earlier, this can be linked to the lengthening of the Oude Roompot channel and breach of the Noordland shoal. Because of this, more of the ebb discharge coming from the Hammen and Schaar channels is pushed into the Banjaard Channel. However, also here we have to acknowledge that wave action might play an important role in redistributing sediment over the terminal lobe and shaping the end of the Banjaard Channel.

Table 3.3: Modelled net yearly sediment transports through the main inlet channels.

Simulation	Roompot	Schaar	Hammen	Total Inlet
1968 open Volkerak (Mm^3/year)	-1.12	-0.98	-0.55	-2.65
1968 closed Volkerak (Mm^3/year)	-1.55	-1.40	-0.79	-3.74
1982 closed Volkerak (Mm^3/year)	-0.99	-0.71	-0.16	-1.86
1982 closed Volkerak with 1968 boundary (Mm^3/year)	-0.85	-0.62	-0.15	-1.61

Table 3.3 shows the net transports through cross-sections across the inlet channels computed by the model. For clarity, the transports are extrapolated to yearly values. The net transport of sediment through the three main channels at the location of the inlet is strongly ebb-directed. There is a clear increase in export in response to the Volkerak dam implementation, and a strong decrease in export when the 1982 bathymetry is applied. This result is in accordance with the observation by Louters *et al.* (1998) that the natural export decreases after 1970. These numbers also give further support to the idea that the original peak in ebb-tidal delta sediment volume around 1980 is erroneous. The export of almost 2 Mm^3 out of the basin given by the model makes it even more unlikely that the ebb-tidal delta could shed a net volume of about 8 Mm^3 per year.

The distribution of the export over the three inlet channels also changes. In the two 1968 simulations, the Roompot takes care of roughly 40% of the sediment export, the Schaar 35%. In the 1982 simulation, this distribution changes to more than 50% for the Roompot. The Schaar still discharges a little more than 35% of the total sediment export, and the Hammen experiences a strong decrease relative to the other inlet channels.

The seaward boundary does not stay the same between 1968 and 1982. De Ronde (1983) shows that the offshore tidal range increases on a scale of roughly 10 cm per century. Also, the tidal range fluctuates due to the so-called nodal tide, which has a period of 18.6 years. Although its amplitude is relatively small, the nodal tide can have a morphological impact. According to De Ronde (1983), the phase of the nodal tide is such, that the average tidal range measured at the mouth of the Western Scheldt has a low point around 1970 (±3.70 m), and a high point around 1979 (±3.85 m).

To investigate the possible influence of this change in seaward boundary, an extra model run has been performed with the 1982 model geometry and bathymetry, but with the 1968 boundary conditions applied. Results from this model run indicate that indeed the change in the seaward boundary has effect (Table 3.3). The transports in the original 1982 simulation are stronger than the transports in the 1982 simulation with the 1968 boundary, indicating that at least part of the morphological activity can be attributed to this change on the seaward boundary. Van den Berg's statement about the tidal volume does seem to be correct: the average tidal volume through the inlet hardly changes between the 1968 and 1982 simulations (1416 Mm^3/tide in the 1968 simulation, and 1408 Mm^3/tide in the 1982 simulation). Note that these numbers are the average volumes over a two month simulation period.

Table 3.4: Modelled net yearly sediment transports through the red transect in Figure 3.14.

Simulation	Keeten channel
1968 open Volkerak (Mm^3/year)	0.01
1968 closed Volkerak (Mm^3/year)	-0.60
1982 closed Volkerak (Mm^3/year)	-1.45
1982 closed Volkerak with 1968 boundary (Mm^3/year)	-1.22

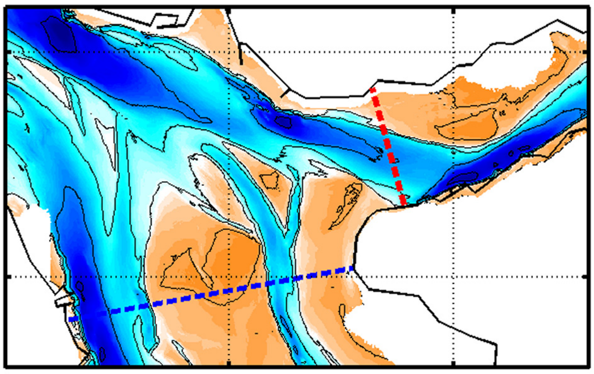

Figure 3.14: Overview of Keeten channel and middle part of the Eastern Scheldt.

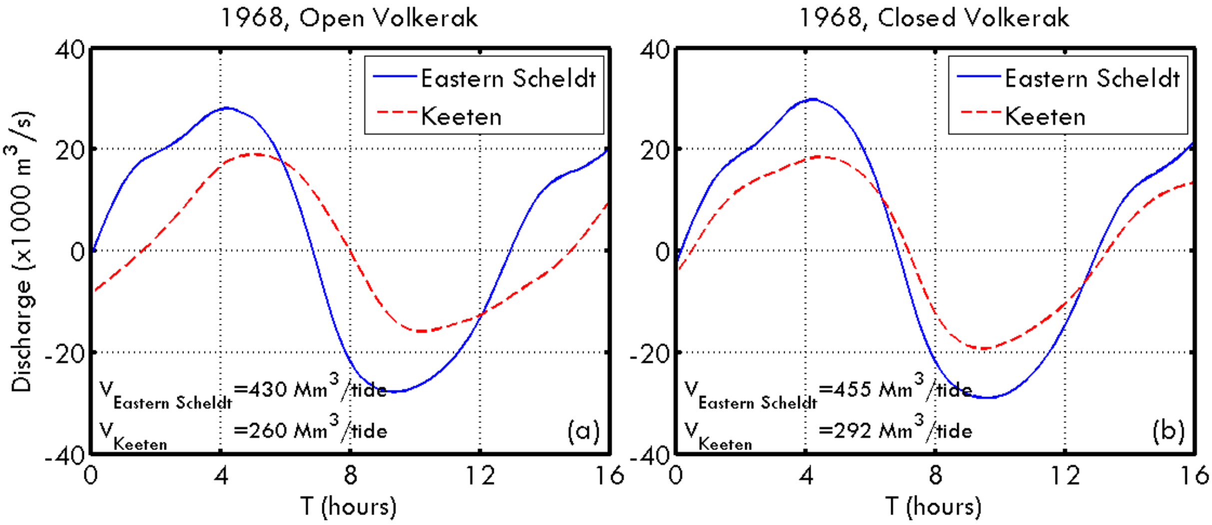

Figure 3.15: Modelled discharge curves through the red and blue transects in Figure 3.14. (a) Simulation with 1968 bathymetry and open Volkerak. (b) Simulation with 1968 bathymetry and closed Volkerak. V= simulated average tidal volume.

Table 3.4 shows the computed net sediment transports through the entrance of the Keeten channel. According to the model, the net transport prior to the closure of the Volkerak were close to zero. The exact value and direction of this transport is somewhat sensitive to the parameters chosen for the discharge boundary at the northern end of the Volkerak. If these parameters are varied within reasonable limits (+/- 15%), the transport also varies between +0.2 and -0.2 Mm^3/year. The variance in the transport through the inlet is roughly the same. In Figure 3.5 it was shown that inside the basin in the Keeten channel, the cross-sectional area decreased between 1968 and 1982. This decrease occurred even though the tidal volume through this channel increased. The model computes that the sediment transport through the same cross-section was larger in 1982 than in 1968 (Table 3.4). This is in line with the hypothesis that this channel section was experiencing an overload of sediment coming from the Zijpe and Volkerak channels. The more south-westerly located Keeten channel received more sediment than it could transport into the Eastern Scheldt basin. Thus, the channel cross-section became smaller. However, because the tidal currents must have increased, also the net sediment transport grew.

Figure 3.5 also shows a small reorientation of the Keeten channel where it connects to the Eastern Scheldt basin. In section 3.2.3 a hypothesis was made that this reorientation was caused by a change in the phase of the tidal discharge going through this channel. Results from the 1968 simulations with and without the Volkerak dam confirm that indeed this phase changed in response to the presence of the dam (Figure 3.15). As a result, the discharge in the Keeten channel becomes more in phase with the discharge in the Eastern Scheldt.

3.5 Discussion & Conclusions

From the observed behaviour as well as a numerical model study it is concluded that for the largest part of the Eastern Scheldt inlet system, the closure of the Volkerak channel merely amplified the previously existing trend for scour and export of sediment. In the inlet area and on the ebb-tidal delta, the closure caused an increase in tidal flow, and coupled to that an increase in transport. At the main inlet channels, most of the sediment was transported by the Roompot channel, which also took care of the larger part of the tidal discharge. Seaward of the inlet, parts of the proximal ebb-tidal delta made way for the ebb channels coming from the inlet which were growing deeper and longer under the increased discharge from the basin.

A considerable part of the deepening inside the Eastern Scheldt since 1960 was a result of dredging. When the remainder of 40 Mm^3 of natural erosion given by Louters *et al.* (1998) is distributed evenly over the period between 1960 and the construction of the storm surge barrier in 1986, an average yearly export of about 1.5 Mm^3 is obtained. However, it is more likely this export showed a peak around 1970, and diminished from that time onward. The model runs confirm this: the simulation with a 1968 bathymetry and a closed off Volkerak produces up to 2 times more sediment export at the inlet than the simulation with the 1982 bathymetry. The nodal tidal cycle caused a slight increase in tidal range between 1968 and 1982. Incorporating this effect in the simulations causes the export rate in 1982 to be larger than it would have been without the nodal cycle. However, even when the nodal tide is incorporated in the simulation, the model still computes transport rates which are far stronger right after construction of the dam than in 1982.

On the ebb-tidal delta, the increased flow from the inlet amplified the morphological activity. The fact that this increased activity persisted even when the sediment supply from the basin dropped, means that this activity is probably mostly driven by the larger flow. The main ebb channels straightened and lengthened, making them more efficient at depositing sediment further away on the main ebb shields and the terminal lobe. The ebb shields located on the northern edge of the ebb-tidal delta were pushed into a region with stronger residual flow. This could explain why the growth and migration speed of these elements hardly decreased over time, although it still remains to be investigated what the effect of waves and the closure of Grevelingen inlet had on this development.

Wave forcing is not included in the model. In general, waves on Dutch ebb-tidal deltas are dominant on the shoal areas and cause redistribution of the sediment towards the coast. They also cause higher sediment concentrations through enhanced bed shear stress, wave breaking and stirring. The exclusion of wave forcing in the model poses limitations on its ability to reproduce the sediment transport patterns on shallow areas. The manner in which waves reshape the ebb-tidal delta of the Eastern Scheldt is addressed in chapters 4 and 5.

From the measured data and model results it can be concluded, that in the decades before the dams were implemented, the basin was already exporting sediment. This export had already lasted for more than a century. The construction of the dams in the nineteen sixties merely amplified the general erosive trend. This leads to the conclusion that the adaptation of the entire Eastern Scheldt system to a new equilibrium state was probably far from completed by 1982.

Chapter 4

MORPHOLOGICAL EFFECTS OF THE STORM SURGE BARRIER ON THE EBB-TIDAL DELTA[6]

4.1 INTRODUCTION

In the previous chapters the evolution of the ebb-tidal delta was described up until the start of the construction of the storm surge barrier in 1983. This chapter describes the behaviour of the ebb-tidal delta since the completion of the storm surge barrier up until the present day. The structure of this chapter is somewhat similar to that of chapter 3. First, observations of hydrodynamics and bathymetry are analysed in section 4.2. Based on this analysis, a conceptual model is made describing the sediment transport on the ebb-tidal delta. This conceptual model is then tested using a process-based model in sections 4.3 and 4.4. The findings from both the data analysis and the model study are integrated in the discussion and conclusions in section 4.5.

Tidal inlets and basins can play an important role in the sediment budget of the adjacent coastal zone (Stive and Wang, 2003). Depending on the history, the geology and the shape of the basin, it can act as either a source or a sink of sediment. Tidal inlet morphology is characterized by complex interactions between currents, waves and sediment on varying spatial and temporal scales. This behaviour can change considerably as a result of human interventions such as dredging, damming, land reclamation, or jetty construction in and around the basin or inlet. Therefore, knowledge of the hydrodynamic and morphological effects of these types of interventions is important for the management of the coastal zone. This chapter focuses on the effects of one particular case of human intervention: the storm surge barrier in the Eastern Scheldt tidal inlet.

The Eastern Scheldt tidal inlet (Figure 4.1), located in the south-western part of the Netherlands, has experienced large changes in hydrodynamics and morphology in

[6] An edited version of this chapter was submitted to Coastal Engineering Journal by authors M. Eelkema, Z.B. Wang, A. Hibma, and M.J.F. Stive.

response to the construction of several dams in its basin (constructed between 1965 and 1970) and a storm surge barrier in the inlet (constructed between 1983 and 1986). This storm surge barrier is open under normal weather conditions, allowing the tide to pass through the inlet, but closes during storm surges. However, even though it was designed as an open barrier, it still has a strong effect on the tidal hydrodynamics, and through that, the morphology.

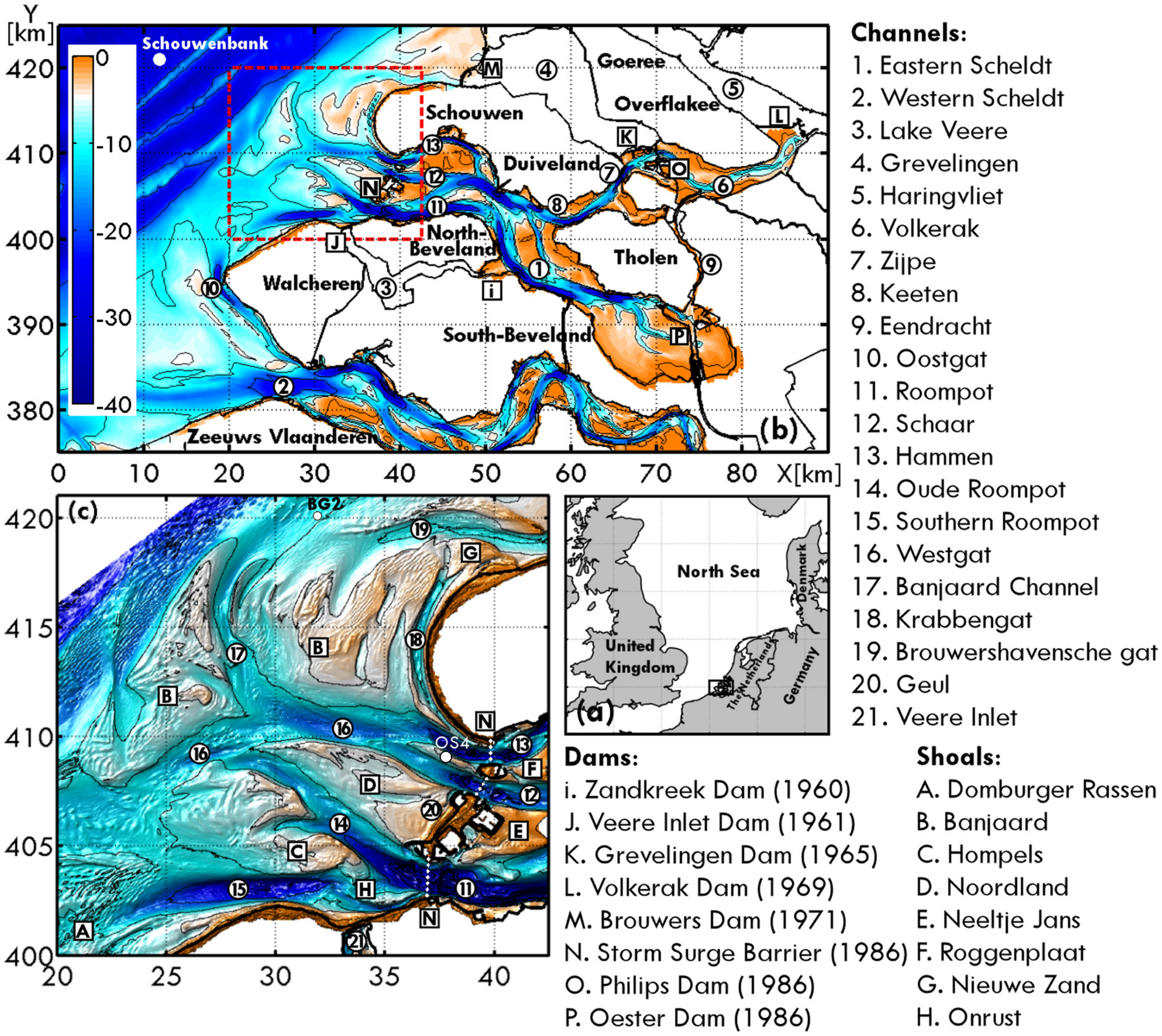

Figure 4.1: Overview of the Dutch south-western delta and the Eastern Scheldt tidal inlet. Depths are in m. Coordinates are based on the Paris coordinate system.

The effects of the storm surge barrier on the morphology of the channels and intertidal flats inside the basin have been well documented in a number of papers and reports (e.g. Ten Brinke *et al.,* 1994; Mulder and Louters, 1994; Vroon, 1994; Louters *et al.*, (1998); Van Zanten and Adriaanse, 2008). As a result of the storm surge barrier, the average tidal flows inside and outside the basin have decreased. Inside the basin this has led to degradation of the intertidal area. Because the tidal current is the main process that enables sediment transport towards the intertidal area, the decrease in currents has also led to a decrease in sediment transport towards the flats. Meanwhile, wind waves inside the Eastern Scheldt, which are the main erosive process for tidal flats, are not affected by the presence of the barrier. As a result, the flats are being eroded more by wind waves than that they are being built up by currents, and thus are experiencing net erosion. This degradation has consequences on navigation, fishery, dike safety, and especially nature values. The sediment budget of the basin indicates that ever since the barrier has been in place, the basin has received virtually no sediment from outside. Apparently, the storm surge barrier is acting as a blockage for sediment transport.

This combination of effects has created a unique situation on the seaward side of the barrier: The ebb-tidal delta has experienced decreased tidal flow coming out of the inlet, but exchanges virtually no sediment with its basin. The morphological activity declined, and the sediment volume has decreased. However, it is yet unclear on what time scale the ebb-tidal delta is adapting, nor where the eroded sediment is transported to (Aarninkhof and Van Kessel, 1999; Cleveringa, 2008; Huisman and Luijendijk, 2008). The response of the sediment budget (surplus or deficit) is an important factor in coastal maintenance policy, as we know from looking at other tidal inlets under the influence of human intervention (Van de Kreeke, 2006; Elias, 2006). Also, knowledge on the behaviour of channels on the ebb-tidal delta can be valuable, because some of those channels are positioned very close to the coastline. A shift in the position of those channels might lead to increased local coastal erosion.

The research goal of this study is to gain understanding of the behaviour of an ebb-tidal delta in response to the construction of a storm surge barrier by studying the Eastern Scheldt Inlet. This chapter describes the observed morphological development of the Eastern Scheldt's ebb-tidal delta for the period between 1986 and 2008, i.e. the period after completion of the storm surge barrier. This chapter also presents results of a process-based model study which is aimed at gaining further understanding of the relevant processes that shape the ebb-tidal delta, and how these processes changed in response to the barrier's construction.

4.2 OBSERVATIONS

4.2.1 Bathymetry and morphology of the ebb-tidal delta before 1983

In the decades before 1965, the Eastern Scheldt exported large quantities of sediment (around 2 million m^3 per year) towards the ebb-tidal delta through its inlet (Haring, 1978). The period between 1965 and 1983 is characterized by the effects of the back-barrier dams in the Eastern Scheldt built in the sixties, called the Grevelingen dam and the Volkerak dam. The implementation of these dams caused a significant increase in tidal prism, which was observable in the response of bathymetry; the sediment export and the rates of channel deepening and ebb-tidal delta growth all increased. This export was caused by the strong ebb-dominant asymmetry in the tidal flow. The construction of the back-barrier dams thus amplified the pre-existing exporting trend by increasing the imbalance between tidal prism and channel area. Van den Berg (1983) and Chapter 3 of this thesis give detailed overviews of this morphological development of the ebb-tidal delta between 1965 and 1983.

4.2.2 Tide, waves and sediment in the vicinity of the inlet

In the present day, the Eastern Scheldt (Figure 4.1) is an elongated tidal basin of approximately 50 km in length and a surface area of 350 km^2. As explained in the previous chapter, the connections to the adjacent estuaries were closed off with dams in the nineteen sixties. The inlet is located between two (former) islands called Schouwen and North-Beveland, and consists of three main channels, separated by shoals. Seaward of the inlet the mean tidal range is 2.9 meters. The tidal range increases to roughly 3.5 meters at spring tide, and decreases to 2.3 meters at neap tide. The total tidal prism passing through this inlet before barrier construction was on average 1200 Mm^3/tide (De Bok, 2001). Most of this prism passed though the southern channel, called Roompot, which reached depths of more than 40 meters. The two smaller northern channels, Schaar and Hammen, had a combined tidal discharge which was less than that of the Roompot, and reached depths of roughly 20 meters.

The ebb-tidal delta consists of a number of shoals, intersected by the ebb channels coming from the inlet. The main southern ebb channel, called Oude Roompot, is flanked by the Hompels and Noordland shoals. The northern edge of the ebb-tidal delta consists of a large shoal, called Banjaard. The southern edge of this shoal area is the Westgat channel, and the shoal itself is intersected by two smaller ebb channels (Banjaard Channel and Krabbengat).

Waves are important for the development of an ebb-tidal delta, because wave-induced currents can transport sediment, and they can stir up sediment leading to higher sediment concentrations. The wave climate observed between 2005 and 2010, measured at Schouwenbank station (Figure 4.2a & Table 4.1) consists mainly of wind-generated waves from the North Sea with only a minor contribution of swell. The long-term mean significant wave height at this location is 1.1 m, and waves higher than 4 m occur less than 0.2% of the time. The directional distribution shows two distinct wave directions (Figure 4.2a), one between 225 and 270 degrees, and one between 315 and 360 degrees. Both directions are more or less equal in strength. Closer to the coast the dominance of certain wave directions might be different. According to Huisman and Luijendijk (2008) there is a north-eastward directed littoral transport along the Walcheren coast, and a southward directed transport along the coast of Schouwen. Both of these transports are in the order of 10.000 m^3 per year.

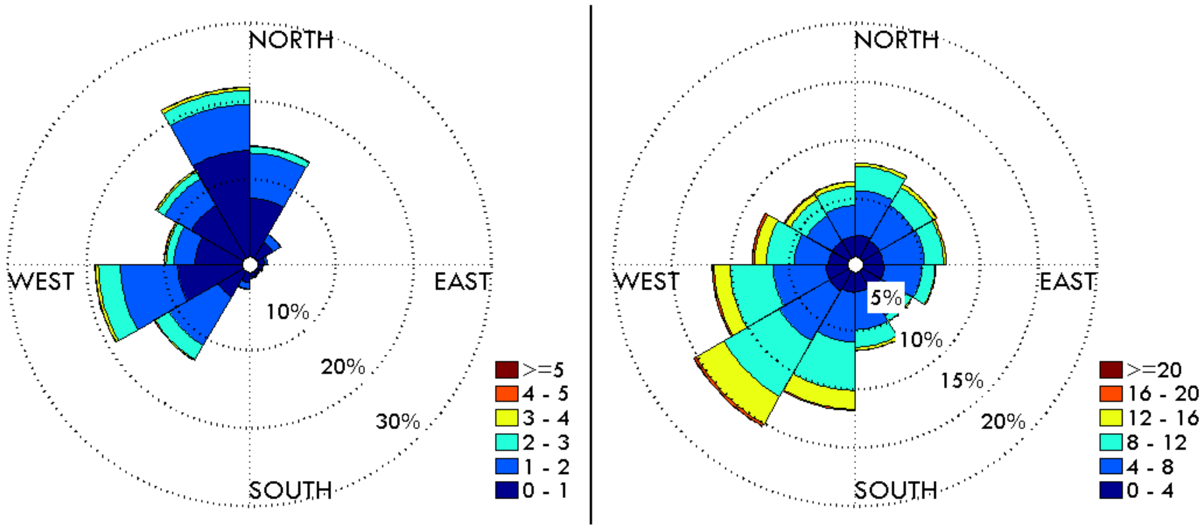

Figure 4.2: (a) Wave rose at Schouwenbank station (offshore). Wave heights are in m. (b) Wind rose at OS4 station (in the inlet). Wind speeds are in m/s. See Figure 4.1 for the locations of the stations.

Table 4.1: Wave climate measured at Schouwenbank station (see Figure 4.1b for location). Quantities are percentages.

H_{sig} (m)	Wave direction class (degrees) 0-45	45-90	90-135	135-180	180-225	225-270	270-315	315-360	Total (%)
<1	9.17	1.67	0.78	0.78	2.61	10.88	9.56	18.09	53.55
1-2	6.47	0.69	0.12	0.20	2.21	13.13	4.30	8.12	35.25
2-3	0.86	0	0	0	0.30	4.59	1.36	2.38	9.49
3-4	0.11	0	0	0	0	0.54	0.34	0.55	1.53
4-5	0	0	0	0	0	0.06	0.03	0.08	0.17
>5	0	0	0	0	0	0	0	0.01	0.01
Total (%)	16.61	2.36	0.90	0.98	5.13	29.20	15.59	29.23	100

The wave gauge known as OS4 (Figure 4.1c) is positioned in the inlet just seaward of the storm surge barrier, and has been measuring wave heights since 1980. The long-term mean significant wave height at this location is only 0.5 m, and has never exceeded 2.8 m. Battjes (1982) showed that these wave heights have a distinct tidal signal (Figure 4.3b). During low water, waves are significantly lower than during high water. This is easily explained: With lower water levels, the shoals in front of the inlet are more effective at dissipating wave energy than with higher water levels. Battjes (1982) also noticed that this effect is hysteretic: The same tidal elevation during ebb produces a lower wave height than the same tidal elevation during flood (Figure 4.4). According to the same source, this effect is due to current-refraction and wave-current interaction on the ebb-tidal delta.

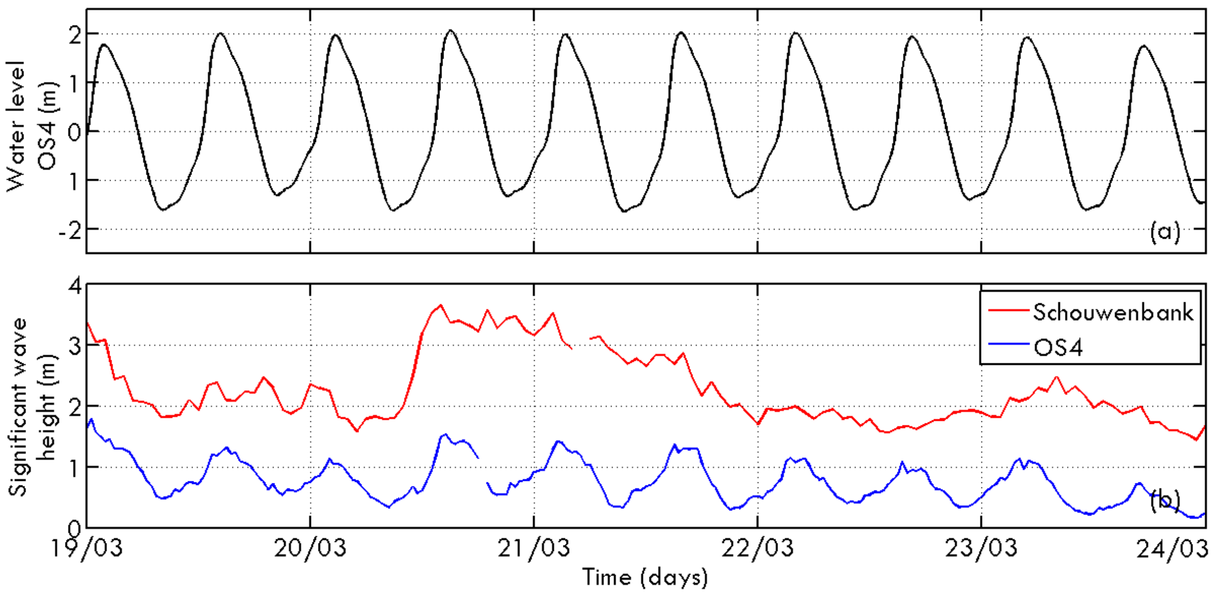

Figure 4.3: (a) Water level at station OS4 (see Figure 4.1 for location) measured in march 2007. (b) Significant wave heights measured offshore (Schouwenbank) and in the inlet (OS4).

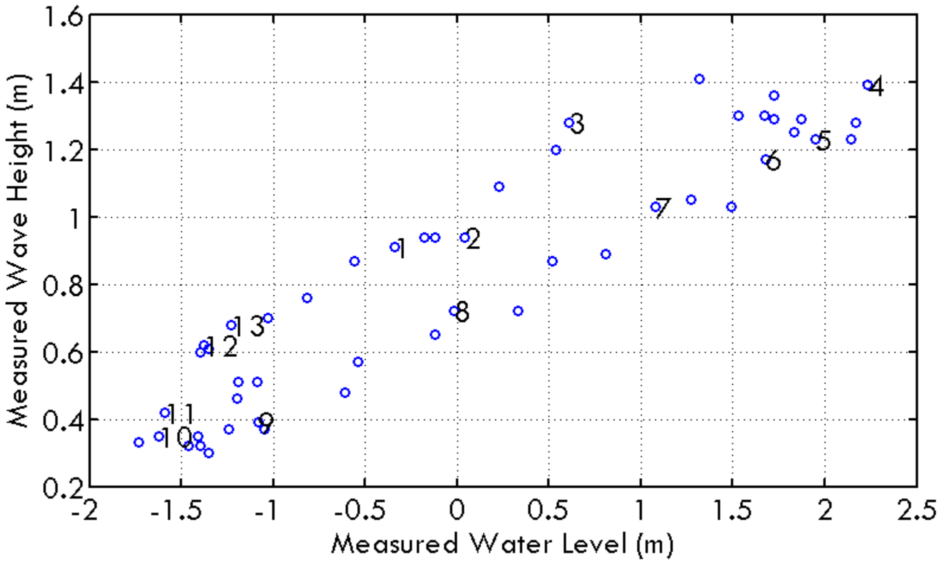

Figure 4.4: Measured water level and significant wave height at OS4 on march 21st 2007. Numbers in the figure indicate hours after midnight.

Figure 4.5 shows the median grain size on the ebb-tidal delta. This figure shows a distribution of relatively coarse material in the channels (250 μm $<d_{50}<$ 400 μm), and more fine material on the shoals ($d_{50}<$250 μm). The scour holes at both sides of the barrier are visible as areas with coarser sediment (d_{50} $>$ 400 μm). Another feature that stands out is the area with very fine material in the middle of the Hompels shoal. This is most likely the old bend at the end of the Oude Roompot, which became abandoned at the end of the nineteen sixties. This bend was probably filled up with fine material from the basin. In the upper left corner the Zeeland sand banks are also clearly visible. The grain size distribution on these shore-parallel sand banks seems correlated to the depth, as is also observed at other sand banks (Walgreen *et al.* (2004). This correlation is not uniform. On some locations, the crests consist of fine sediment, and the troughs are coarse. However, on other locations this correlation is reversed, with fines in the troughs and coarse sediments on the crests.

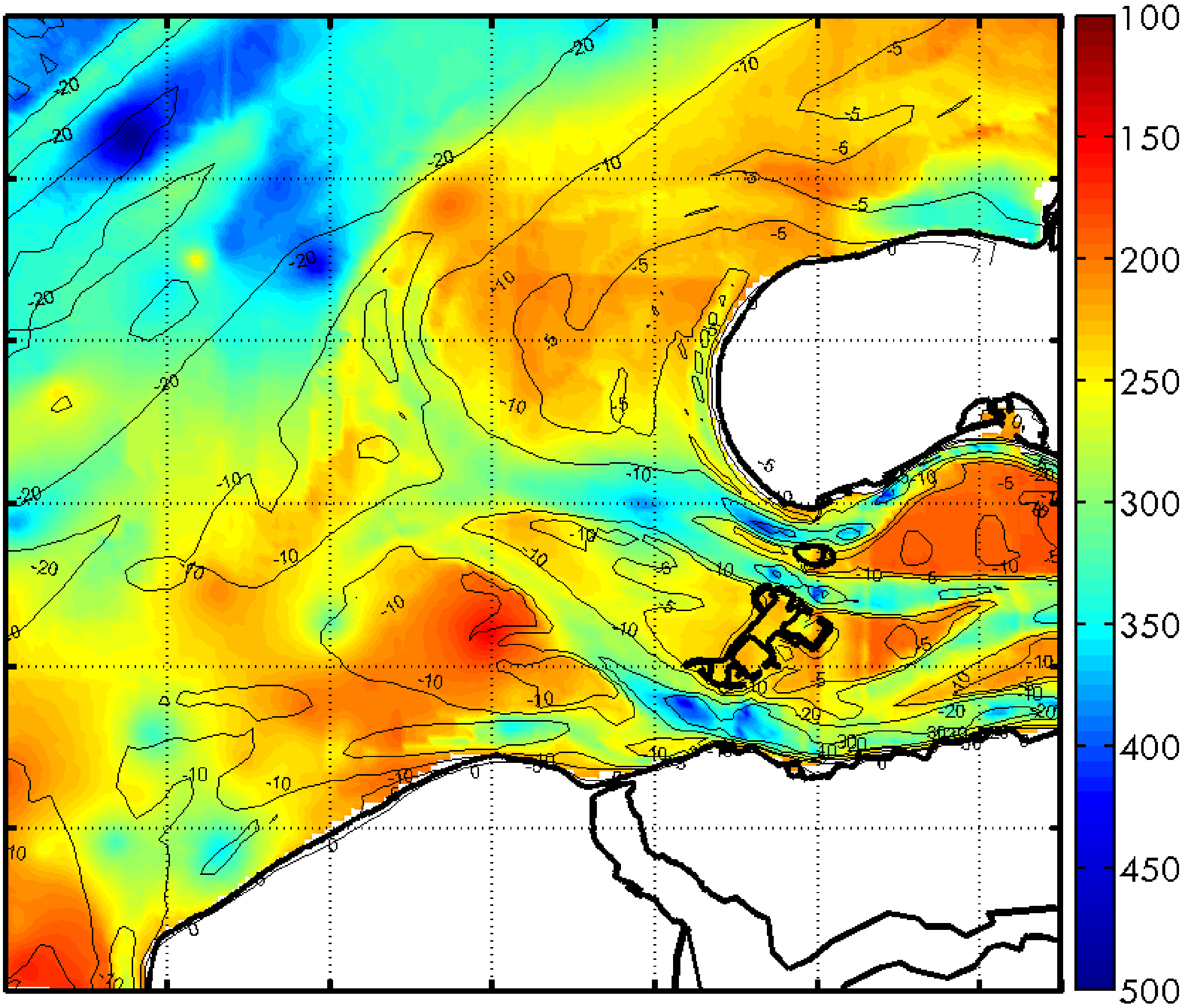

Figure 4.5: Median grain size (d_{50}) on the ebb-tidal delta (red = fine sediment). Contour lines are the 2008 bathymetry (depths in m below MSL). Units on the colour bar are in microns. (Source: TNO Bouw en Ondergrond).

4.2.3 Hydrodynamic changes in response to the storm surge barrier

Between 1983 and 1986 a storm surge barrier was built in the inlet channels in order to safeguard against flooding during storms while retaining the tidal current inside the basin during normal conditions. Coupled to the barrier's construction, also two more back-barrier dams (the Philips dam and Oester dam) were built near the landward end of the Eastern Scheldt basin. These dams were constructed in order to restrict the decrease of the tidal range by limiting the basin length and thereby increasing the reflection and amplification of the tidal wave.

The storm surge barrier reduced the effective cross-sectional area of the inlet from approximately 80.000 m^2 to 17.900 m^2 (Vroon, 1994). This constriction causes large amounts of local turbulence and a large loss in the energy head over the barrier. This loss is visible as a decrease of the tidal range inside the basin, accompanied by a shift in the phase of the tidal wave (Vroon, 1994). The average decrease in tidal range along the basin was around 20%. The two back-barrier dams, which were finalized shortly after the storm surge barrier, caused the loss in tidal range to be reduced from 20 to 10% by reducing the basin length (Figure 4.6). However, these dams also decreased the basin area from 452 km^2 to 351 km^2. The combined effect of the barrier and dams was that the tidal prism decreased by roughly 25% from 1200 Mm^3/tide to around 900 Mm^3/tide (de Bok, 2001). According to Vroon (1994), the maximum flow velocities in the western part of the basin reduced by roughly the same percentage.

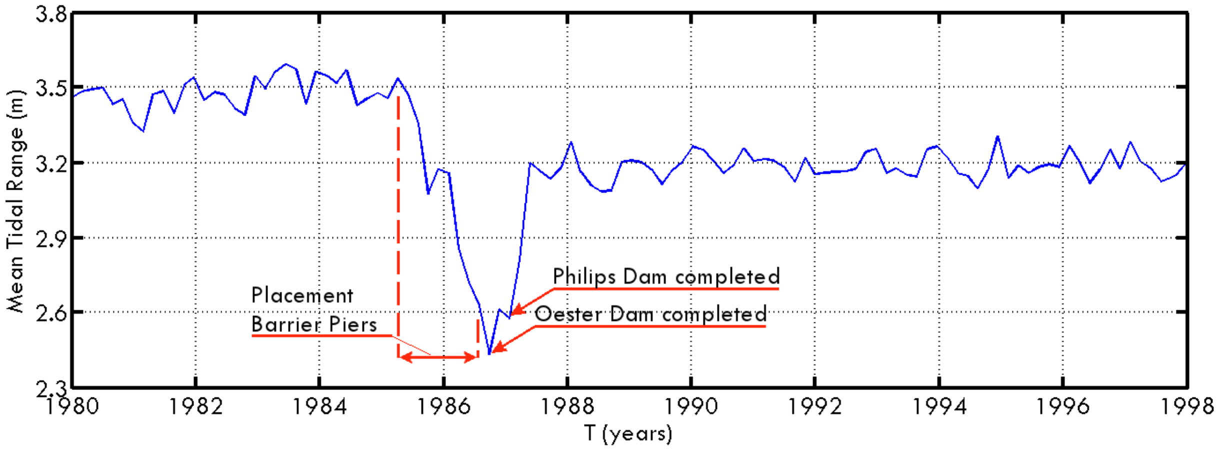

Figure 4.6: Mean tidal range measured in the central part of the Eastern Scheldt basin.

Measurements of the tidal discharges in the Roompot, Schaar, and Hammen channels (Table 4.2) have been performed since 1982 in a number of years (Rijkswaterstaat 1984). These 13-hour measurement campaigns are not performed frequent enough to determine changes in the average discharges throughout the years. The measurements do give valuable information on the distribution of discharges over the various channels.

More than half of the total discharge enters and leaves the basin through the Roompot channel. From the limited number of measurements it is not clear whether the flows through the inlet channels are flood- or ebb-dominant, or how the residual discharges are distributed over the inlet. Further out on the ebb-tidal delta the dominance seems stronger. The Oude Roompot, Westgat, and Krabbengat channels are clearly ebb-dominated (see the 2009-measurement in Table 4.2). Flood-dominance is observed in the Southern Roompot channel and over the Hompels shoal.

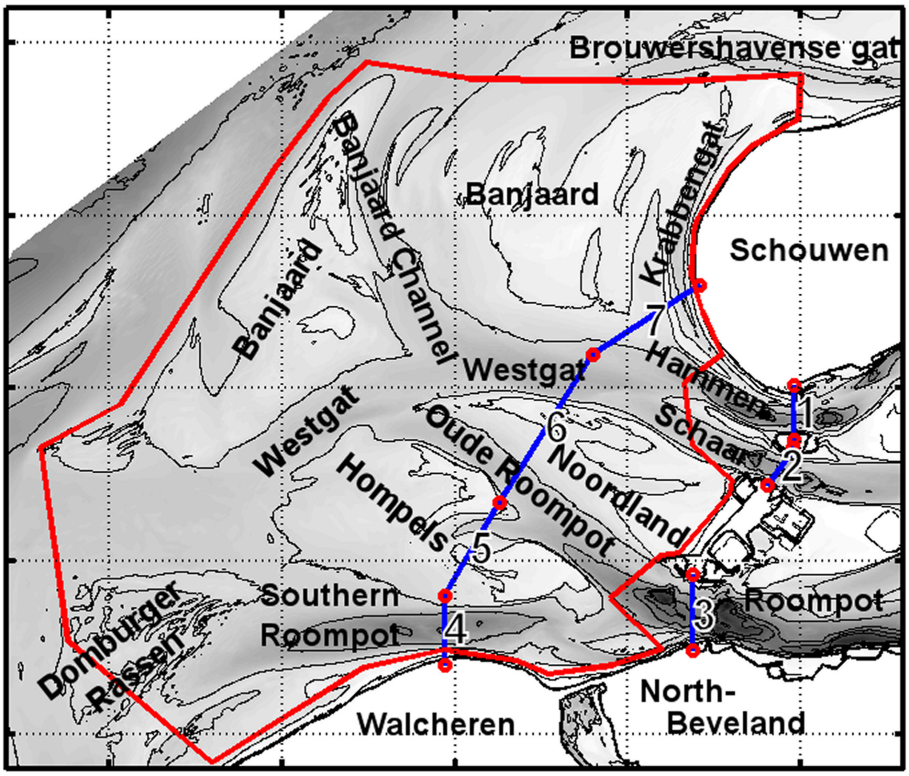

Figure 4.7: Location of discharge measurement transects (blue lines) in Table 4.2. The red polygon indicates the area used for calculation of sediment volumes and morphological activity.

Table 4.2: Tidal volume measurements in various transects (see Figure 4.7 for locations). Units are in Mm^3/tide.

Transect name		Hammen	Schaar	Roompot	Southern Roompot	Hompels	Westgat & Oude Roompot	Banjaard & Krabbengat
Transect number		1	2	3	4	5	6	7
Year								
1982	Ebb	237	282	699	-	-	-	-
	Flood	238	257	698	-	-	-	-
1988	Ebb	205	185	598	-	-	-	-
	Flood	198	206	483	-	-	-	-
1993	Ebb	-	-	-	229	-	-	-
	Flood	-	-	-	268	-	-	-
1995	Ebb	190	197	550	-	-	-	-
	Flood	185	209	485	-	-	-	-
1997	Ebb	-	-	-	247	-	-	-
	Flood	-	-	-	291	-	-	-
1999	Ebb	188	200	620	252	-	-	-
	Flood	224	218	511	302	-	-	-
2009	Ebb	144	214	568	328	151	449	174
	Flood	154	221	572	381	175	411	128

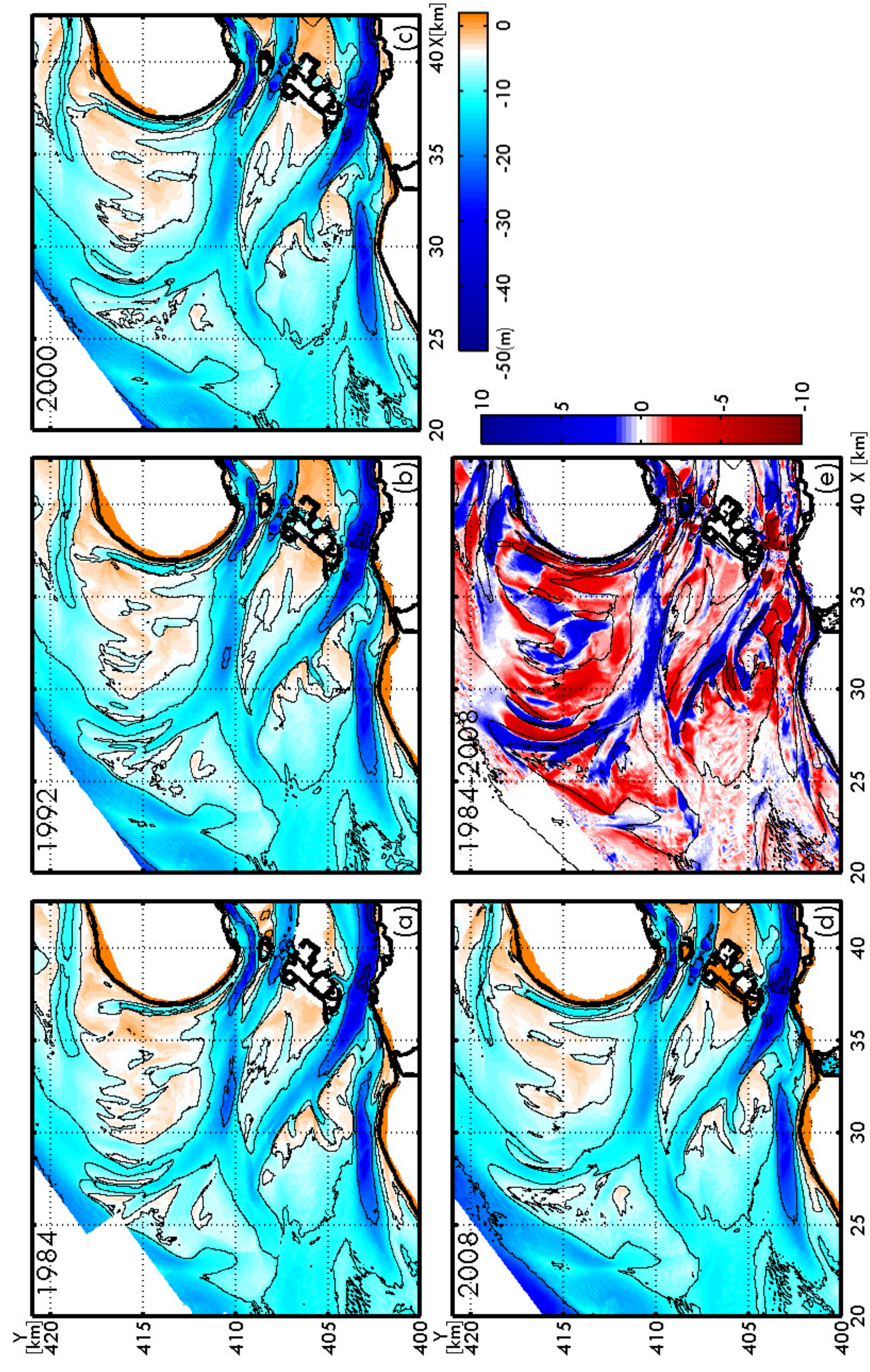

Figure 4.8: Bathymetry of the ebb-tidal delta between 1984 and 2008. (e) Difference in bed level between 1984 and 2008 (red=erosion). Depths and differences in bed level are in m.

4.2.4 Morphological changes in response to the storm surge barrier

General morphological developments

The bathymetry of the ebb-tidal delta has been measured every 4 years since 1960 (De Kruif, 2001). The digital bathymetrical data consists of a 20 m x 20 m grid with depth values in cm. From this dataset, a view emerges of an ebb-tidal delta that is affected by the storm surge barrier (Figure 4.8).

As explained in Chapter 3 and Van den Berg (1986), the period before 1983 was characterized by the effects of the back-barrier dams built in the sixties, causing significant increase in tidal prism and sediment export. After completion of the storm surge barrier in 1986, the magnitudes of the sediment transports must have decreased due to the decrease in flow velocities. This decrease in sediment transport is relatively stronger than the decrease in flow, because of the non-linear relation between flow and sediment transport. Most of the channels are no longer scouring, and some are becoming shallower. Since 1986, several sawtooth shaped bars on the Banjaard shoal are visibly growing and migrating (Figure 4.9). These bars migrate in eastern direction towards the coast, which indicates that they are probably wave-driven features.

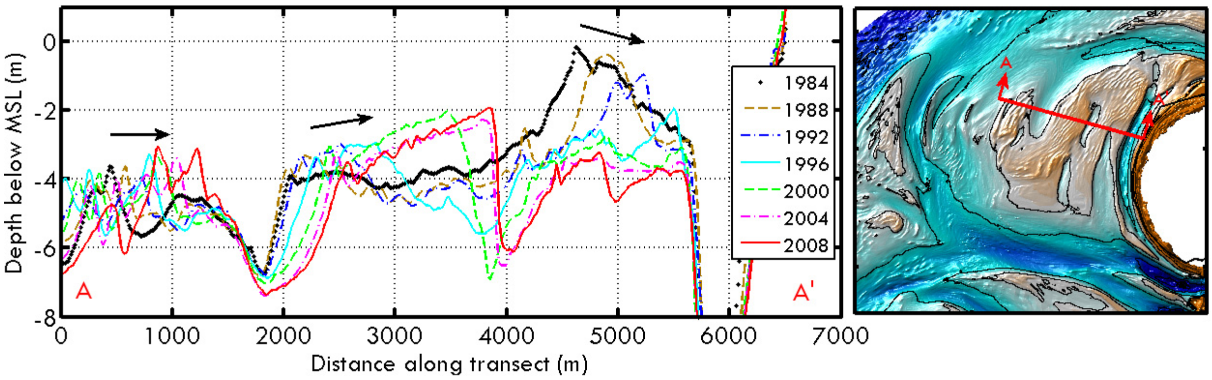

Figure 4.9: Cross-section of the bathymetry of the Banjaard shoal in different years.

The construction of the storm surge barrier has caused a small clockwise reorientation of the main channels on the ebb-tidal delta, effectively caused by sedimentation on the southern sides and erosion on the northern sides of these channels. The growth of the Westgat and Roompot channels in seaward direction has stopped, and both channels are depositing in the areas seaward of the scour holes near the barrier. This trend is not seen everywhere on the ebb-tidal delta. Krabbengat and Banjaard Channels are still lengthening in northern direction. Krabbengat channel has also become deeper.

The reorientation of the channels and shoals can be related to the interaction between the alongshore tidal current and the tidal current coming out of the inlet (Aarninkhof and Van Kessel, 1999). According to Sha and Van den Berg (1993), the orientation and protrusion of ebb-tidal deltas are related to the relative phases and strengths of alongshore currents and cross-shore currents. Because the current flowing in and out of the Eastern Scheldt has decreased in strength, the alongshore current going from southwest to northeast should have become relatively stronger on the ebb-tidal delta. This explains the clockwise reorientation of channels and shoals.

The overall decrease in dynamics is clearly visible when this is quantified by computing the Morphological Activity Index (MAI). This index is the mean of the absolute bed-changes calculated from the bathymetrical data of the ebb-tidal delta from 1960 to 2008 (Figure 4.10a). The MAI is calculated according to:

$$MAI(t) = \frac{\sum_{i=1}^{n} \left| z_{year2}(x_i, y_i) - z_{year1}(x_i, y_i) \right|}{n(year_2 - year_1)} \tag{1}$$

herein $t = (year_1 + year_2)/2$, $z_{year1}(x_i, y_i)$ and $z_{year2}(x_i, y_i)$ are the bottom depths with coordinates x_i and y_i measured in year$_1$ and year$_2$, respectively, and n is the total number of locations where bottom depths are compared. Only locations which have data points for every measurement are included. The area for which the activity is calculated is shown as the red polygon in Figure 4.7. This area is also used for calculation of the sediment volume.

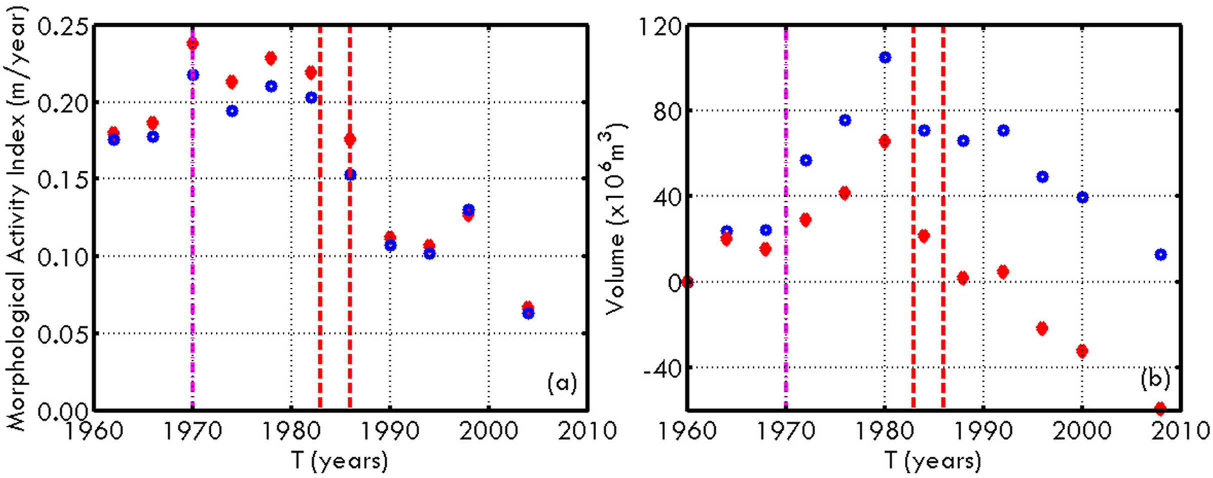

Figure 4.10: (a) Morphological activity (average absolute bed-level change) between 1960 and 2008. (b) Cumulative sediment volume change of the ebb-tidal delta relative to 1960. For the area used in the calculation, see Figure 4.7. The red diamonds are the result when the scour holes are included. The blue circles are the result when the scour holes are omitted. The coloured vertical lines note the construction of the Volkerak dam (1970) and the storm surge barrier (1983-1986).

In Figure 4.10a the MAI is shown along with the periods when the Volkerak dam and the storm surge barrier were constructed. The area for which the MAI is calculated is shown as the red polygon in Figure 4.7. Several features stand out in Figure 4.10a. Apparently, between 1960 and 1964 the morphological activity was already quite high as compared to the post-1986 period, indicating that the ebb-tidal delta was still undergoing large changes in response to previous developments inside the basin. This activity increased in response to the implementation of the Volkerak dam in 1970, and remained more or less stable during the seventies and early eighties. This activity is mostly due to the increased flow coming from the basin. There was also a supply of sediment coming from the basin, but this supply decreased significantly during the seventies, while the morphological activity persisted (Eelkema *et al.*, 2012). The decrease in the sediment supply during the seventies is not visible in Figure 4.10b.

However, in Chapter 3 it was already stated that there is probably a systematic error in the bathymetry of 1980 (Figure 3.6), and the real increase in sediment volume between 1976 and 1980 is probably smaller.

The plot of the morphological activity (Figure 4.10a) also shows the effect of the storm surge barrier. After the completion in 1986, the activity decreased sharply and continued to decrease even further after 2000. This indicates that the new situation on the ebb-tidal delta is such that there are hardly any large-scale or high amplitude bed-level changes occurring, and the area is characterized by a slow but continuous development towards a new state. The decline in activity is probably caused by the general decrease in flow velocity over the area. Because of the non-linear relation between flow velocity and transport, the morphodynamics are diminished much more than the hydrodynamics.

According to Walton and Adams (1976), the sediment volume of an ebb-tidal delta is related to the tidal prism passing through its inlet. In the case of the Eastern Scheldt Inlet, the tidal prism has decreased by 25% as a result of the storm surge barrier and the back-barrier dams. This would mean that there is a large difference between the equilibrium state and the actual state of the ebb-tidal delta sediment volume. However, even though there is a large difference between the equilibrium sediment volume and the actual volume, the flow velocity is not high enough to produce strong sediment transports and large bed-level changes. This would mean that the morphological activity is not an indicator of morphological equilibrium, but rather a measure of the transport capacity.

Figure 4.10b shows the cumulative sediment volume relative to 1960 of the area inside the polygon shown in Figure 4.7. Similar to Figure 4.10a, the closure of the Volkerak and the construction of the storm surge barrier mark changes in the trend of the sediment volume. From 1970 onward (closure of the Volkerak channel) the volume grew at roughly 2 to 3 Mm^3 per year. After 1986, the trend changed into an eroding trend. If the bathymetrical data for calculating the sediment volumes are used without any kind of filtering or correction, the ebb-tidal delta loses sediment at a rate of roughly 2.5 Mm^3 per year. However, Cleveringa (2008) states that this rate is likely an overestimation due to measurement inaccuracies. If bathymetrical changes smaller than a certain threshold are omitted, the rate of sediment loss since 1986 becomes smaller, between 1.2 Mm^3 of erosion or even 0.4 Mm^3 of accretion per year, dependent on the value for the threshold. However, the choice for this threshold is somewhat arbitrary (also see the note on generating sediment budgets on page 81). The rate of 2.5 Mm^3 per year can be seen as an upper limit of this rate.

The boundaries of the area in which the sediment volume is calculated (the red polygon in Figure 4.7) are supposed to represent the boundaries of this particular ebb-tidal delta. However, it is not possible to define exactly where an ebb-tidal delta 'ends'. Also, the areas with the scour holes in front of the barriers are omitted from the calculation, because these areas are not considered as representative for the rest of the ebb-tidal delta. Shifting the location of the northern, western, or southern boundaries by 500 m yields small variations in the calculated sediment volumes (± 8 Mm^3 around the values shown in Figure 4.10b). The same holds for the morphological activity. Including the scour holes results in less total sedimentation between 1960 and 1984. However, the amount of eroded material between 1984 and 2008 remains roughly the same (-64 Mm^3 with scour holes, in stead of -59 Mm^3 when no scour holes are included).

Whatever the precise rate is, its order of magnitude is comparable to that which existed before 1986. This seems counterintuitive, because Figure 4.10a also shows that the morphological activity is much lower, and the basin is not receiving any of this sediment loss. One way to make the observed behaviours of the morphological activity and the sediment volume changes consistent with each other, is to say that although since 1986 the bed-changes are relatively small, most of them are negative. This means that since 1986 erosion is more wide-spread than before 1986.

The initial response of the ebb-tidal delta is also observable in the hypsometry. The hypsometric curve (Figure 4.11a) shows that at roughly 10 m depth there is a tipping point in the morphological response. Since 1986, the sediment volume above 10 m depth has decreased, signifying erosion of the shallow areas (Figure 4.11b). The sediment volumes below 10 m depth have increased since 1986, indicating a sedimentation trend in the channels. The erosion on the shallow parts of the ebb-tidal delta does not seem to have slowed since 1986. The volumes of the deeper parts on the other hand do seem to have levelled out. It should be noted that the sediment volumes lost from the shallow parts are much larger than the volumes gained in the deeper parts, so the ebb-tidal delta as a whole is losing sediment.

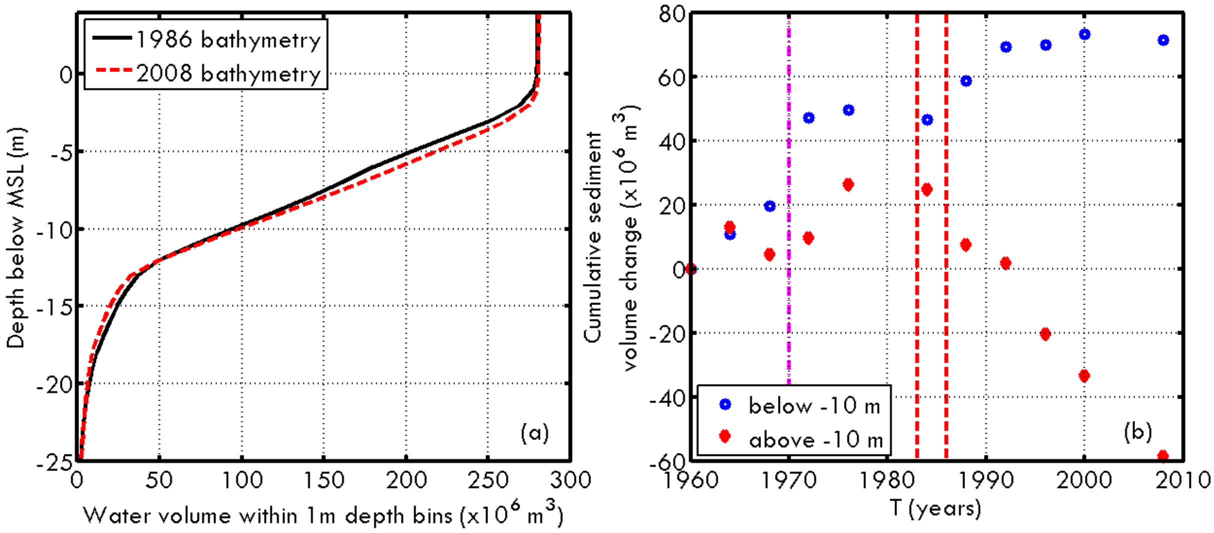

Figure 4.11: (a) Hypsometric curves of 1984 and 2008. (b) Cumulative sediment volume changes above and below 10 m depth on the ebb-tidal delta. Negative change means channel deepening or shoal erosion. For the area used in the calculation, see Figure 4.7.

The wave gauge located in the Eastern Scheldt inlet (station OS4, see Figure 4.1) has been measuring wave heights since 1980. If the erosion of the shallow areas had an effect on the dissipation of short waves on the ebb-tidal delta, this should be visible in the measured wave data. Looking at the percentage of wave heights over 0.5 m measured in a period of two years (Figure 4.13) and comparing it to 1982, it is difficult to discern a trend. It does seem like the percentage of higher waves in the inlet is rising on a time scale of more than 10 years. However, the scatter around this trend is rather large.

A note on calculating sediment budgets.

The construction of a sediment budget seems like a straightforward procedure. Differences in sediment volume are determined by subtracting two sets of bathymetric data and summation of all the differences. However, these data are subject to small measurement errors. These errors are either stochastic or systematic errors. Stochastic (random) errors vary in size and sign over one measurement campaign, while systematic errors are usually constant for one campaign. Stochastic errors can stem from the movement of the measuring vessel, variation of the velocity of sound in water, and the settings of the software for data-handling. Systematic errors can stem from the squat of the measuring vessel, the width of the beam of the echo sounder, errors in the water level reduction, calibration of the echo sounder, and human errors in data-handling (Marijs and Parée, 2004). Although the errors in measured bathymetry are usually small, they can lead to large errors in the sediment budget because of the large spatial scales involved (Cleveringa, 2008). For instance, a systematic error of 1 cm over an area of 100 km^2 leads to an error of 1 Mm^3 in the sediment volume. In the case of measurements performed every four years, this value is of the same order as the natural variability.
One method of 'correcting' for these inaccuracies is to omit bed level differences which are smaller than a certain threshold, under the assumption that differences that small stem from measurement errors and not from real morphology. Figure 4.12 shows the sediment budgets from Figure 4.10 and Figure 4.11 with this type of correction applied to them. These budgets look roughly the same until 1984, after which the three lines give very different trends. This is because after 1984, the average bed level differences became smaller, and many of these differences fall below the threshold. Depending on this threshold value, the ebb-tidal delta either gains or loses sediment between 1984 and 2008. Most of these supposed errors are located on the shallow areas above 10 m depth. However, the choice for these threshold values, or any other kind of correction is somewhat arbitrary. Also, if the time period between subsequent data sets is increased, the true morphological trends also become clearer. If for the budgets presented below only the data of 1960, 1984 and 2008 is used, both the red and green data points more or less coincide with the blue, uncorrected values.

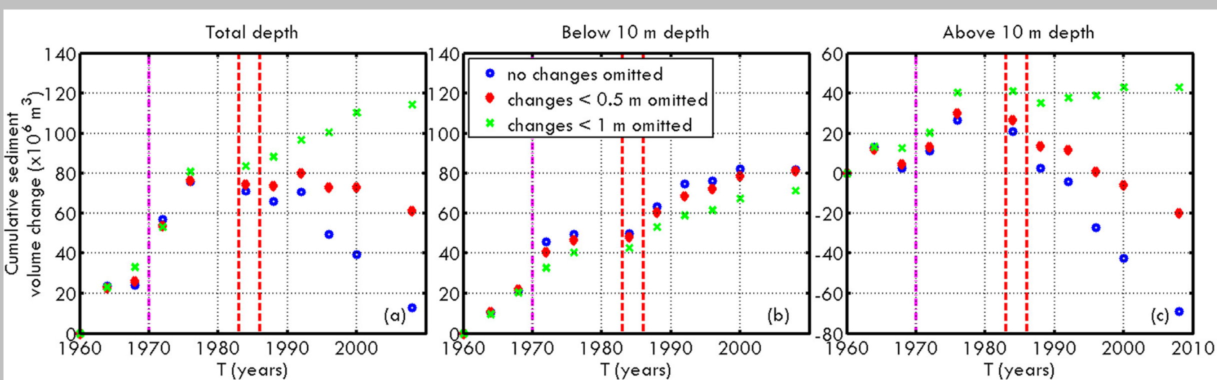

Figure 4.12: (a) Cumulative sediment volume change on the ebb-tidal delta. Blue circles denot the original, unaltered data. Red diamonds mean all bed level differences smaller than 0.5 m are omitted. Green crosses mean all bed level differences smaller than 1 m are omitted. (b) Cumulative sediment volume change below 10 m depth. (c) Cumulative sediment volume change above 10 m depth.

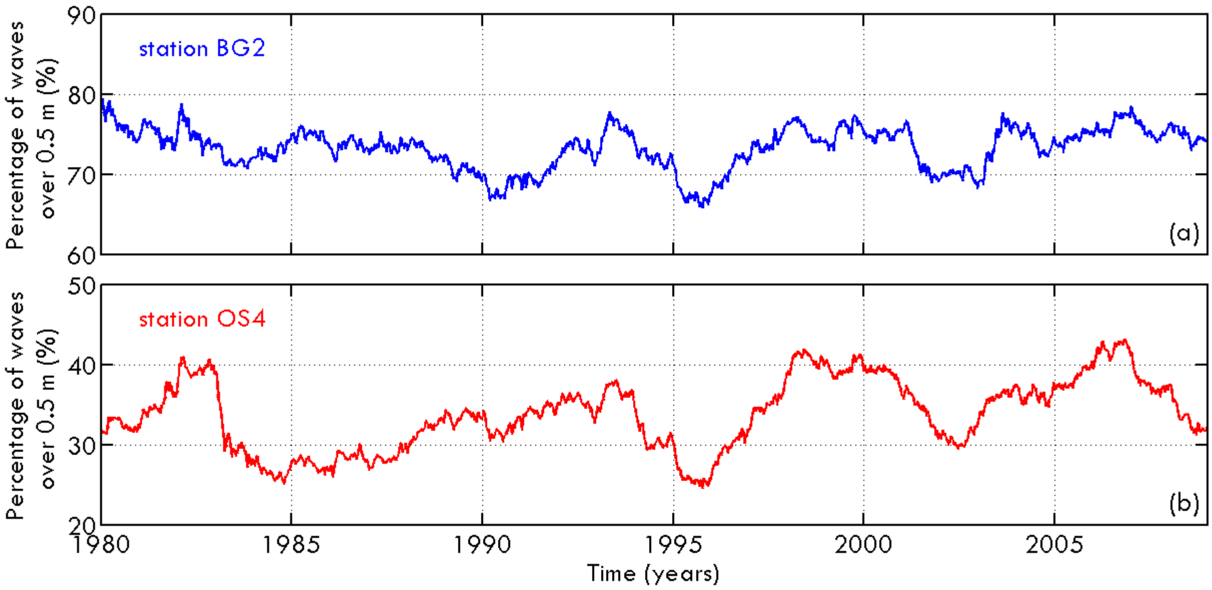

Figure 4.13: Percentages of measured significant wave heights higher than 0.5 m in a two year period. (a) Measured in station BG2 (see Figure 4.1). (b) Measured in the inlet in station OS4.

Local morphological developments

On the seaward side of the inlet channels, the flow constriction caused by the barrier induces strong flows during ebb tide. As a result, large scour holes have developed in front of the barrier at the location where the scour protection ends. These holes can reach depths of 40 to 50 meters. For the calculation of the sediment volumes mentioned in the previous subsection, the immediate area around the storm surge barrier which includes these scour holes was omitted. When looking at the hypsometry of this specific area (Figure 4.14), it is noticed that the sediment volume above -20 m experienced a sharp decrease immediately after the barrier was built, but has been stable ever since. The volumes below -20 m are still decreasing slightly. This indicates that the deepest parts of the scour holes are still getting deeper. However, the total volume of scour holes has remained stable since 2000 (Figure 4.14d).

The scour holes are not seen on every location where the scour protection ends. On the southern side of the Roompot channel, the Onrust sill actually reaches the beginning of the scour protection (Figure 4.15). At this location, the net sediment transport is most likely directed towards the barrier, and sediment particles transported by the current would not have to pass any deep scour hole before reaching the barrier. There is a deep scour hole just north of the Onrust sill. At this location the net sediment transport direction is most likely away from the storm surge barrier.

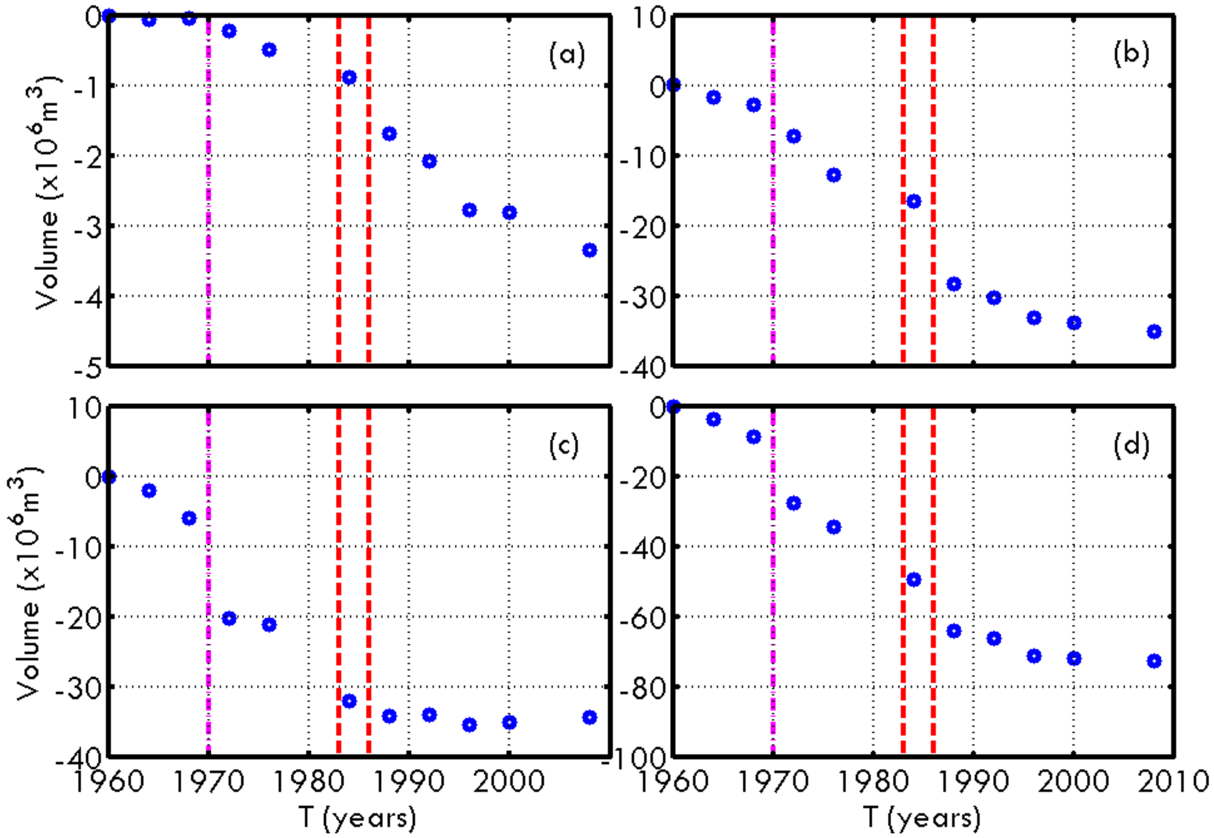

Figure 4.14: Cumulative sediment volume changes between various depths around the inlet: (a) Below 40 m depth. (b) Between 40 and 20 m depth. (c) Above 20 m depth. (d) Total cumulative sediment volume. Note that the scale on the vertical axis changes per plot. The vertical lines note the construction of the Volkerak dam (1970) and the storm surge barrier (1983-1986). Downward trends indicate erosion. For the area used for calculation see Figure 4.16.

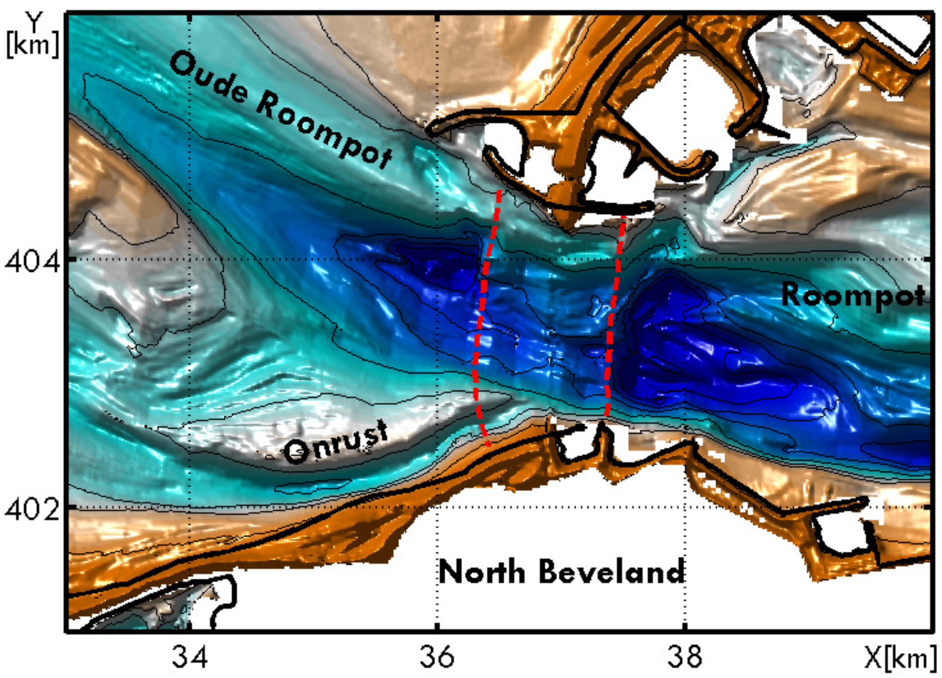

Figure 4.15: Bathymetry of the scour holes on both sides of the Roompot gate of the storm surge barrier. Red dashed lines indicate where the scour protection ends.

In the twenty years before the barrier was constructed, the small ebb-channels on the northern side of the Hompels shoal migrated with a rate of about 1 km in four years (Eelkema *et al*, 2012, see also Figure 3.8). After construction of the barrier, these ebb chutes hardly migrated, and the generation of new ebb chutes on the Onrust sub-tidal sill ceased. One large chute remains in place, but hardly migrates. The linear bar which marks the edge between the Hompels shoal and the Oude Roompot channel is pushed north-eastward, where it forms steep channel edges and even starts filling the channel. Consequently, this channel is pushed north-eastward. This development will likely result in the remaining ebb-chute becoming larger, drawing more current. At the same time, the connection between the Oude Roompot and Westgat channels will most likely silt up.

The part of the Banjaard shoal westward of Banjaard Channel exhibits highly dynamic behaviour during this period. The seaward front has been eroding, probably because the supply of sediment has stopped and the waves have started to re-work the delta front. The small ebb-channels on the inlet-side of the shoal have filled up with sediment, and there have been large amounts of deposition along the outer bend of Banjaard Channel. This deposition is making the northern tip of this shoal grow in northward direction. The linear bars in the middle of the Banjaard Channel are still migrating to the west. The creation and migration of these bars is a cyclic process. It takes roughly 40 years for one of these bars to migrate from the eastern to the western side of the Banjaard channel.

The Banjaard shoal also shows signs that waves have become more important in shaping the shoal. Bathymetrical measurements show multiple saw-tooth shaped bars being pushed eastward towards the coast. At the same time the entire shoal system has become lower. The Krabbengat channel is still deepening and expanding in northern direction. The rate of growth of the channel cross-section shows a distinct jump around 1986 (Figure 4.16a). Especially the part of the channel below -10 m is growing steadily since 1986. Between 1986 and 2008 also the ebb-shield on the northern side of the Krabbengat channel has been growing in increasing rate. The Brouwershaven channel, which marks the northern edge of the Banjaard shoal, used to be a more or less straight channel running from east to west. However, nowadays this channel shows a distinct bend at the location where the Krabbengat channel terminates. The Brouwershaven channel itself is acting as a sink for the sediment transported over the northern edge of the Banjaard shoal. This is also an effect of the closure of the Brouwershaven Inlet in 1971. However, the clockwise rotation of the Eastern Scheldt ebb-tidal delta is only observed after 1986.

The deepening of the Krabbengat channel seems counter-intuitive. As discussed in the previous section, the tidal prism through the inlet decreased in response to the storm surge barrier. As a consequence, the channels near the inlet should also decrease in size. The Krabbengat channel, on the other hand, became larger, indicating that the discharge through this channel should have increased (Figure 4.16a). There are, however, no measurements of tidal currents in this channel available to confirm this. The Southern Roompot channel shows similar behaviour (Figure 4.16b). Its deeper parts have gained some wet volume since 1986, albeit not as strong as in the Krabbengat. This deepening is not a general trend on the rest of the ebb-tidal delta. The channels in the central part of the ebb-tidal delta, i.e. the

Westgat and Oude Roompot, experienced sedimentation in their deeper parts (Figure 4.16c&d).

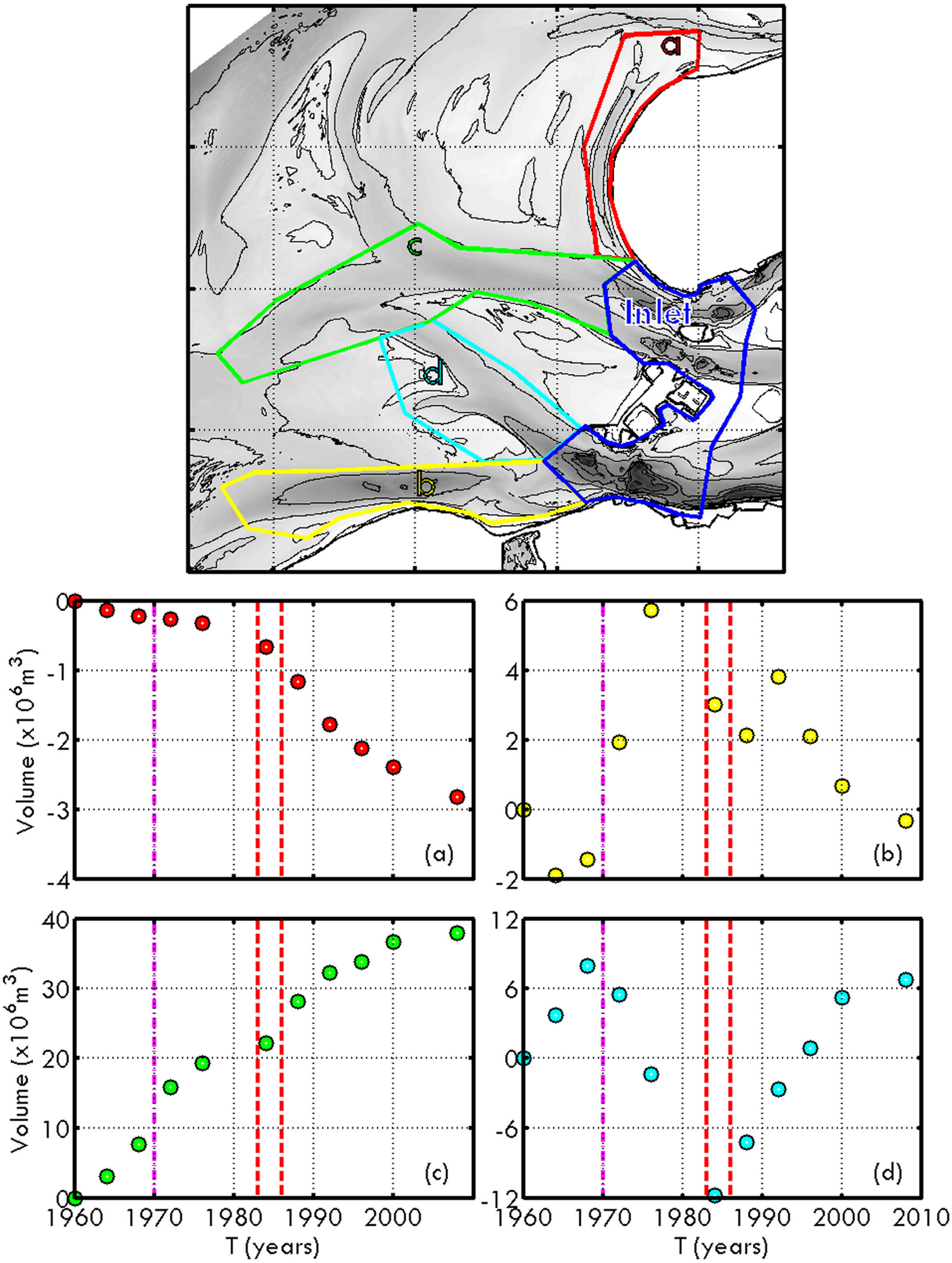

Figure 4.16: Cumulative sediment volume changes below 10 m depth in various channels. (a) Krabbengat channel. (b) Southern Roompot channel. (c) Westgat channel. (d) Oude Roompot channel. Downward trends indicate erosion.

4.2.5 Summary of observations

The storm surge barrier caused a major shift in the equilibrium state of the ebb-tidal delta, resulting in an adaptation of both its volume and its shape. Though the bed-level changes of the ebb-tidal delta are not very large (low morphological activity), they are mostly in the same direction (persistent erosion). Without any kind of correction, the erosion rate is 2.5 Mm^3 per year. With different types of corrections, Cleveringa (2008) estimates the erosion rate between 1.2 Mm^3 of erosion and 0.4 Mm^3 of accretion per year.

Even though the ebb-tidal delta has most likely lost between 30 and 50 Mm^3 of sediment since 1986, it is not clear where the eroded material has ended up. The Eastern Scheldt basin has received virtually no sediment since the barrier has been in place. The Grevelingen ebb-tidal delta, as well as the Western Scheldt ebb-tidal delta, located south of Eastern Scheldt, show net erosion since 1986 (Cleveringa, 2008). The dunes adjacent to Eastern Scheldt Inlet have not grown significantly since 1986. It is also unlikely that the sediment has been transported seaward, as there is no process present which could plausibly transport these amounts of sediment per year. We hypothesize that the most plausible location for the eroded sediment is the abandoned Brouwershaven channel, which has been filling up with sediment since the closure of Grevelingen Inlet. However, the deposition in this area is limited to 10 Mm^3 at the most.

The erosion is primarily located on the parts above -10 m depth. The deeper parts of the ebb-tidal delta have gained some sediment since 1986, but not as much as the shallow parts have lost. Also, this gain in the deeper parts has levelled off, while the shallow parts still seem to be losing sediment nowadays at the same rate as in the eighties. Apparently, the shallow shoal areas require more time to reach a new equilibrium state than the channels. Elias (2006) notices a similar development on the Texel Inlet ebb-tidal delta, and states that this is due to the fact that sediment transports are largest in the channels. On the shoals, the capacity for the tidal current to transport sediment is smaller, although wave action will probably help in stirring up the sediment.

This development of the hypsometry is not seen on the ebb-tidal deltas north of the Grevelingen and the Haringvliet, north of the Eastern Scheldt. Both these ebb-tidal deltas are under the influence of the total closure of their inlets (Cleveringa, 2008). Like at the Eastern Scheldt, the most seaward parts of these ebb-tidal deltas have been eroding, and their channels have been acting as sinks for sediment (Steijn *et al.*, 1989). However, what sets these ebb-tidal deltas apart from the Eastern Scheldt's, is that at the Grevelingen and Haringvliet, the waves are actually pushing sediment towards the coast and build up large shore-parallel bars. This development is absent at the Eastern Scheldt.

The reorientation of the channels and shoals can be related to the interaction between the alongshore tidal current and the tidal current coming out of the inlet, as described by Sha and Van den Berg (1993). Because the horizontal tide going in and out of the Eastern Scheldt has decreased in strength, the alongshore current going from southwest to northeast should have become more important on the ebb-tidal delta, resulting in the clockwise reorientation of most channels and shoals.

The Krabbengat and Southern Roompot channels have not just reoriented themselves, they have also deepened. It is hypothesized that the barrier causes a small amplification of the tidal amplitude on the ebb-tidal delta because of a partial reflection of the tidal wave. Because of this amplification, the average water level gradients between this ebb-tidal delta and its surroundings should also increase, leading to higher current velocities and discharges in the channels running more or less shore-parallel. This hypothesis, which is already mentioned in Aarninkhof and Van Kessel (1999), remains to be tested.

From this description of the ebb-tidal delta based on observations it becomes clear that some understanding of its behaviour is still missing. First of all, the erosion and transport rates do not seem to have slowed down since 1986, at least according to the sediment budget. It would be worthwhile to see whether this trend also follows from the changes in currents and wave climate on the ebb-tidal delta. Second, it seems as if the alongshore currents have become more important, although there are insufficient measurements to confirm this. In the next sections a process-based numerical model based on Delft3D will be applied in order to give insight into these processes.

4.3 PROCESS-BASED MODELLING

4.3.1 Method

Process-based numerical models are useful tools in coastal and estuarine research (De Vriend *et al.*, 1993). These models describe water motion, sediment transport and bed-level changes by solving a coupled set of mathematical equations. The model itself usually consists of several modules, each of which is dedicated to computing a different process. Recent studies (e.g. Lesser, 2009; Van der Wegen, 2010) have shown that these types of models can aid in the interpretation of field data. In this sense the model is applied as a clever way of interpolating behaviour that is observed in only a limited number of points in space at a limited number of moments in time. One of the prerequisites for this kind of model usage is that the model is well-calibrated for those points where measurements are available.

In this study a process-based model is applied in order to gain information on the governing current and sediment transport patterns in two different periods, to see how these patterns have changed in response to the presence of the storm surge barrier, and to be able to link the changes in hydrodynamics to the changes in the sediment transport and bathymetrical evolution. It is not the ultimate aim of this study to reproduce the exact transport magnitudes. The aim of this study is to determine how changes in direction and magnitudes of tidal currents and waves might have led to changes in bathymetry.

The focus of this model study will be firstly on the tidal currents and wave forcing which in turn force the sediment transport. First, the situation in 1986, directly after the completion of the storm surge barrier is modelled. This situation should display the strongest signal, since the ebb-tidal delta had only just started to adapt. Second, the 2007 situation is modelled. This situation should give the best indication of the present-day state of the ebb-tidal delta. In all these model instances, the model is run for a two month simulation period. For each time step the model computes flow, sediment transport and bed-level change. These types of output from the simulations are then compared to see in what manner they differ.

4.3.2 Model Setup

For this research the Delft3D-Flow model (version 3.55.05.00) is used in two-dimensional depth-averaged mode. The depth-averaged mode is warranted, because the basin has a negligible fresh water inflow (Peelen, 1970), and three-dimensional effects are assumed to have minor influence on the large-scale sediment exchange between basin and ebb-tidal delta. Each model run is performed two times; one with tidal, wave, and wind forcing enabled, and one with tidal forcing only. From the difference between these runs the relative influence of waves and wind can be deduced.

The Delft3D-Flow model is discussed in detail in Lesser *et al.* (2004). For application in and around the Eastern Scheldt, a specific model application has been made, called the *KustZuid*-model (Figure 4.17). The *KustZuid*-model has been designed and constructed as an operational model for predicting water levels for the present-day situation. This model application and its calibration are described in detail in Chapter 3 (also see Appendix A for the *KustZuid*-model parameter settings).

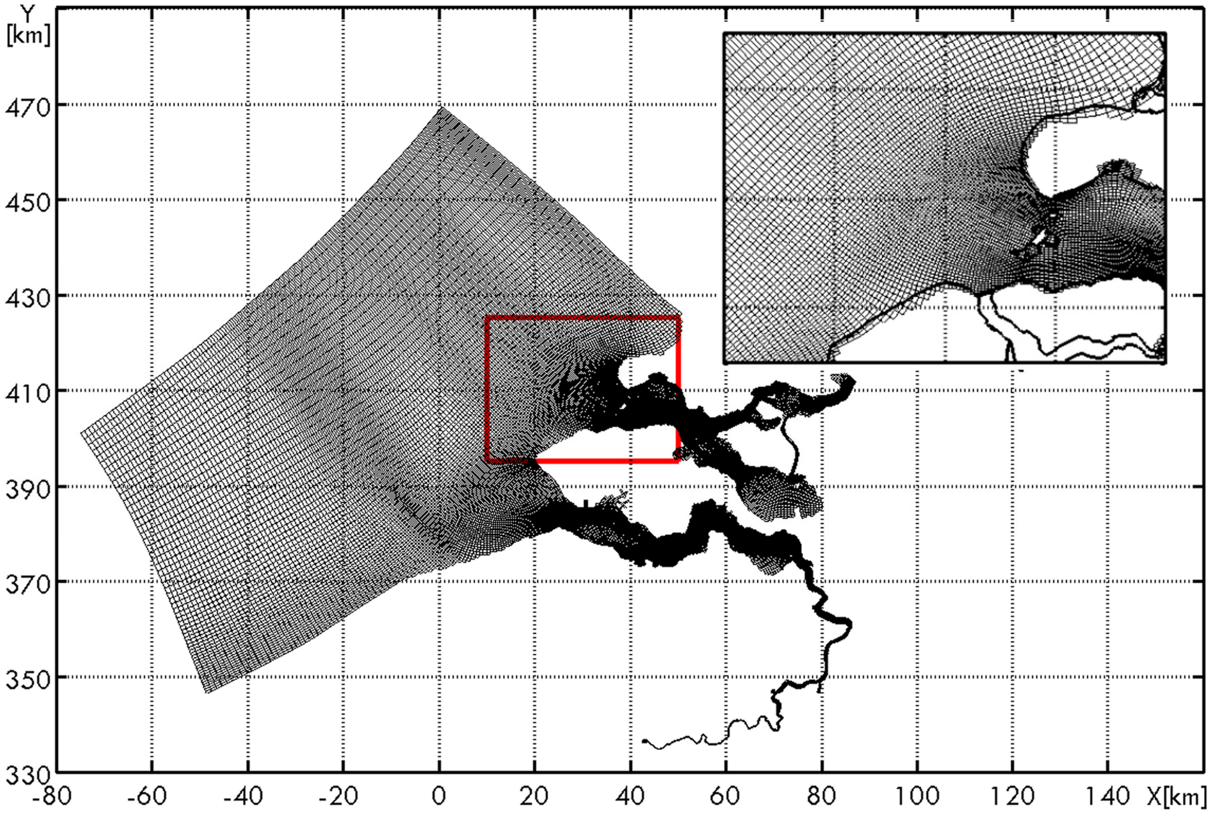

Figure 4.17: Delft3D computational grid.

All model implementations are run for a two-month period (31-01-1986 to 01-04-1986, and 31-01-2007 to 01-04-2007) with a time step of 60 seconds. There is no complete bathymetry data set available from one measurement period which covers the entire delta and basin. Therefore, the bed topography for the 1986 simulation is composed out of the 1984 bathymetrical measurement of the ebb-tidal delta, and the 1987 measurement of the Eastern Scheldt basin. The bed topography for the 2007 simulation is composed out of the 2008 bathymetrical measurement of the ebb-tidal delta, and the 2007 measurement of the basin.

Each run starts from a uniform water level and zero velocities. A period of one day is long enough for the hydrodynamics to spin up before morphological changes are computed. For the eddy viscosity as well as eddy diffusivity a value of 1 m^2/s is chosen. For the bottom roughness, a Manning coefficient of 0.025 $s/m^{1/3}$ is applied.

In each run the sediment transport rate is calculated using the Van Rijn (1993) transport formula. From data on sediment grain size diameters of the Dutch continental shelf (Geological Survey of the Netherlands, 2007), it is known that the median grain size has a spatial variability. This variability is mostly visible as coarser sediment (d_{50}≈350 μm) in the channels and finer sediment (d_{50}≈150 μm) on the shoals. This knowledge is incorporated in the model by using a spatially varying grain size based on this data. Also, the scour protection on both sides of the storm surge barrier are incorporated by reducing the sediment availability to zero near the storm surge barrier.

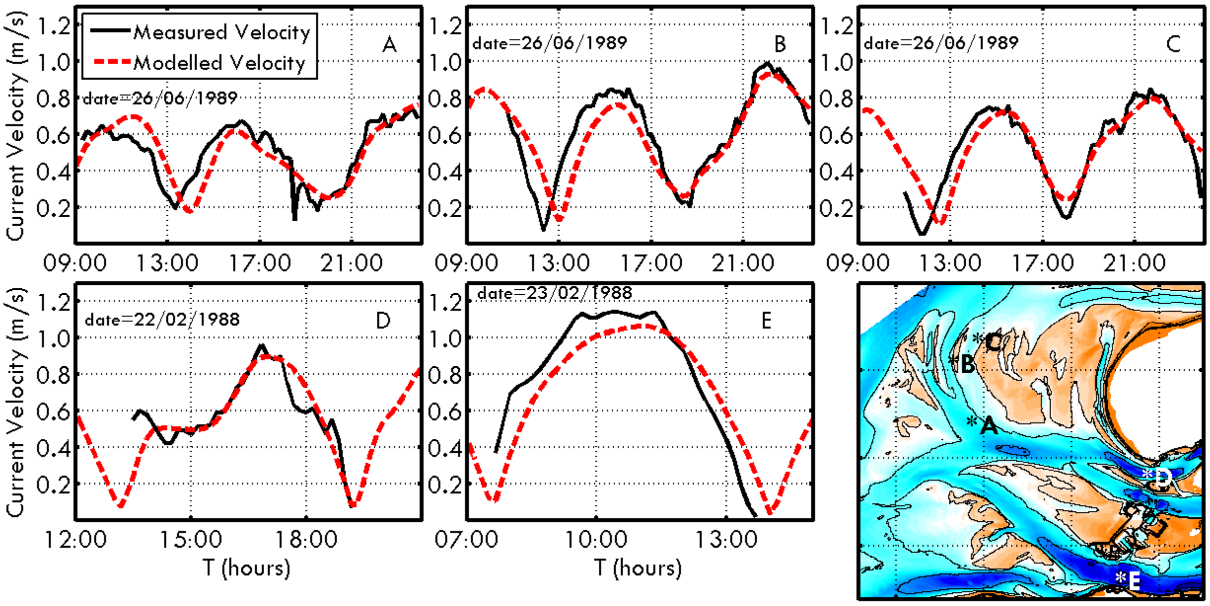

Figure 4.18: Measured and modelled current velocity in various points in the inlet and on the ebb-tidal delta. See lower right figure for locations.

So far, the model described here is the same as the model used in Eelkema *et al.,* (2012). New for this particular study are the addition of the storm surge barrier and the inclusion of wave forcing. The storm surge barrier is modelled as so-called porous plates across the inlet which cause the loss of energy head. With these porous plates, there is no need to incorporate the barrier in the bathymetry. This type of barrier implementation has the advantage that the model is stable and less computationally intensive. A disadvantage is that the local hydrodynamic conditions around the barrier (less than 400 m from the barrier) are not represented well. However, the simulated hydrodynamic conditions further away from the barrier and on the rest of the ebb-tidal delta are far less sensitive to the type of barrier implementation, and show good agreement with measured data (e.g. Figure 4.18).

The wave forcing is modelled using the SWAN model (Booij *et al.*, 1999). This model computes wave propagation, growth due to wind, and dissipation due to depth-induced breaking, bottom friction, white capping, and non-linear triad interactions. The grid applied in this model is the same as the flow-grid, only in this case with most of the Eastern and Western Scheldt basins and the southern part of the grid in front of the Belgian coast cut off. On the north eastern boundary the grid is extended in order to keep the disturbances caused by the lateral boundaries out of the area of interest. The bathymetry is adopted from the flow module. The spatially constant, time-varying boundary conditions are applied on the western boundary of this grid. The boundary conditions applied for both simulations (1986 and 2007) consist of time series of wave heights and directions measured at Schouwenbank station during February and March of 2007 (Figure 4.20b and c). The same period is applied for the wind forcing measured at station OS4 (see Figure 4.1 for locations of Schouwenbank and OS4 stations). These two months were chosen because the wave climate observed during this period is fairly representative of the long-term wave climate measured at the same location between 2005 and 2010 (Table 4.1). The wave field computed with SWAN is updated every 60 minutes. Reducing this period to 30 minutes does not result in significant changes in model output.

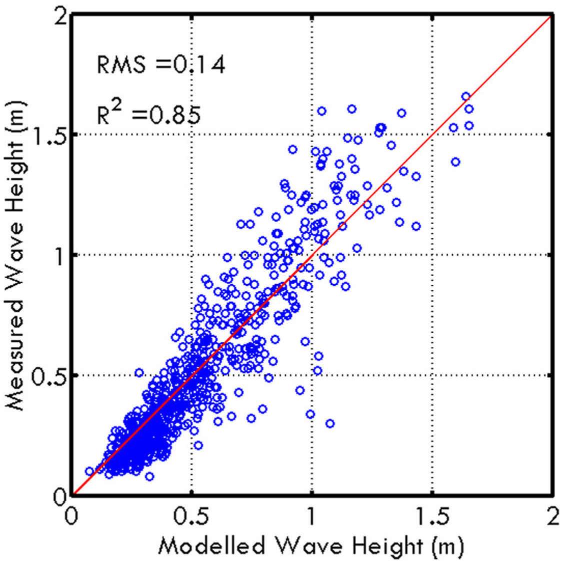

Directional class at Schouwenbank station	R^2	RMS	Occurrence (%)
0-30	0.85	0.11	13
30-210	0.60	0.15	9
210-240	0.85	0.12	14
240-270	0.87	0.17	20
270-300	0.91	0.14	11
300-330	0.82	0.14	14
330-360	0.86	0.12	19
All directions	0.85	0.14	100

Figure 4.19: Comparison between measured and modelled significant wave heights in station OS4 in the inlet from 31-01-2007 to 01-04-2007. The red line indicates the line of perfect agreement. The table shows the R^2-values and the root mean squared errors of the measured and modelled significant wave heights in station OS4 per directional class.

In the previous chapter the calibration of the flow module and its capability to reproduce measured flow velocity was discussed. However, the accuracy of the wave module was not discussed. In order to assess the accuracy of the modelled wave field over the ebb-tidal delta, the model output at location OS4 was compared to wave heights measured at the same location. Unfortunately, measurements consisted only of wave height, and not direction. The comparison between measured and modelled significant wave height for the 2007 simulation period (Figure 4.19) shows good agreement.

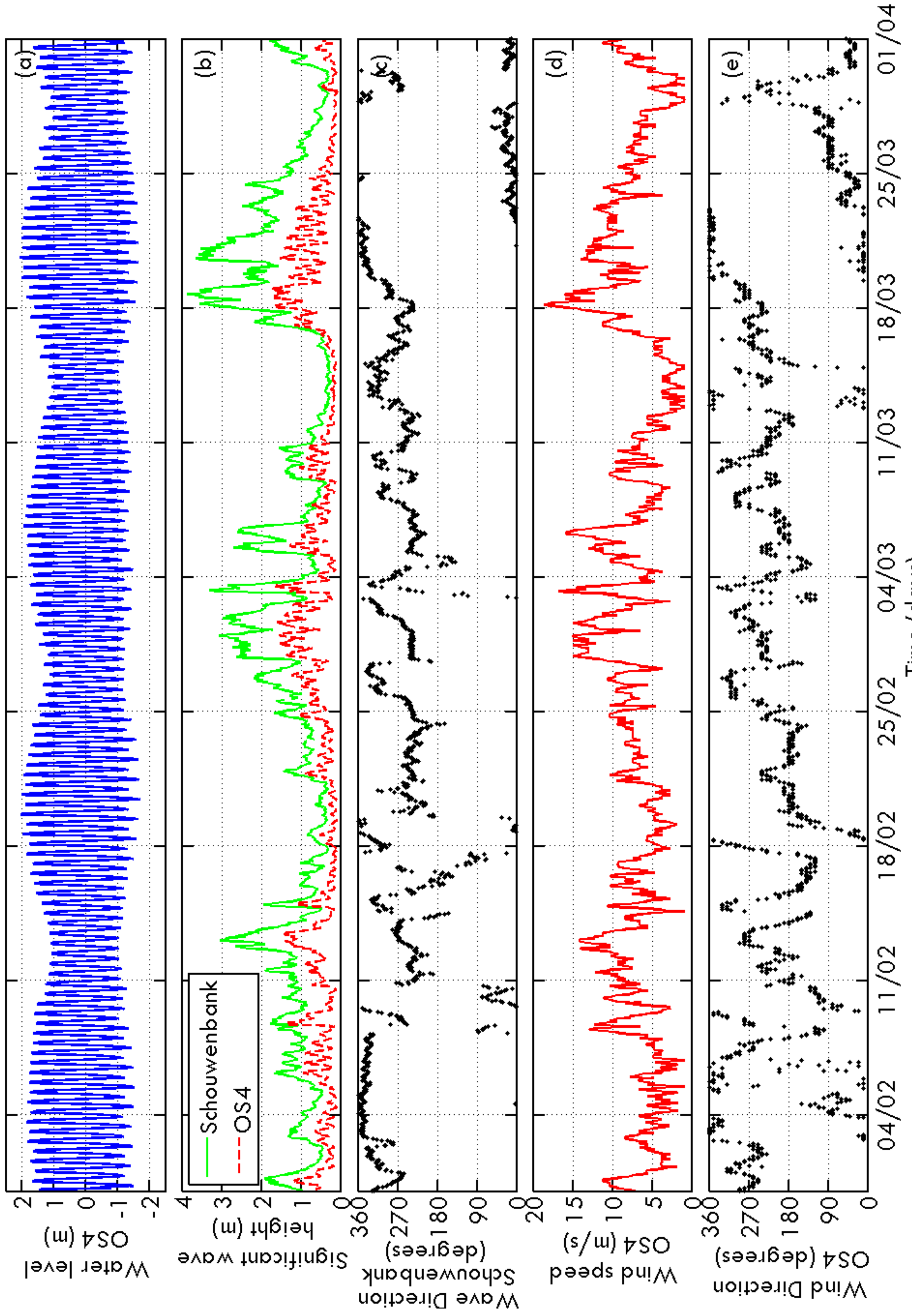

Figure 4.20: Overview of various forcing types. (a) Water level at station OS4, (b) significant wave height measured offshore (Schouwenbank) and in the inlet (OS4), (c) wave direction at Schouwenbank, (d) wind speed and (e) directions at station OS4.

4.4 Model Results

4.4.1 Simulated flow patterns

Figure 4.21 shows the residual flow velocity from the 2-month simulations with the 1986 and 2008 bathymetries. Both simulations show similarities in the overall distribution of residual velocities over the ebb-tidal delta. Flood-directed residuals prevail in the Southern Roompot channel and over the Hompels and Noordland shoals. The residual flow through the Westgat and Oude Roompot channels is ebb-directed, creating a tide-residual eddy on the north-western tip of the Hompels shoal. The residual flow on the Banjaard shoal is mostly directed northward, and seems to be stronger closer to the coast of Schouwen. The residual flow coming out of Banjaard Channel curves westward, and creates a large eddy which rotates counter-clockwise around the western part of the Banjaard shoal. The point where this eddy flows onto the ebb-tidal delta again is visible in the bathymetry as the large notch in the seaward face of the Banjaard shoal.

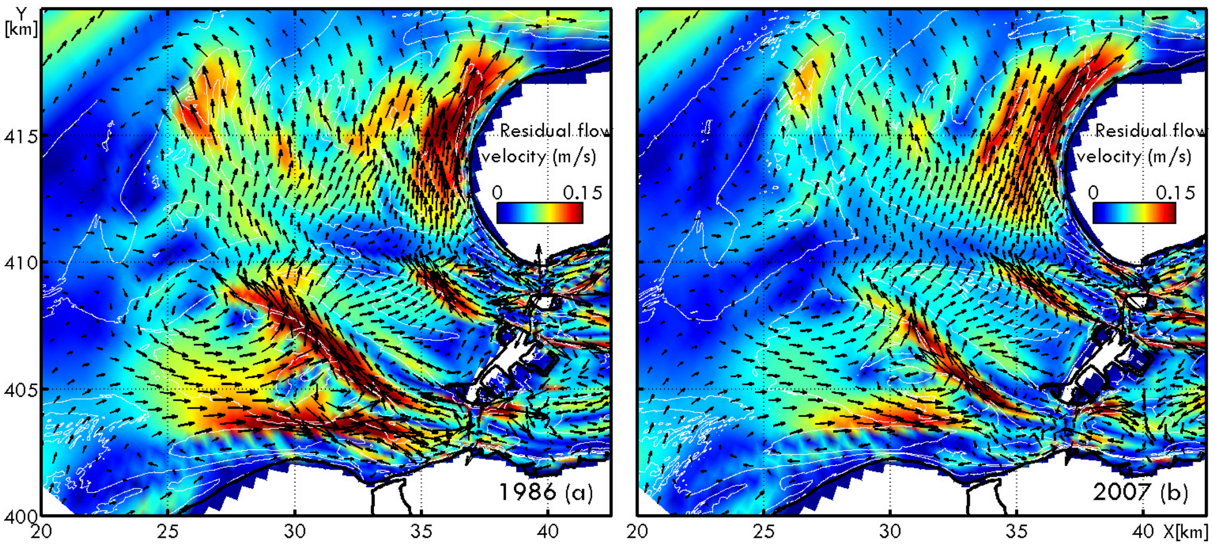

Figure 4.21: Modelled residual flow velocities: (a) 1986 bathymetry, (b) 2007 bathymetry.

The residual flow patterns also show differences between both situations. Most notably, the residual flow seems to be deflected more in northward direction. The overall residual flows over the Banjaard shoal have become stronger, especially in the vicinity of the Krabbengat channel, while the ebb-directed residual flows through the Oude Roompot channel have decreased significantly in strength.

In the observations section it was hypothesized that the barrier caused an increase in alongshore tidal current. To test this hypothesis, an extra model run is required for the 1986 situation without the barrier and back-barrier dams. For this simulation, the barrier is removed by removing the porous plates which schematize the barrier. The back-barrier dams (Oester dam and Philips dam) are removed by removing the thin dams which cut off the backward part of the grid.

From comparing these two simulations, the instantaneous effect of the barrier on the hydrodynamics becomes apparent (Figure 4.22 and Figure 4.23). First of all, the average flow velocity magnitudes decrease on the entire ebb-tidal delta, except for some small areas around the barrier and the north-western tip of the Banjaard shoal (Figure 4.22a). This decrease is strongest in the channels and weaker on the shoals. However, in the Krabbengat and Southern Roompot channels the discharges and average flow velocity magnitudes also decreased according to the model. As mentioned before, measurements indicate these channels are growing in cross-sectional area. Apparently, this growth is not caused by an increase in tidal discharge or average tidal flow velocities through these channels.

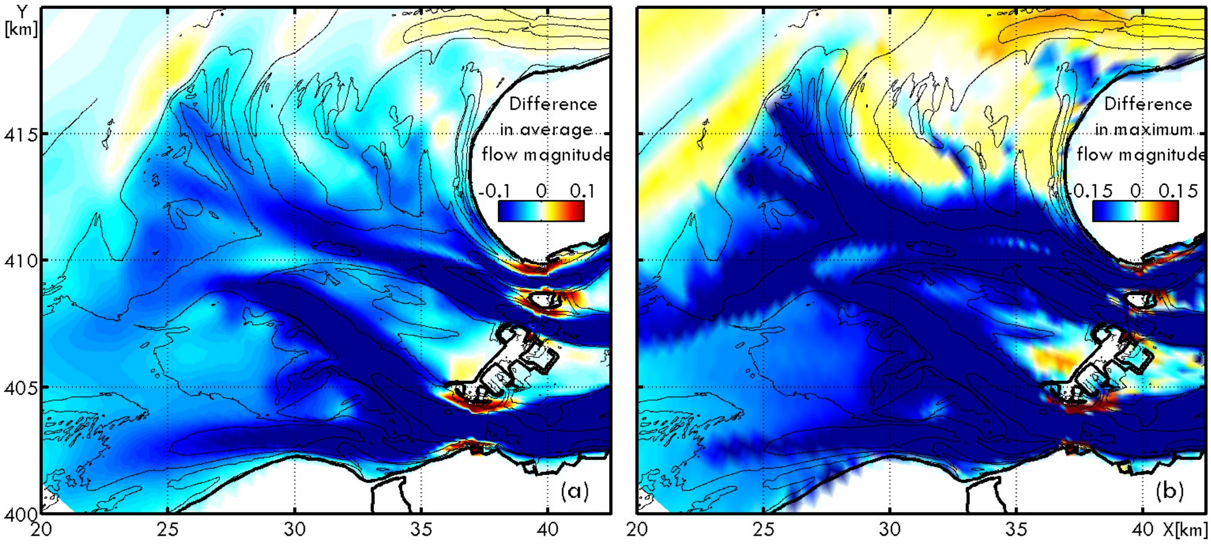

Figure 4.22: Comparison of model runs with and without the storm surge barrier. (a) Tide-averaged flow velocity magnitude differences. (b) Maximum flow velocity magnitude differences.

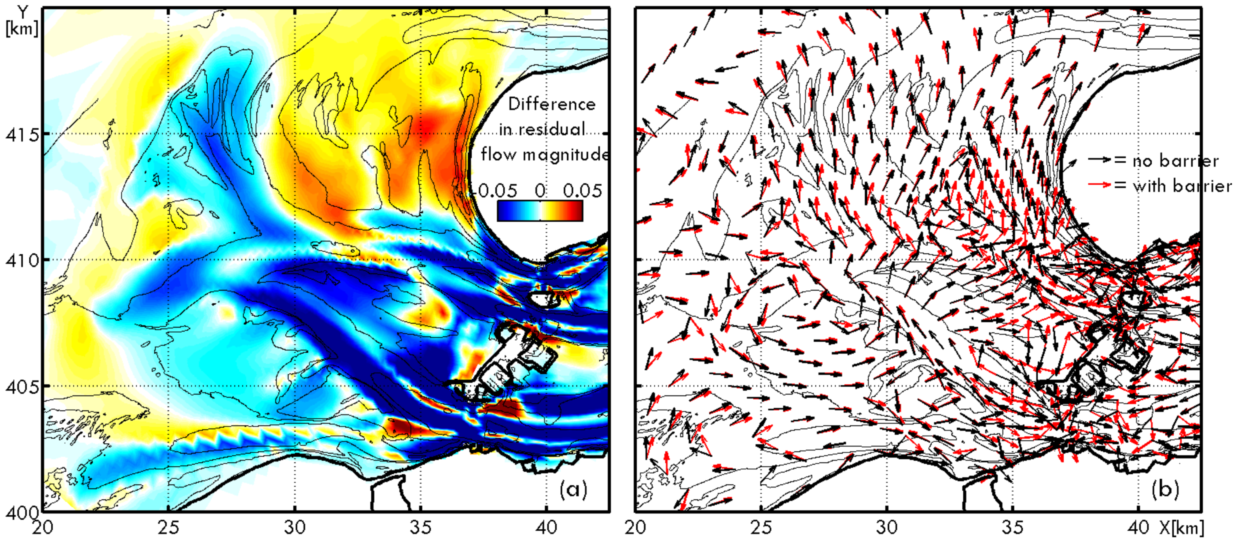

Figure 4.23: (a) Residual flow magnitude difference (m/s) between simulations with and without a storm surge barrier (red = increase). (b) Vector plot of residual currents with and without a storm surge barrier. The vectors have been normalised, so they all have the same length.

However, it is also observed that the residual currents and the maximum tidal flow velocities over the Banjaard shoal increase when the barrier is included in the model (Figure 4.22b and Figure 4.23). This indicates that, although the tide-averaged flow velocities have decreased, the flow velocities have also become more asymmetric (larger maximum velocities). The residual flow and tidal asymmetry constitute the major contribution to the net sediment transport (Van de Kreeke and Robaczewska, 1993). Figure 4.23b also shows that the directions of the residual currents have been changed. Especially in the vicinity of the Westgat channel, the residual currents have been pushed to the north. Therefore, the erosion of the Krabbengat channel is not an effect of increased currents, but rather a result of increased residual flow and tidal asymmetry.

4.4.2 Simulated transport patterns

The residual sediment transports have the largest magnitude on the edges of the Oude Roompot channel and the northern edge of the Banjaard shoal (Figure 4.24). The magnitudes on these locations are weaker in the 2007 simulation as compared to the 1986 simulation. As with the tidal flow, most sediment enters the domain from the southwest and is pushed westward by the flow coming out of the inlet.

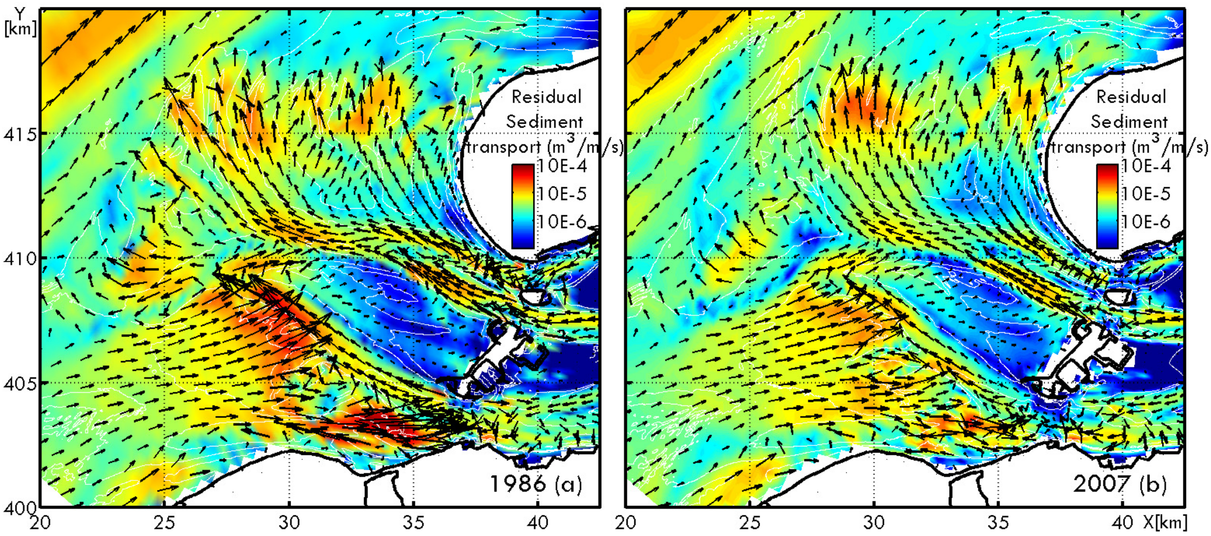

Figure 4.24: Modelled residual sediment transports: (a) 1986 bathymetry, (b) 2007 bathymetry.

When looking at the transport patterns on the Hompels shoal in detail (Figure 4.25), the model gives a good explanation for the morphological behaviour observed in this region. The sediment transport over the shoal is primarily flood-directed, while transports through the Oude Roompot channel are ebb-directed. This can explain the observed migration of the shoal edge into the channel: Due to the construction of the storm surge barrier the tidal flow and transports through the channel have decreased. The eastward transport over the shoal has also decreased, but not as much as in the channel, and thus is pushing the shoal into the channel. As a result, the shoal edge has migrated eastward. This process is visible in model runs with and without wave action, so it is mainly related to the altered tidal current, although wave action does seem to amplify it.

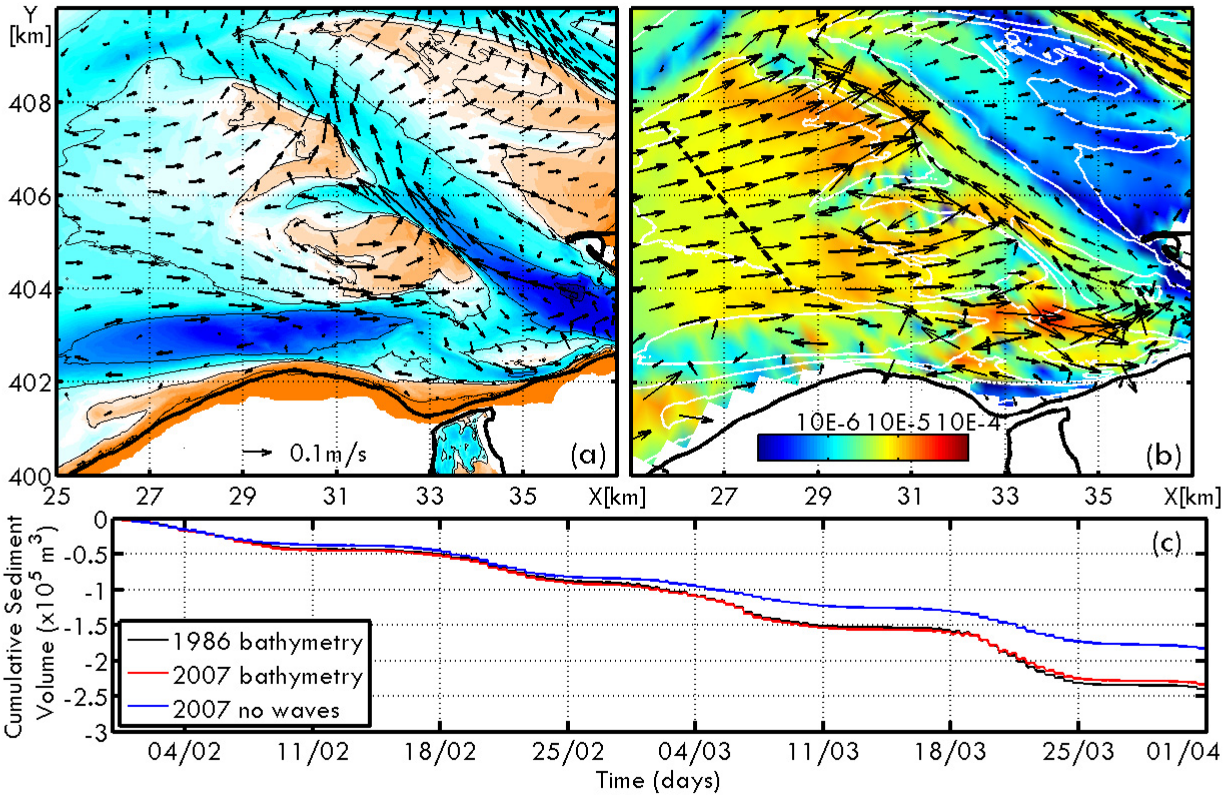

Figure 4.25: Model output around the Hompels shoal for the 2007 simulation with waves. (a) Tide-residual flow. (b) Tide-residual transport. (c) Sediment transport through the transect shown with the dashed line in (b).

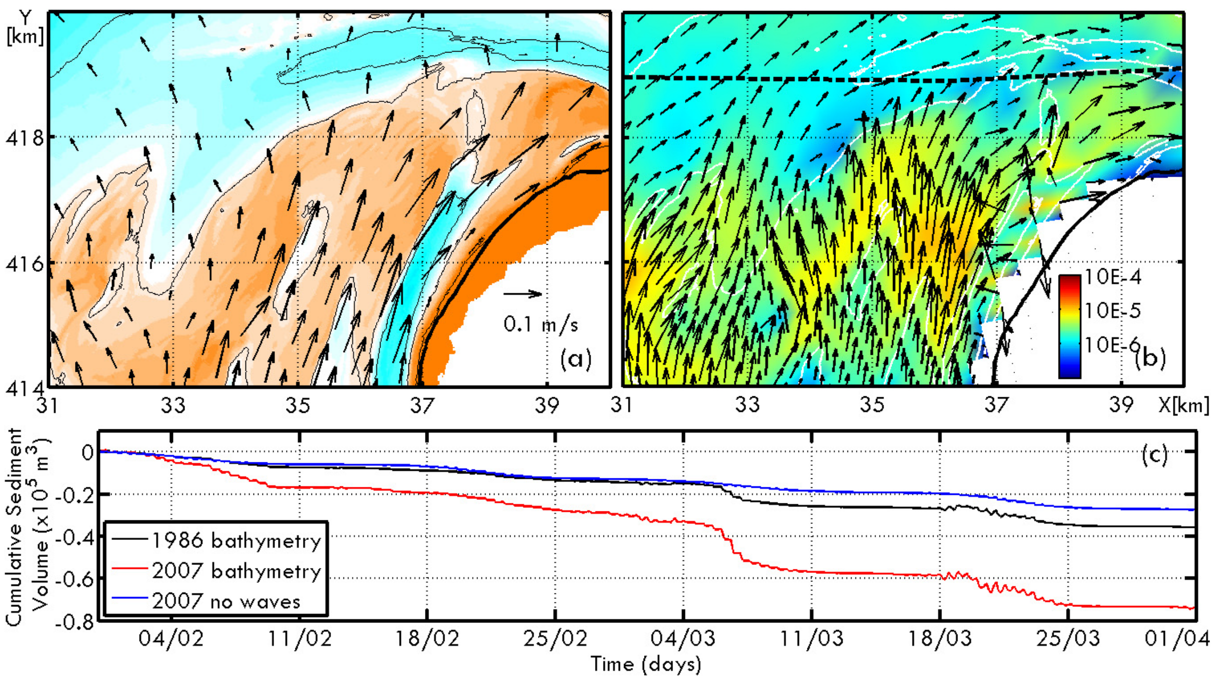

Figure 4.26: Model output around the Krabbengat channel for the 2007 simulation with waves. (a) Tide-residual flow. (b) Tide-residual transport. (c) Sediment transport through the transect shown with the dashed line in (b).

The migration of the Hompels shoal makes it possible, that in future decades the northern part of the Hompels shoal will attach to the Noordland shoal. The Oude Roompot channel will then be redirected in western direction through the ebb-chute in the middle of the Hompels shoal. This scenario seems plausible, also because this new configuration has been present at the same location in the past (Eelkema *et al.*, 2012).

The part of the Banjaard shoal between Krabbengat and Banjaard Channel loses sediment according to the model as well as the measured data. The influence of waves becomes apparent when comparing the transport magnitudes and residual transport vectors from the simulations with and without waves. Without waves, the simulated transports are directed mainly from south to north. When wave forcing is included, the transport vectors are significantly more coastward directed, especially on the part just west of Krabbengat channel (Figure 4.26). Also, the transport magnitudes are much larger when wave forcing is applied. This model result is in agreement with the idea that the saw-tooth shaped bars observed on the Banjaard shoal are wave driven features.

By comparing the modelled changes in sediment volume in certain areas of the ebb-tidal delta with the measured trends in the same areas, we see that the model reproduces most of the trends (sedimentation vs. erosion) observed in reality. The computed sediment transport through the barrier is negligible. Most of the morphological activity in the model is located around the Oude Roompot channel edge and the northern side of the Banjaard shoal, as is also seen in measurements. However, the model does seem to overestimate the amount of sedimentation in some places. This overestimation is in fact so strong, that the sediment volume of the entire ebb-delta shows an increase in both the 1986 and 2007 simulations, instead of the measured decrease (Figure 4.27).

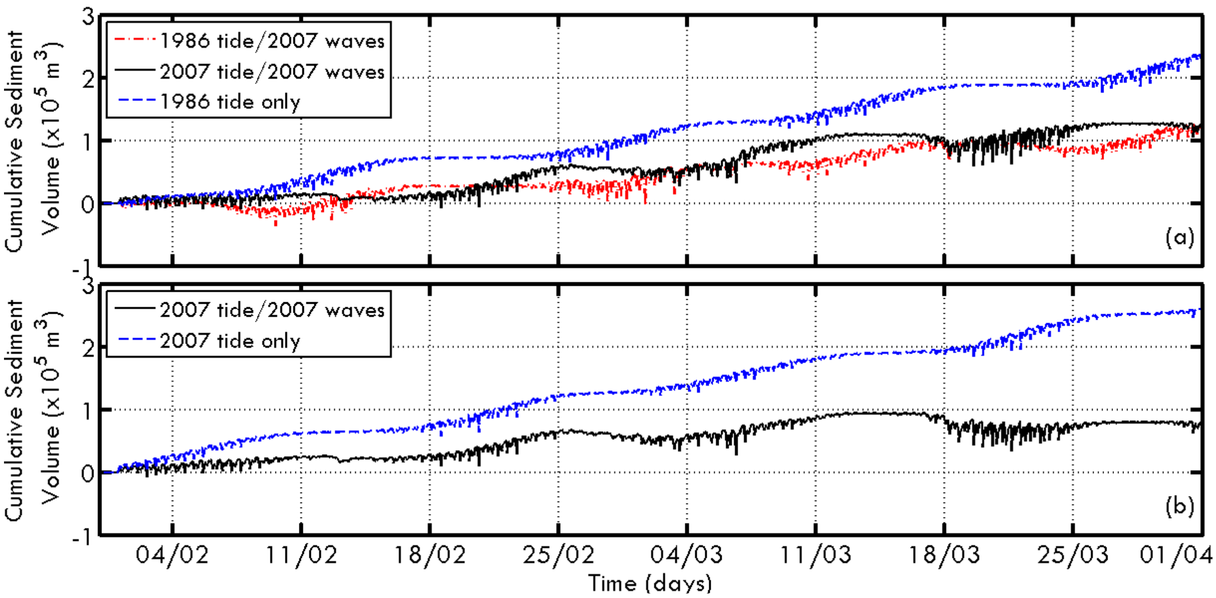

Figure 4.27: Evolution of the cumulative sediment volume change of the ebb-tidal delta in different simulations. (a) 1986 bathymetry simulations. (b) 2007 bathymetry simulations. Legends indicate which types of forcing are applied.

The modelled evolution of the sediment budget confirms the idea that tidal currents on the ebb-tidal delta make the sediment volume increase, while wave action makes it decrease. The simulations with only tidal forcing and no wave forcing (blue lines in Figure 4.27) produce a sediment volume increase which is more than 2 times larger than the increase produced by a simulation with wave forcing applied (black lines in Figure 4.27). Hence, the waves temper the growth of the ebb-tidal delta, although in the model not enough to cause a decrease in sediment volume.

The differences in overall bathymetric changes between the 1986 and 2007 simulations are small. After two months of simulation, the bathymetry of 2007 produces only slightly less change in total sediment volume than the 1986 bathymetry (black lines in Figure 4.27). However, it is worth to note that the 1986 and 2007 simulations are almost completely out of phase with regard to their spring-neap tidal phase. When a spring tide occurs in the 1986 simulation, the 2007 simulation experiences neap tide, and vice versa. The time series for the wave forcing is identical for both simulations, so in one simulation a high-energy wave event can occur during a spring tide period, while in the other simulation the same event occurs during neap tide. Therefore, the question arises whether this difference in the phase of the spring-neap cycle has an effect on the outcome. To answer this question, an extra simulation has been performed with the 1986 bathymetry, but with the 2007 tidal forcing. The wave forcing is left unaltered. This simulation shows that while there is some variation on a 14-day scale, the average trends are the same (black and red lines in Figure 4.27a). Hence, the differences in bed-level changes which might arise from the difference in phasing apparently even out on longer time scales.

The difference between simulations with and without waves is even more noticeable when looking at the modelled evolution of the hypsometry (Table 4.3). When no wave forcing is applied, the parts above -10 m depth gain sediment volume, while these same parts lose volume when wave forcing is applied, which is also observed in reality (Figure 4.11). The parts deeper than -10 m show a similar, yet opposite trend: Without wave forcing, these parts lose sediment. With wave forcing, these parts gain sediment, as is observed in reality. Apparently, the division in the behaviour of shallow and deeper parts is strongly related to the wave action.

Table 4.3: Measured and modelled hypsometric evolution. "+" = net sedimentation. "-" = net erosion.

Measurement/Model	Depths below -10 m	Depths above -10 m	Entire delta
Measured 1984 - 1988	+	-	-
1986 tide only	-	+	+
1986 waves + tide	+	-	+
Measured 2004 - 2008	=	-	-
2007 tide only	+	+	+
2007 waves + tide	+	-	+

4.5 DISCUSSION AND CONCLUSIONS

It has been roughly 25 years since the Eastern Scheldt storm surge barrier has been in place. From the observed evolution of the bathymetry since the barrier's completion a number of questions arose about the effects of the barrier on the ebb-tidal delta. A process-based numerical model was applied in order to gain insight into the mechanisms behind the observed behaviour. The combined results of data analysis and model output are illustrated in Figure 4.28.

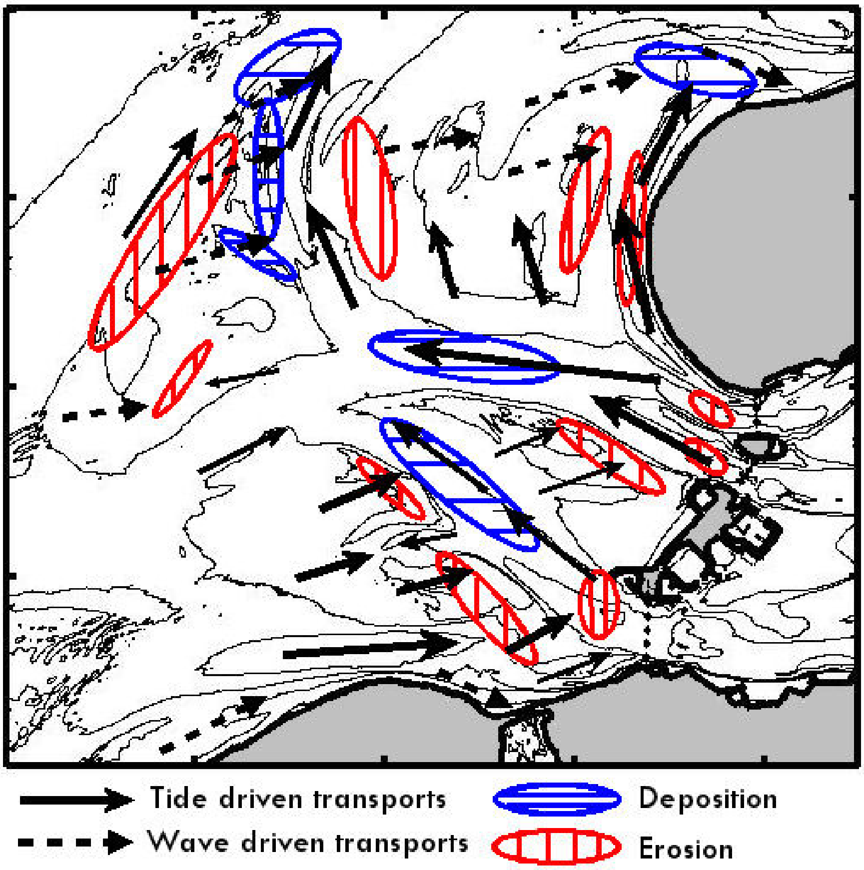

Figure 4.28: Schematization of the sediment transports and main erosion and deposition areas on the ebb-tidal delta.

The initial response of the ebb-tidal delta is characterized by a reorientation of the channels and a redistribution of sediment. The primary mechanism behind the reorientation is the relative change in strength of the alongshore and cross-shore tidal currents. Because the cross-shore current out of the inlet decreased in strength, the alongshore component gained in importance. As a result, the channels rotated clockwise, and the shoals have been expanding in northward direction. This mechanism is also described by Van der Vegt (2006), who explains how the tide-residual eddies can be pushed down drift by an alongshore residual current (Figure 4.29).

Overall, the shallow parts of the ebb-tidal delta are eroding, while the deeper parts gain sediment. However, this trend is not seen everywhere on the ebb-tidal delta. The channels on the ebb-tidal delta which run close to the shore have shown scouring since the barrier's construction, even though the tidal currents through these channels have decreased. The probable causes for this erosion are stronger residual flows and tidal asymmetries.

The processes governing the redistribution of sediment are the decreased tidal currents in combination with the increased relative strength of the wave action. The overall decrease in currents also caused a strong decrease in morphological activity, i.e. the average size of the bed-level changes has become smaller. In spite of this, the sediment budget still shows a distinct erosive trend. So even though the bed-level changes are small on average, they are mostly negative.

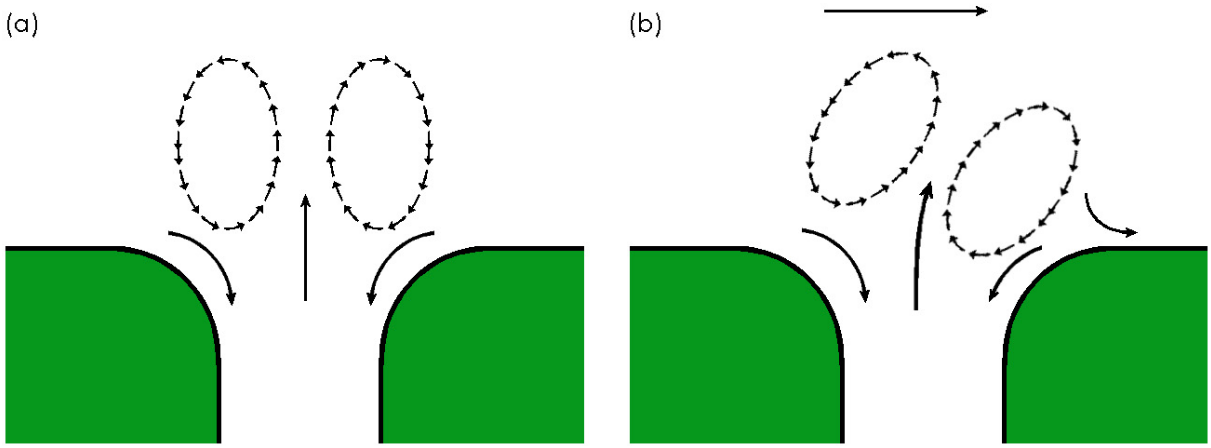

Figure 4.29: Schematised residual flow patterns on an ebb-tidal delta, adapted from Van der Vegt (2006). (a) Standing tidal wave along the coast. (b) Propagating tidal wave along the coast (left side to right side).

With the results of the process-based model, we have gained insight into the relevant processes governing the sediment redistribution, and the transport paths that are associated with this redistribution. The process-based model simulations indicate that wave forcing is important in the reduction of the sediment volume of the ebb-tidal delta. Without wave forcing, the model produces more sedimentation than when wave forcing is applied. More specifically, the model needs wave forcing to adequately reproduce the observed change in the hypsometry, in which deeper parts gain sediment, while shallow parts erode. This trend is only reproduced when tidal forcing and wave forcing are applied simultaneously.

Import of sediment onto the ebb-tidal delta still occurs in the south-western part, with the flood-dominated current pushing sediment through Southern Roompot channel and up the Hompels shoal. The sediment transports over the Banjaard shoal are mainly directed northward. As a result of the barrier, the ebb currents coming out of the inlet have decreased in transport capacity, but still transport sediment away from the inlet and onto the distal parts of the ebb-tidal delta, where this sediment is further reworked by a combination of wave and tidal action. Two main deposition areas for this sediment where this mechanism is most visible are the northern ends of Krabbengat and Banjaard Channels.

Although the model applied in this study has aided in testing hypotheses and gaining insight into the mechanisms behind the adaptation of the ebb-tidal delta, improvements to the model application are still possible. The model fails to reproduce the erosive trend measured in reality. This is probably because of the delicate balance between wave and tidal forcing. Due to the large spatial scales involved, a small underestimation of the wave- or tide-related erosion or sedimentation can lead to a simulated trend which differs from the measured trend.

With the knowledge gained from observed behaviour and model results, a view emerges of an ebb-tidal delta which is still far from any kind of morphological equilibrium, and which is steadfastly adapting itself to the new hydraulic forcing regime, even though sediment transport capacities have decreased. It is yet unclear what a new equilibrium state of the ebb-tidal delta will possibly look like, or how long it will take for this area to reach this new state. The measured trends have not yet shown signs of levelling out. The future ebb-tidal delta will become smoother, with smaller differences in depth between shoals and channels. However, at what point the shoals will stop losing sediment remains unclear.

This lack of clarity also comes from the differences between the Eastern Scheldt ebb-tidal delta and the neighbouring ebb-tidal deltas of the Grevelingen and the Haringvliet. On these ebb-tidal deltas the waves are actually turning the sub-tidal swash platforms into large intertidal shore-parallel bars. This development is absent at the Eastern Scheldt, which gives rise to the hypothesis that the way in which a swash platform like the Banjaard shoal responds to changed hydrodynamics depends on how much tidal current is still present. If there is virtually no tidal current, like at the Grevelingen, the waves can form large bars. If the tidal current is diminished, but still sufficient, then the bars will not form, and the current will simply transport the sediment stirred up by the waves. However, while this tidal current may be sufficient to transport sediment off the swash platform, it might be too weak to transport sediment onto the same platform, causing net erosion.

Which range of tidal currents actually puts the swash platform in any particular state is the knowledge which is needed to say anything about a possible end state of the Eastern Scheldt ebb-tidal delta. The erosion of the shoals might stop when either the sediment transport towards the shoal picks up again, or when the sediment transport from the shoal towards deeper water decreases. The first condition might be met if the main channels become even more shallow, which would concentrate the tidal currents running through them. The second condition might be met if the shoals become so deep that either the waves are hardly effective at stirring up sediment anymore, or the tidal currents are hardly effective at transporting the sediment. At what point these conditions are met, if at all, remains unknown.

The Eastern Scheldt storm surge barrier was the first of its kind ever implemented in a tidal inlet. As such, it gives valuable insight into the effect of storm surge barriers on estuarine morphology. In general, the most important feature of a storm surge barrier is its constriction of the cross-sectional area of the inlet. This constriction caused a general decrease in flow velocity magnitudes inside and outside the basin. This effect causes a sharp decrease in sediment transport capacity, which in turn causes eroding shoals and flats, sedimentation in channels, and probably even the blockage of sediment exchange between the basin and the ebb-tidal delta. These effects have to be kept in mind whenever the construction of a storm surge barrier is considered anywhere else in the future.

Chapter 5

LONG-TERM EFFECTS OF A STORM SURGE BARRIER ON AN EBB-TIDAL DELTA

5.1 INTRODUCTION

The previous chapters describe the evolution of the Eastern Scheldt tidal inlet up until the present day. However, the aim of this thesis is not just to present descriptions and explanations of past behaviour, but also to give an outlook on what this behaviour might be for the next 200 years. This chapter aims to give an outlook on possible future developments, by discussing the possible evolution of an ebb-tidal delta under the influence of a storm surge barrier on longer timescales, viz. timescales of several decades to centuries. This is done by applying a process-based model to simulate the evolution of an ebb-tidal delta with a highly schematized geometry. By comparing simulations with and without a storm surge barrier, we hope to gain insight into the effects and timescales of these interventions.

The outline of this chapter is as follows: Section 5.2 explains in more detail the problem in making a prediction on future developments. In section 5.3 the method and models used for investigating future behaviour are explained. In sections 5.4 and 5.5 the results of these models are presented and discussed.

5.2 PROBLEM DESCRIPTION

Tidal inlets are openings along barrier coastlines through which tidal waters flow, thereby connecting the sea to estuaries and tidal basins (Fitzgerald *et al.*, 2002). Human intervention in and around tidal inlet systems can have far reaching consequences on the behaviour of these inlets and the basins and coasts which they connect (Stive and Wang, 2003). Depending on the magnitude of the intervention, the state of the system can be brought far out of morphological equilibrium.

This system, usually subdivided in a basin, an inlet, an ebb-tidal delta and the adjacent coasts, will typically evolve back towards a new equilibrium by redistributing sediment between its elements. In the case of a tidal prism decrease, the basin will require sediment in order to fill up channels which have become oversized relative to the currents running through them. In the same case, the ebb-tidal delta will have a surplus of sediment due to the same decrease in tidal prism (Walton and Adams, 1976). Thus, the basin will typically receive the required sediment from the ebb-tidal delta.

In the nineteen eighties, the Eastern Scheldt inlet was partially closed off from the North Sea with a storm surge barrier. This storm surge barrier is unique in the world, not only in its design and age, but also in the manner in which it altered the exchange of sediment through the inlet. The barrier consists of rows of concrete piers across the three main inlet channels. The piers hold the barrier gates, which can be lowered to cut off the tidal current through the barrier in case of a storm surge. The three gate sections are connected with two construction islands, built on top of former intertidal flats. On both sides of the barrier the bed is protected against erosion. This scour protection is about 600 m long measured from the barrier. Simultaneously with the storm surge barrier, also two back-barrier dams were built in the Eastern Scheldt basin in order to restrict the decrease of the tidal range by limiting the basin length and thereby increasing the reflection and amplification of the tidal wave. However, these dams also reduced the basin area from 450 km^2 to 350 km^2.

Judging by the sediment budget of the basin, virtually no sediment has been imported or exported by natural processes since the completion of the barrier (Louters *et al.*, 1998). Tidal currents have also been reduced, which caused an even stronger decrease of the sediment transports. Jongeling (2007) gives an overview of sediment transport measurements performed in 1988, and concludes that the sediment transport through the barrier is very small.

The time required for the sediment surpluses and deficits to level out depends on the size of the basin and ebb-tidal delta, how far each of these elements is from its equilibrium and how strong these elements are interacting with each other (Kragtwijk *et al.*, 2004). For Dutch tidal inlets these time scales can easily reach decades or even centuries. In the case of Texel Inlet, for instance, this inlet is influenced by a large reduction of the back-barrier basin by the Afsluitdijk (Enclosure Dike). This closure in 1928 created a large sediment deficit in the remaining Marsdiep basin. By the year 2000, there was still a significant sediment import into the Marsdiep basin in the order of 5 to 6 Mm^3/year (Elias, 2006). The driving mechanisms behind this net import are the strong tidal currents in the inlet, the vicinity of a large supra-tidal shoal in front of the inlet (Noorderhaaks) which can supply sediment, and the large sediment demand inside the basin.

The Marsdiep basin is of comparable size as the Eastern Scheldt, and also the tidal volumes are of the same order. However, where the Marsdiep basin and its ebb-tidal delta can freely exchange sediment through the inlet, the Eastern Scheldt basin cannot do this because of the storm surge barrier. The Eastern Scheldt's ebb-tidal delta only remaining pathway to get rid of its excess sediment is through interaction with its adjacent coastline. However, in the case of the Eastern Scheldt, this adjacent coastline consists of the former Grevelingen ebb-tidal delta, which is also dealing with a surplus of sediment after closure of its inlet in 1971. This makes it likely that the adaptation of the Eastern Scheldt ebb-tidal delta will take even longer than the Marsdiep ebb-tidal delta.

From the analysis in the previous chapter of the observed morphology of the Eastern Scheldt ebb-tidal delta, a couple of predictions can be made. Between 1986 and 2008, the 10 m depth contour was the point on the hypsometric curve above which there was net erosion, and below which there was net sedimentation, as compared to the 1984 bathymetry. The erosion of the shallow areas will continue for the coming decades. This erosion of the shallow areas will probably sustain itself due to the decrease of the sheltering effect created by the seaward shoals. As they become lower, their ability to dissipate wave energy will also decrease. As a result, shoals that are located more inward, such as the Hompels and Noordland shoals, will experience more wave attack. This also means that it is probable that the maximum significant wave heights measured seaward of the barrier will increase over the coming decades.

The sediment volume below 10 m depth seems stable as of 2008, but is also likely to start decreasing. This is because eroding areas of the ebb-tidal delta that used to be above 10 m depth, will simply erode beyond this depth and keep on eroding. Primary locations of this development are the terminal lobe and the Banjaard shoal.

These future morphological developments described here are hypothetical, based purely on the observed morphology between 1986 and 2008. It would be interesting to test these hypotheses to get more confidence in our ideas about what the ebb-tidal delta might look like in 100 to 200 years. In order to do this, a process-based numerical model is applied.

5.3 PROCESS-BASED MODELLING

5.3.1 Approach

The traditional, ‘virtual reality’ modelling philosophy consists of designing and calibrating a model to represent the real situation as close and detailed as possible, and then use this model to forecast the coming period. According to Dissanayake (2011), this traditional approach has several shortcomings when it is applied to longer time periods (100 years or more). The modelled bathymetrical development will most likely deviate from the real trend early in its evolution. This can be due to several causes: 1) The model will start with adjusting the bathymetry in order to counter the imbalance between the initial model bathymetry and modelled forcing conditions and model parameters. This behaviour can be looked at as morphological spin-up, and can lead to nonsensical solutions. 2) Long-term modelling requires either serious computational power, or significant input reduction in order to keep the computation time within limits. 3) In order to have confidence in a 200 year forecast, the calibration period needs to be of comparable length. However, only the period since 1986 is suitable for this calibration.

In light of these shortcomings, a different approach is used for this investigation, known as the 'realistic analogue' (Roelvink and Reniers, 2011). This approach is similar to that used by Dissanayake *et al.* (2009), who used a schematized model approach to develop a qualitative representation of a Wadden Sea inlet. For the present study, the approach consists of using a process-based numerical model, Delft3D, to generate basin and inlet morphology in a schematized model geometry similar to that of the Eastern Scheldt. In this approach, the model starts from a uniform bed, and is allowed to produce a morphology which is in equilibrium with its forcing. Once this morphology is sufficiently established, the model is used to make an actual forecast.

The criterion of being 'sufficiently established' means that the simulated morphology has to be compared to real data to see whether the simulated morphology behaves similar to reality. Not every combination of input and model parameters results in a morphology that passes this criterion. Appendix B gives an overview of the model parameter settings that have been considered for this study. For the rest of this chapter, only the parameter settings that were deemed to be best are discussed.

The model domain consists of a rectangular area representing the open sea and coast. Halfway along this coast, the Eastern Scheldt basin is attached (Figure 5.1). This basin has the same geometry as the real Eastern Scheldt basin. This geometry is adopted because it makes this model more comparable to the real situation around the Eastern Scheldt.

The morphological model with this geometry is first run for three hydrodynamic years with a morphological scale factor of 200. Thus, the model simulates 600 years of morphological evolution. This simulation will serve as a baseline simulation. The effects of a storm surge barrier are investigated by implementing a barrier in the bathymetry generated by the model after 400 years, and then letting this new simulation run for another 200 morphological years. The effects of the modelled barrier become apparent when results of this altered simulation are compared to the last 200 years of the unaltered simulation.

For the purpose of this study, it is important that the simulated bathymetry behaves in the same way as the real ebb-tidal delta. In order for this to be true, the simulation needs a minimum morphological simulation time of 400 years. This period is required for the bathymetry to establish an ebb-tidal delta with approximately the same hypsometry as found in reality. Especially the shallow parts with a water depth above 10 m need this time to approach realistic values. If the simulation with storm surge barrier is started with a younger bathymetry from the baseline simulation, the model will simply continue to build up the shoals, while in reality the shoals are eroding in response to the barrier.

5.3.2 Model setup

The model domain consists of a stretch of coast 60 km long and 25 km wide with a tidal basin attached halfway its long side (Figure 5.1a). This basin has the geometry of the Eastern Scheldt basin, which is approximately 50 km long and 7 km wide. The size of the grid cells varies over the domain. In and around the inlet the cell size is 150 by 150 m, widening to about a kilometre near the boundaries.

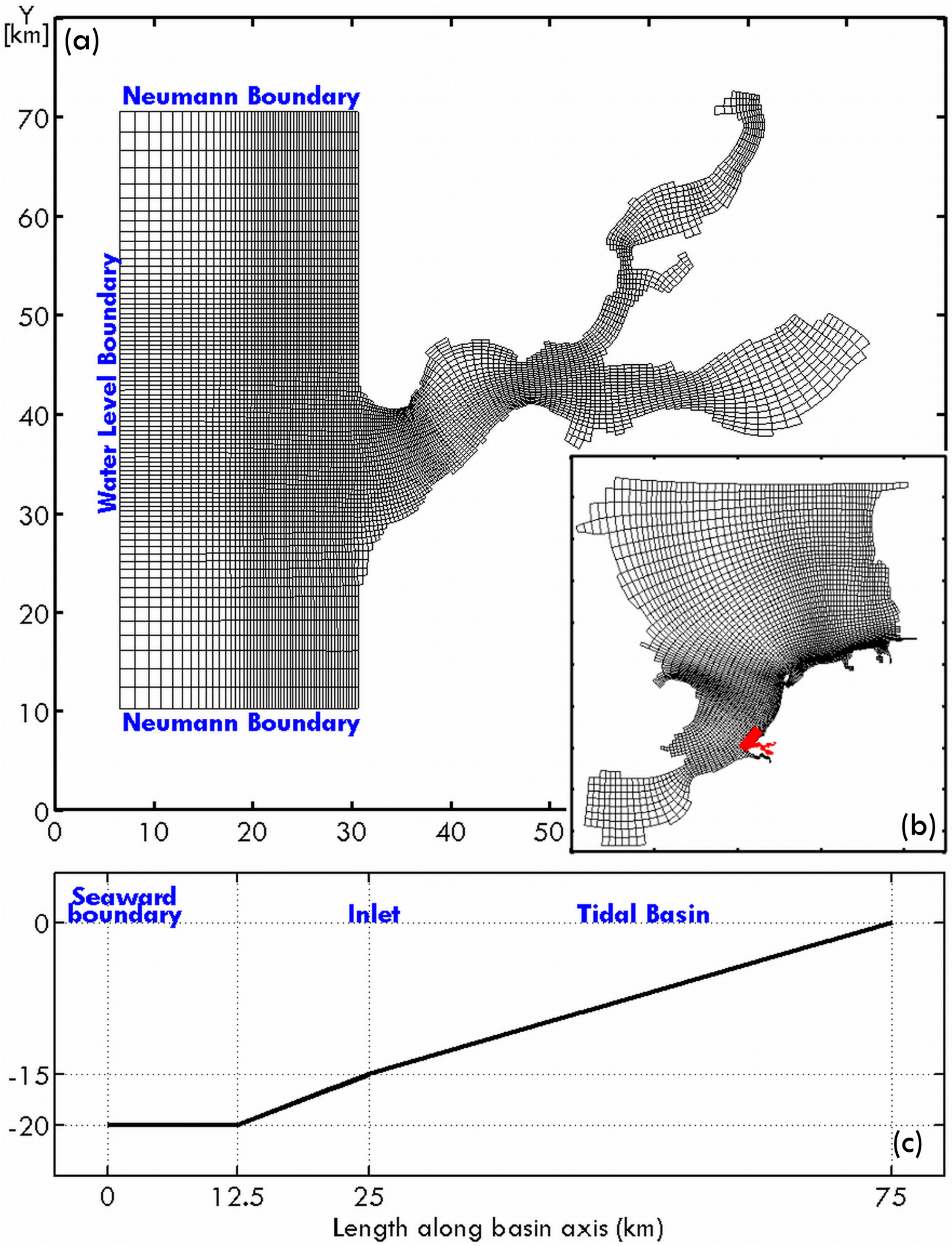

Figure 5.1: (a) Model grid with boundary configuration. (b) North Sea grid with nested model grid (red). (c) Initial depth profile along the basin axis.

The model is forced by a combination of water level boundaries on its alongshore edge and Neumann boundaries (i.e. water-level gradient boundaries) on its cross-shore edges. All other boundaries are closed. The boundary conditions were created by nesting this detailed grid in a much larger and coarser model covering most of the southern North Sea (Roelvink *et al.*, 2001). The smaller model is nested at the location of the Eastern Scheldt in the coarser model (Figure 5.1b). The only tidal constituents considered are the M_2 tide and its first two harmonic overtides M_4 and M_6. The values for the amplitudes and phases of the Neumann boundaries were derived following the method described by Dissanayake (2011). This configuration of boundary conditions results in a progressive tidal wave running from south to north along the coast. The model produces a tidal amplitude at the location of the inlet of 1.3 m, which is very similar to the average tidal amplitude measured seaward of the Eastern Scheldt inlet in reality.

The initial bathymetry of all simulations consists of a uniform sloping bottom with a depth of 0 m at the landward end, linearly increasing to 15 m in the inlet. Seaward of the inlet, the depth increases linearly to 20 m over a distance of 12.5 km. Seaward of this, the bed has a constant depth of 20 m (Figure 5.1c).

The initial bed composition is an important parameter for the result of the simulation. In reality, there is a distinct segregation in grain sizes between the shoals and the channels (Figure 4.5). The median grain size in the channels is larger than on the shoals. Running the Delft3D-simulations with a single uniform grain size would lead to unrealistically deep channels. Therefore, the initial bed composition consists of an even mixture of three non-cohesive sediment fractions of 100, 300, and 500 microns, respectively. To further keep the channels from growing too deep, the transverse bed slope factor is set at 100. This value deviates far from the value 1.5 suggested by Ikeda (1982). However, values lower than 100 result in less realistic hypsometries.

To investigate the influence of waves on the evolution of the ebb-tidal delta, two types of simulations are run, one with tidal forcing only, and one with both tidal and wave forcing. The wave forcing is kept simple, with a single wave, in shore-normal direction on the western boundary which stays constant in time. The significant wave height and period are the same as the average wave height and period measured offshore of the Eastern Scheldt tidal inlet: H_s= 1.4 m, T_p = 4.5 s.

The evolution of the wave field is simulated using online coupling of the SWAN model (Booij *et al.*, 1999) with the Delft3D FLOW-module. The SWAN module uses the bathymetry, water levels and current velocities from the FLOW module to compute wave heights, periods and directions. The results are coupled back to the FLOW-module. The wave field computed with SWAN is updated every 60 minutes.

After 400 years of computed morphology, a barrier is implemented in the bathymetry. This barrier consists of three elements: Dry points across the islands at the barrier's location, decreased depths in the channel openings, and non-erodible layers on both sides of these openings. The dry points have the same effect as the construction islands by cutting off the flow over these tidal flats. The decreased depths in the remaining channel openings act as the sills and piers of the barrier by significantly reducing the cross-sectional area (Figure 5.2). These openings are also made non-erodible. The total size of the openings has been calibrated to cause the same relative decrease in tidal amplitudes as the real barrier, which reduced the tidal amplitude by 20%. The total reduction of cross-sectional area is 81%. With this kind of barrier implementation in the bathymetry, there is no need for the porous plates used in the *KustZuid*-model applied in the previous chapter. The resolution of the grid in the vicinity of the barrier is such, that the barrier openings are only three or four grid cells wide. The non-erodible layers next to the barrier act as the scour protection.

Apart from the barrier, also the back-barrier dams (Oester dam and Philips dam) have a serious effect on the tidal range and prism, because they reduce the basin length and basin area. These dams have been incorporated in the model by placing a thin dam which reduces the basin area by 22%.

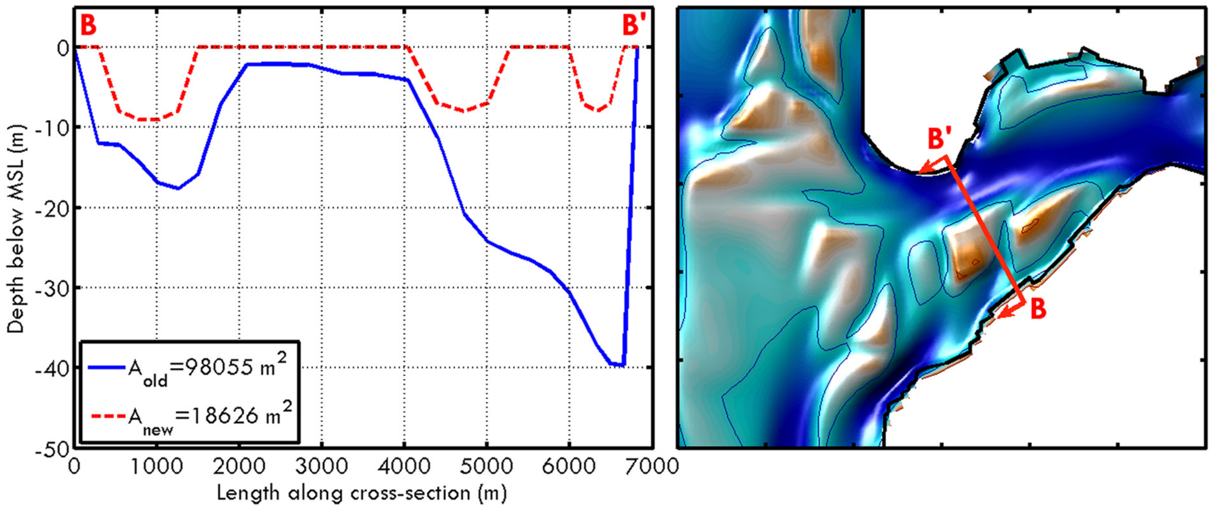

Figure 5.2: Model inlet cross-sectional area before and after implementation of the storm surge barrier.

5.4 Results

5.4.1 Baseline simulations

The model reproduces the general location of the main shoals and channels on the ebb-tidal delta (Figure 5.3). On the northern side of the ebb-tidal delta, the model generates a large shoal which extends roughly 10 km into sea and curves around the inlet. This shoal looks similar to the Banjaard shoal in reality. Both the Banjaard shoal and the shoal in the simulation are also intersected by small shallow channels. In the simulations one of these channels runs around the coastline, similar to how the Krabbengat channel runs around the Schouwen coastline.

The southern part of the simulated ebb-tidal deltas is dominated by two or three main channels. The pattern of these channels and the shoals and sills between them looks similar to the Westgat and Roompot channels with the Noordland and Hompels shoals between them. The orientation of the main channels and shoals is in accordance with the conceptual model by Sha and Van den Berg (1993). This configuration of channels and shoals is generated by the model even when there is only tidal forcing applied in the simulation. This implies that the configuration is mainly governed by tidal interactions, and waves play a secondary role.

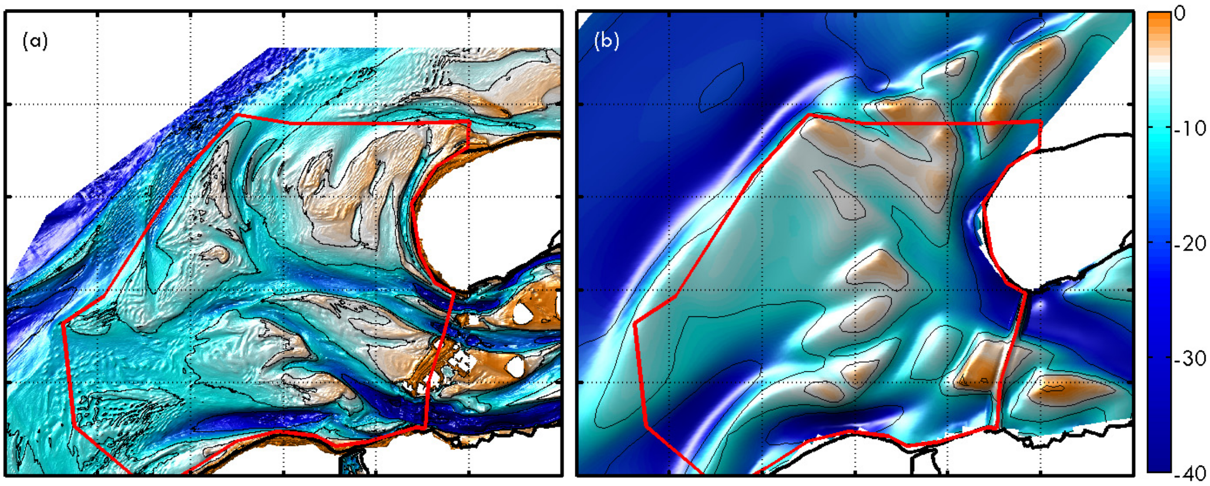

Figure 5.3: (a) Eastern Scheldt ebb-tidal delta bathymetry in 2008. (b) Modelled baseline bathymetry after 400 morphological years. The red polygon indicates the area used in determining the hypsometry and sediment budget.

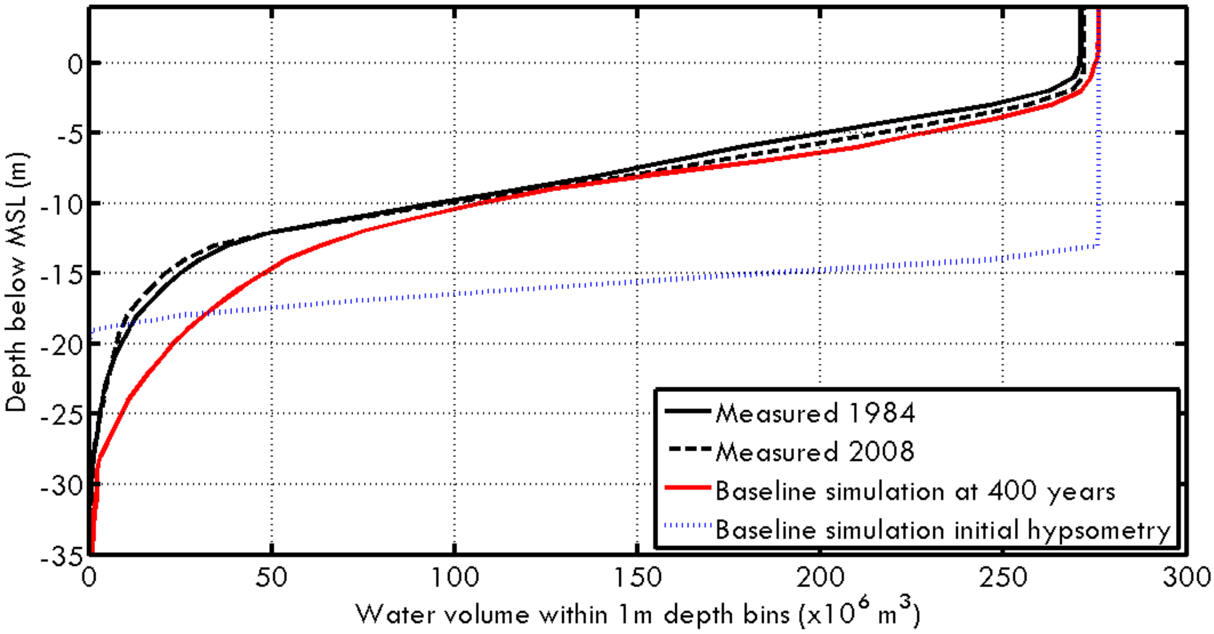

Figure 5.4: Hypsometric curves of the real ebb-tidal delta (black lines and dots), and modelled ebb-tidal delta (red line). The considered area is shown as the red polygons in Figure 5.3.

The hypsometry of the ebb-tidal delta needs at least 400 years of morphological computation to stabilize. Comparison between the modelled hypsometry and the hypsometry measured in 1984 shows that the shape of the hypsometric curves look similar, although the model overestimates the water volumes (Figure 5.4).

The inclusion of the multiple sediment fractions generates a segregation of grain sizes which is again also observed in reality (Figure 4.5 and Figure 5.5). This segregation consists of coarser grains in the channels and finer grains on the shoals. The larger grain sizes found just seaward of the terminal lobe are also reproduced by the model.

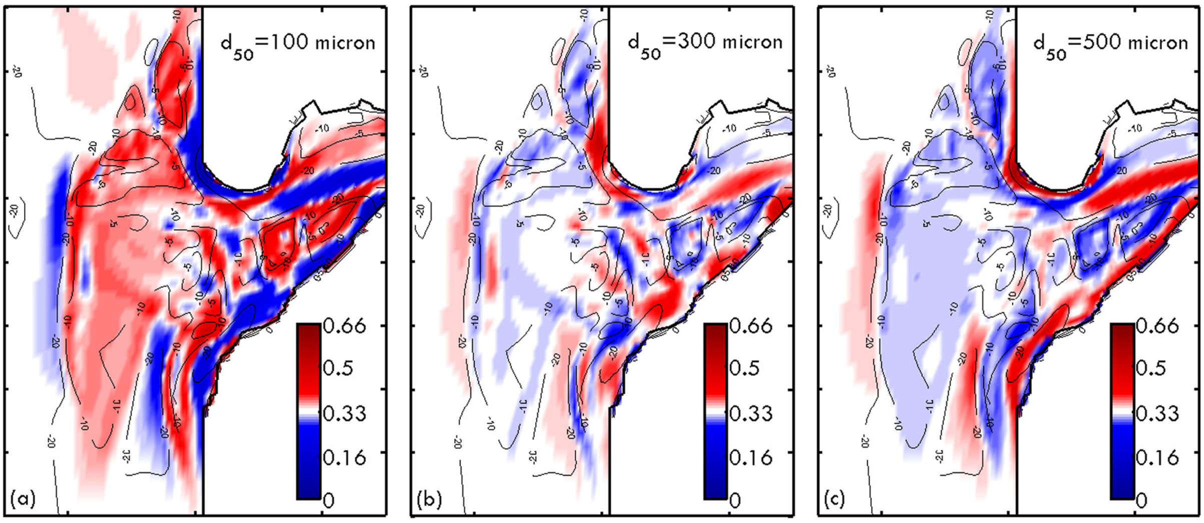

Figure 5.5: Sediment mass fraction distribution (%) after 400 years of simulation, starting from a uniform distribution (33% for each fraction).

5.4.2 Storm surge barrier

The storm surge barrier has several effects on the ebb-tidal delta hydrodynamics. First of all, it decreases the tide-averaged absolute flow velocities on the entire ebb-tidal delta except for a small region near the storm surge barrier.

The modelled storm surge barrier has a strong effect on the exchange of sediment between the sea and the basin (Figure 5.6). The basin receives hardly any sediment in the model, as is also observed in reality. The fact that this model reproduces this property with its simple implementation of the barrier, its relatively coarse grid, and its depth-averaged calculation, means that the sediment blockage has little do with any three-dimensional structure of the flow around the barrier and the scour holes. This result is in agreement with Hoogduin (2009), who also saw that a 2DH-model could reproduce the sediment blocking effect of the barrier, and that making adaptations to the scour holes such as filling them up and/or extending the scour protection had little effect on the exchange of sediment through the barrier. The study by Hoogduin (2009), as well as De Bruijn (2012) showed that the ebb- and flood-jets on both sides of the barrier play an important role in the direction and magnitude of the net sediment transports around the scour holes.

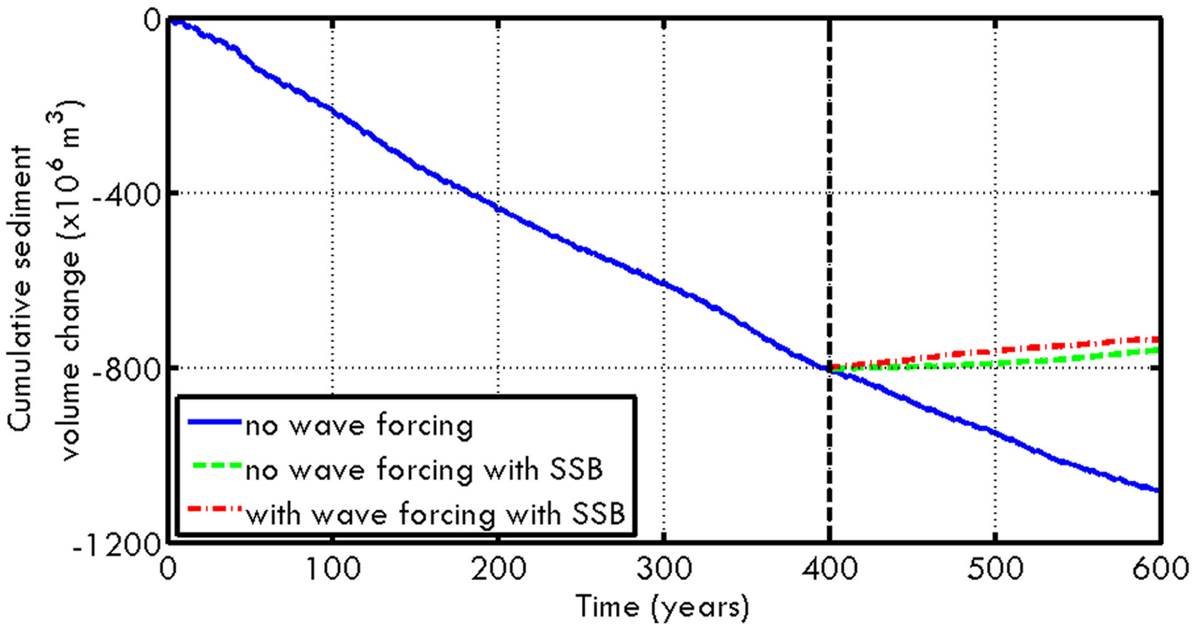

Figure 5.6: Cumulative sediment volume change of the basin behind the storm surge barrier.

When the cumulative sediment volume changes of the simulated ebb-tidal delta are considered, it is noticed that the model does not reproduce the measured trend in the sediment budget. According to measurements, the ebb-tidal delta began losing sediment with a rate between 1 and 2 Mm^3 per year after the barrier was completed. Most of this measured erosion is located in the shallow areas with depths less than 10 m below MSL. However, the simulations with storm surge barrier show either no net erosion in these shallow parts (black and dashed blue lines in Figure 5.7a), or they show less erosion compared to the same simulation without storm surge barrier (dashed red and dotted green lines Figure 5.7a).

The differences in the results between the simulations restarted with waves and the simulations with only tidal forcing are mainly the effect of the short waves being activated within the model. The activation makes that the model bathymetry starts to adapt itself to the presence of waves. In the simulation without storm surge barrier (dotted green line), this is visible as a period with high erosion rates, which lasts for roughly 50 years. After 50 years, the erosion rate becomes more or less equal to the erosion rates of the other simulations. The simulation with both waves as well as a storm surge barrier (dashed red lines) results in less erosion in the first 125 years than if waves are included and the inlet remains open (dotted green line). This behaviour of the model is considered as not consistent with the measured trends.

In order to isolate the effect of the storm surge barrier in these simulations, one has to compare either the two simulations with tidal forcing only (black and dashed blue lines in Figure 5.7d), or the simulations with both tide and wave forcing (dashed red and dotted green lines Figure 5.7d). None of these results show a clear difference in response between the altered and the unaltered simulations.

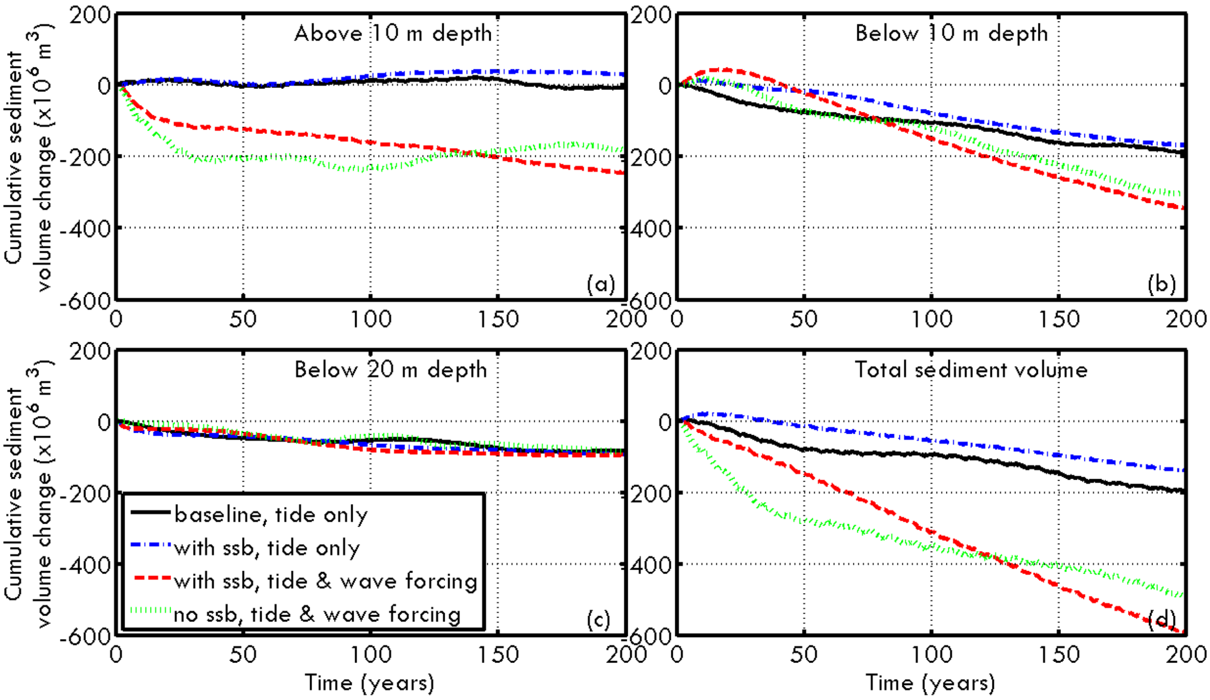

Figure 5.7: Cumulative sediment volume changes above and below various depths of the ebb-tidal deltas for the simulations starting from a baseline created with tidal forcing only.

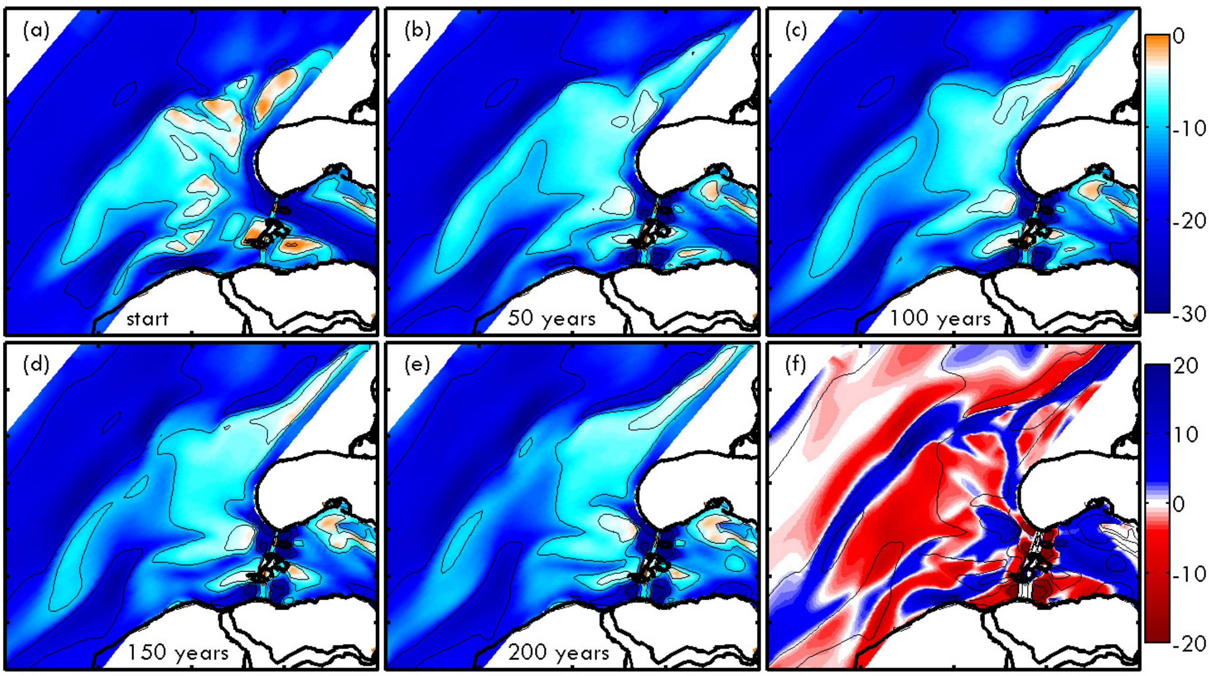

Figure 5.8: Simulated bathymetry of the ebb-tidal delta after barrier implementation in the simulation with both waves and tidal forcing, starting from the baseline bathymetry created with tidal forcing only. (f) Cumulative difference after 200 years (red=erosion).

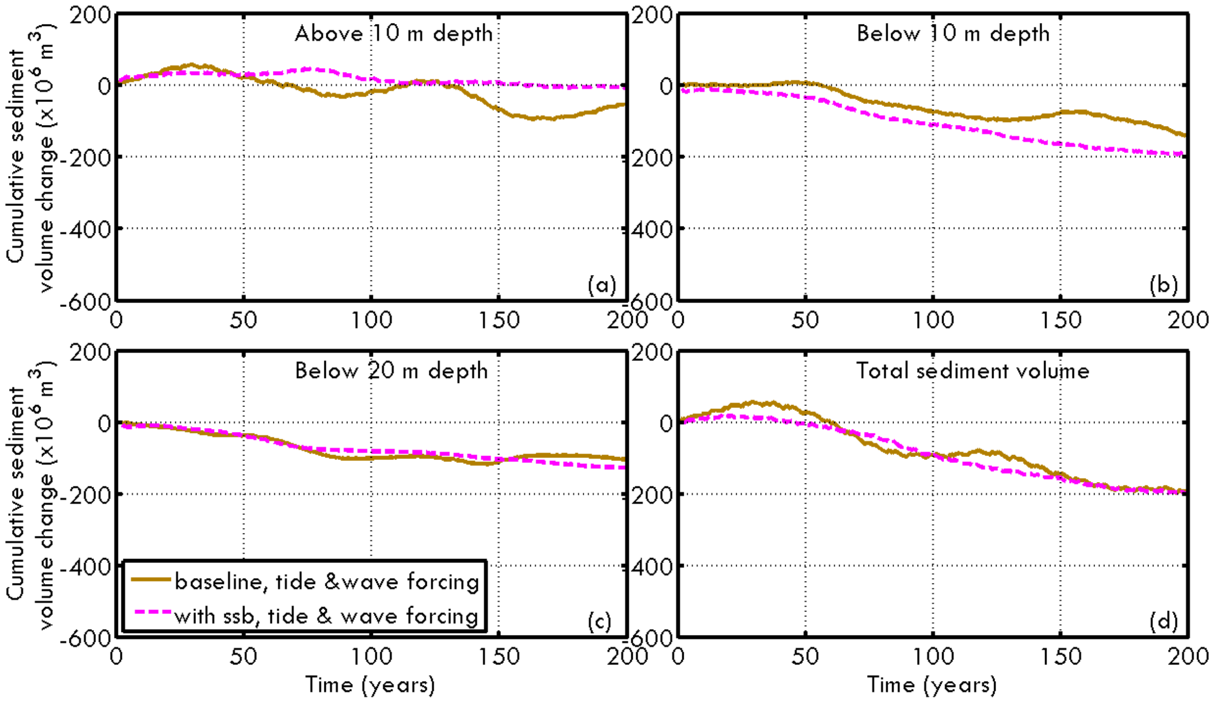

Figure 5.9: Cumulative sediment volume changes above and below various depths of the ebb-tidal deltas for the simulations starting from a baseline created with waves as well as tidal forcing

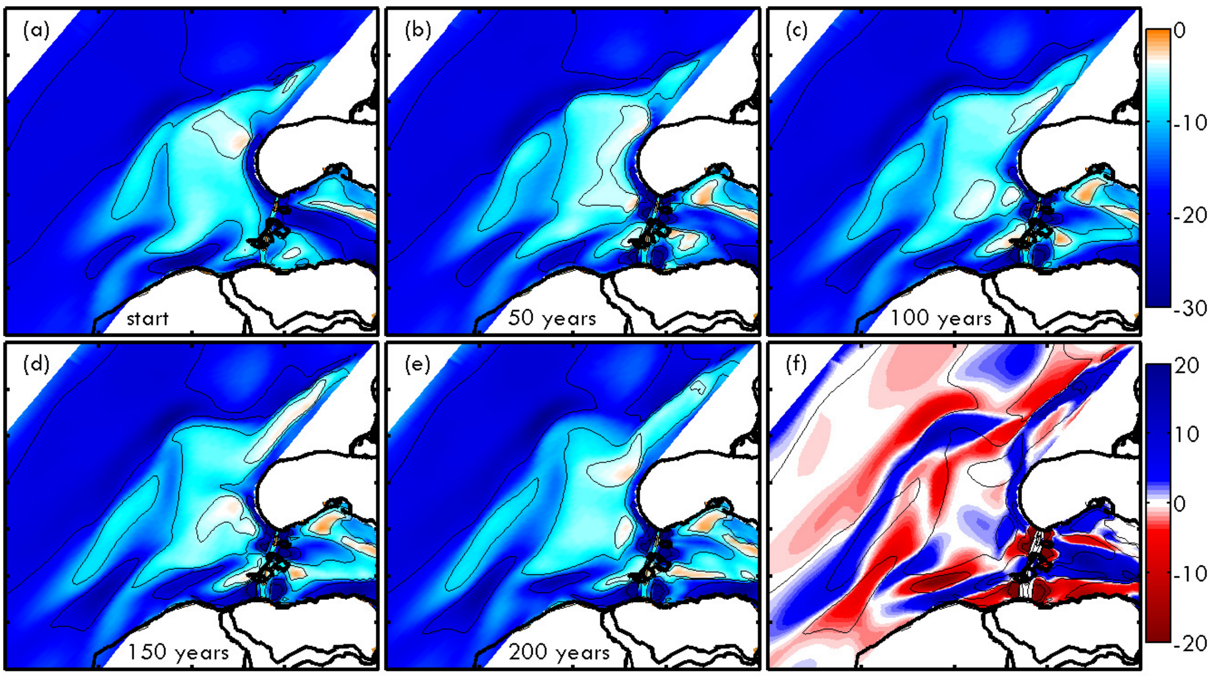

Figure 5.10: Simulated bathymetry of the ebb-tidal delta after barrier implementation in the simulation with both waves and tidal forcing, starting from the baseline bathymetry created with waves and tidal forcing. (f) Cumulative difference after 200 years (red=erosion).

The problems of the unrealistic effects which arise when a model bathymetry created without waves is used as the initial bathymetry in a simulation with waves should be averted if the baseline morphology is also created with both tide and wave forcing. The drawback of this approach is that the baseline simulation takes a lot more time to complete. When the new bathymetry created in this way is used as initial bathymetry in a simulation with a storm surge barrier (Figure 5.9), the results still show no clear difference in behaviour between the altered (dashed pink lines) and unaltered simulations (brown lines). Aside from this, both these simulations show a slight accretion of sediment in the first 25 years instead of erosion.

One plausible cause is the simplification of the wave forcing. The single wave condition of 1.4 m significant wave height might not be enough to cause the erosion on the ebb-tidal delta. Also, the single shore-normal wave direction does not create any littoral drift, which might be important. However, Dastgheib (2012) already states that the variation of wave directions is not a determining factor in the reshaping of an ebb-tidal delta, but the relative importance of waves and tidal forces are essential.

This statement seems related to the hypothesis made at the end of the previous chapter. This hypothesis was that the morphological response of an ebb-tidal delta depends on the intensity of the tide remaining on the ebb-tidal delta after a large-scale intervention in the inlet. If the tide is reduced far enough, then the waves will start reworking the shoals into large intertidal shore-parallel bars, as is observed at the Grevelingen and Haringvliet inlets (e.g. Steijn *et al.,* 1989; Cleveringa, 2008). The ebb-tidal delta as a whole still suffers net erosion. This situation can be seen as a wave-dominated erosive regime.

However, if the tide is reduced, but not by much, the remaining tidal current interferes with the cross-shore wave-driven sediment transport, and the intertidal shore-parallel bars are not created. Instead, the waves on a shoal simply stir up sediment which gets transported away from the shoal by the remaining tidal current. However, this tide is not strong enough to transport sediment from deeper water towards the same shoal, so the shoal suffers net erosion. This can be seen as a tide-dominated erosive regime.

The old situation of the Eastern Scheldt ebb-tidal delta, in the period before the barrier was built, can be seen as a tide-dominated accretive regime. The tidal current coming out of the inlet had an abundant source of sediment from the scouring channels, and had more than enough transport capacity to carry the sediment from the channels onto the shoals.

In light of this hypothesis, the behaviour of the model could be explained by stating that the simulations, with their particular hypsometry and parameter settings, do not reproduce the same regime changes as occurred in reality. These regime changes are dependent on the balance between wave-driven and tide-driven sediment transports. In order to reproduce the regime changes, these wave- and tide-driven transport magnitudes, or at least their relative ratios have to be reproduced well. What makes this even more challenging is that it is difficult on a shoal to distinguish between these two processes: Waves are affected by wave-current interaction, and the tide-driven transport can be enhanced by the wave stirring.

The response of the simulations (Figure 5.8 and Figure 5.10) looks more similar to the morphological response observed at the Grevelingen and Haringvliet ebb-tidal deltas. This would mean that the model overestimates the decrease in tide-driven transport relative to the wave-driven transport. Apparently, the sediment transport capacity in reality is still somewhat larger than the model predicts. It would be worthwhile to investigate whether tuning of the tide-driven sediment transport parameters would lead to the proper change in morphological regime.

5.5 DISCUSSION AND CONCLUSION

The Eastern Scheldt ebb-tidal delta has been adapting itself to the presence of a storm surge barrier in the inlet for the past 25 years. This adaptation has shown no sign so far that it is stabilising. This has given rise to the question how long this adaptation might possibly take.

The most likely development of the ebb-tidal delta is a further redistribution of its sediment surplus along the coast in northern, down drift direction. The seaward front and the shallow areas of the ebb-tidal delta will most likely be eroded further by a combination of waves and alongshore current. This erosion will sustain itself by the deterioration of the wave-sheltering effect of the eroded areas. As a consequence, maximum significant wave heights just seaward of the barrier are likely to increase in the coming decades.

The model applied in this chapter falls short at reproducing the morphological trends observed in reality, and does not show a clear difference in the morphological response between simulations with and without a storm surge barrier. As such, the model cannot assist in answering the question of how long the adaptation of the ebb-tidal delta might take.

In all likelihood, the timescale of the adaptation is in the order of centuries, rather than decades. This conclusion is based on the notion that the decrease in tidal prism created a large sediment surplus on the ebb-tidal delta. The ebb-tidal delta cannot exchange its sediment with any area in need of sediment in its neighbourhood. The Eastern Scheldt basin is out of reach because of the storm surge barrier, and the Grevelingen ebb-tidal delta is also dealing with its own excess sediment. Aside from this, the tidal flow velocities have decreased in response to the barrier's construction. This should imply that the sediment transport capacity also decreased. This combination implies a long adaptation timescale.

Chapter 6

CONCLUSIONS & RECOMMENDATIONS

The goal of this study is to gain understanding of the effects of several human interventions in and around the Eastern Scheldt tidal inlet. In the previous chapters several of these interventions and their effects were examined by looking at measured data as well as model simulations. Having investigated these different phases in the evolution of the Eastern Scheldt, the main research questions posed in chapter 1 can now be answered. This chapter also includes a discussion on how this knowledge can help us in coastal maintenance, how this knowledge fits into the Building With Nature framework, and what knowledge is still missing.

6.1 CONCLUSIONS

6.1.1 Morphology of the Eastern Scheldt tidal inlet before the storm surge barrier

What was the state of the Eastern Scheldt before the Delta Plan was implemented?

The shape of the Eastern Scheldt estuary has been determined predominantly by human intervention since the Middle Ages. The gains and losses of land had a decisive influence on the tidal hydrodynamics and morphology. The state of the Eastern Scheldt estuary by 1950 AD is characterised by a persistent export of sediment out of the inlet. This export has probably been going on since the inundation of South-Beveland in 1530, and was further strengthened by the incorporation of the Volkerak channel. An important factor in the evolution seems to be the erosion-resistant clay layer underneath the inundated parts of South-Beveland. This layer has limited the erosion in this area, and also limited the supply of sediment towards the rest of the basin. This gave the basin a chance to deepen considerably. The disappearance of the tidal watershed in the Zijpe channel during the 18th century is an indirect result of the inundation of South-Beveland. Due to the inundation, the tidal amplitude and phase difference on the Eastern Scheldt side of the watershed started to change. After some time, this caused the watershed to be pushed northward into the Grevelingen estuary.

What was the state of the Eastern Scheldt just before the storm surge barrier was constructed?

The first stages of the Delta Plan consisted of the construction of two dams in the northern branch of the Eastern Scheldt, turning the estuary into a basin. These dams caused amplification of the tidal range, and subsequently caused the sediment export to be amplified. The basin and inlet channels adapted to the new hydraulic regime in the following years by means of deepening and widening channels and accreting flats. As a result of this adaptation, the sediment export through the inlet declined after the initial increase. In the decades before the dams were implemented, the estuary was already exporting sediment. The construction of the dams merely amplified the general erosive trend. This leads to the conclusion that the adaptation of the entire Eastern Scheldt system to a new equilibrium state was probably far from completed by 1983.

On the ebb-tidal delta, the increased flow from the inlet amplified the morphological activity. The main ebb channels straightened and transported sediment further away from the inlet onto the terminal lobe. The fact that this increased activity persisted even when the sediment supply from the basin declined, means that this activity is probably mostly driven by the larger tidal flow, and was not directly dependent on the sediment supply from the basin. The northern shoals were not only influenced by this development, but also by the effects of the closure of the Grevelingen inlet in 1971.

6.1.2 Present-day situation of the Eastern Scheldt ebb-tidal delta

What were the short-term hydrodynamic and morphological effects of the storm surge barrier on the ebb-tidal delta?

The morphological response of the ebb-tidal delta to the construction of the storm surge barrier is characterised by two developments: 1) a small reorientation of the main channels and shoals, and 2) a decrease in sediment volume. The decrease in sediment volume mostly takes place at depths above 10 m. The channels of the ebb-tidal delta with depths below 10 m show some minor accretion since 1986, although some channels actually experience more erosion after 1986 than before.

Overall, the presence of the barrier has caused a decrease in average tidal flow velocity magnitudes. The effect of this decrease is that the morphological activity, i.e. the average magnitude of the bed-level changes also decreased. In spite of this, the sediment budget still shows a strong erosive trend. So even though the bed-level changes are small on average, they are mostly negative. The decrease in flow velocities also causes the shallow parts of the ebb-tidal delta to erode, while the deeper parts gain sediment. Due to the lower flow velocities, sediment transport towards the shoals has decreased. Waves, on the other hand, still enhance sediment transport from these shoals towards deeper parts by means of wave stirring. The strength of this erosion has remained more or less the same. As a result, the shallow parts of the ebb-tidal delta are eroding, and the channels are gaining sediment. The process-based model shows that the erosion of shallow parts and accretion of deeper parts can only be reproduced if waves are included in the model.

However, the trend of accreting channels is not seen everywhere on the ebb-tidal delta. The channels which run close to the shores of Walcheren and Schouwen have shown scouring since the barrier's construction, even though tidal currents through these channels have decreased. Most of the eroded sediment is deposited at the northern ends of Krabbengat and Banjaard Channel, where this sediment is further reworked by a combination of wave and tidal action. The probable cause for the erosion of these channels are stronger residual flows and tidal asymmetries. This development is a specific element of the small clockwise reorientation of the ebb-tidal delta's shoals and channels. The reorientation is a result of the change in the balance between the cross-shore and the alongshore tidal currents. Because the storm surge barrier decreased the strength of the cross-shore currents, the alongshore currents gained in relative strength. As a result, the shoals and channels are pushed slightly northward by the alongshore currents. This hydraulic effect is also reproduced by the process-based model. Comparison of simulations with and without the storm surge barrier shows an increase in tide-residual flow velocity and tidal flow velocity asymmetry on the Banjaard shoal and in the Krabbengat channel.

According to the process-based model simulations, wave forcing is crucial in the reduction of the sediment volume of the ebb-tidal delta. Without wave forcing, the model produces significantly more sedimentation than when wave forcing is applied. More specifically, the model needs wave forcing to adequately reproduce the observed change in the hypsometry, in which deeper parts gain sediment, while shallow parts erode.

With the knowledge gained from observed behaviour and model results, a view emerges of an ebb-tidal delta which is still far from any kind of morphological equilibrium, and which is steadfastly adapting itself to the new hydraulic forcing regime, even though sediment transport capacities have decreased. In general, the most important feature of the storm surge barrier is its constriction of the cross-sectional area of the inlet. A major effect of this constriction is a general decrease in tidal flow velocity magnitudes inside and outside the basin. This effect causes a sharp decrease in sediment transport capacity, which in turn causes eroding shoals and flats, accreting channels, and probably even the observed lack of exchange of sediment between basin and ebb-tidal delta.

It is yet unclear what a new equilibrium state of the ebb-tidal delta will possibly look like, or how long it will take for this area to reach this new state. The measured trends have not yet shown signs of levelling out. The future ebb-tidal delta will become smoother, with smaller differences in depth between shoals and channels. However, at what point in time or bed elevation the shoals will stop losing sediment remains unclear. The most important lack of understanding lies in the particular balance of wave and tidal forces which is needed to put an ebb-tidal delta in a certain morphological regime. At present, the ebb-tidal delta is in a regime characterised by shoals being eroded by tidal currents which are still strong enough to erode (with the help of waves) and transport sediment away from the shoals, but which are not strong enough to transport sediment towards the shoals from deeper water.

6.1.3 The ebb-tidal delta in 200 years

What are the possible long-term effects of the storm surge barrier?

The timescale of the adaptation of the ebb-tidal delta is relatively long, because the surplus of ebb-tidal delta sediment has no obvious deficit to fill. The sediment deficit inside the basin would be an obvious sink. However, the storm surge barrier is blocking the exchange of sediment. The adjacent ebb-tidal deltas are also dealing with sediment surpluses. Apart from this, it has to be kept in mind that the storm surge barrier caused a sharp decrease in sediment transport capacities on the ebb-tidal delta. This makes that the exchange of sediment between the ebb-tidal deltas also occurs on longer timescales.

Model simulations of a schematised version of the Eastern Scheldt inlet show that the general location of the main shoals and channels is mainly determined by tidal interactions. However, these models fail to reproduce the measured trend of erosion of the shallow areas in response to the construction of the storm surge barrier. This is probably because the model fails to capture the proper ratio between wave- and tide-driven sediment transports.

The erosion of the shallow areas will continue for the coming decades. The build-up of large intertidal bars as seen on the Grevelingen and Haringvliet ebb-tidal deltas is not observed at the Eastern Scheldt. This is probably because at the Eastern Scheldt, the remaining tidal currents interfere with the wave-driven cross-shore processes. This prevents the bars from forming, and instead causes erosion of these shoals. This erosion of the shallow areas will probably sustain itself due to the decrease of the sheltering effect created by the seaward shoals. This also means that it is probable that the maximum significant wave heights measured seaward of the barrier will increase over the coming decades.

6.2 RECOMMENDATIONS

6.2.1 Recommendations for coastal maintenance in and around the Eastern Scheldt

The main cause for the lack of sediment import is a lack of sediment transport capacity, not the presence of scour holes

The low sediment transport capacity inside and outside the basin lies at the root of many of the problems in the Eastern Scheldt. The intertidal flats inside the basin have been decreasing in height and area since the construction of the barrier. The cause for this is a lack of sediment transport from the channels towards the flats, brought on by the general decrease in tidal flow velocity magnitudes. Meanwhile, the erosion of the flats by wind waves continues. The lack of net sediment transport through the storm surge barrier is caused by the same general decrease in flow velocities.

The situation inside the basin could be improved by increasing the tidal flow velocities in some way. However, this is easier said than done. Removing the barrier would increase flow velocities, probably to the point where shoal build up would take place again (e.g. Das, 2010; De Pater, 2012). However, this might not be a cost-effective solution due to the adaptations that would have to be made to the levees around the basin.

Another method of dealing with degradation of tidal flats is to nourish them with sediment. In other words, sediment is placed mechanically on top of the flats, after which natural processes will redistribute it. Benefits of this solution are its cost-effectiveness and flexibility. Disadvantages are the temporary disturbance of the estuarine biology on top of the flats, and the fact that the nourishments will have to be applied for as long as the storm surge barrier remains in place.

In the case of the Eastern Scheldt, there are no viable possibilities to stimulate sediment import in quantities that are sufficient to counter the deficit. The solution of maintaining some of the intertidal area with nourishments is more efficient, even on the timescale of the design lifetime of the barrier.

On the ebb-tidal delta, the main trend consists of eroding shoals and accreting channels. However, channels close to the coast are still becoming deeper, not shallower.

The main coastal erosion problems around the Eastern Scheldt inlet occur where the Onrust and Krabbengat channels approach the coasts of North-Beveland and Schouwen, respectively. The bathymetric data measured since 1960 clearly show a change in trend in these channels in response to the construction of the barrier. This development will probably remain the leading cause for the shoreline erosion of Schouwen and North-Beveland for the foreseeable future. Until now, these coasts have been maintained by a combination of breakwaters and beach nourishments. The relatively large size of these channels makes that this combination of measures remains the most suitable solution for maintaining this coast. It is recommendable, however, to keep a close eye on these coastlines, as the channels in front of them are still growing larger.

6.2.2 Recommendations for future research

The process-based models applied in this study for predicting long-term behaviour did not reproduce some of the changes in morphological behaviour caused by the storm surge barrier. The most probable cause for this inability is a lack of understanding of the different morphological states that an ebb-tidal delta can be in. Which range of tidal currents relative to the wave forcing actually puts the ebb-tidal delta in any particular state is the knowledge which is needed to say anything about a possible end state of the Eastern Scheldt ebb-tidal delta.

In the Dutch Delta there are several tidal channels which run relatively close to the shoreline. Especially the Oostgat channel near Walcheren, the Onrust channel near North-Beveland, and the Krabbengat channel near Schouwen all run very close to the beaches of these islands. If such a channel shifts position or becomes deeper, beach erosion can be severe. However, most knowledge on beach morphology is based on situations without channels like these in front of the beach, and little is known about the effects of tidal channels so close to the shoreline.

The topic of channel-beach interaction is closely related to channel-shoal interaction. Most of the numerical models which are applied to predict the evolution of the intertidal flats inside the Eastern Scheldt still have problems in determining when increase or decrease of shoal height is to occur. Causes for this could be the flooding and drying procedures in combination with short waves, lack of resolution, or lack of knowledge on which processes are essential for modelling sediment transport on intertidal area. Therefore, it is recommendable to acquire field data from these areas with sufficient temporal and spatial coverage to give insight into what is actually happening on these channel edges. This knowledge and associated data can then be used to make morphological models more robust in these areas.

The small-scale morphology of the scour holes on both sides of the barrier deserves further scientific attention. The scour holes are still growing, albeit slowly. From recent studies (e.g. Hoogduin, 2009; De Bruijn, 2012) it is known that the ebb- and flood-jets on both sides of the barrier play an important role in the direction and magnitude of the net sediment transports around the scour holes. Recently, there have been signs that the edges of the scour protection are suffering from damage and erosion. Further insight into the hydrodynamic and morphological processes inside the scour holes may help in countering or preventing further damage.

6.2.3 Integration in the Building with Nature framework

The goal of the Building with Nature program is to find new ways of creating wet infrastructure while also creating opportunities for nature to develop. The knowledge gained through this particular study can help the Building with Nature program in several ways. The developments in the Eastern Scheldt over the past 50 years give a comprehensive view of how different types of human intervention affect estuarine morphology. An important lesson learned is that interventions in estuaries can have a large reach in both space and time. A second important lesson is that the phasing of multiple interventions is something that can be optimised. In the case of the Eastern Scheldt, for instance, this phasing was far from optimal. The first phase, initiated by the construction of the Volkerak dam, caused the period between 1969 and 1986 to be dominated by sediment export with an estimated cumulative volume of 40 million m^3. The following phase, initiated by the completion of the storm surge barrier in 1986, is characterised by a deficit of sediment. Although the sediment deficit inside the basin is much larger than this 40 million m^3, it would have been smaller than it is in reality today if the barrier been built sooner after completion of the Volkerak dam.

In the case of future storm surge barriers, it would be recommendable to make the wet cross-sectional area of any barrier as large as feasible. This would be the best way to preserve the hydraulic and morphological characteristics of any body of water behind the barrier.

Recently, the hydrodynamic model for the Eastern Scheldt used in this study has also been of use for ecological research purposes (Cozzoli *et al.*, 2013). A model like the one designed for this study can give the spatial distribution of certain hydrodynamic parameters which influence the distribution of biological species. This combining of models gives a powerful tool for assessing hydrodynamic, morphological, and possibly also ecological effects of human interventions in estuaries.

Bibliography

Aarninkhof, S.G.J. and Van Kessel, T. (1999). Data analyse Voordelta: Grootschalige morfologische veranderingen 1960-1996. WL/Delft Hydraulics, Z2694.

Battjes, J.A. (1982). A case study of wave height variations due to currents in a tidal entrance. Coastal Engineering, 6, 47-57.

Beekman, F. (2007). De kop van Schouwen onder het zand: Duizend jaar duinvorming en duingebruik op een Zeeuws eiland. Uitgeverij Matrijs.

Beets, D.J. and Van der Spek, A.J.F. (2000). The Holocene evolution of the barrier and the back-barier basins of Belgium and the Netherlands as a function of late Weichselian morphology, relative sea-level rise and sediment supply. Netherlands journal of Geosciences, 79 (1), 3-16.

Beets, D.J., van der Valk, L. and Stive, M.J.F. (1992). Holocene evolution of the coast of Holland. Marine Geology, 103, 423-443.

Booij, N., Ris, R.C. and Holthuijsen, L.H. (1999). A third generation wave model for coastal regions. 1. Model description and validation. Journal of Geophysical Research, 104 (C4), 7649-7666.

Bruun, P. and Gerritsen, F. (1959). Natural bypassing of sand at coastal inlets. Journal of the Waterways and Harbors, 85, 75-107.

Cleveringa, J. (2000). Reconstruction and modelling of Holocene coastal evolution of the western Netherlands. PhD-thesis, Universiteit Utrecht, The Netherlands.

Cleveringa, J. (2008). Morphodynamics of the Delta coast (southwest Netherlands): Quantitative analysis and phenomenology of the morphological evolution 1964-2004. Alcyon, A1881.

Das, I.L.L. (2010). Morphodynamic modelling of the Galgeplaat. MSc-thesis, Delft University of Technology, The Netherlands. Available at http://repository.tudelft.nl/view/ir/uuid%3A56998e1f-729c-4924-9a4b-67003c1355ff/

Dastgheib, A., Roelvink, J.A., and Wang, Z.B. (2008). Long-term process-based morphological modeling of the Marsdiep tidal basin. Marine Geology, 256, 90-100.

Dastgheib, A. (2012). Long-term process-based morphological modeling of large tidal basins. PhD-thesis, UNESCO-IHE, The Netherlands.

De Bok, C. (2001). Long-term Morphology of the Eastern Scheldt. Rijkswaterstaat RIKZ, RIKZ/2002.108x.

De Bruijn, R.A. (2012). The future of the Oosterschelde with a new inlet channel. MSc-thesis, Delft University of Technology, The Netherlands. Available at http://repository.tudelft.nl/view/ir/uuid%3Adb879ccf-3cb1-448f-adea-4d9e221be35f/

De Kruif, A.C. (2001). Bodemdieptegegevens van het Nederlandse kustsysteem. RIKZ/Rijkswaterstaat, RIKZ/2001.041.

De Pater, P.D. (2012). Effects of removal of the Oosterschelde storm surge barrier. MSc-thesis, Delft University of Technology, The Netherlands. Available at http://repository.tudelft.nl/view/ir/uuid%3A852d5a80-6998-4b3e-bcd2-9124fb3ed21a/

De Ronde, J.G. (1983). Changes of relative mean sea-level and mean tidal amplitude along the Dutch coast. Seismicity and seismic risk in the offshore North Sea area. A.R. Ritsema and A. Gurpunar.

De Vriend, H.J. (1991). Mathematical modelling and large-scale coastal behaviour. Part 1: Physical processes. Journal of Hydraulic Research, 29, 727-740.

De Vriend, H.J. (1996). Mathematical modeling of meso-tidal barrier island coasts. Part 1: Empirical and semi-empirical models. Advances in coastal and ocean engineering, Singapore, World Scientific Publishing Company.

De Vriend, H.J., Louters, T., Berben, F, and Steijn, R.C. (1989). Hybrid prediction of a sandy shoal evolution in a mesotidal estuary. In R.A. Falconer, P. Goodwin & R.G.S. Matthew (eds.), Hydraulic and Environmental Modelling of Coastal, Estuarine and River Waters, Int. Conf. Bradford, England, vol. 14: 145-156.

De Vriend, H.J., Zyserman, J., Nicholson, J., Roelvink, J.A., Péchon, P. and Southgate, H.N. (1993). Medium-term 2DH coastal area modelling. Coastal Engineering, 21, 193-224.

Dissanayake, D.M.P.K. (2011). Modelling morphological response of large tidal inlet systems to sea level rise. PhD-thesis, UNESCO-IHE, The Netherlands.

Dissanayake, D.M.P.K., Roelvink, J.A. and van der Wegen, M. (2009). Modelled channel patterns in a schematized tidal inlet. Coastal Engineering, 56, 1069-1083.

Eelkema, M., Wang, Z.B. and Stive, M.J.F. (2012). Impact of back-barrier dams on the development of the ebb-tidal delta of the Eastern Scheldt. Journal of Coastal Research, 28 (6), 1591-1605.

Elias, E. (2006). Morphodynamics of Texel Inlet. PhD thesis, Delft University of Technology, The Netherlands.

Elias, E.P.L., Cleveringa, J., Buijsman, M.C., Roelvink, J.A. and Stive, M.J.F. (2006). Field and model data analysis of sand transport patterns in Texel tidal inlet (the Netherlands). Coastal Engineering, 53, 505-529.

Escoffier, F.F. (1940). The stability of tidal inlets. Shore and Beach, 114-115.

Eysink, W.D. (1990). Morphological response of tidal basins to change. Proceedings 22nd International conference on Coastal Engineering, Delft, 1948-1961.

Fitzgerald, D.M., Buynevich, I.V., Davis, R.A. and Fenster, M.S. (2002). New England tidal inlets with special reference to riverine-associated inlet systems. Geomorphology, 48, 179-208.

Fitzgerald, D.M., Kraus, N.C. and Hands, E.B. (2000). Natural Mechanisms of Sediment bypassing at Tidal Inlets. US army corps of engineers.

Friedrichs, C.T. and Aubrey, D.G. (1988). Non-linear tidal distortion in shallow well-mixed estuaries: a synthesis. Estuarine, costal and shelf science, 27, 521-545.

Haring, J. (1953). Inhouds- en diepteveranderingen van de Oosterschelde over de periode 1933-1947-1951. Rijkswaterstaat, rapport nº 13.

Haring, J. (1955). Zandbalansen van de zuidwestelijke wateren van Nederland over de perioden 1872-1933 en 1933-1952. Rijkswaterstaat, rapport nº 3.

Haring, J. (1978). De geschiedenis van de ontwikkeling van de waterbeweging en van het profiel van de getijdewateren en zeegaten van het zuidelijk deltabekken. Rijkswaterstaat, K77M031E.

Hayes, M.O. (1979). Barrier island morphology as a function of tidal and wave regime. Barrier Islands: From the Gulf of St. Lawrence to the Gulf of Mexico, S.P. Leatherman, ed., Academic Press, New York, 3-22.

Hayes, M.O. (1980). General morphology and sediment patterns in tidal inlets. Sedimentary geology, 26, 139-156.

Hoogduin, L. (2009). Sediment transport through the Eastern Scheldt storm surge barrier. MSc-thesis, Delft University of Technology, The Netherlands. Available at http://repository.tudelft.nl/view/ir/uuid%3Ab574822d-377d-43ff-894c-8e4b74a2a476/

Huisman, B.A. and Luijendijk, A.J. (2008). Sand demand of the Eastern Scheldt. Deltares, Z4581.

Jongeling, T.H.G. (2007). Zandhonger Oosterschelde: maatregelen ter vergroting van doorstroomcapaciteit en zanddoorvoer stormvloedkering Oosterschelde. WL/Delft Hydraulics, Q4264.

Kohsiek, L.H.M., Mulder, J.P.M., Louters, T. and Berben, F. (1987). De Oosterschelde; naar een nieuw onderwaterlandschap. RWS dienst getijdewateren, DGW.AO.87.029.

Kragtwijk, N.G., Zitman, T.J., Stive, M.J.F. and Wang, Z.B. (2004). Morphological response of tidal basins to human interventions. Coastal Engineering, 51, 207-221.

Lesser, G.R. (2009). An approach to medium-term coastal morphological modelling. PhD-thesis, UNESCO-IHE, The Netherlands.

Lesser, G.R., Roelvink, J.A., van Kester, J.A.T.M. and Stelling, G.S. (2004). Development and validation of a three-dimensional morphological model. Coastal Engineering, 51, 883-915.

Louters, T., Van den Berg, J.H. and Mulder, J.P.M. (1998). Geomorphological changes of the oosterschelde tidal system during and after the implementation of the delta plan. Journal of Coastal Research, 14 (3), 1134.

Marijs, K. and Parée, E. (2004). Nauwkeurige vaklodingen Westerschelde en -monding: "de praktijk". Meetinformatiedienst Zeeland, ZLMD-04.N.004.

Mulder, J.P.M. and Louters, T. (1994). Changes in basin geomorphology after implementation of the Oosterschelde estuary project. Hydrobiologia, 282/293, 29-39.

O'Brien, M.P. (1969). Equilibrium flow areas of inlets and sandy coasts. Journal of waterway, port, coastal, and ocean engineering, 95, 43-55.

Oertel, G.F. (1975). Ebb-tidal deltas of Georgia Estuaries. Estuarine research, L.E. Cronin, ed., Academic Press, New York, 267-276.

Partheniades, E. (1965). Erosion and deposition of cohesive soils. Journal of the Hydraulic Division, ASCE, 91, (No. HY1).

Peelen, R. (1970). Changes in salinity in the delta area of the rivers Rhine and Meuse resulting from the construction of a number of enclosing dams. Netherlands Journal of Sea Research, 5 (1), 1-19.

Rijkswaterstaat, (1961). Verslag over de stormvloed van 1953. Samengesteld door de Rijkswaterstaat en het Koninklijk Nederlands Meteorologisch Instituut. Staatsdrukkerij- en uitgeverijbedrijf 's-Gravenhage.

Rijkswaterstaat, (1984). Vastlegging uitgangssituatie Oosterschelde (T2). Rijkswaterstaat, WWKZ-84.V005.

Roelvink, J.A. and Reniers, A.J.H.M. (2011). A guide to modelling coastal morphology. Advances in Coastal and Ocean Engineering, World Scientific.

Roelvink, J.A., Van der Kaaij, T. and Ruessink, B.G. (2001). Calibration and verification of large-scale 2D/3D flow models, phase 1. Delft Hydraulics report, Z3029.11.

Roelvink, J.A., and Walstra, D.J. (2004). Keeping it simple by using complex models. 6th International Conference on Hydroscience and Engineering, Advances in Hydro-Science and –Engineering, Brisbane, Australia.

Sha, L.P. and Van den Berg, J.H. (1993). Variation in ebb-tidal delta geometry along the coast of the Netherlands and the German Bight. Journal of Coastal Research, 9 (3), 730-746.

Speer, P.E., and Aubrey, D.G. (1985) A study of non-linear tidal propagation in shallow inlet/estuarine systems, part II: theory. Estuarine, coastal and shelf science, 21, 207-224.

Steijn, R.C., Louters, T., Van der Spek, A.J.F., and De Vriend, H.J. (1989). Numerical model hindcast of the ebb-tidal delta evolution in front of the Deltaworks. In R.A. Falconer, P. Goodwin & R.G.S. Matthew (eds.), Hydraulic and Environmental Modelling of Coastal, Estuarine and River Waters, Int. Conf. Bradford, England, vol. 14: 255-264.

Stive, M.J.F. and Wang, Z.B. (2003). Morphodynamic modeling of tidal basins and coastal inlets. Advances in Coastal Modeling, 367-392.

Ten Brinke, W.B.M. (1993). The impact of biological factors on the deposition of fine grained sediment in the Oosterschelde (the Netherlands). PhD thesis, Universiteit Utrecht, The Netherlands.

Ten Brinke, W.B.M., Dronkers, J. and Mulder, J.P.M. (1994). Fine sediments in the Oosterschelde tidal basin before and after partial closure. Hydrobiologia, 282/283, 41-56.

Tran, T.T. (2011). Morphodynamics of seasonally closed coastal inlets at the central coast of Vietnam. PhD-thesis, Delft University of Technology, The Netherlands.

Van de Kreeke, J. (2006). An aggregate model for the adaptation of the morphoogy and sand bypassin after basin reduction of the Frisian Inlet. Coastal Engineering, 53, 255-263.

Van de Kreeke, J. and Robaczewska, K. (1993). Tide-induces residual transport of coarse sediment; application to the Ems estuary. Netherlands Journal of Sea Research, 31, (3), 209-220.

Van den Berg, J.H. (1986). Aspects of sediment- and morphodynamics of subtidal deposits of the Oosterschelde (the Netherlands). Rijkswaterstaat, no. 43/1986.

Van der Spek, A.J.F. (1994). Large-scale evolution of Holocene tidal basins in the Netherlands. PhD-thesis, Universiteit Utrecht, The Netherlands.

Van der Spek, A.J.F. (1997). Tidal asymmetry and long-term evolution of Holocene tidal basins in the Netherlands: simulation of paleo-tides in the Schelde estuary. Marine Geology, 141, 71-90.

Van der Vegt, M. (2006). Modeling the dynamics of barrier coasts and ebb-tidal deltas. PhD-thesis, Universiteit Utrecht, The Netherlands.

Van der Wegen, M. (2010). Modeling morphodynamic evolution in alluvial estuaries. PhD-thesis, UNESCO-IHE, The Netherlands.

Van der Wegen, M. and Roelvink, J.A. (2008). Long-term morphodynamic evolution of a tidal embayment using a two-dimensional, process-based model. Journal of Geophysical Research, 113, (C03016), 23.

Van der Wegen, M., Wang, Z.B., Savenije, H.H.G., and Roelvink, J.A. (2008). Long-term morphodynamic evolution and energy dissipation in a coastal plain, tidal embayment. Journal of Geophysical Research, 113, F03001.

Van Rijn, L.C. (1993). Transport of fine sands by current and waves. Journal of waterway, port, coastal, and ocean engineering, 119 (2), 123-143.

Van Veen, J., Van der Spek, A.J.F., Stive, M.J.F. and Zitman, T.J. (2005). Ebb and flood channel systems in the Netherlands tidal waters. Journal of Coastal Research, 21 (6), 1107-1120.

Van Zanten, E. and Adriaanse, L.A. (2008). Verminderd getij; verkenning naar mogelijke maatregelen om het verlies van platen, slikken en schorren in de Oosterschelde te beperken. Rijkswaterstaat.

Vos, P.C., and Van Heeringen, R.M. (1997). Holocene geology and occupation history of the Province of Zeeland (SW Netherlands). Mededelingen Nederlands Instituut voor Toegepaste Geowetenschappen TNO, 59, 5-109.

Vos, P.C., Bazelmans, H.J.T., and van der Meulen, M.J. (2011). Atlas van Nederland in het Holoceen. Bert Bakker, Amsterdam, 94pp.

Vroom, J. (2011). Tidal divides: A study on a simplified case and the Dutch Wadden Sea. MSc-thesis, Delft University of Technology, The Netherlands. Available at http://repository.tudelft.nl/view/ir/uuid%3A7c28338b-7a43-489f-8b57-98af6a00561c/

Vroon, J. (1994). Hydrodynamic characteristics of the Oosterschelde in recent decades. Hydrobiologia, 282/283, 17-27.

Walgreen, M., De Swart, H.E. and Calvete, D. (2004). A model for grain-size sorting over tidal sand ridges. Ocean Dynamics, 54, 374-384.

Walton, T.L. and Adams, W.D. (1976). Capacity of inlet outer bars to store sand. Proc. 15th International Conference on coastal Engineering, Honolulu.

Wang, Z.B., Louters, T. and De Vriend, H.J. (1995). Morphodynamic modelling for a tidal inlet in the Wadden sea. Marine Geology, 126, 289-300.

Wilderom, M.H. (1961). Tussen Afsluitdammen en Deltadijken 1: Noord-Beveland. Littooy & Olthoff, Middelburg.

Wilderom, M.H. (1964). Tussen Afsluitdammen en Deltadijken 2: Noord-Zeeland (Schouwen-Duiveland, Tholen, en St. Philipsland). Littooy & Olthoff, Middelburg.

Wilderom, M.H. (1968). Tussen Afsluitdammen en Deltadijken 3: Midden-Zeeland (Walcheren en Zuid-Beveland). Littooy & Olthoff, Middelburg.

Zagwijn, W.H. (1986). Nederland in het Holoceen.Geologie van Nederland. Rijksgeologische dienst, Haarlem.

PUBLICATIONS

Thesis related publications

Eelkema, M., Wang, Z.B. and Stive, M.J.F. (2009). Historical morphological development of the Eastern Scheldt tidal basin (the Netherlands). *Proceedings of Coastal Dynamics 2009.*

Eelkema, M., Wang, Z.B. and Stive, M.J.F. (2011). Sediment transport dynamics in response to a storm surge barrier. *Proceedings of Coastal Sediments 2011.*

Eelkema, M., Wang, Z.B. and Stive, M.J.F. (2012). Impact of back-barrier dams on the development of the ebb-tidal delta of the Eastern Scheldt. *Journal of Coastal Research,* 28(6), 1591-1605.

Eelkema, M., Wang, Z.B., Hibma, A., and Stive, M.J.F. (2012). Morphological effects of the Eastern Scheldt storm surge barrier on the ebb-tidal delta. *Submitted to Coastal Engineering Journal.*

Cozzoli, F., Eelkema, M., Bouma, T., Ysebaert, T., Escavarge, V., and Herman, P. (in preparation). Coastal Defence: long-term impacts on benthic habitats suitability.

Other publications

Jacobs, W., Eelkema, M., Limburg, H., and Winterwep, J.C. (2009). A new radiometric instrument for in situ measurements of physical sediment properties. *Marine and Freshwater Research,* 60, 727-736.

Appendix A KUSTZUID MODEL PARAMETERS

Parameter	*Description*	*Unit*	*Value*
Flow			
delta t	flow time step	s	60
Rho w	water density	kg/m^3	1023
Roumet	roughness formulation	-	Manning
C	Manning coefficient	$s/m^{1/3}$	0.025
Vicouv	horizontal eddy viscosity	m^2/s	1
Dicouv	horizontal eddy diffusivity	m^2/s	1
Rouwav	stress formulation due to wave forces	-	FR84
Dryflc	Threshold depth	m	0.1
Rhoa	air density	kg/m^3	1.205
Waves			
spectrum	shape of spectrum	-	JONSWAP
gamma1	peak enhancement factor JONSWAP spectrum	-	3.3
wave setup	wave related water level setup	-	false
forcing	computation of wave forces	-	radiation stress
generation	generation mode for physics	-	3rd
breaking	depth-induced breaking model	-	B&J model
alfa1	coefficient for wave energy dissipation in the B%J model	-	1
gamma2	breaker parameter	-	0.73
triads (LTA)	non-linear triad interaction	-	true
alfa2	coefficient for triad interaction	-	0.1
beta	coefficient for triad interaction	-	2.2
bottom friction	bottom friction formulation	-	JONSWAP
coeff	bottom friction coefficient	m^2/s^3	0.067
diffraction		-	false
wind growth	formulation for exponential wind growth	-	true
white capping	formulation for white capping	-	true
quadruplets	quadruplet wave-wave interaction	-	true
ref	refraction for wave propagation in spectral space	-	true
freq	frequency shift for wave propagation in spectral space	-	true
Sediment transport			
MorFac	morphological scale factor	-	1
MorStt	spin-up interval from TStart till start of morphological changes	min	1440
Thresh	Threshold sediment thickness for transport and erosion reduction	m	0.05
MorUpd	update bathymetry during FLOW simulation	-	true
EqmBc	equilibrium sand concentration profile at inflow boundary	-	true
DensIn	include effect of sediment concentration on fluid density	-	false
AksFac	van Rijn's reference height factor	-	1
Rwave	wave related roughness coefficient	-	2
AlfaBS	streamwise bed gradient factor for bed load transport	-	1
AlfaBN	transverse bed gradient factor for bed load transport	-	50
Sus	multiplication factor for suspended sediment reference concentration	-	1
Bed	multiplication factor for bed load transport vector magnitude	-	1
SusW	wave-related suspended sediment transport factor	-	0.05
BedW	wave-related bed load sediment transport factor	-	1
SedThr	minimum water depth for sediment computations	m	0.1
ThetSD	factor for erosion of adjacent dry cells	-	0
Rhosol	specific density	kg/m^3	2650
CDryB	dry bed density	kg/m^3	1600

Appendix B LONG TERM MODEL SENSITIVITY ANALYSIS

The morphological model used in Chapter 5 requires some specific parameter settings in order to give the model the desired behaviour. The most pressing issue is the fact that with certain values, the model produces an ebb-tidal delta which is too deep and/or too wide. The problem is mainly to find a combination of settings that generates both a realistic hypsometry as well as a realistic shape of the ebb-tidal delta. Some combinations result in a hypsometry that is close to reality, but give a shape that is seemingly missing certain bathymetrical elements found in reality. Other combinations do generate these elements, but have problems approaching the real hypsometry.

The main problem with reproducing the hypsometry is that the numerical model has a tendency to make channels deeper than they should be. One method for limiting this behaviour is to make use of multiple sediment fractions with different median grain sizes instead of just one. This will result in a simulated ebb-tidal delta with higher median grain sizes in the channels, and lower median grain sizes on the shoals. This kind of distribution is also found in reality.

Apart from the multiple sediment fractions, also the choice for the value of the transverse bed slope factor for the bed load transport ('AlfaBn' in Delft3D) has an influence on the shape of the channels. Generally, low values (<10) for the transverse bed slope factor result in narrow and deep channels, while high values (>50) result in shallower channels (Tran, 2011). This means that this factor can be used to limit the erosion of the channels by increasing it to high, non-physical values in the range of 50 to 100.

For the study described in Chapter 5 on the possible long term evolution of the Eastern Scheldt ebb-tidal delta, four different combinations of bed composition and bed slope factors were examined. Two of those combinations used a single sediment fraction with a median grain size of 200 microns, and bed slope factors of 50 and 100, respectively. The other two combinations used three sediment fractions with median grain sizes of 100, 300, and 500 microns, and bed slope factors of 50 and 100, respectively.

The hypsometries (Figure A.1) and bathymetries (Figure A.2) generated with these settings show that increasing the bed slope factor results in a much smoother bathymetry, and decreases the channel volumes. Adding more sediment fractions decreases these volumes even further, and also prevents the formation of the bars around the terminal lobe that are seen in the simulations with a single sediment fraction.

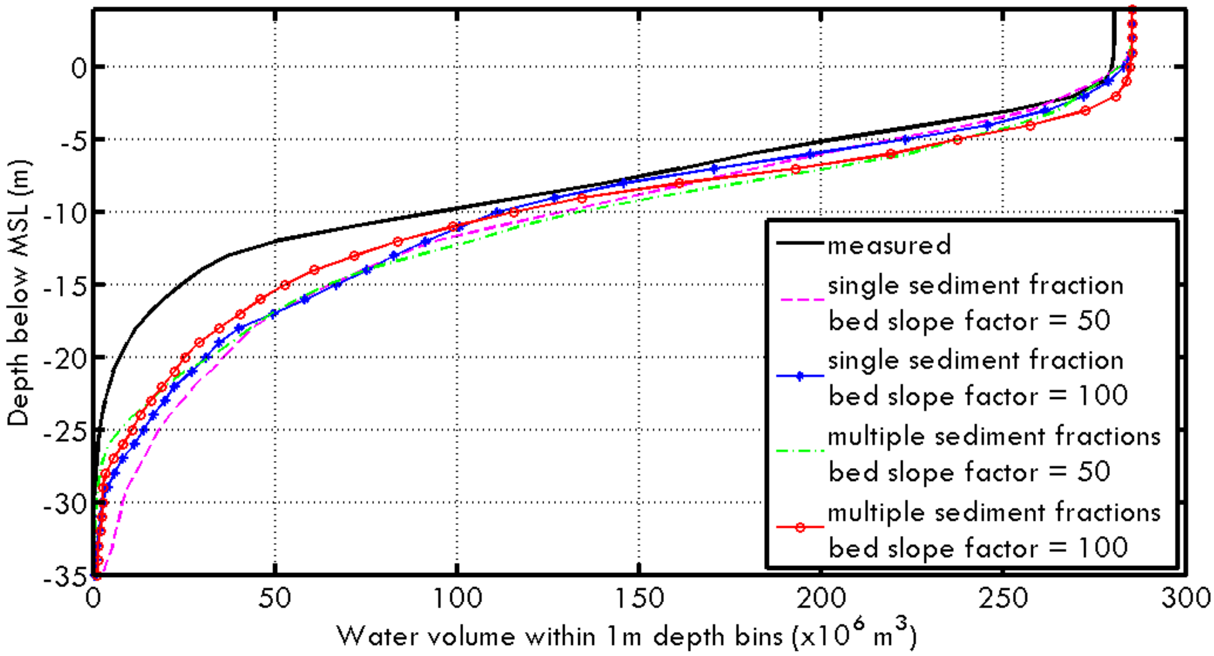

Figure A.1: Hypsometric curves of the ebb-tidal deltas of different parameter combinations after 400 morphological years.

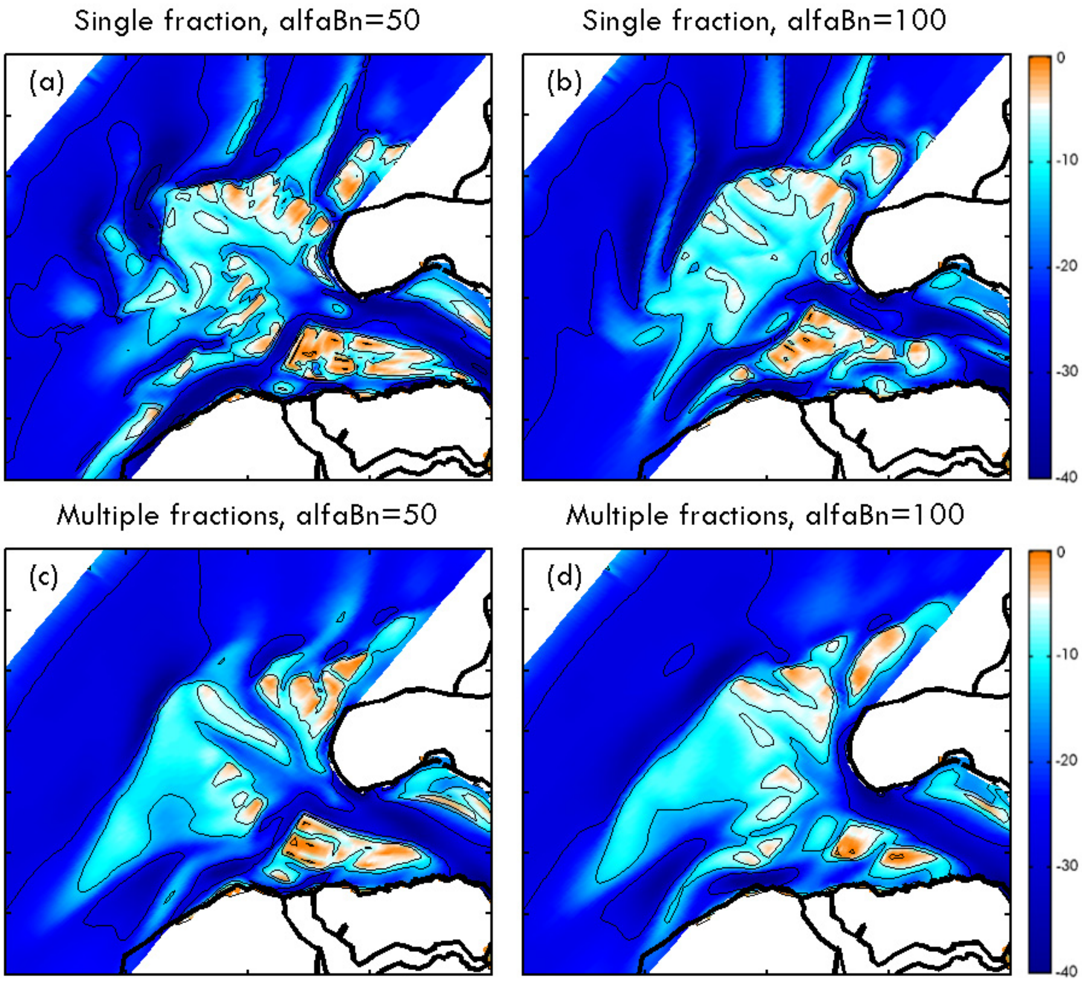

Figure A.2: Bathymetries of the ebb-tidal deltas for different parameter settings

Appendix C Ebb-tidal delta Bathymetry of 2008

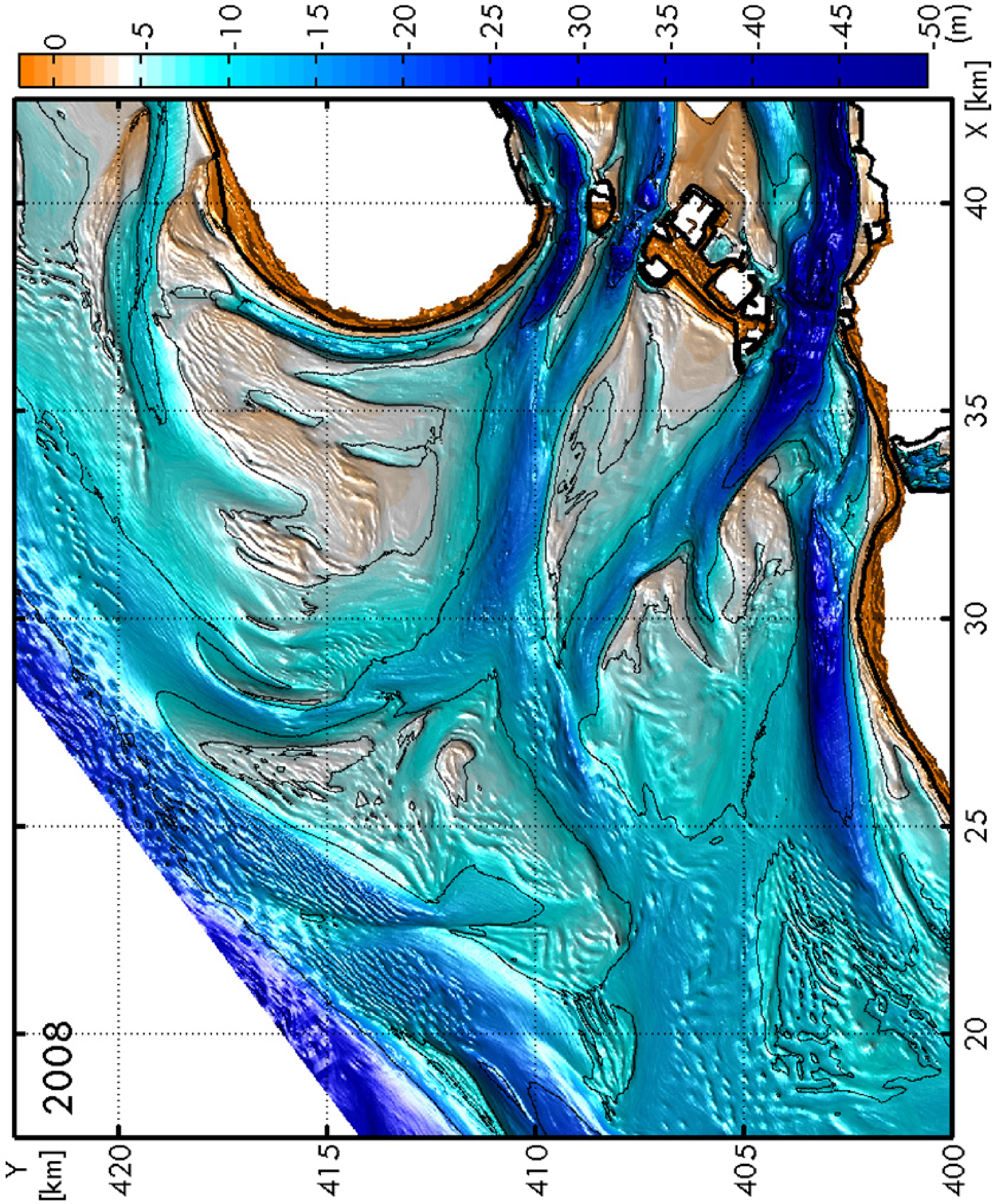

Appendix D 2010 Eastern Scheldt Basin Bathymetry

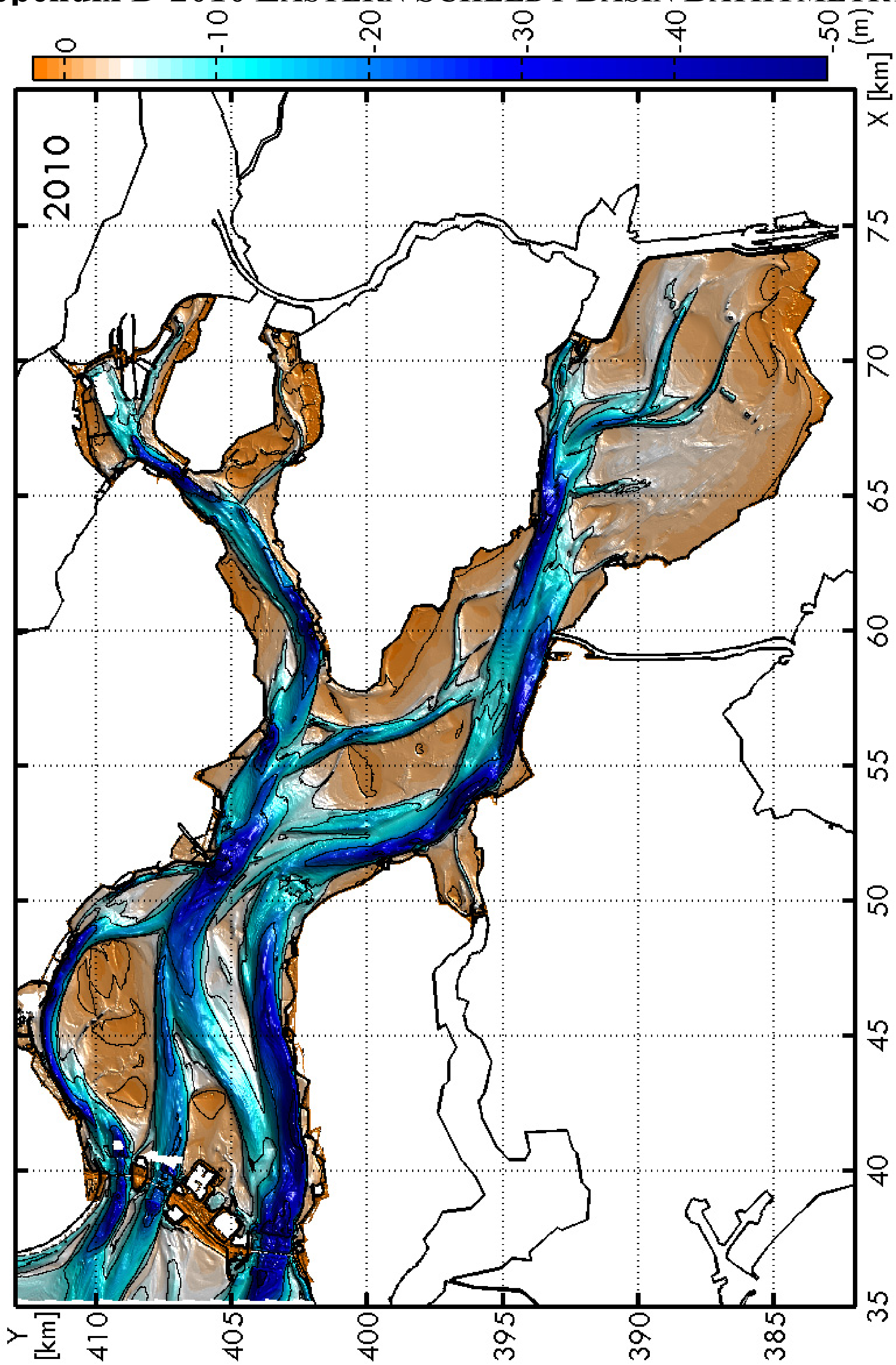

ACKNOWLEDGEMENTS

It was a little over 5 years ago, during the time when I was finalising my master thesis, when I asked my graduation professor: “Hey Huib, What is this “Building-with-Nature” thing I keep hearing about?” Five years later, this dissertation is part of the answer to that question.

In my undoubtedly biased opinion, it has come out pretty nice, and it incorporates all the things that I like about civil engineering: morphology, fluid mechanics, hydraulic structures, ecology, history, measurements, etc. There are a lot of people who have helped me in making this dissertation what it is. I feel grateful for spending so much time with so many cool people, and I sure want to thank them for it. So here it goes.

Marcel Stive, thank you for being such a great boss over the years, and for spurring me on or slowing me down whenever I needed to be.

Zheng Bing Wang, your knowledge is rivalled only by your patience and enthusiasm. Thank you for all those fruitful discussions and your helpful comments.

Huib de Vriend, thank you for inventing the Building with Nature program, and for inviting me into it.

I also want to express my gratitude towards the other members of the committee for reviewing my manuscript and offering valuable feedback: Prof.dr.ir. Dano Roelvink, Prof.dr.ir. Piet Hoekstra, Dr. Ad van der Spek, and Dr.ir. Anneke Hibma.

Thanks to all the people involved in the Building with Nature program, either as part of my user committee, or as part of other programs: Anneke Hibma, John de Ronde, Mark van Koningsveld, Stefan Aarninkhof, Tom Ysebaert, Leo Adriaanse, Martin Baptist, Claire van Oeveren Theeuwes, Brenda Verhaeghe de Naeyer, Francesco Cozzoli, and all the other Building with Nature PhD’s.

Thanks to Jan Slager and all the other people at Rijkswaterstaat Zeeland who helped me dig up some very useful measurement data.

To the Building with Nature MSc-students with whose graduation I was involved, in chronological order: Lars Hoogduin, Ingrid Das, and Pim de Pater; Thank you for taking some work out of my hands.

To all my roommates at work, past and present; Cong Mai Van, Wim Kanning, Duong Bach, Bas Huisman, Bas Hoonhout, and Saulo Meirelles; Thank you for making room 3.95 the best room in the building.

Special thanks goes to my Coastal Dynamics exam buddies, with whom I also went to Miami for Coastal Sediments conference (and who are also my paranymphs), Ronald Brouwer and Sierd de Vries. I think we made a good team.

Over the years I've had the privilege of working with many different colleagues at the faculty of Civil Engineering; Arjen, Bas, Bianca, Bram, Chu, Cornelis, Dirk-Jan, Fedor, Gerben, Jaap, Jasper, Jessica, Joao, Judith, Kees, Madelon, Marije, Martijn, Matthieu, Meagan, Miguel, Nici, Rosh, Ruben, Steven, Timo, Tomo, Trung, Vana, Walter, Willem, Wim, and many others; My thanks goes out to all of you.

To the people who keep the department running: Agnes, Chantal, Inge, Judith, Mark; Thank you for all the logistical and administrative support.

Finally I want to thank all my family and friends in Delft, The Hague, De Bilt, and many other parts of the world. A special thanks goes out to my parents, who have blessed me with a fascination for beaches, dunes, tidal basins, barrier islands, Zeeland, the Wadden Sea, and many other things water-related.

Menno Eelkema

Februari, 2013

ABOUT THE AUTHOR

Menno Eelkema was born on May 10th 1983, in the village of Bilthoven (the Netherlands), and grew up in De Bilt. After graduating from the Utrecht Stedelijk Gymnasium in 2001, he moved to The Hague, and started studying Civil Engineering at Delft University of Technology. In 2007 he conducted research in the Western Scheldt for his master thesis, entitled "Measuring sediment properties in the field using MEDUSA RhoC". As part of his thesis, he went onto several tidal flats in the Western Scheldt, and applied a new device which can measure mud content and sediment density in the field. Back in the laboratory he compared these measurements with sediment samples taken at the same locations.

Since June 2008 Menno has been employed at the faculty of Civil Engineering, department of Hydraulic Engineering, to work on his research on the morphology of the Eastern Scheldt tidal inlet. This research was funded by both the Building With Nature program and the Cornelis Lely foundation. During the final months of his employment he also developed a new website for the NEMO-project (Nearshore Monitoring & Modelling).

In his spare time he enjoys playing guitar and sailing.